Biomimetic asymmetric catalysis with bioinspired helical foldamers

Antoine Hacihasanoglu

THÈSE EN COTUTELLE PRÉSENTÉE

POUR OBTENIR LE GRADE DE

DOCTEUR DE

L'UNIVERSITÉ DE BORDEAUX

ET DE L'UNIVERSITÉ DU PAYS BASQUE

ÉCOLE DOCTORALE UBX

ÉCOLE DOCTORALE UPV/EHU

SPÉCIALITÉ CHIMIE ORGANIQUE

Par ANTOINE HACIHASANOGLU

Biomimetic asymmetric catalysis with bioinspired helical foldamers

Sous la direction de Gilles GUICHARD
et de Mikel OIARBIDE

Soutenue le 13 Mai 2022

Membres du jury :

M. Daniel TATON, Professeur des universités, Université de Bordeaux, Président
Mme. Renata MARCIA DE FIGUEIREDO, Chargée de recherche, Ecole Nationale Supérieure de Chimie de Montpellier, Rapporteur
M. Claude TAILLEFUMIER, Directeur de recherche, Université Clermont Auvergne, Rapporteur
M. Aitor LANDA, Professeur des universités, Universidad del Pais Vasco, Examinateur
M. David AITKEN, Professeur des universités, Université Paris-Saclay, Examinateur

List of commonly used abbreviations:

Ac: Acetate
Aib: 2-aminoisobutyric acid
Ala: Alanine
BAMOL: 1,1'-biaryl-2,2'-dimethanol
BINOL: (1,1'-bi-2-naphthol)
Boc: *tert*-butyloxycarbonyl
BPA: BINOL derived phosphoric acid
Cbz: benzyl chloroformate
CPBA: Chloroperoxybenzoic acid
DCM: Dichloromethane
DIAD: Diisopropyl azodicarboxylate
DIPEA: Diisopropylethylamine
DMAP: 4-Dimethylaminopyridine
DMF: Dimethylformamide
DSC: N,N'-Disuccinimidyl carbonate
***ee*:** Enantiomeric excess
h: Hour
HBA: Hydrogen bond acceptor
HBD: Hydrogen bond donor
HDA: Hetero Diels Alder
HPLC: High performance liquid chromatograpy
HRMS: High resolution mass spectrometry
IBCF: Isobutyl chloroformate
IPDA: Isophorone diamine
Leu: Leucine
MBH: Morita Baylis Hillman
min: Minute
Ms: Methanesulfonyl
Naph: -Naphthyl
NCS: N-chlorosuccinimide
NMM: N-methyl morpholine
NMR: Nuclear magnetic resonance spectroscopy
Nu: Nucleophile
RT: Room temperature
Su: Succinimide
TADDOL: (α,α,α',α'-tetraaryl-1,3-dioxolane-4,5-dimethanol
TEA: Triethylamine
TFA: Trifluoroacetic acid
THF: Tetrahydrofuran
Thr: Threonine
TLC: Thin-layer chromatography
Tle: *tert*-Leucine
Val: Valine

Contents

Chapter 1

Chirality and the tools to access it

I.1- On chirality and its importance

From the day we open our eyes and until we close them, we have always been able to notice asymmetry. Our hands and feet, while similar, are never the exact same. Given a mirror, our left hand reflects an image onto which, only our right hand can be superposed. And it is precisely from this observation of the hand that the term *chirality* (χέρι, or "hand" in Greek) would originate. Life, as well as many things surrounding us in the observable universe is based on this asymmetry, from our right-handed DNA helix, to the naturally occurring L-amino acids to the pattern that can be seen on ammonoidea, chirality is intrinsic to our existence.[1]

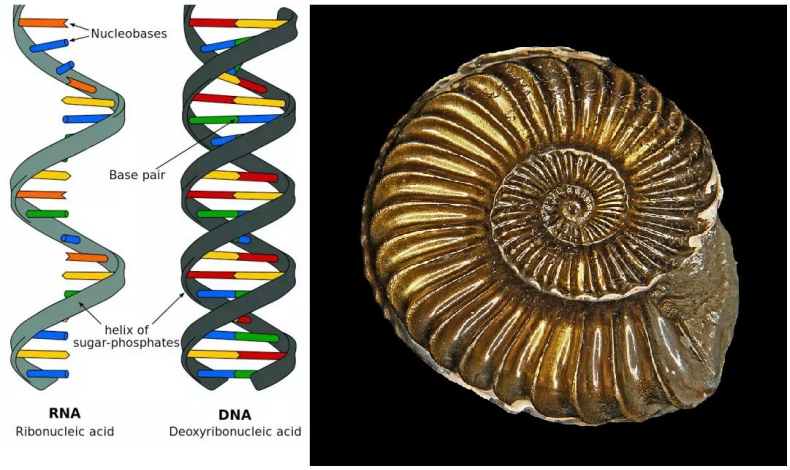

Figure 1.1 RNA and DNA helices (left) and ammonoidea fossil (right)

While chirality is a naturally occurring phenomenon, it has been a subject of interest as our capabilities in all scientific fields has advanced. Accompanying these advancements, our need to better understand and control asymmetry has also dramatically risen notably in organic synthesis[2] and pharmaceutical research[3], without forgetting the enthusiasm of total synthesis chemists for challenging and increasingly complex natural substances[4]. A search for the keyword "asymmetry" in the context of chemistry shows the importance that this subject has had in the last century as can be seen in **Fig 1.2**.

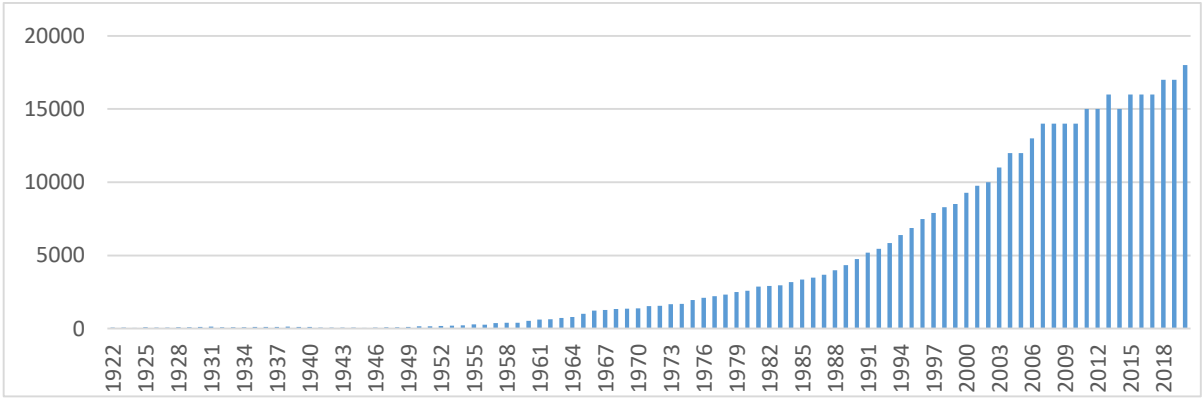

Figure 1.2 Publications containing "asymmetry" in the last 100 years (data from scifinder.org)

As the number of publications on the subject of asymmetry has virtually exploded in the last decades, our ways of accessing these asymmetric molecules has also evolved in order to respond to the increased complexity that modern scientific community demands.

While the original discoveries and research on chirality at the molecular level has been performed on simpler compounds found in nature, such as the different crystal structure of tartaric acids discovered by Louis Pasteur. Nowadays, new tools have become unavoidable in order to access specific species and chemical synthesis has had to adapt its tools to accommodate the structural challenges presented by the newer substances of interest. Modern asymmetric syntheses of chiral compounds mostly employ three main strategies:

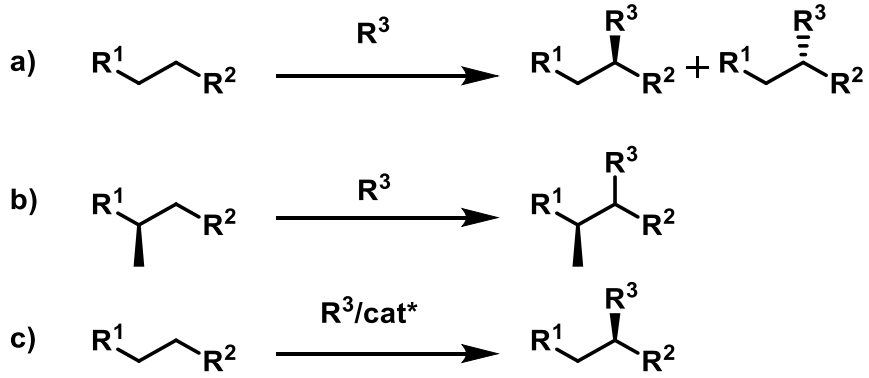

Scheme 1.1 *Various methods to access asymmetric molecules*

- Non-stereoselective synthesis, resulting in the obtention of multiple isomers, followed by separation or transformation of the unwanted compound to keep the target enantiomerically pure molecule[5] **(Scheme 1.1 a)**. This method is largely applicable as it is often easier to synthesise a racemic mixture than products with the very high enantiomeric purity required both academically and industrially. However the main drawback stems from the separation which can prove challenging[6], and the inherent loss of half of the employed mass.
- Using readily available chiral molecules **(Scheme 1.1 b)**. Mostly coming from the natural chiral pool, optically pure starting materials are used as reactants in various reactions leading to enantiopure products as a consequence[7]. The objective of these methods consists of taking an existing stereogenic center and employ it in the target compound, either directly by not modifying said center or by using it to create a new and controlled center elsewhere. This approach has the advantage of saving cost on expensive starting materials as usual chiral pool building blocks are rather inexpensive as well as not necessitating asymmetric catalysis. It does however require to examine the reaction mechanism in order to ensure that the chiral information is not lost along the synthesis, as well as being strongly reliant on the availability of the starting materials in entantiomerically pure form.
- Stereoselective synthesis **(Scheme 1.1 c)**. In this case, a stereogenic center is created *de novo* during the reaction. This method relies on three different strategies: the usage of chiral reagents or of chiral auxiliaries, both of which can present limitations to their

application, and the usage of asymmetric catalysis to create a new chiral center on the product molecule. Both transition-metal catalysed[8] and organocatalysed[9] reactions are widely reported in literature as the field of asymmetric catalysis has seen very high interest during the last decades, as demonstrated by the important amount of Nobel Prizes awarded in the field (2001, W. Knowles, R. Noyori, B. Sharpless; 2005, Y. Chauvin, R.H. Grubbs, R.R. Schrock; 2018, F.H. Arnold, G.P. Smith, G.P. Winter; 2021, B. List, D.W.C. MacMillan).

I.2 Catalysis for asymmetric synthesis

While there are multiple ways of controlling reactivity, the field of catalysis in particular plays a big role in modern synthetic chemistry. Both the transition metal catalysis and organocatalysis branches enjoy a very important academic and industrial success as they each offer respectively exclusive benefits. Although neither field is deemed "more important" than the other, an analytical summary of the whole field is beyond the scope of this body of work and the focus will be restrained to the field of organocatalysis and more particularly the sub-category of hydrogen bond catalysis.

Enzymes represent the most famous example of catalysts in nature. Found in all living beings, they were first identified by French chemist Anselme Payen in 1833[10] and only 130 years had their structure resolved by x-ray crystallography[11] due to their complexity **(Fig 1.3)**.

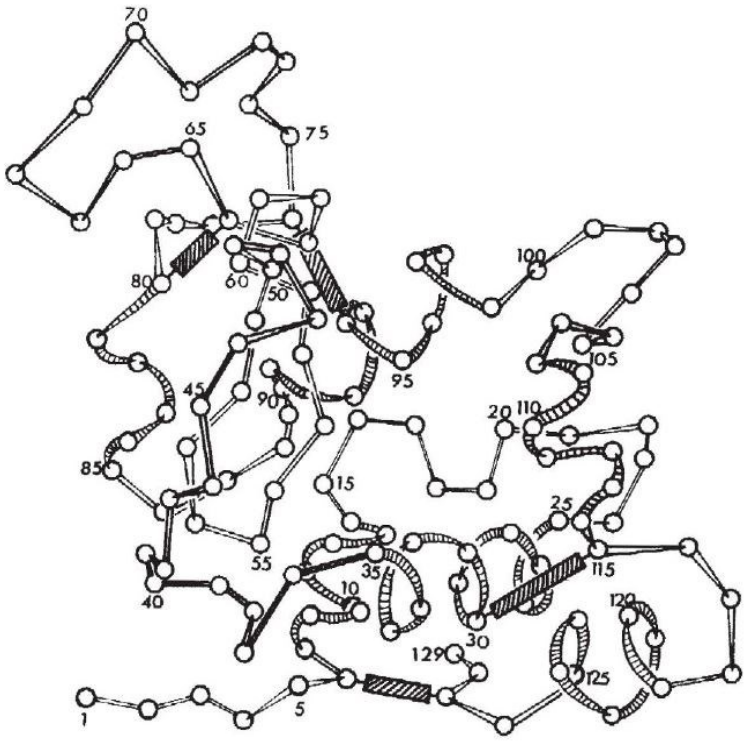

Figure 1.3 *Main chain conformation of Lysozyme*[11]

While they play numerous roles in organisms, some enzymes are known to play a catalyst role for certain reactions such as aldolase in the breakdown of 1,6-biphosphate. As a result of years of evolutionary optimisations, they show extremely high chemo-, regio- and often stereoselectivities thanks to their highly structured nature and because the reactions they catalyse take place in physiological media, they present tremendous activity under very mild reaction conditions.

The high selectivity properties are, however, also a barrier to general application in research or industrial-scale synthesis. Their high molecular weight and high substrate and reaction specificity explain why examples of enzyme use remain rare in literature, although *de novo* design and directed evolution approaches have caused accelerated improvements in the field.

As a result, in order to answer the challenges of modern synthesis, chemists have turned to the use of smaller molecules as organocatalysts. Compounds such as proline were shown to be able to catalyse the aldol addition reaction in an analogous way to enzymes **(Fig 1.4)** by Hajos and Parrish in the 1970s[12] and later by B. List *et al.*[13] The use of smaller structures with comparable selectivities but without the high specificity issue comes with very relevant advantages such as the easy availability or cheap accessibility of small organocatalysts, the possibility to use both enantiomers, the ease of separation from the product and even the reuse of the catalysts. The extreme usefulness of this method of catalysis was recognized by the attribution of the 2021 Nobel Prize of chemistry to B. List for his work on enamine mediated catalysis and D. MacMillan for his imminium ion mediated catalysis.

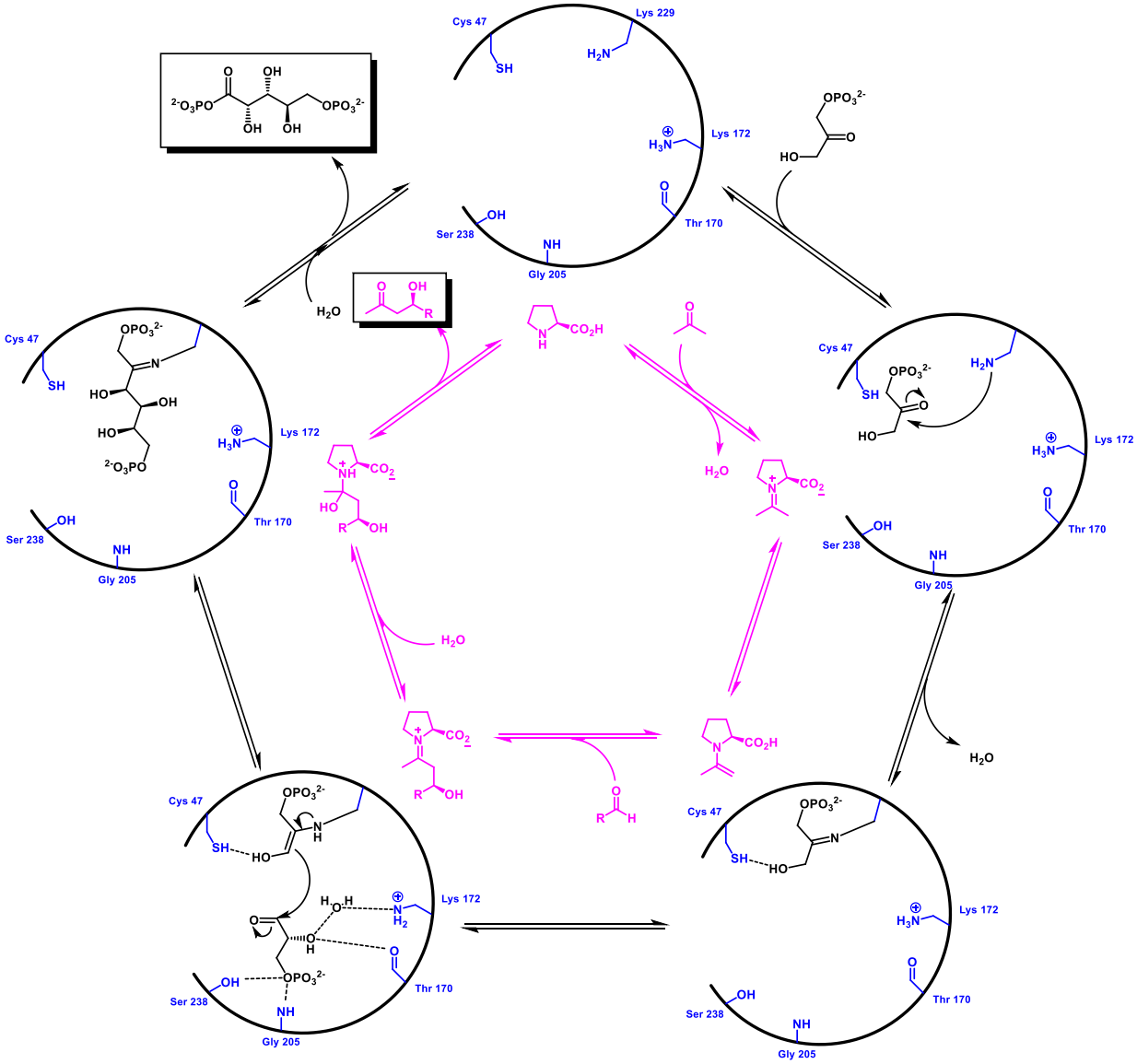

Figure 1.4 *Simplified enzyme/proline catalysed aldol reaction*[14]

One important aspect of enzymatic catalysis that has been of particular interest in the field of modern organocatalysis has been the role played by the hydrogen bond.

A/ The hydrogen bond: powerful tool for catalysis.

The hydrogen bond (H-bond) is a phenomenon that has generated considerable interest among the scientific community for years.[15] It is an interaction with an electrostatic character between an acceptor atom or group referred to as hydrogen bond acceptor (HBA) and a hydrogen containing donor group referred to as hydrogen bond donor (HBD). Although the strength of this interaction varies **(Table 1.1)** depending on the nature of the HBD and HBA respectively, the hydrogen bond is longer than covalent bonds (in ice: O-H distance 0.97Å; O- - - -H distance 1.79Å) and as a result is also weaker (50-100kcal/mol for covalent bonds; 1-40kcal/mol for H-bonds).

	Strong	Moderate	Weak
Type of bonding	**Mostly covalent**	**Mostly electrostatic**	**Electrostatic**
Length of H-bond (Å)	1.2–1.5	1.5–2.2	2.2–3.2
Bond angles (°)	175–180	130–180	90–150
Bond energy (kcal/mol)	14–40	4–15	<4

***Table 1.1** H-bond properties[16]*

The concept of weaker noncovalent bonds, in the case of catalysis, is an incredible boon as it allows for reversible temporary interactions between the potential catalyst and the reaction partners. As such, it is important to differentiate between two different types of catalysis: hydrogen-bond catalysis and Brønsted-acid catalysis. Whereas H-bond catalysis consists of temporary activation of the target molecule without changing its valency, Brønsted-acid catalysis results from the transfer of the proton from the HBD to the HBA and therefore, the formation of an ion pair. **(Fig 1.5)**

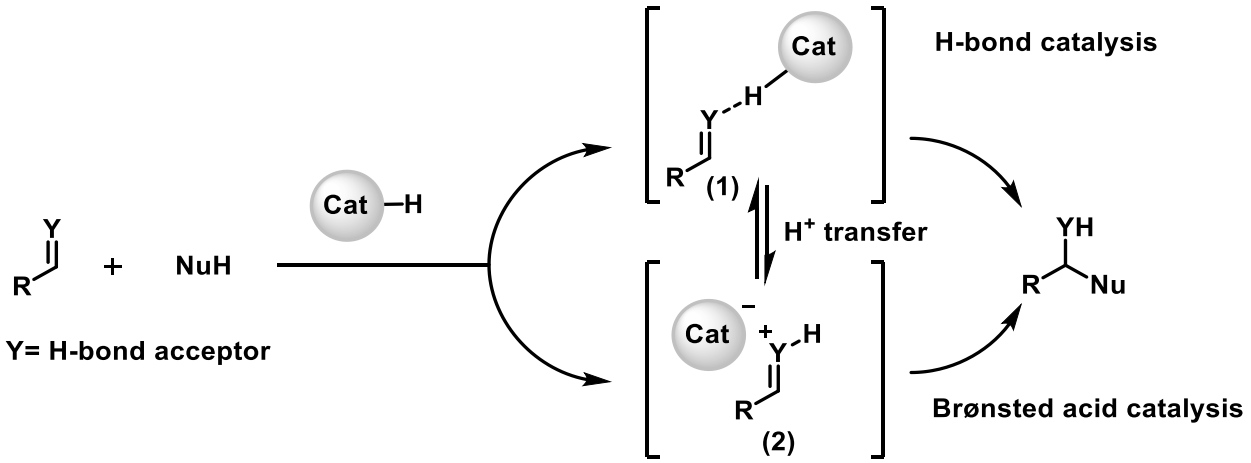

***Figure 1.5** H-bond & Brønsted-acid catalysis*

As the H-bonded intermediate **(1)** is in an equilibrium with the ion pair **(2)**, differentiating between H-bond and Brønsted-acid catalysis is not always straightforward. While more acidic catalysts such as phosphoric

acids will tend to favour the Brønsted-acid catalysis way, for instance, in reactions involving imines[17], weakly acidic species such as thioureas or squaramides are most often considered as hydrogen bond catalysts.

B/ Hydrogen bond catalysts.

Whereas the phenomenon of hydrogen bonding has been known for a century[18], its use in catalysis, such as the promotion of the Diels-Alder reaction by the solvent[19], is a much younger concept. Selected examples of the development of this field will be presented herein in an attempt to better understand its place in the current field.

- *TADDOL and BINOL derivatives: O-H-----X catalysis.*

Alcohols, and especially diols have represented a well-studied family of compounds for organocatalysis[20] and asymmetric synthesis. Among this large family of compounds, two stand out particularly: TADDOL (α,α,α',α'-tetraaryl-1,3-dioxolane-4,5-dimethanol) and BINOL (1,1'-bi-2-naphthol) **(Fig. 1.6)** derivatives have demonstrated their usefulness both as catalysts[21] as well as chiral resolving agents.[22]

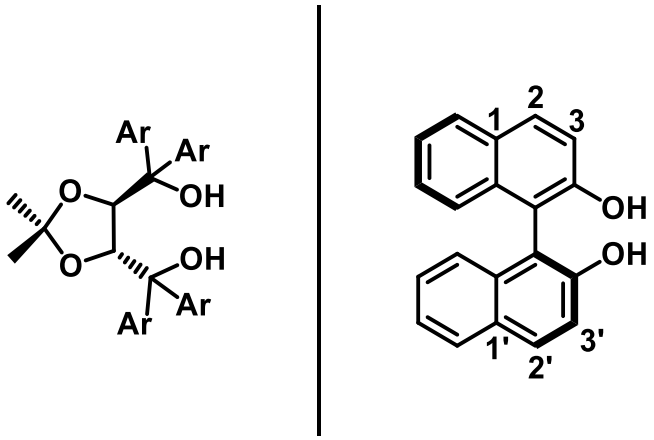

Figure 1.6 *General structure of TADDOL and (S)-BINOL*

The discovery that the addition of certain phenols accelerated phosphine-catalysed Baylis-Hillman reactions[23] opened the door to an important development of a new class of catalysts. BINOL derivative catalysis has enjoyed success in the field of organocatalysis with the works of Schaus *et al.* reporting on the Morita-Baylis-Hillman (MBH) reaction mediated by BINOL derivative diols[24] or Sasai & co. extending the reaction to an aza-MBH under a Lewis base containing bifunctional BINOL catalyst.[25]

After reporting that H-bonding solvents appeared to be catalysing some hetero Diels-Alder (HDA) reactions[26,19], Rawal *et al* investigated the application of BINOL-like 1,1'-biaryl-2,2'-dimethanol (BAMOL) scaffolds to the same type of reactivity.[27] The presented results showed that this family of catalysts greatly accelerated the cycloadditions of aromatic and aliphatic aldehydes to activated dienes, as well as providing good to excellent enantioselectivities **(Scheme 1.2)**

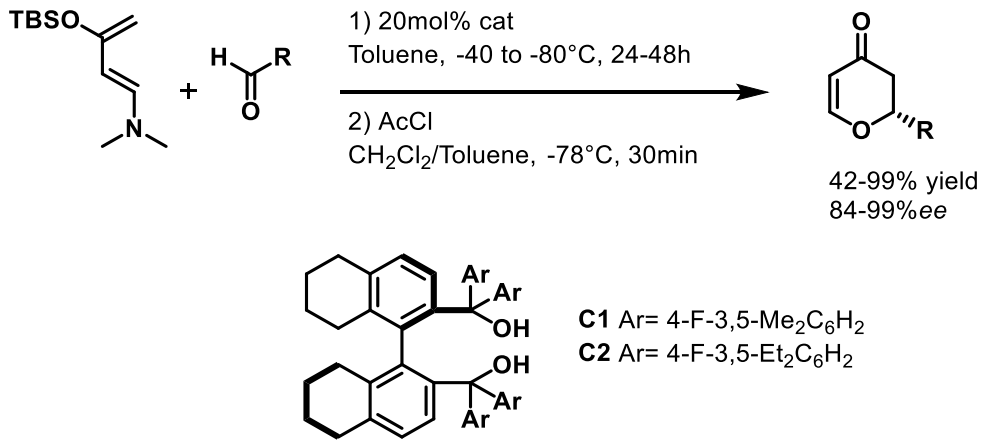

Scheme 1.2 *BAMOL catalysed Hetero Diels-Alder reaction*

While they do not strictly act as H-bond donating catalysts, chiral phosphoric acids have been employed in reactions where they have more of a H-bonding character than a Brønsted acid one. While this character differentiation can be difficult to discern, the importance of this branch of catalysis deserves to be mentioned in the general context of BINOL and H-bonding catalysis. BINOL derived phosphoric acid catalysed (BPA) aza-ene type reactivity between aldehydes and enecarbamates was reported by Terada *et al.*[28] whereby the catalyst activates the carbonyl group of the electrophile **(Fig. 1.7)**. The authors point out that, unlike in previous imine activation cases with this family of catalysts, simple substituents in positions 3-3' give excellent results and that bulk in *ortho* and *para* positions of the aromatic substituents severely degrade yields and enantioselectivities.

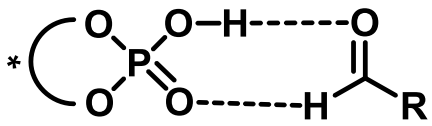

Figure 1.7 *Phosphoric acid carbonyl activation*

Building on their previous work, the Akiyama group described the enantioselective alkylation of indoles with nitroalkenes mediated by BPAs.[29] The reaction was shown to tolerate a large panel of nitroalkenes with high *ee*s as well as being able to be conducted at gram scale without loss of yield or enantioselectivity. Methylation of the indole –NH led to the expected severe decrease of the reaction yield as well as giving the product as a racemate. The authors postulate that the catalyst plays a bifunctional role and activates both reaction partners **(Fig. 1.8)**

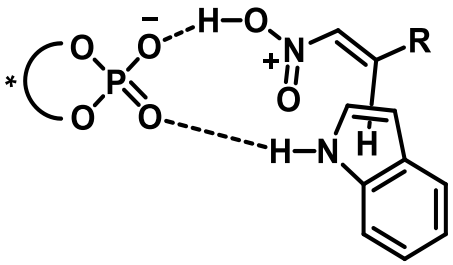

Figure 1.8 *Proposed dual activation transition state*

Nevertheless, it is not the only family of interest: catalysts incorporating the TADDOL motif have also met considerable success.

The Diels-Alder reaction is a reaction that has had tremendous impact in the field of organic chemistry and has been extensively studied. From an asymmetric synthesis side, the reaction has been reported with

chiral starting materials[30] and under organometallic asymmetric catalysis[31] while MacMillan *et al.* have also described organocatalysed Diels-Alder with chiral amines[32] and H-bonding.[33]
In 2004, Rawal's group reported a TADDOL derivative H-bond catalysed Diels-Alder reaction between acrolein dienophiles and aminosiloxydienes.[34] While the reaction displayed slightly lower enantioselectivities than usually expected in literature and presented scope limitations, it was one of the first examples of the application of H-bond catalysis to this reaction with useful *ee*s. The reaction mechanism was not elucidated, however the authors proposed a three-point activation of the carbonyl system: an intramolecular H-bond between the two diols which activates the remaining hydroxyl group by rendering it more acidic, activation of the carbonyl group through H-bonding to the oxygen, lowering the lowest unoccupied molecular orbital, and interaction between the carbonyl double bond and the aromatic groups of the catalyst. **(Scheme 1.3)**

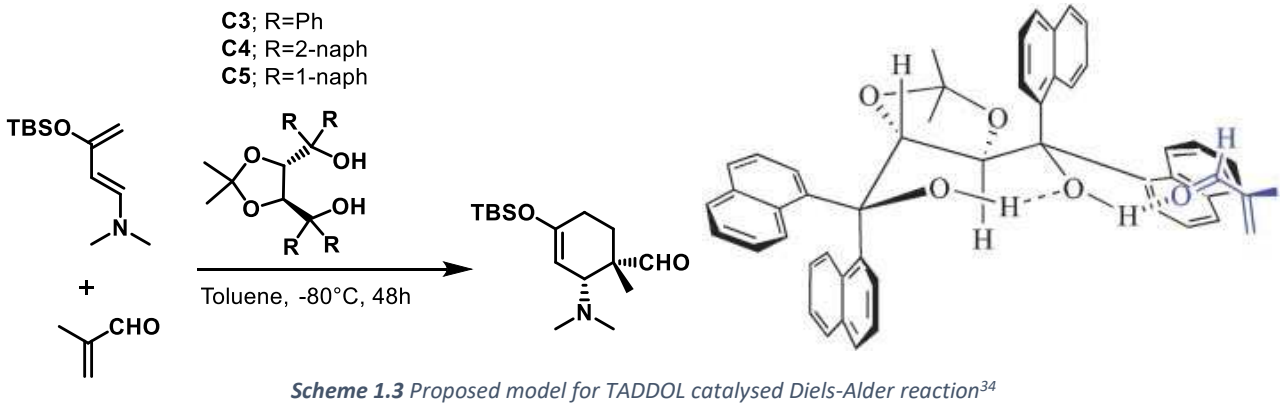

Scheme 1.3 *Proposed model for TADDOL catalysed Diels-Alder reaction[34]*

A year later, the Yamamoto group described a TADDOL-catalysed nitroso aldol reaction.[35] While this type of reactivity had been reported using chiral enamines[36] and with proline catalysts[37], this work constituted the first Brønsted acid catalysed nitroso aldol using achiral enamines. The authors showed that depending on the nature of the catalyst, the reaction provided two distinct pathways: using TADDOL, the reaction proceeded to give the N-nitroso aldol exclusively whereas using an aryl-glycolic acid led to the O-nitroso aldol **(Scheme 1.4)**. The authors proposed that the protonation of the nitrogen atom followed by nucleophilic attack on the oxygen atom would lead to the O-product while the H-bonding interaction of the catalyst with the oxygen atom lead to an activated nitroso intermediate which provided the N-product after nucleophilic attack.

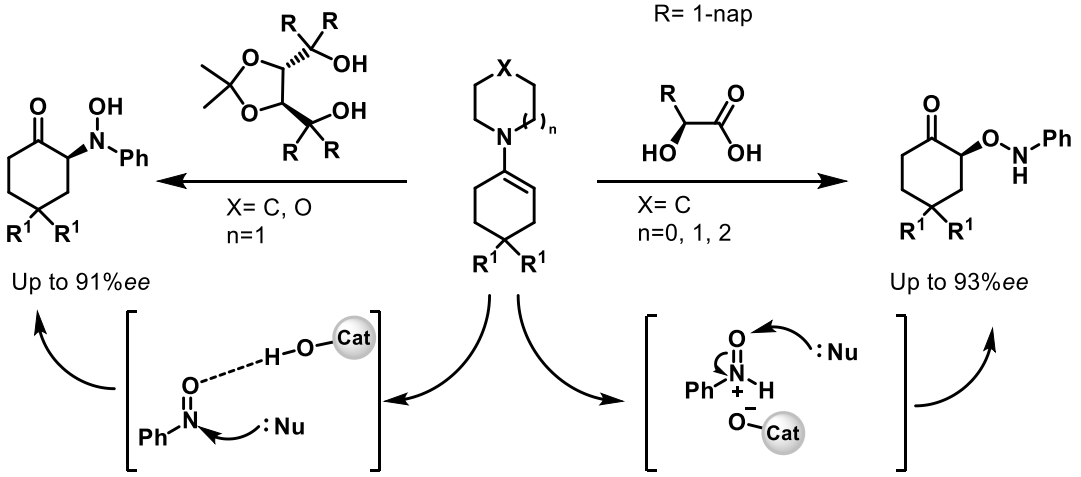

Scheme 1.4 *Brønsted acid and H-bond catalysed nitroso aldol reaction*

- *(Thio)Ureas, Squaramides and peptides: N-H-----X catalysis.*

While diols have shown their capabilities as H-bonding catalysts, a second motif has attracted the attention of researchers with an interest in H-bond organocatalysis. Ureas and thioureas are known to interact with various charged and neutral species[38]. The (thio)urea motif presents the interesting properties of two –NH groups playing a bidentate H-bond donor role as well as the (thio)carbonyl group potentially playing a H-bond acceptor role. Schreiner *et al.* have reported the use of an achiral thiourea promoting various reactions through H-bonding[39] and since then, even more reactions involving Schreiner's thiourea have been described[40]

In 1998, Jacobsen's group presented pioneering results while studying the Strecker reaction[41]. A catalyst structure optimisation study was carried out by screening libraries of both solid-state and soluble catalysts. From the results of the optimisation study, a general structure yielded the best result **(Fig 1.9)**. The combination of an amino acid moiety with a chiral diamine motif and capped with a salicylimine Schiff base gave the best selectivities among the three screened libraries with 80%*ee* when grafted on a solid-state support and 91%*ee* in solution.

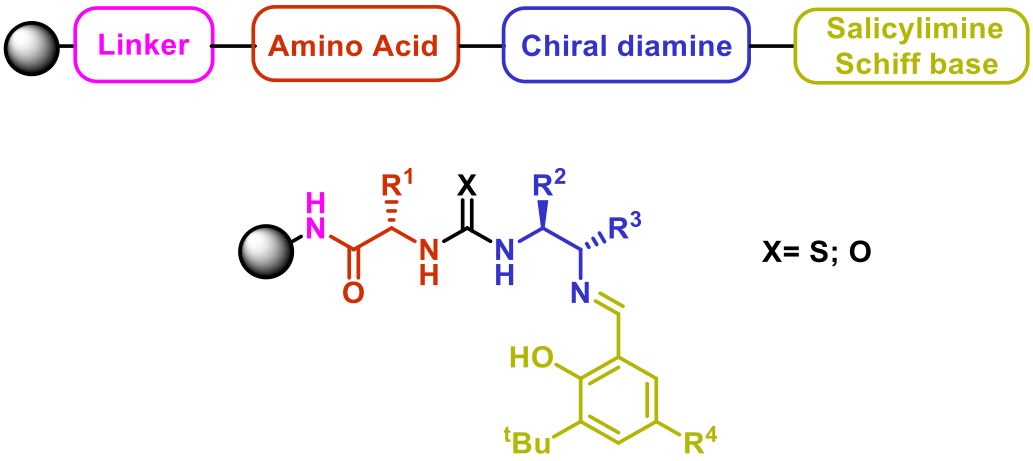

Figure 1.9 *Strecker reaction general optimized catalyst structure*

The group underlined that the bulk of the substituents (R^1) at the amino-acid moiety played a key role in the stereoselectivity of the Strecker reaction with a 40% reduction of *ee* between *tert*-leucine (Tle) and threonine (Thr). The substituent at position 3 of the salicylimine aryl group and the nature of the diamine motif, although not as crucial as the amino acid side chain, also had a great impact on the enantiomeric control of the reaction.
With the optimization study done, the scope of the reaction was probed[42]: catalyst **C6** proved effective at loadings as low as 2 mol% at -78°C and the reaction was found to tolerate both aryl- and alkyl-imines with good yields and high enantioselectivities **(Scheme 1.5)**. The reaction was tested with the catalyst in solution as well as grafted on solid-support and while enantioselectivity was lowered by small amounts (1-2%), yields were higher thanks to the easier purification process.

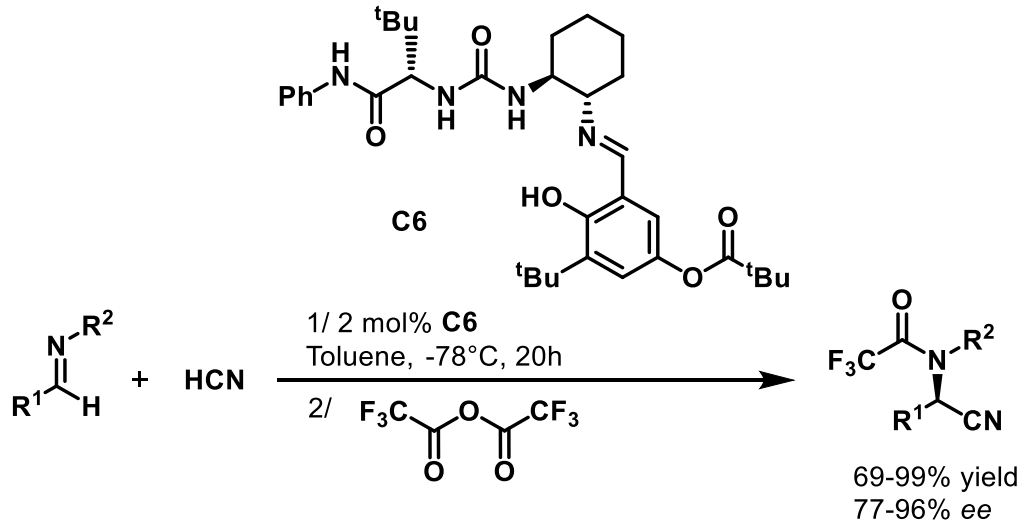

Scheme 1.5 *Optimised urea catalysed Strecker reaction scheme*

After reporting of an achiral thiourea catalysed TMSCN and silyl ketene acetal nucleophilic additions to nitrones and aldehydes[43] , the Takemoto group took an interest to the Michael reaction and the application of thiourea catalysis. The same year, the group described a thiourea catalysed enantioselective addition of malonates to nitro-olefins.[44]

The group took an interest in the nitro functionality under the hypothesis that unlike previously described imines, aldehydes or nitrones, these substrates possess two oxygen atoms that could therefore interact with the bidentate thiourea motif of the catalyst. While this approach may be considered as "classic", the most important part of this work was the addition of a secondary basic motif in the form of a tertiary amine to activate the nucleophile and thus, to obtain a catalyst with two functions, spaced by a chiral linker interacting synergistically to activate both partners. **(Fig 1.10)**

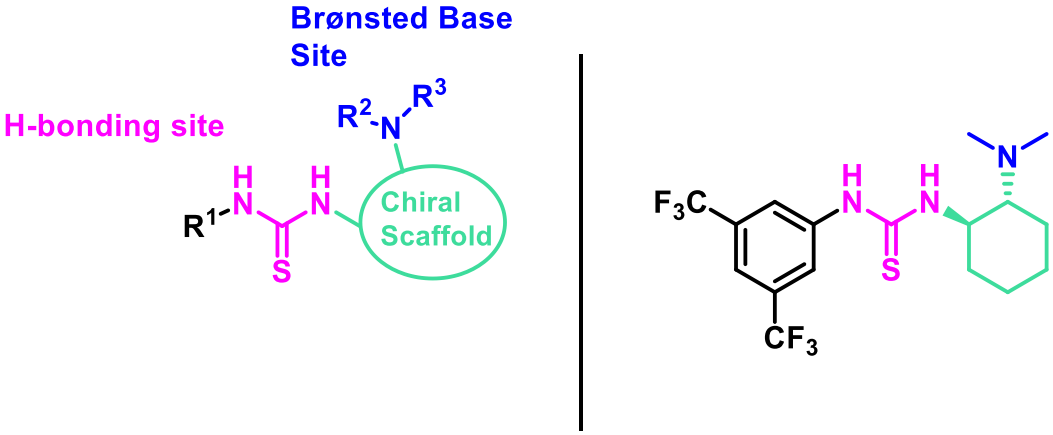

Figure 1.10 *Takemoto's bifunctional catalyst*

An important point underlined by the authors was that in the presence of only one of the two functions, the reaction took place (although with a much lower yield) with no stereoselectivity **(Fig 1.11, entries 1 & 2)** and that even with a mixture of a simple thiourea catalyst and triethylamine, only moderate yields were obtained **(Fig 1.11, entry 3)**. Therefore, it was concluded that the two functions taking part in this catalysis had to be present in the same structure in order to provide any asymmetric induction and useful yields.

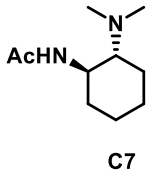

C7

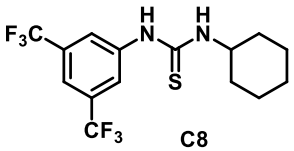

C8

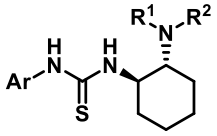

C9; Ar= 3,5-$(CF_3)_2C_6H_3$, R^1, R^2= *o*-$(CH_2)_2C_6H_4$
C10; Ar= 3,5-$(CF_3)_2C_6H_3$, R^1=Me, R^2= ^{i}Pr
C11; Ar=Ph, R^1, R^2= Me

entry	additive	time (h)	% yield[b]	% ee[c,d]
1	TEA	24	17	–
2	**C7**	24	14	35
3	TEA+**C8**	24	57	–
4	**C9**	48	29	91
5	**C10**	48	76	87
6	**C11**	48	58	80

Figure 1.11 *Bifunctional catalysis optimisation*[44]

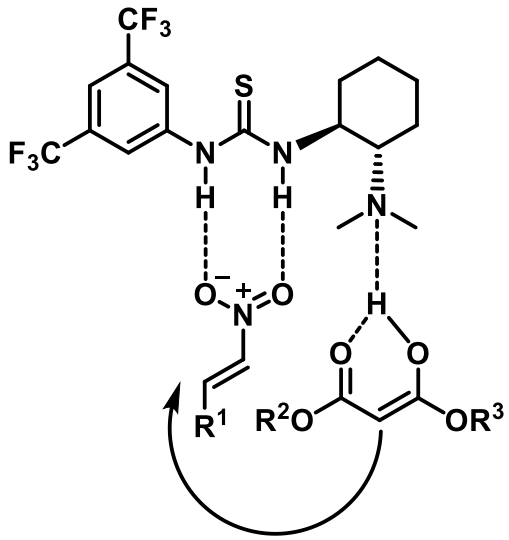

Figure 1.12 *Bifunctional catalyst double activation*

This first account of a bifunctional catalyst by Takemoto thus demonstrated the Michael addition of malonates to both aryl- and alkyl-substituted nitro-olefins with excellent yields and *ee*s under fairly mild conditions through a double activation mechanism as proposed by the authors. **(Fig. 1.12)**

This work proved to be quintessential to the field of organocatalysis and more specifically H-bond catalysis as variations of Takemoto's catalyst have been used to develop enantioselective transformations such as Morita-Baylis-Hilman(MBH)[45], Alkylation of Indoles[46] or Nitroaldol[47] reactions among many other.

Almost a decade after Takemoto's first bifunctional catalyst description, the Palomo group developed a new family of catalysts[48] following the report by Schreiner indicating that (thio)urea catalysts with a bis-3,5-(trifluoromethyl)phenyl group functioned better compared to those differently capped thanks to a secondary interaction by the *ortho* –CH of the aromatic ring[49].

By adding a peptide-like *gem* diamino- moiety, the group envisioned that this new class of catalysts would be highly tunable for different reactions owing to: (*i*) a third –NH for more potential interaction while mimicking the *ortho*-CH secondary interaction that was previously mentioned[50], (*ii*) the introduction of a new stereocenter in close proximity of all –NH the interaction sites and (*iii*) the Brønsted base motif being kept to maintain the bifunctional nature of the catalyst.

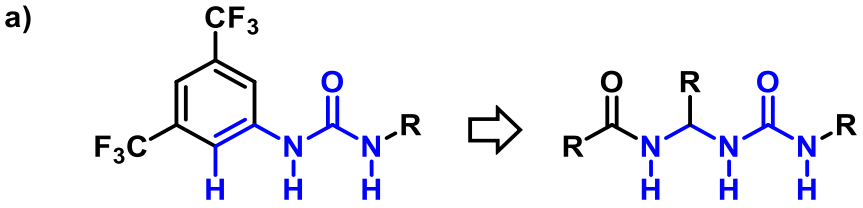

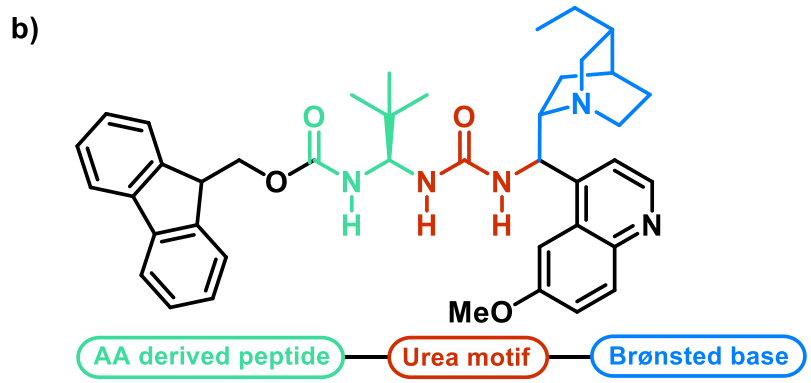

Figure 1.13 *Palomo group's ureidopeptide bifunctional catalyst architecture*

The group has subsequently described the stereoselective: synthesis of tertiary thiols by thiazolone addition to nitro-olefins[51] **(Fig 1.14, a)**, formation of β-aminonitriles from (arylsulfonyl)acetonitriles and Boc-protected imines[48] **(Fig 1.14, b)** and the aldol reaction of α-keto imides[52] **(Fig 1.14, c)**, all promoted by bifunctional ureidopeptide catalysts.

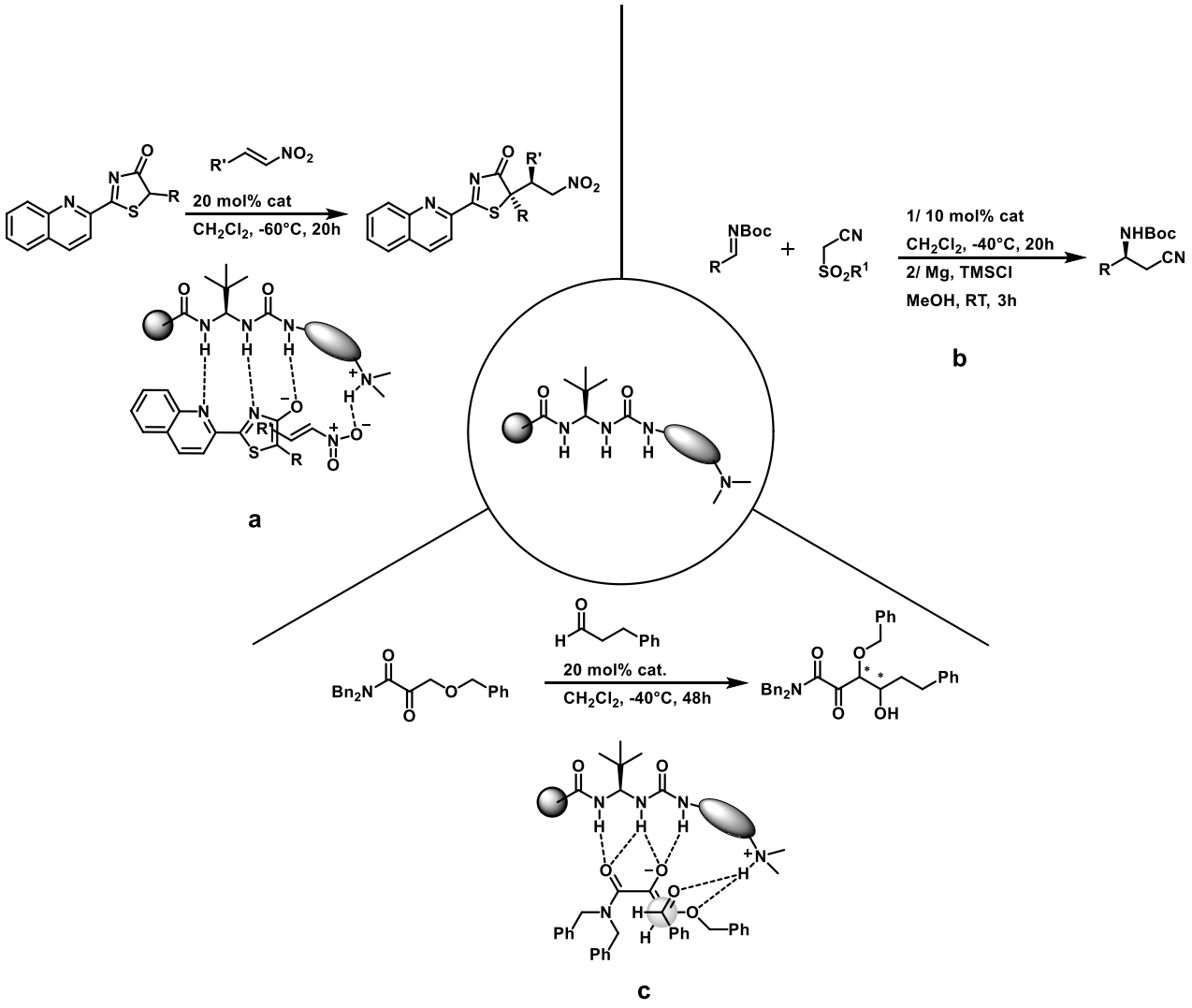

Figure 1.14 *Palomo group's bifunctional ureidopeptide mediated transformations*

As interest in H-bonding catalysis grew and different catalyst structures were developed, urea and thiourea motifs have appeared in an important part of the described transformations, although other functions have also been studied. Squaramides, much like ureas and thioureas are good H-bond donor candidates that bring interesting features for catalysis such as a more rigid structure, a pseudo-aromatic configuration leading to an enhanced N-H acidity as well a change of both the separation of the –NH groups and geometry of the H-bonds they establish.[53] **(Fig 1.15)**

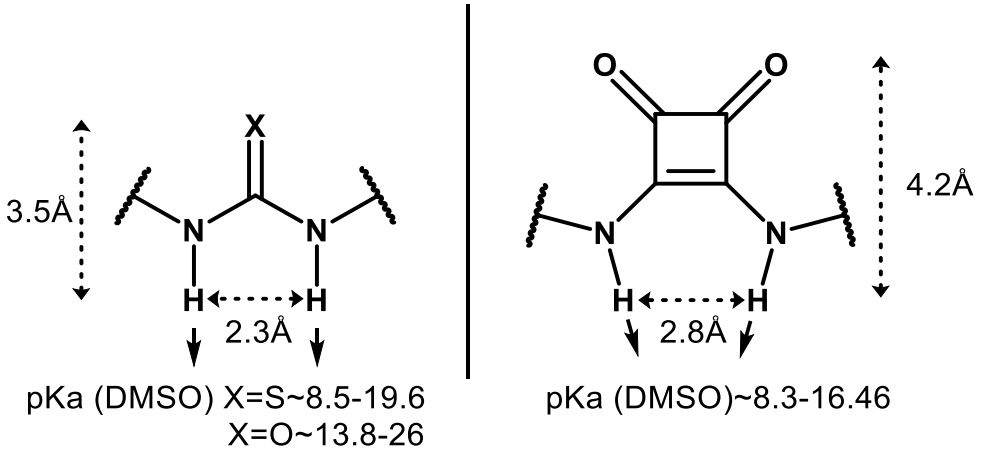

Figure 1.15 *(Thio)Urea and squaramide H-bond differences*[54]

The Michael reaction between dicarbonyl compounds and nitroalkenes being a good test candidate to study new H-bond catalysts, Rawal *et al* reported the first attempt at the asymmetric Michael addition catalysed by squaramide derivatives.[55] Under optimized conditions, the group obtained excellent yields and enantioselectivities with catalyst loadings as low as 0.1 mol% under mild conditions. **(Scheme 1.6)**

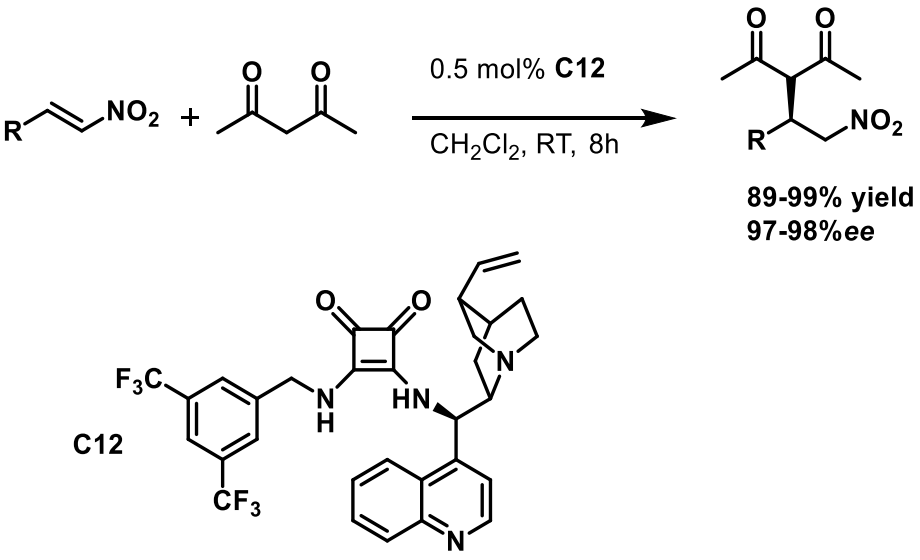

Scheme 1.6 *Squaramide derivative catalysed Michael reaction*

After the admirable results obtained by Rawal's group using catalysts that incorporate a squaramide motif, this class of catalyst attracted the attention of other groups. Dai and co-workers described a Michael-type

addition of thiols to activated alkenes with a squaramide derived H-bond catalyst **(Scheme 1.7)**.[56] This type of reactivity has previously been reported with different acceptors (such as nitro-olefins, enones or carboxylic acid derivatives) or with chalcones although with low yields[57] or low enantioselectivities.[58] The reported results indicate excellent catalyst activity under mild conditions and with good substrate tolerances again, thus corroborating the usefulness of the squaramide motif in H-bond catalysis.

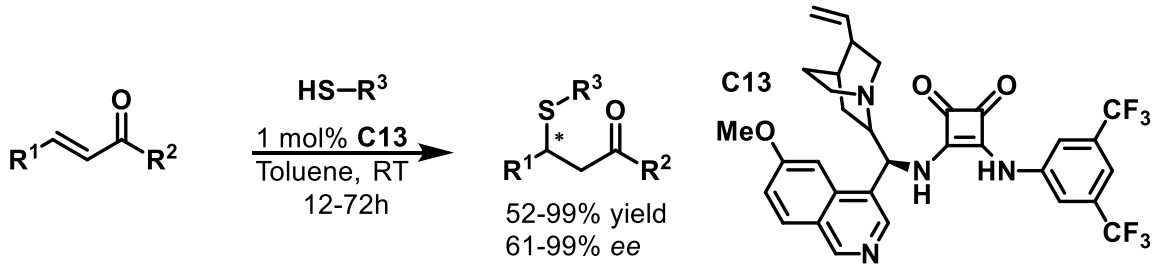

Scheme 1.7 *Squaramide catalysed Michael-type thiol addition*

Although squaramide catalysts proved to provide outstanding results in Michael-type reactions, it has since then been successfully employed in other reactions. Rawal *et al* demonstrated that although the structure had to be specifically tuned in order to obtain any sort of enantioselectivity, this class of catalysts was able to promote the Friedel-Crafts alkylation of indoles with imines.[59] **(Fig 1.16 a)** The same group demonstrated that the same catalyst family, owing to its modularity enabled the α-hydrazination of dicarbonyl compounds.[60] **(Fig 1.16 b)** The Palomo group also contributed to this field of catalysts by employing the squaramide motif instead of the ureidopeptide it had developed. The group reported that, using squaramide catalyst **C17 (Fig 1.16 c)** instead of the previously described ureidopeptides, the Mannich reaction between α-keto imides and imines proceeded with a 92%*ee* (against 30%).[61] More recently, the group described a Michael reaction between aryl acetaldehydes and nitro-olefins promoted by a hybrid bifunctional catalyst containing a squaramide motif as well as the additional peptidic motif that it had developed in its previous works.[62] **(Fig 1.16 d)**

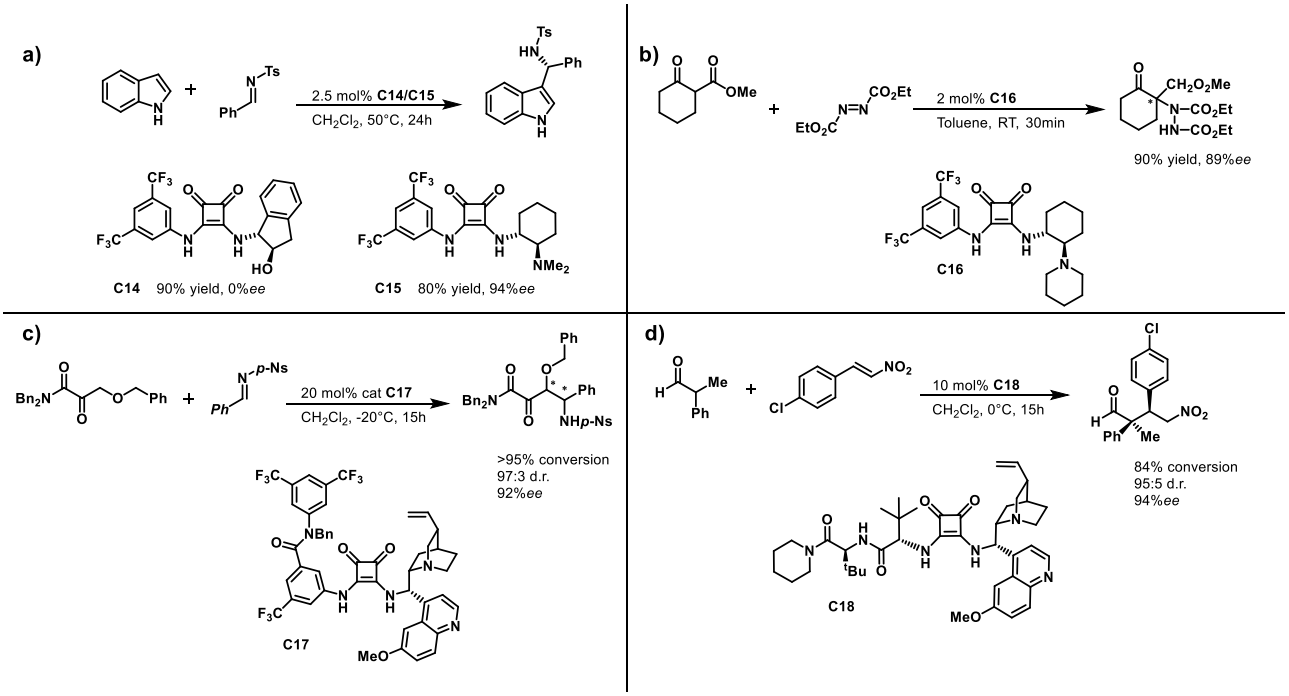

Figure 1.16 *Examples of squaramide catalysed transformations*

- *Bis-(thio)ureas: towards more complex catalyst architectures.*

While studying the application of (thio)urea H-bond donor catalysis to the Morita-Baylis-Hillman reaction, Nagasawa *et al* determined through NMR experiments that the simple achiral catalyst they used interacted with both the enone and aldehyde reaction partners at different stages of the reaction.[63] After obtaining mediocre yields and no selectivity with single H-bond donor catalysts **C19** and **C20 (Fig 1.17)**, the group thus had the idea of synthesising a new type of catalyst with two (thio)urea units to activate both partners in a controlled spatial conformation.

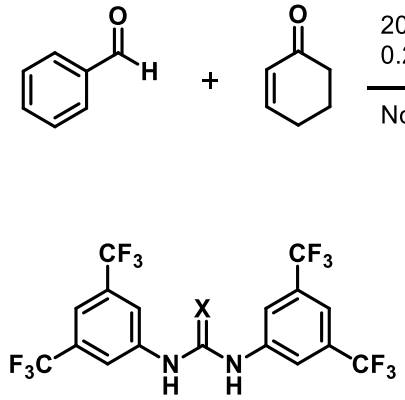

Entry	Catalyst	Yield (%)	Ee (%)
1	None	1	—
2	**C19**	52	—
3	**C20**	60	—
4	**C21**	72	33 (*R*)

Figure 1.17 *Catalyst screening for the MBH reaction*[63]

Much to their delight, bis-thiourea **C21** provided better catalytic activity and some enantioselectivity. Through optimisation of the reaction conditions, the authors concluded that the base also had an impact on both the yield and the selectivity that was observed. After determination of the major stereoisomer, the group proposed a reaction mechanism involving a transition state where both the aldehyde and enone are coordinated to the catalyst, therefore blocking the spatial conformation before the conjugated addition step **(Fig 1.18).**

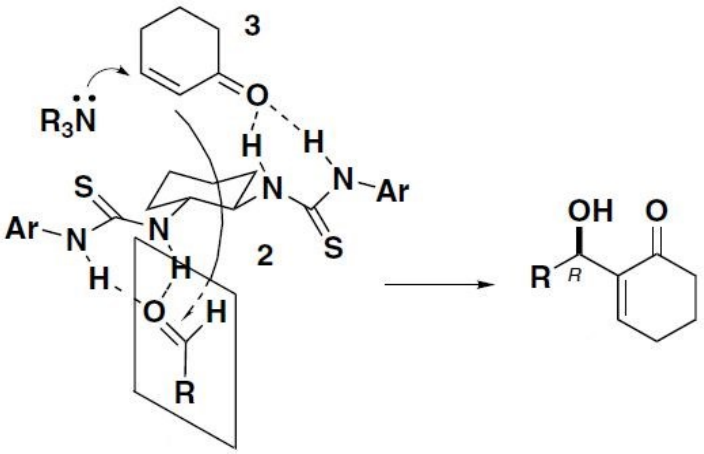

Figure 1.18 *Proposed transtion state for the bis-thiourea catalysed MBH reaction*[63]

Although this new class of catalysts improved the MBH reaction compared to previously described mono-(thio)urea catalysts, these first results that were reported by the Nagasawa group proved slightly disappointing with very variable yields and enantioselectivities ranging from moderate to excellent (33-99% yield and 19-90% *ee*). Two years after this initial report, Berkessel and collaborators attempted to improve upon the shortcomings of described the MBH reaction results.[64] The new catalysts were derived from isophorone diamine (IPDA) and the optimisation process led to the ideal conditions shown below **(Scheme 1.8)**

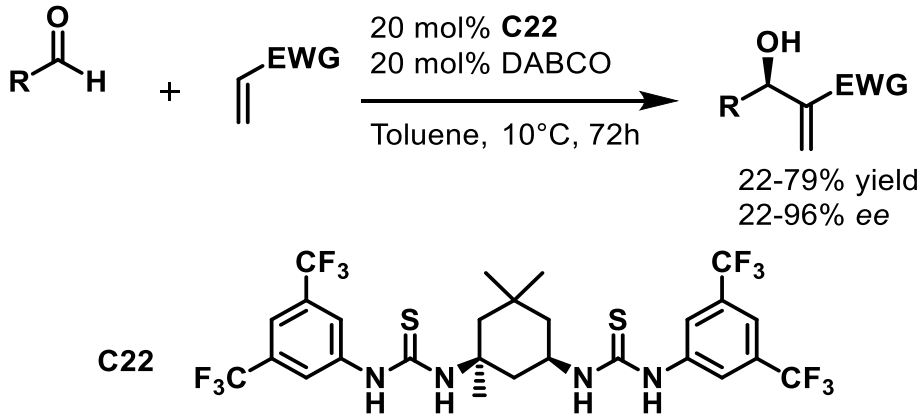

Scheme 1.8 *IPDA derived bis-thiourea catalysed MBH reaction*

Even with moderate success, the reports of bis-HBD catalysts by Nagasawa and Berkessel proved that this family of compounds had promising potential in the field of H-bond catalysis.

I.3 Foldamers and catalysis.

As discussed previously, enzymes are capable of exceptional reaction rate accelerations and stereochemical control often by the way of a set of noncovalent interactions leading to a locked conformations of the involved substrates within the active site. These properties have, in turn, made enzymes an important source of insight and inspiration in the development of new synthetic catalysts. Inspiration from what can be seen in nature leads to questioning how we can reproduce or reuse the tools found in living systems to recreate them or even to improve upon them. One field that has attempted to find a middle ground between the complex structures of complete enzymes and small molecule catalysts is that of foldamers. Defined by Gellman as "synthetic polymers with a strong tendency to adopt a specific compact conformation"[65], foldamers offer exclusive properties that can find a use in the design of new catalyst architectures.

Structures with a robust and fixed backbones can allow for a controlled organisation of the functional groups involved in catalysis. In the same way, these rigid structures provide an important platform to better control the transition states of reactions and their geometry for the development of asymmetric reactions.

A majority of the foldamers described in literature tend to adopt helical structures[66], whether from the use of strained residues forcing this conformation[67] or through self-organisation resulting from intramolecular H-bonding.[68] While the helical conformation is the most prevalent, the way to achieve such secondary structures can be quite varied. Structuration of oligomers backbones can be achieved through the use of constrained bond geometries or directing subunits among the foldamer **(Fig 1.19)**

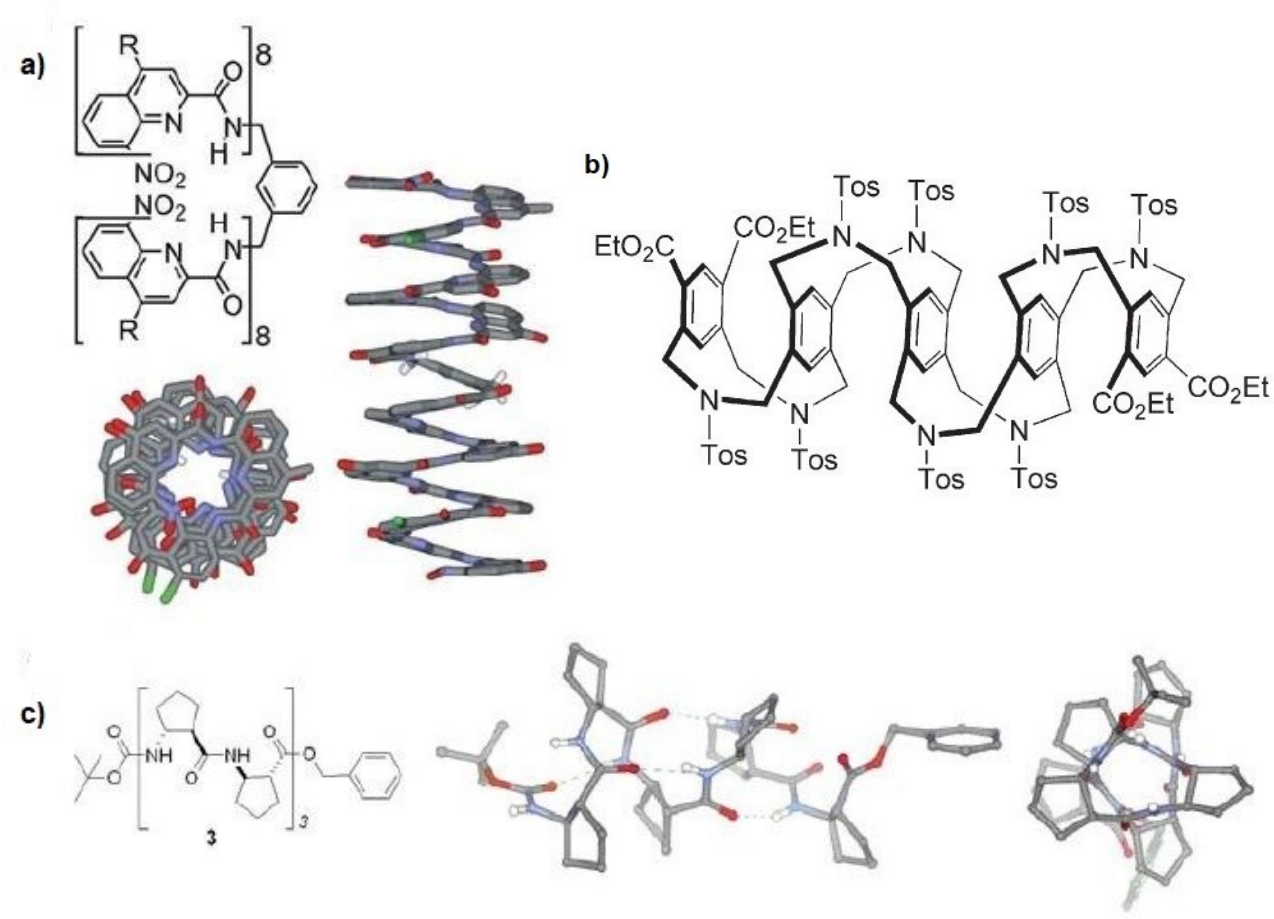

Figure 1.19 *Diverse foldamer designs: a) based on local conformation preferences, b) based on solvophobic effects, c) based on non-covalent intramolecular H-bonds* [66]

Compared to enzymes whose tertiary structures can be considered as a combination of various secondary structures often packed through the formation of a hydrophobic core resulting from the hydrophobic effect, these simpler and more readily tunable structures offer better predictability when considering their use as potential catalysts.

The Gellman group has taken a strong and long-standing interest in the development of new foldamers for various applications including catalysis. Following a report by Pihko *et al* showing that pyrrolidine activates both partners in the organocatalysed aldol reaction[69] the group has studied ring-constrained β-amino acid based helical foldamers in an effort to develop better catalytic systems[70]. While reported after some of the following examples, this work is presented out of chronological order as it elegantly combines enamine and iminium type catalysis although no stereoselectivity was offered by this initial system. Under the hypothesis that two properly spaced pyrrolidine moieties should lead to increased activity, a library of foldamer backbones containing the two catalytic functions (as pyrrolidine-based residues) were synthesised and tested. The screening of the 16 different structures showed the importance of minute control and easy tunability of the spatial and distance arrangement of the activity sites in larger catalysts as the best candidate was able to increase the acceleration rate of the reaction by a factor of 143. **(Fig 1.20)**

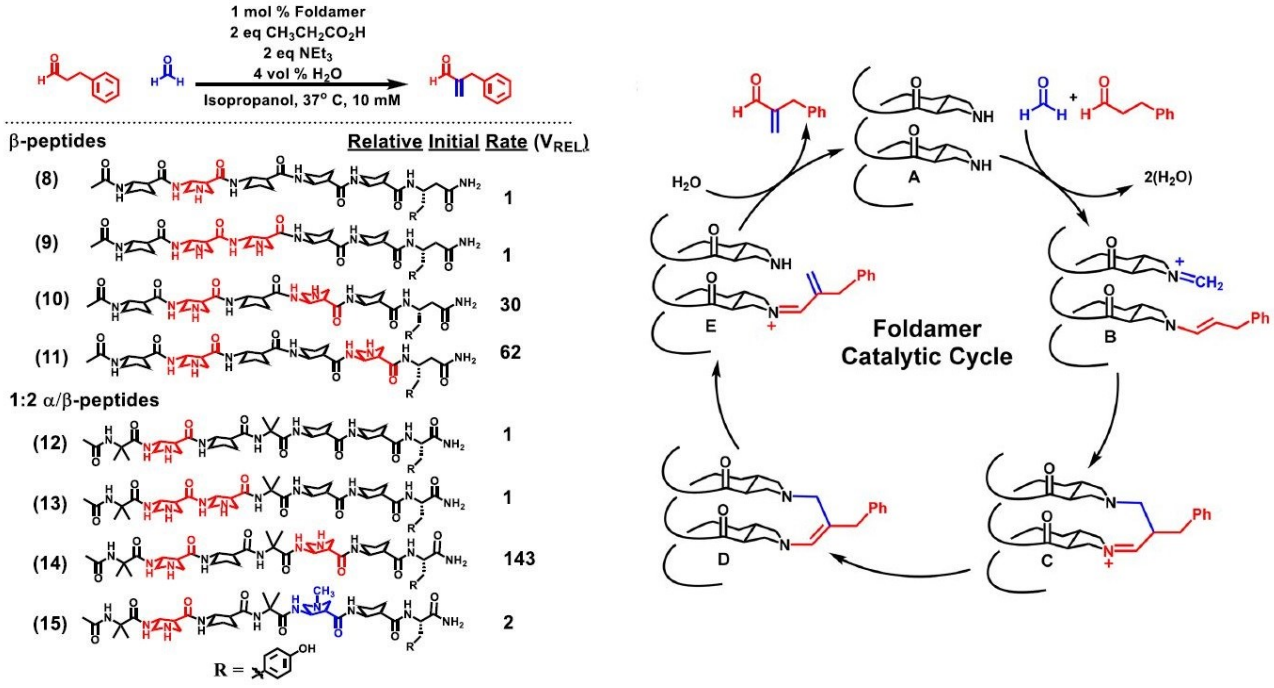

Figure 1.20 *α/β-Helical foldamers to catalyse aldol reactions*[71]

The reported works indicate that foldamers provide an interesting platform with easy functionalisation and most importantly the ability to easily predict and tune the spacing and geometry of the catalytic sites. These properties, modulated by optimisation of the reaction conditions, would allow for new catalysts that show increased activity and stereoselectivity while being sufficiently modifiable to avoid the disadvantages presented by enzymatic catalysis.

While foldamer catalysis is still young, the reported examples prove that it as a field rife[71] with opportunity as foldamers represent an important platform towards more difficult challenges awaiting the domain of catalysis.

Proline and derivatives have been shown to catalyse aldol and aldol-like reactions.[72] While good activities and selectivities have been obtained, large catalyst loadings often proved necessary and more so in cases of

low activity substrates. These complications are hard to address on small catalysts such as Proline due to the limited tunability of these compounds. In 2005, the Wennemers group screened a library of 3375 tripeptide catalyst combinations to determine an optimal structure for the aldol reaction.[73] The study resulted in two promising sequences **C29** and **C30** as shown below **(Fig 1.21)**

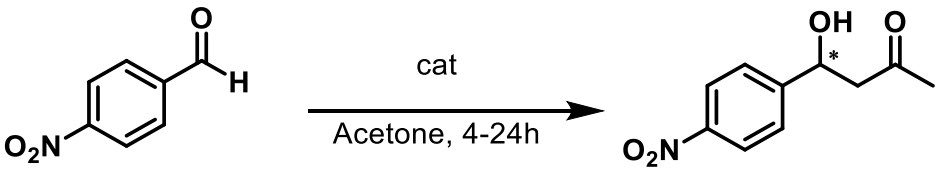

C29= H-^{L}Pro-^{D}Ala-^{D}Asp-NH_2 **C30**= H-^{L}Pro-^{L}Pro-^{L}Asp-NH_2

entry	catalyst	mol %	temp (°C)	yield (%)	ee (%)	abs conf
1	**C29**	10	rt	73	70	*R*
2	**C29**	10	−20	53	81	*R*
3[c]	**C30**	1	rt	99	80	*S*
4	**C30**	5	−20	98	90	*S*
5[d]	proline	30	rt	68	76	*R*
6	proline	30	−20	30	71	*R*

Figure 1.21 *Tripeptide catalysed aldol reaction*[73]

The group reported that catalyst **C30** is highly active with loadings as low as 1 mol% leading to 99% conversion in 4h at ambient temperature. It was also noted that while catalyst **C29** showed lesser activity, it allowed access to the opposite absolute configuration due to the change of turn direction in the overall conformation of the catalyst.

With organocatalysed Michael reactions having been described in literature (see previous examples), the group noted that compared to prolines, the amine and carboxylic group were approximately 3Å further apart in their tripeptide catalyst. Based on that observation, they decided to assess the applicability of these tripeptides in 1,4-additions of aldehydes to nitro-olefins.[74]

A process of optimisation and catalyst screening allowed for a highly active and selective catalyst structure to be determined. Additionally, a simple stereoisomer change on the tripeptide catalyst allowed access to the opposite absolute configuration, demonstrating one key advantage of this family of catalysts.

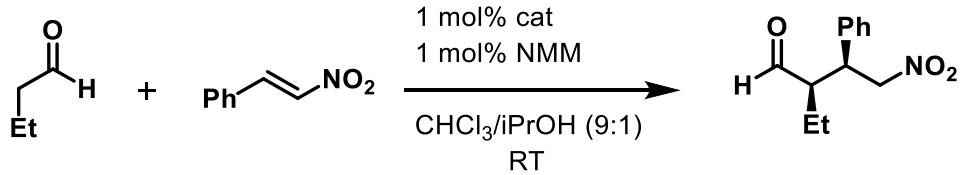

Proline **C30:** H-^{L}Pro-^{L}Pro-^{L}Asp-NH_2 **C31:** H-^{D}Pro-^{L}Pro-^{L}Asp-NH_2

Catalyst	t (h)	yield (%)	syn:anti	ee (%)	Abs. Conf.
Proline	24	85	8:1	39	(*R,S*)
C30	6	96	10:1	85	(*R,S*)
C31	12	93	25:1	95	(*S,R*)

Figure 1.22 *Tripeptide catalysed 1,4-Michael additions*

After their success with nitro-olefins as Michael acceptors, Wennemers *et al*, attempted to employ nitro ethylene to access mono-substituted γ^2-amino acids instead of their disubstituted counterparts.[75] Catalyst **C30**, which had successfully promoted aldehyde additions to nitro-olefins was engaged in the new reaction as a first attempt. While it provided promising results, replacing the ^{L}Asp unit with ^{L}Glu led to increased yields and selectivities. The reaction scope was explored with 10 aldehydes providing good to excellent enantioselectivity. **(Scheme 1.9)**

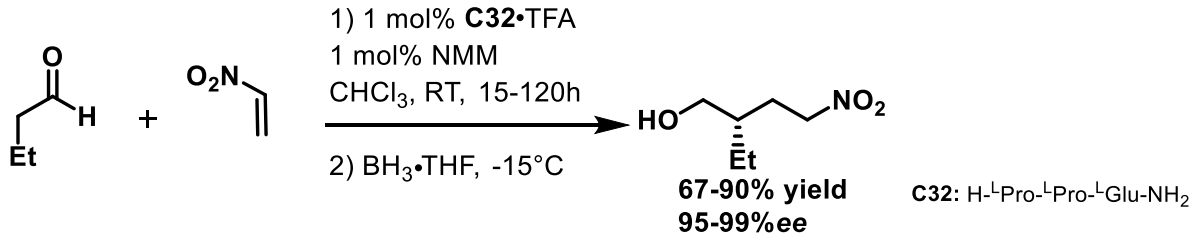

Scheme 1.9 *Tripeptide catalysed aldehyde addition to nitroethylene*

Kudo and co-workers have also used resin-supported peptidic catalysts to promote various in aqueous media reactions such as asymmetric transfer hydrogenations of unsaturated aldehydes[76], asymmetric α-oxyamination of aldehydes[77] or the Michael-type addition of nitromethane to α,β-unsaturated aldehydes[78] **(Fig 1.23)**. Throughout their studies, the group highlighted that the helical part of the catalyst (polyleucine or leucine-Aib moieties) plays an important role in the efficiency of the catalyst.

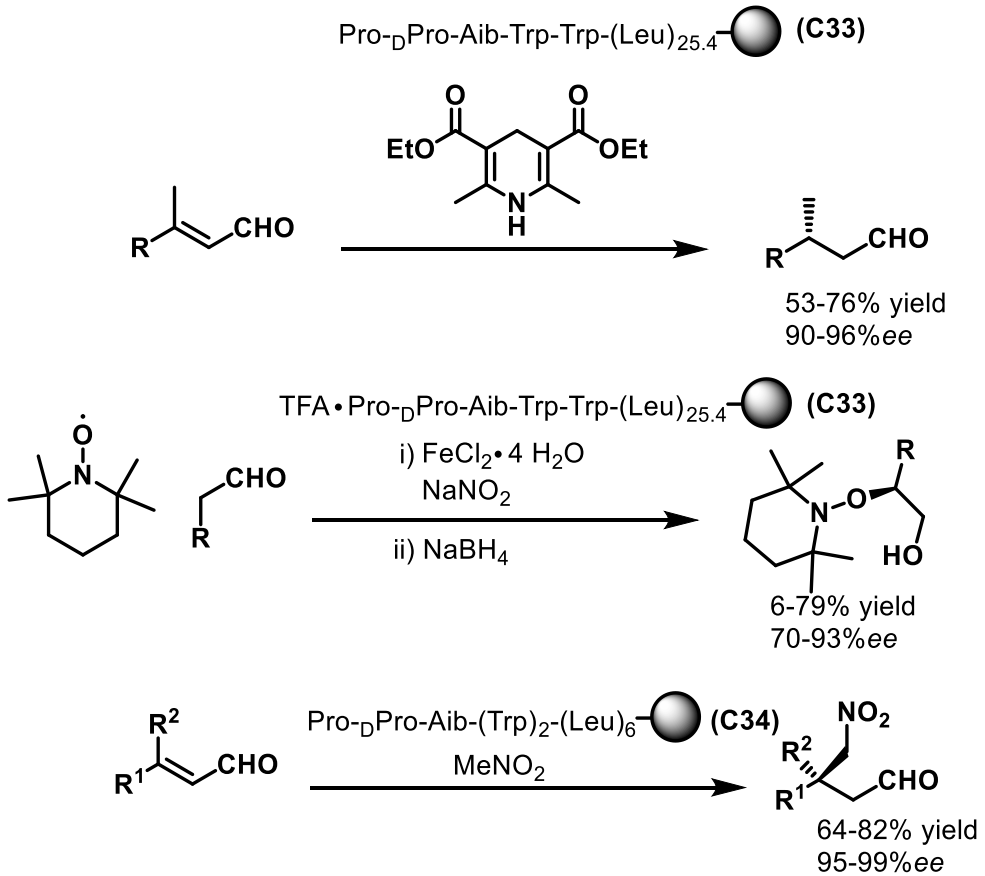

Figure 1.23 *Resin-supported peptide catalyst promoted transformations described by Kudo et al*

In 2013 the Maillard group described the synthesis of foldamers based on γ-amino acids containing a thiazole motif. [79] As part of their initial work, the conception of building blocks based on the thiazole ring allowed the team to synthesise oligomers that adopt a 3 residue per turn helical conformation. This well-defined structure is maintained through intramolecular H-bonds and the geometry and rigidity provided by the thiazole. The group attempted to probe the possibility of using this helical scaffold in the context of organocatalysis by introducing specific units with pyrrolidine side chains. [80] The Michael-type addition of cyclohexanone to nitrostyrenes was identified to be a good candidate for study **(Scheme 1.10)**.

Initial screening of the reaction with monomeric catalysts revealed a strong selectivity for the *syn* addition product but showed fairly low enantioselectivities. Moving to a trimeric catalyst reinforced the previously noted *syn*-selectivity as well as increasing the enantiomeric excess from 52% to 74%, thus demonstrating that the structuration brought by the helical backbone of the foldamer catalyst had an impact on the reaction.

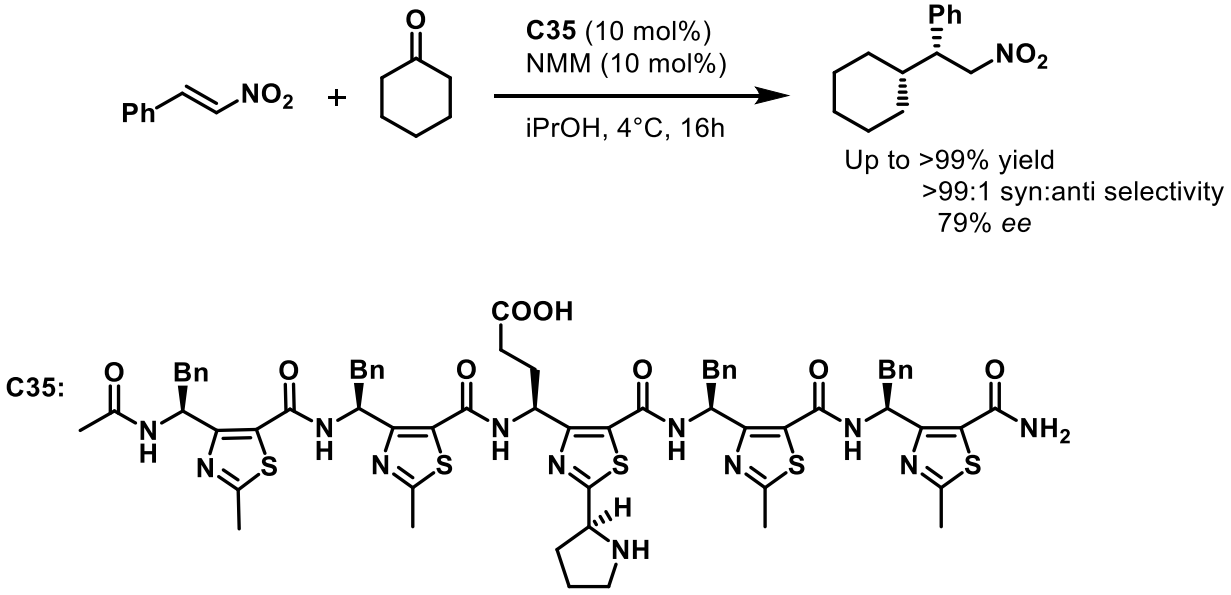

Scheme 1.10 *Thiazole-based foldamer catalysed Michael-type addition of cyclohexanone to nitrostyrenes*

Increasing the length of the foldamer led to only moderate enantioselectivity increase while shortening the carboxylic acid-bearing side chain lowered the yield by half. The team also studied the effect of said carboxylic acid-bearing side chain's position along the backbone of the pentameric foldamer however no major effect could be observed. Finally, introducing steric strain at the N-terminus of the catalyst greatly reduced the yield of the reaction with nitrostyrene and *p*-methylnitrostyrene but not with *p*-methoxynitrostyrene. This example once again shows the high capacity of foldamer catalysts to be tuned specifically for certain reactions and substrates.

Michaelis and co-workers have described the synthesis of a helically folded peptide-based catalyst allowing for controlled spatial arrangement of a catalytic site and a binding site.[81] **(Fig 1.24)** The 11-residue foldamer scaffold was declined in four variations. Bifunctional catalyst **C36** and monofunctional catalysts **C37** and **C38** respectively carrying the catalytic imidazolidinone side chain and H-bond donor binding sites all incorporating 2-aminoisobutyric acid (Aib) motif so as to form the well-defined helical structure while catalyst **C39** acted as the control catalyst by adopting a random coil conformation due to the replacement of Aib residues by two proline residues. All the synthesised catalysts were functionalised post-synthesis to graft the imidazolidinone and thiourea functions for catalysis.

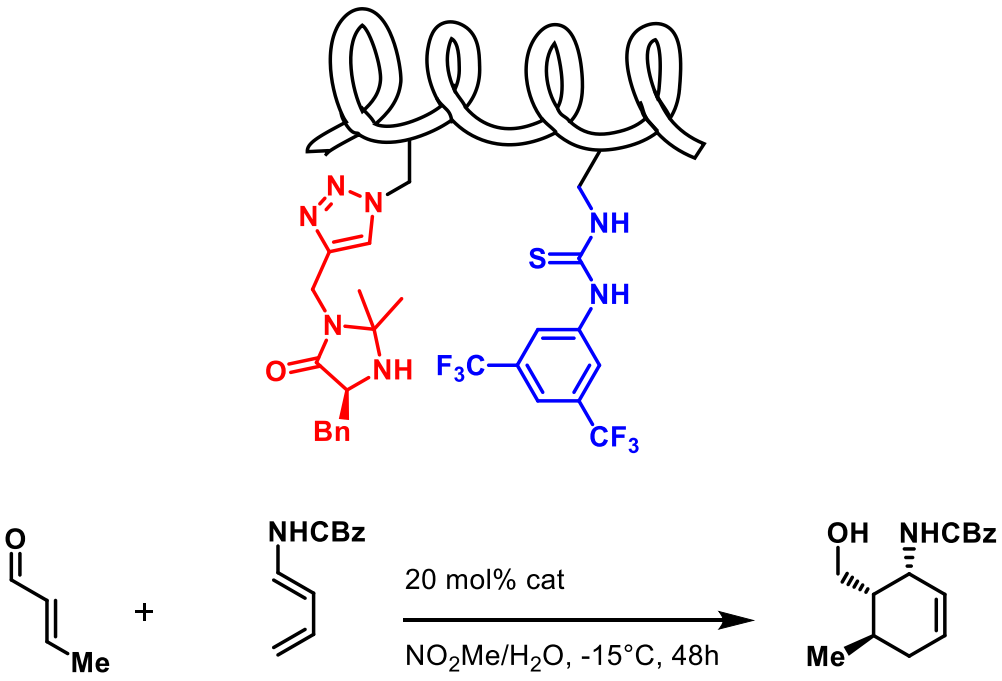

Catalyst	Conversion (%)
Uncatalysed	3.4
C36	88% (80%)[a]
C37	7.1
C37+C38	7.6
C39	- (2%)[a]

C36: AcNH-VXLBZVLBVAL-NHMe
C37: AcNH-VALBZVLBVAL-NHMe
C38: AcNH-VXLBAVLBVAL-NHMe
C39: AcNH-VXLPZVLPVAL-NHMe

X= Thiourea H-bond donor function.
Z= Imidazolidinone function. (catalytic site)
P: Proline
B: Aib
[a] reaction conducted at [diene]=10mM

Figure 1.24 *Helical α-peptides as bifunctional catalysts for Diels-Alder reactions*

Control reactions showed that the disruption of the helical conformation led to diminished catalytic activity (**C36** vs **C39**) and that the presence of both functions on the same molecule was primordial as their separation did not allow for good catalyst activity (**C37** + **C38**). However, although the catalyst **C36** accelerated the reaction by a factor of 10, it did not produce interesting enantioselectivities (30%*ee*).

The previously mentioned works have focused on catalysis through the foldamer side chains (e.g. pyrrolidine-based units or thiourea containing side chains), another method of using foldamer-based catalysts is through the main chain of the catalyst with the side chains being involved more in the stereochemical control of the reaction.

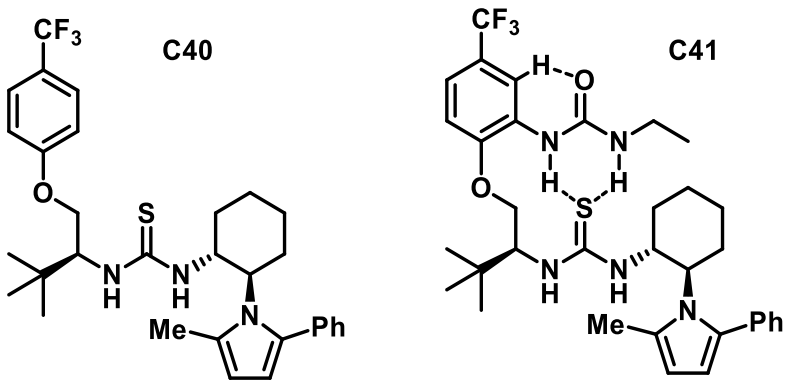

Figure 1.25 *Single urea catalyst* ***C38*** *and cooperative catalyst* ***C39*** *developed by Smith et al*

Smith and co-workers have provided an important source of inspiration with their work on bis-(thio)ureas as catalysts for Mannich type reactions.[82] In this cornerstone report, the group presented the benefits of well-defined folded architectures and activation of H-bond donating groups in catalyst architectures **(Fig 1.25)**. The study of simple thiourea catalyst **(C40)** and its comparison to **(C41)** demonstrated that the activation of the main thiourea unit by an intramolecular urea moiety can lead to higher catalytic activity and enantioselectivity **(Scheme 1.11)** These folded catalysts were further refined by the Pihko group and showed excellent results in enantioselective Mannich reactions between malonates/ β-ketoesters and both aliphatic and aromatic imines. [83]

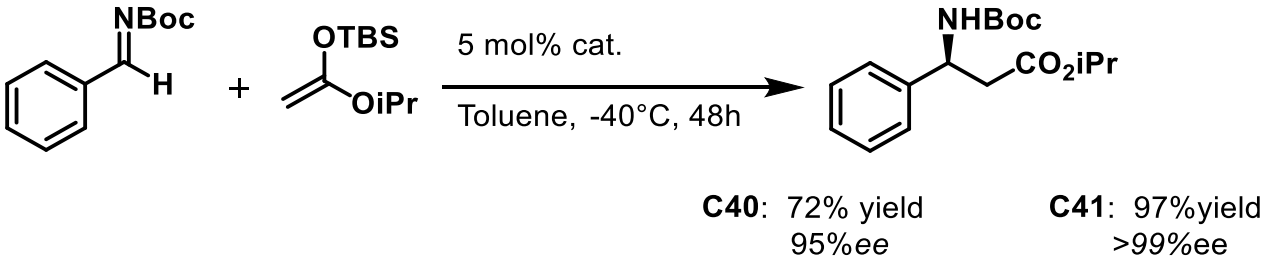

Scheme 1.11 *Mannich type reaction catalysed by an intramolecular H-bond activated catalyst*

The Clayden group demonstrated an elegant use of the foldamer structure by highlighting its ability to transmit stereochemical information between its two termini.[84] Starting from Aib homo-oligomers that adopt a 3_{10} helical conformation which can exist in both right- and left- screw-sense[85], the group elegantly demonstrated that a preferential screw-sense can be induced by addition of a chiral terminus. As the ligation of this terminal element leads to the organisation of the ultimate β-turn of the helix, one screw-sense is preferred over the other, thus leading to the desymmetrisation of the foldamer. The group proved this concept by adding a photoswitchable *C*-terminal –AlaBni (Bni= 5-bromo-7-nitroindoline) moiety to a bifunctional thiourea catalyst. Under normal conditions, addition of the unswitched catalyst **(C42)** to a mixture of dimethylmalonate and nitrostyrene lead to 84% yield with a 37:63 *er*. Irradiation in the presence of isopropylamine gives the *C*-terminal secondary amide, inducing a left-handed screw-sense to catalyst **(C43)** and leading to a 78% yield with a 77:23 *er.* **(Fig. 1.26)**

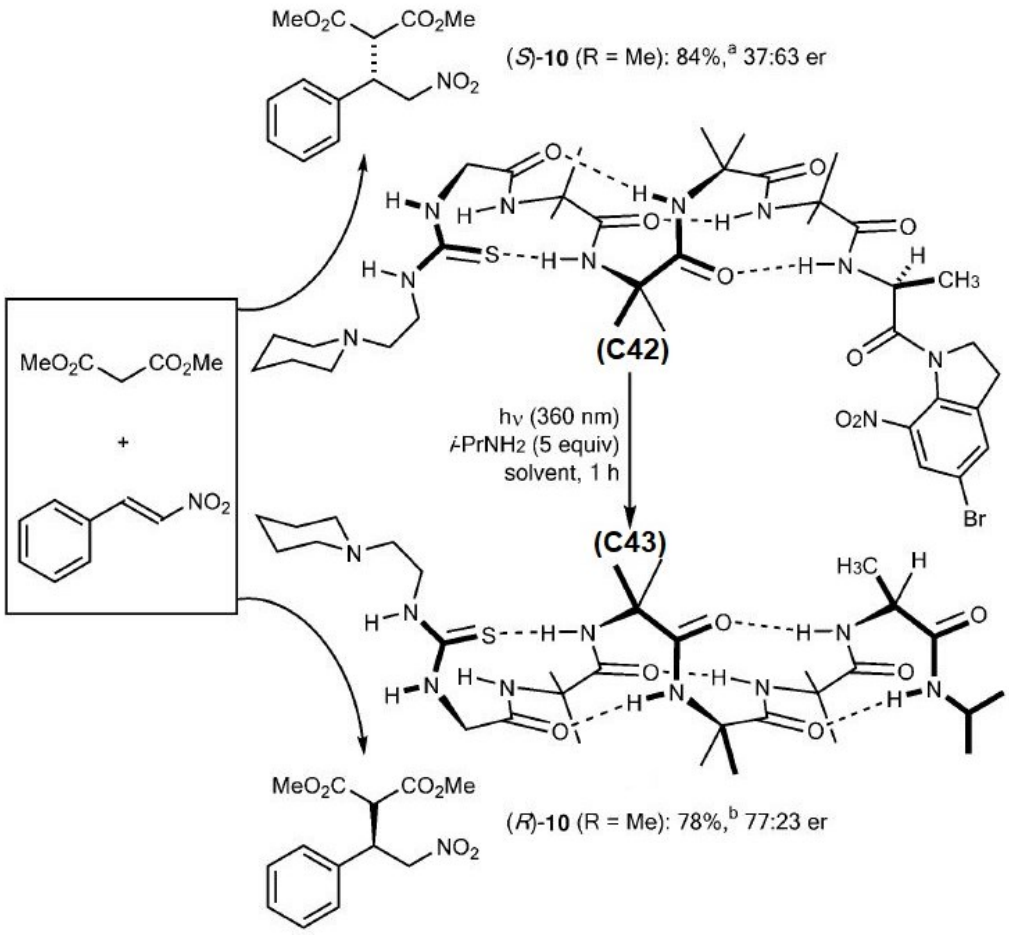

Figure 1.26 *Photoswitchable helical foldamer catalysis*

Building upon the work of Smith *et al*, the Guichard group has described amino acid derived urea-motif based foldamers that adopt a 2.5 residue per turn helix conformation.[68] This conformation is maintained by the formation of intramolecular H-bonds between the H-bond acceptor carbonyl and H-bond donor urea –NH groups at the [i+2] position. **(Fig 1.27)**

With the penultimate and ultimate ureas not being engaged in H-bonding, they are left free to bind potential target molecules or anions[86] and thus could be used as catalysts.

In cooperation with the Palomo group, the group investigated the catalytic activity of oligo-urea foldamers in the asymmetric addition of malonates to nitro-olefins.[87] Good to excellent reactivity with catalyst loadings as low as 0.01 mol% was observed. **(Scheme 1.12)** Increasing enantioselectivity was linked to the size growth of the foldamers with 5 or 6 residues

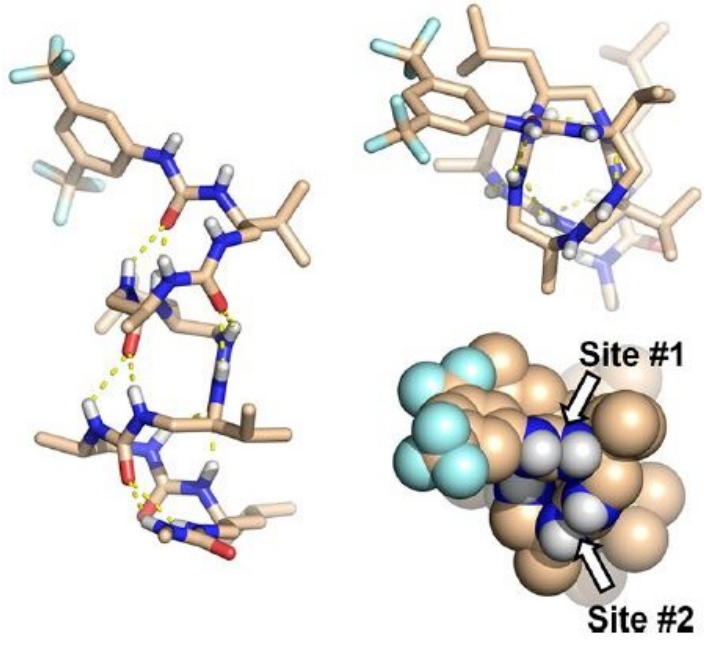

Figure 1.27 *X-Ray structure of the 6-residue oligourea foldamer catalyst* ***C44****, showing a well-defined helical conformation and accessible H-bond donor sites*[87]

representing the ideal length. While the exact rationalisation of the mechanism has not been given, the group points to the formation of the helix starting at 4 residues and the conformation being reinforced in the 5- and 6-residue catalysts leading to a better controlled spatial arrangement of the reaction partners during the transition state owing to better activated H-bonding urea motifs.

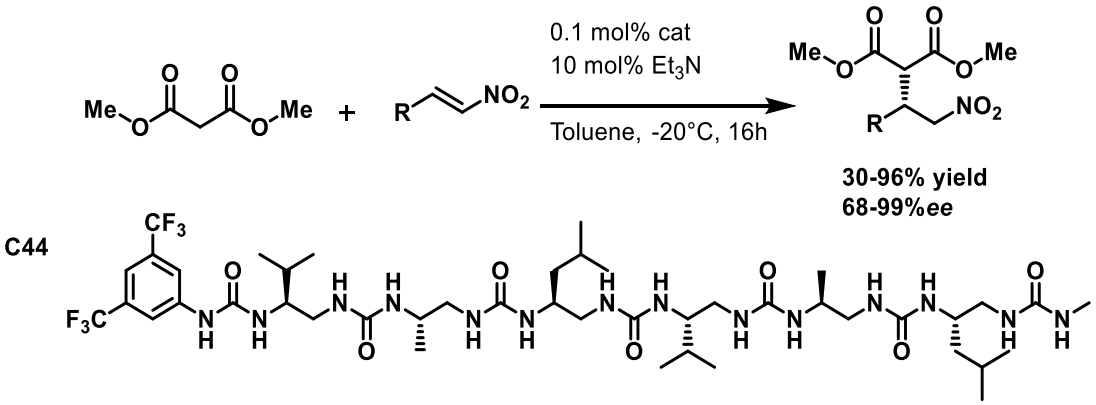

Scheme 1.12 *Oligo-urea foldamer catalysed malonate additions to nitro-olefins*

The examples that were presented give a taste of the possibilities that are opened by the integration of catalytic activity to foldamer scaffolds and the potential applications that this chemistry can offer but also shows that much development is still needed in the field to expand the scope of asymmetric reactions accessible with such catalysts.

I.4 Thesis outline

This body of works presents the results of the continuation of the previously studied chemistry, and as such, is focused in two parts. With the excellent results that have been obtained by the group when applying oligourea foldamer catalysts to the addition of malonates to nitro-olefins, the group has shown an interest in derivatising its most active catalyst in an effort to establish and understand how various parameters of the oligourea affect both the observed reactivity and stereoselectivity. Concurrently, and encouraged by the results they had obtained with their initial attempt, the team has intended to explore other catalytic reactions using oligourea catalysts. This project is therefore constituted of the abovementioned two objectives and will be presented in two parts.

The initial works will focus on the effect of the catalyst structure variations on reactivity and stereoselectivity for the reference addition reaction. To complement this study and as an intermediary step, the Michael type addition of β, γ-unsaturated ketones to nitro-olefins was investigated as an extension of the previous chemistry.

Finally, with the oligoureas from the group having demonstrated the ability to selectively bind anions, a new way of using our foldamer catalysts in anion-binding catalysis was explored in collaboration with the Palomo group at the UPV (Universidad del País Vasco).

Reference

[1] G.H. Wagnière, *On chirality and the universal asymmetry,* Verlag Helvetica Chimica Acta, Zürich, **2007**

[2] F. Zhou, Y. L. Liu, J. Zhou, *Adv. Synth. Catal.* , **2010**, *352*, 1381-1407; C. Najera, J. M. Sansano, *Chem. Rev.*, **2007**, *107*, 4584-4671

[3] E. Sanganyado, Z. Lu, Q. Fu, D. Schlenk, J. Gan, *Water Research*, **2017**, *124*, 527-542; V. Farina, J. T. Reeves, C. H. Senanayake, J. J. Song, *Chem. Rev.*, **2006**, *106*, 2734-2793

[4] For reviews on total syntheses: J. S. Chen, K. C. Nicolaou, *Chem. Soc. Rev.*, **2009**, *38*, 2993-3009 ; T. Gaich, P. S. Baran, *J. Org. Chem.* **2010**, *75*, 14, 4657–4673 ; *Chem. Soc. Rev.*, **2021**, *50*, 2320-2336
Some examples of total syntheses from well-known groups: W.R. Gutekunst, P. S. Baran, *J. Am. Chem. Soc.*, **2011**, *133*, 19076-19079; L. Furst, J. M. R. Narayanam, C. R. J. Stephenson, *Angew. Chem. Int. Ed.*, **2011**, *Vol.50 (41)*, 9655-9659; Y. Kanda, Y. Ishihara, N. C. Wilde, P. S. Baran, *J. Org. Chem.*, **2020**, *85*, 16, 10293-10320

[5] P.Camps, S. Gimenez, M. Font-Bardia, X. Solans, *Tetrahedron: Asymmetry* **1995**, *6*(4), 985–990

[6] Y. Wang, A. M. Chen, *Org. Process Res. Dev.* **2008**, *12*, 2, 282–290

[7] J. Rudolph, F. Hannig, H. Theis, R. Wischnat, *Org. Lett.* **2001**, *3*, 20, 3153–3155; N. K. Anand, E. M. Carreira, *J. Am. Chem. Soc.* **2001**, *123*, 43, 10782–10783, E. D. Nacsa, B. C. Fielder, S. P. Wetzler, V. Srisuknimit, J. P. Litz, M. J. Van Vleet, K. Quach, D. A. Vosburg, *Synthesis*, **2015**, *47*(17): 2599-2602

[8] W. Zhang, J. L. Loebach, S. R. Wilson, E. N. Jacobsen, *J. Am. Chem. Soc.*, **1990,** *112*(7), 2801-2803; Z. H. Zhang, X. Y. Dong, X. Y. Du, Q. S. Gu, Z. L. Li, X. Y. Liu, *Nat. Commun.*, **2019**, *10*(1), 5689

[9] S. E. Denmark, S. K. Ghosh, *Angew. Chem. Int. Ed.*, **2001**, *40*, 4759-4762; B. List, *J. Am. Chem. Soc.,* **2002**, *124*(20), 5656-5657

[10] A. Payen, *Annales de chimie et de physique. 2nde,* **1833,** *53, pp73–92*

[11] C. C. F. Blake, D. F. Koenig, G. A. Mair, A. C. T. North, D. C. Phillips, R. R. Sarma, *Nature* , **1965**, *vol. 206*, p 757–761

[12] Z. G. Hajos, D. R. Parrish, German Patent DE 2102623 **1971;** Z. G. Hajos; D. R. Parrish, *J. Org. Chem.,* **1974,** *39 (12)*, 1615–1621

[13] B. List, R. A. Lerner, C. F. Barbas, *J. Am. Chem. Soc.*, **2000**, *122*, 2395

[14] M. Haridas, E.M.M. Abdelraheem, U. Hanefeld, *Appl. Microbiol. Biotechnol.*, **2018**, *102*, 9959-9971

[15] M. J. Calhorda, *Chem. Commun.* , **2000**, 801-809

[16] G. A. Jeffrey, *An introduction to hydrogen bonding,* Oxford University Press, Oxford, **1997;** T. Steiner, *Angew. Chem. Int. Ed.* **2002***, 41,* 48 - 76

[17] J. Itoh, K. Yokota, K. Fuchibe, T. Akiyama, *Angew. Chem. Int. Ed.*, **2004**, *43*, 1566-1568

[18] W. M. Latimer, W. H. Rodebush, *J. Am. Chem. Soc.*, **1920**, *42*, 1419-1433

[19] Y. Huang, V. H. Rawal, *J. Am. Chem. Soc.*, **2002**, *124*, 9662-9663

[20] T. P. Yoon, E. N. Jacobsen, *Science*, **2003,** *299*, 1691-1693

[21] J. Itoh, K. Fuchibe, T. Akiyama, *Adv. Synth. Catal.*, **2006**, *348*, 999-1010, D. Seebach, A.K. Beck, A. Heckel, *Angew. Chem. Int. Ed.*, **2001**, *1*, 92-138

[22] S. H. Wilen, J. Z. Qi, P. G. Williard, *J. Org. Chem.*, **1991**, *56*, 485-487

[23] T.M.A. Yamada, S. Ikegami, *Tetrahedron Lett.*, **2000**, *41*, 2165-2169

[24] N. T. McDougal, S. E. Schaus, *J. Am. Chem. Soc.*, **2003**, *125*, 12094-12095

[25] K. Matsui, S. Takizawa, H. Sasai, *J. Am. Chem. Soc.*, **2005**, *127*, 3680-3681

[26] Y. Huang, V. H. Rawal, *Org. Lett.*, **2000**, *2*, 3321

[27] A.K. Unni, N. Takenaka, H. Yamamoto, V.H. Rawal, *J. Am. Chem. Soc.*, **2005**, *127*, 1336-1337

[28] M. Terada, K. Soga, N. Momiyama, *Angew. Chem. Int. Ed.*, **2008**, *47*, 4122-4125

[29] J. Itoh, K. Fuchibe, T. Akiyama, *Angew. Chem. Int. Ed.*, **2008**, *47*, 4016-4018

[30] K. Rück-Braun, H. Kunz, *Chiral Auxiliaries in Cycloadditions*, Wiley, New York, **1999**

[31] E. J. Corey, *Angew. Chem. Int. Ed.*, **2002**, *41*, 1650-1667

[32] A. B. Northrup, D. W. C. MacMillan, *J. Am. Chem. Soc.*, **2002**, *124*, 2458-2460

[33] T. Schuster, M. Bauch, G. Dürner, W. Göbel, *Org. Lett.*, **2000**, *2*, 179-181

[34] A. N. Thadani, A. R. Stankovic, V.H. Rawal, *Proc. Natl. Acad. Sci. USA*, **2004**, *101*, 5846; Y. Huang, A.K. Unni, A.N. Thadani, V.H. Rawal *Nature,* **2003**, *424***,** 146

[35] N. Momiyama, H. Yamamoto, *J. Am. Chem. Soc.*, **2005**, *127*, 1080-1081

[36] K. Tomioka, K. Ando, K. Yasuda, K. Koga, *Tetrahedron Lett.*, **1986**, *27*, 715-716

[37] T. Tejero, P. Merino, *Angew. Chem. Int. Ed.*, **2004**, *43*, 2995-2997

[38] M.C. Etter, Z. Urbanczyk-Lipkowska, M. Zia-Ebrahimi, T.W. Panunto, *J. Am. Chem. Soc.*, **1990**, *112*, 8415-8426; V. Amendola, L. Fabbrizzi, L. Mosca, *Chem. Soc. Rev.*, **2010**, *39*, 3889-3915

[39] P. R. Schreiner, *Chem. Soc. Rev.*, **2003**, *32*, 289

[40] Z. Bao, H. Xing, Z. Zhang, *Org. Biomol. Chem.*, **2014**, *12*, 3151-3162

[41] M. S. Sigman, E. N. Jacobsen, *J. Am. Chem. Soc.*, **1998**, *120*, 4901-4902

[42] M. S. Sigman, P. Vachal, E. N. Jacobsen, *Angew. Chem. Int. Ed.*, **2000**, *39*, 1279-1281

[43] T. Okino, Y. Hoashi, Y. Takemoto, *Tetrahedron Lett.*, **2003**, *44*, 2817-2821
[44] T. Okino, Y. Hoashi, Y. Takemoto, *J. Am. Chem. Soc.*, **2003**, *125*, 12672-12673
[45] J. Wang, H. Li, X. Yu, L. Zu, W. Wang, *Org. Lett.*, **2005**, *7*, 4293-4296
[46] R. P. Herrera, V. Sgarzani, L. Bernardi, A. Ricci, *Angew. Chem. Int. Ed.*, **2005**, *44*, 6576-6579
[47] Y. Sohtome, Y. Hashimoto, K. Nagasawa, *Adv. Synth. Catal*. **2005**, *347*, 1643 – 1648
[48] S. Diosdado, R. Lopez, C. Palomo, *Chem. Eur. J.*, **2014**, *20*, 6526-6531
[49] K. M. Lippert, K. Hof, D. Gerbig, D. Ley, H. Hausmann, S. Guenther, P. R. Schreiner, *Eur. J. Org. Chem.*, **2012**, *30*, 5919-5927
[50] L. Fischer, C. Didierjean, F. Jolibois, V. Semetey, J.M. Lozano, J.P. Briand, M. Marraud, R. Poteau, G. Guichard, *Org. Biomol. Chem.*, **2009**, *6*, 2596-2610
[51] S. Diosdado, J. Etxabe, J. Izquierdo, A. Landa, A. Mielgo, I. Olaizola, R. Lopez, C. Palomo, *Angew. Chem. Int. Ed.*, **2013**, *52*, 11846-11851
[52] H. Echave, R. Lopez, C. Palomo, *Angew. Chem. Int. Ed.*, **2016**, *55*, 3364-3368
[53] T. J. Auvil, A. G. Schafer, A. E. Mattson, *Eur. J. Org. Chem.*, **2014**, *13*, 2633-2646
[54] R.I. Storer, C. Aciro, L.H. Jones, *Chem. Soc. Rev.*, **2011**, *40*, 2330-2346; M. Zabka, R. Sebesta, *Molecules*, **2015**, *20*, 15500-15524
[55] J. P. Malerich, K. Hagihara, V. H. Rawal, *J. Am. Chem. Soc.*, **2008**, *130*, 14416-14417
[56] L. Dai, S. X. Wang, F. E. Chen, *Adv. Synth. Catal.*, **2010**, *352*, 2137-2141
[57] J. Skarzewski, M. Zielinska-Blajet, I. Turowska-Tyrk, *Tetrahedron: Asymmetry*, **2001**, *12*, 1923-1928
[58] P. Suresh, K. Pitchumani, *Tetrahedron: Asymmetry*, **2008**, *19*, 2037-2044
[59] Y. Qien, G. Ma, A. Lv, H. L. Zhy, J. Zhao, V. H. Rawal, *Chem. Commun.*, **2010**, *46*, 3004-3006
[60] H. Konishi, T. Y. Lam, J. P. Malerich, V. H. Rawal, *Org. Lett.*, **2010**, *12*, 2028-2031
[61] H. Echave, I. Bastida, R. Lopez, C. Palomo, *Chem. Eur. J.*, **2018**, *24*, 11554-11558
[62] A. Garcia-Urricelqui, A. de Cosar, T. E. Campano, A. Mielgo, C. Palomo, *Eur. J. Org. Chem.*, **2021**, *25*, 3604-3612
[63] Y. Sohtome, A. Tanatani, Y. Hashimoto, K. Nagasawa, *Tetrahedron Lett.*, **2004**, *45*, 5589-5592
[64] A. Berkessel, K. Roland, J. M. Neudörfl, *Org. Lett.*, **2006**, *8*, 4195-4198
[65] S. H. Gellman, *Acc. Chem. Res.*, **1998**, *31*, 173-180
[66] G. Guichard, I. Huc, *Chem. Commun.*, **2011,** *47***,** 5933-5941; S. Hecht, I. Huc, *Foldamers: Structure, Properties and Applications*, Wiley-VCH, Weinheim, **2007**
[67] M. W. Giuliano, S. J. Maynard, A. M. Almeida, L. Guo, I. A. Guzei, L. C. Spencer, S. H. Gellman, *J. Am. Chem. Soc.*, **2014**, *136*, 15046-15053; J.R. Gord, P.S. Walsh, B.F. Fisher, S.H. Gellman, T.S. Zwier, *J. Phys. Chem. B.*, **2014**, *118*, 8246-8256
[68] V. Semetey, D. Rognan, C. Hemmerlin, R. Graff, J. P. Briand, M. Marraud, G. Guichard, *Angew. Chem. Int. Ed.*, **2002**, *41*, 1893-1895
[69] A. Erkkilä, P. M. Pihko, *Eur. J. Org. Chem.*, **2007**, *25*, 4205-4216
[70] Z.C. Girvin, S.H. Gellman, *J. Am. Chem. Soc.*, **2018**, *140*, 12476–12483
[71] Z.C. Girvin, S.H. Gellman, *J. Am. Chem. Soc.*, **2020**, *142*, 17211-17223
[72] L. Moisan, P. I. Dalko, *Angew. Chem. Int. Ed.,* **2004**, *43*, 5138-5175
[73] P. Krattiger, R. Kovasy, J. D. Revell, S. Ivan, H. Wennemers, *Org. Lett.*, **2005**, *7*, 1101-1103
[74] M. Wiesner, J. D. Revell, H. Wennemers, *Angew. Chem. Int. Ed.*, **2008**, *47*, 1871-1874
[75] M. Wiesner, J. D. Revell, S. Tonazzi, H. Wennemers, *J. Am. Chem. Soc.*, **2008**, *130*, 5610-5611
[76] K. Akagawa, H. Akabane, S. Sakamoto, K. Kudo, *Org. Lett.*, **2008**, *10*, 2035-2037
[77] K; Akagawa, T. Fujiwara, S. Sakamoto, K. Kudo, *Org. Lett.*, **2010**, *12*, 1804-1807
[78] K. Akagawa, K. Kudo, *Angew. Chem. Int. Ed.*, **2012**, *51*, 12786-12789
[79] L. Mathieu, B. Legrand, C. Deng, L. Vezenkov, E. Wenger, C. Didierjean, M. Amblard, M. C. Averlant-Petit, N. Masurier, V. Lisowski, J. Martinez, L. T. Maillard, *Angew. Chem. Int. Ed.*, **2013**, *52*, 6006-6010
[80] J. Aguesseau-Kondrotas, M. Simon, B. Legrand, J. L. Bartignies, Y. K. Kang, D. Dumitrescu, A. Van der Lee, J. M. Campagne, R. M. de Figueiredo, L. T. Maillard, *Chem. Eur. J.*, **2019**, *25*, 7396-7401
[81] M. J. Kinghorn, G. A. Valdivia-Berroeta, D. R. Chantry, M. S. Smith, C. C. Ence, S. R. E. Draper, J. S. Duval, B. M. Masino, S. B. Cahoon, R. R. Flansburg, C. J. Conder, J. L. Price, D. J. Michaelis, *ACS Catal.*, **2017**, *7*, 7704-7708
[82] C.R. Jones, G. D. Pantos, A.J. Morrison, M.D. Smith, *Angew. Chem. Int. Ed.*, **2009**, *48*, 7391-7394
[83] N. Probst, A. Madarasz, A. Valkonen, I. Papai, K. Rissanen, A. Neuvonen, P.M. Pihko, *Angew. Chem. Int. Ed.*, **2012**, *51,* 8495-8499; A.J. Neuvonen, P.M. Pihko, *Org. Lett.*, **2014**, *16*, 5152-5155
[84] B.A.F. Le Bailly, L. Byrne, J. Clayden, *Angew. Chem. Int. Ed.,* **2016**, *55*, 2132-2136
[85] R.-P. Hummel, C. Toniolo, G. Jung, *Angew. Chem. Int. Ed.*, **1987**, *26*, 1150–1152
[86] R. Wechsel, J. Raftery, D. Cavagnat, G. Guichard, J. Clayden, *Angew. Chem., Int. Ed*., **2016**, *55*, 9657–9661
[87] D. Becart, V. Diemer, A. Salaün, M. Oiarbide, Y. R. Nelli, B. Kauffmann, L. Fischer, C. Palomo, G. Guichard, *J. Am. Chem. Soc*,. **2017**, *139*, 12524–12532

Chapter 2

I- History of the project:

The Guichard group has been specialized in the study of foldamers based on the urea motif to provide the desired scaffold structuration. As early as 2002, the synthesis of oligourea macrocycles was described by the group[1] with the goal of self-assembly into nanotubes maintained by intermolecular H-bonds. These oligoureas are obtained through a linear iterative synthesis from α-amino-acid derived subunits.

Non-macrocyclic oligoureas have been a family of high-interest compounds among the team as they have the ability to fold into a 2.5 residue per turn helix after four residues have been introduced in the chain[2]. This scaffold is maintained by a three-centered intramolecular H-bonding scheme between the acceptor carbonyl oxygen (*i*+3) and the donor –NH groups from the urea positioned in (*i*) and (*i*+1). **(Fig 2.1)**

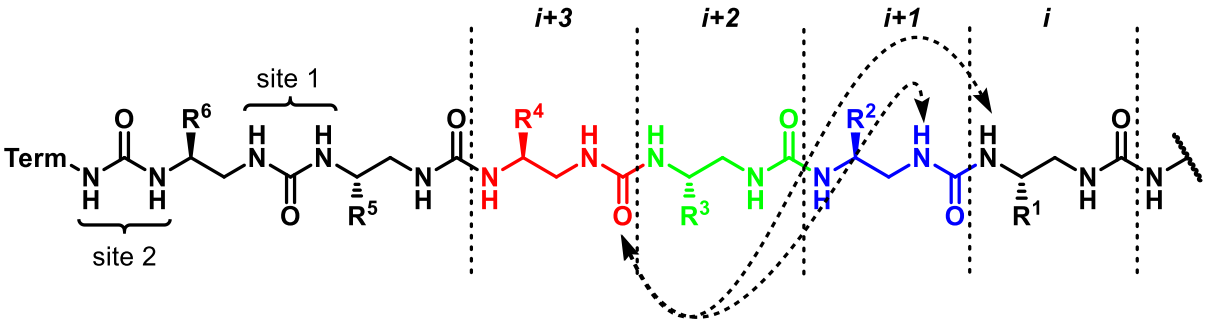

Figure 2.1 *Intramolecular H-bonding network in oligoureas*

These molecules have been shown to recognize and bind anions in previous works[3]. Indeed, two urea moieties that present free –NH groups can be found at the N-terminus of the oligoureas (site 1 and site 2, Fig. 2.1) which also correspond to the positive pole of the helix macrodipole, allowing interaction with external targets without disrupting the helix.

Following these reports, the group has investigated the ability of oligourea foldamers to be used as organocatalysts. In results published in 2017, Guichard *et al* have shown that the Michael addition of malonates to nitro-olefins was indeed activated by foldamer catalysts, providing the desired addition products under very low catalytic loadings with excellent yields and enantioselectivities[4]. In this work, the catalytic system was formed by the foldamer (chiral catalyst) and a simple achiral Brønsted base cocatalyst acting synergistically. To differentiate the two sites available for molecular recognition and catalysis a 4,5-bis(trifluoromethyl)phenyl urea was introduced to increase the polarity and polarisability of the first urea bond **(Fig 2.2)**.

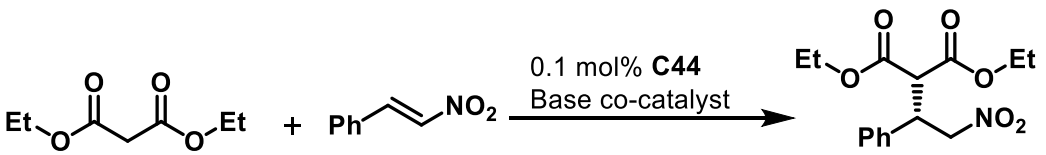

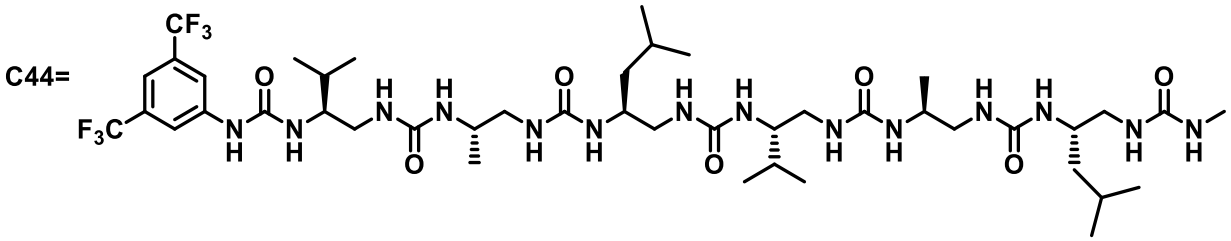

entry	foldamer loading (mol %)	temp (°C)	reaction time (h)	Et_3N (mol %)	conversion (%)	yield (%)	ee (%)
1	–	−20	48	10	7	n.d.	0
2	0.1	−20	48	10	100	86	95
3	0.05	−20	48	10	100	85	94
4	0.01	−20	48	10	98	82	91
5	0.005	−20	48	10	93	82	84
6	0.001	−20	48	10	67	49	74

Figure 2.2 *Oligourea foldamer catalysed Michael addition*

The chain length as well as the nature of the side chains of the catalysts were shown to have an impact on the selectivity of the reaction, demonstrating the strong correlation between folding propensity of the oligomer and its catalytic performance. As mentioned above, the studied oligoureas do not adopt the expected helical conformation before at least four residues have been incorporated (subtle differences were observed when the first urea in **(C44)** was replaced by a thiourea, see Figure 2.3). However, even though the helix is formed at four residues, it did not lead to useful enantioselectivity. Optimal oligourea length was demonstrated to be either five or six residues with longer 9-mer sequences surprinsingly resulting in lower yield and selectivity (unpublished data from the Guichard group).

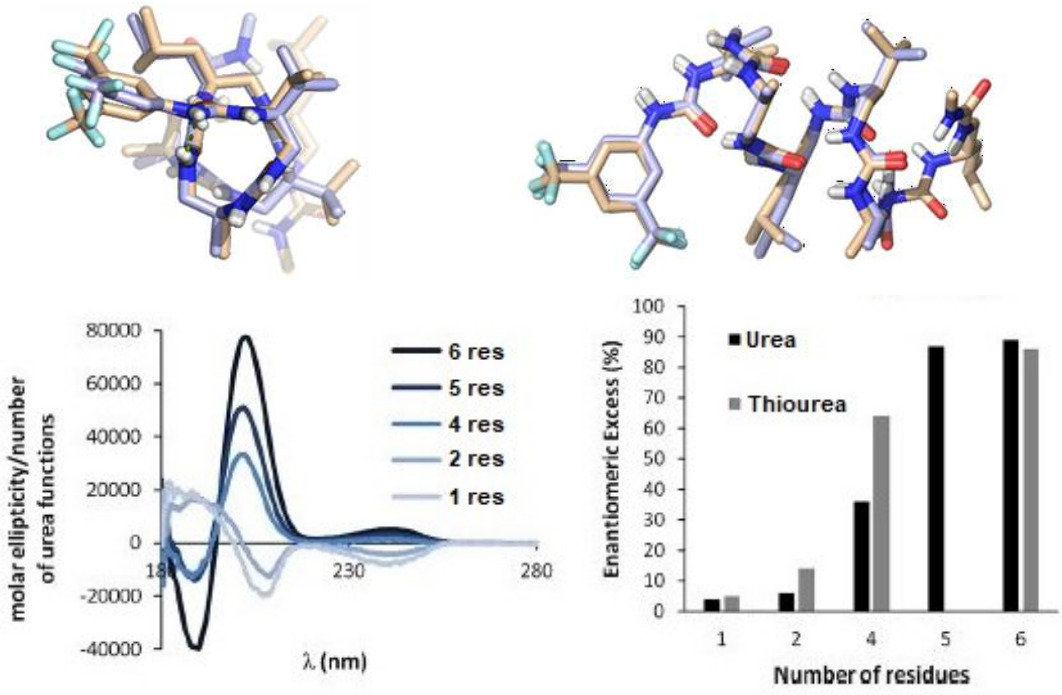

Figure 2.3 *Optimal catalyst chain-length studies in oligo (thio)ureas and overlay of the X-ray structures of* ***C44*** *and the cognate pentaurea sequence*

Following the encouraging results that have been obtained in the case of the foldamer catalysed Michael addition with **C44**, the team has taken a keen interest in further exploring the rules that govern catalysis in these systems and in trying to identify new reactions that could be mediated by this new type of organocatalysts to establish their scope and limitations.

This project follows in the steps of the predecessors according to the discoveries that they have transmitted. In order to study new reactivities, new catalyst structures could prove necessary to optimize in the case of a successful reaction but also to provide insight into the workings of potential newfound reactivity.

II- Synthesis of oligourea foldamers:

1) Objectives and initial considerations:

The initial objectives of our work has been threefold:

- The design and evaluation of structural modifications on the original catalyst that was used in the previous works from the group in order (i) to perform structure-activity relationship studies and study the requirements for effective addition of carbonyl pronucleophiles to nitroalkenes and (ii) to expand the library of available foldamers that could serve to screen new reactions.
- The synthesis of the original catalyst at a scale sufficient to allow for the screening of new reactions as well as to be given to co-workers collaborating with our group for the application to the organocatalysed polymerisation of lactide (cooperation with Taton and co-workers at the Laboratoire des Polymères Organiques, Bordeaux).
- Provide a general strategy for anchoring the catalyst on solid support to evaluate the potential of solid-supported oligourea foldamers as reusable heterogeneous catalysts.

The attempted structural modifications to the initial catalyst are summarily presented in **Figure 2.4.** The areas of modification are highlighted over the reference catalyst **(C44)** and the resulting catalyst structures are specified.

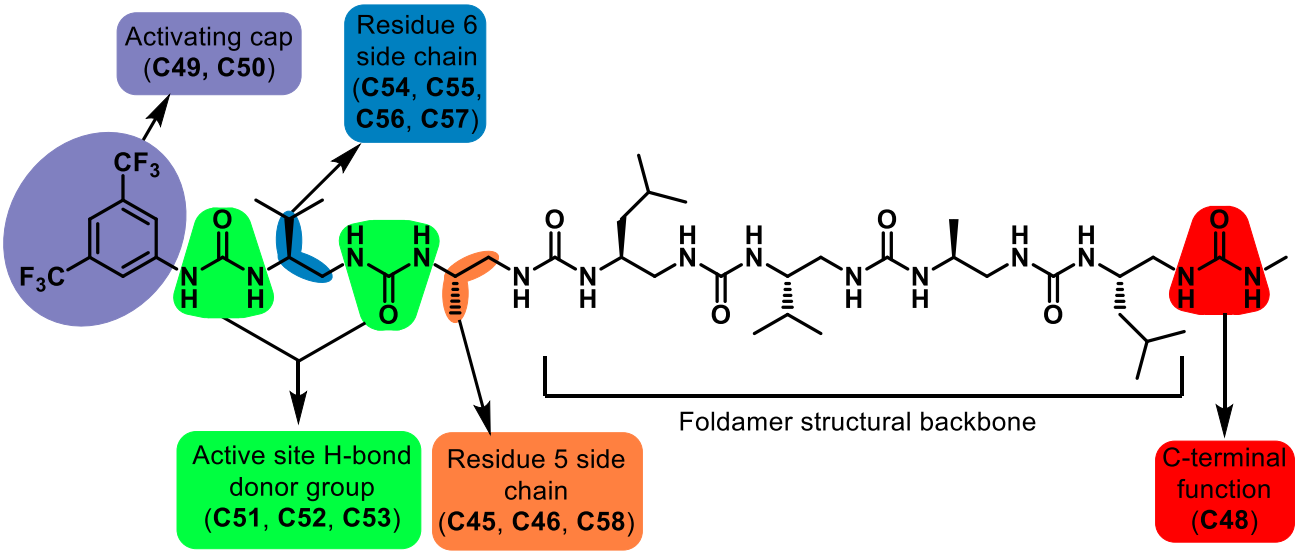

Figure 2.4 *Representation of catalyst modifications envisioned in this work to modulate the catalytic activity of* ***C44***

The idea was to evaluate additional catalyst variations that were not previously investigated in the first account published on oligourea catalysts. We focused on new backbone and sequence variations to gain additional insight into the principles governing the catalytic activity of the oligoureas and as a mean to improve next generation foldamer-based catalysts. In addition to variations of the nature of the side chains, substitution patterns (position of the side chain on the backbone)[2] and isosteric backbone modifications (e.g. urea versus thiourea) can be used to modulate the helix properties and generate different spacing and projection of side chains at the surface. For example, the thiourea moiety is potentially useful to increase the acidity of the NHs along the backbone.[5] Furthermore, the introduction of other catalytic moieties replacing the bis-trifluoromethyl phenyl urea at the terminal end of the helix have also been considered to study how the catalytic properties may be influenced.

For our study of the structure-activity relationship of oligourea catalysts, we both synthesised new catalyst sequences (e.g. **(C45)**, **(C46)** – variation of side chains and substitution patterns – and **(C50)** – backbone modification) and used sequences made by previous co-workers of the group but never tested in head-to-head comparison.

As such, the first step of this work has been the synthesis of both the previously tested model catalyst sequence **(C44)** and modified catalyst structures to have a diverse set of options to probe new reactivity. The synthesis method of oligourea sequences is one of iterative addition of amino acid derived building blocks which need to be prepared beforehand.

2) Synthesis of building blocks

The iterative synthesis of the foldamer catalysts is accomplished by using simple building blocks obtained by transforming amino-acids, whether natural or not. In the work shown here, a Boc- protection strategy has been employed all along the preparation of the blocks and the synthesis of oligomers for which solution phase was selected[6].

The usual synthesis plan of building blocks shown in **scheme 2.1** starts with the reduction of the Boc-protected amino-acid **(1)** into its alcohol analogue **(2)** through activation by isobutyl chloroformate followed by treatment with sodium borohydride. The alcohol group was then substituted by a phthalimide group in a Mitsunobu reaction to give the masked diamine **(3)**. The second amine function was unmasked by the way of phthalimide hydrazinolysis to afford mono-protected diamine **(4)**. The free amine was coupled with disuccinimidyl carbonate to afford the Boc-protected activated succinimidyl carbamate **(5)**.

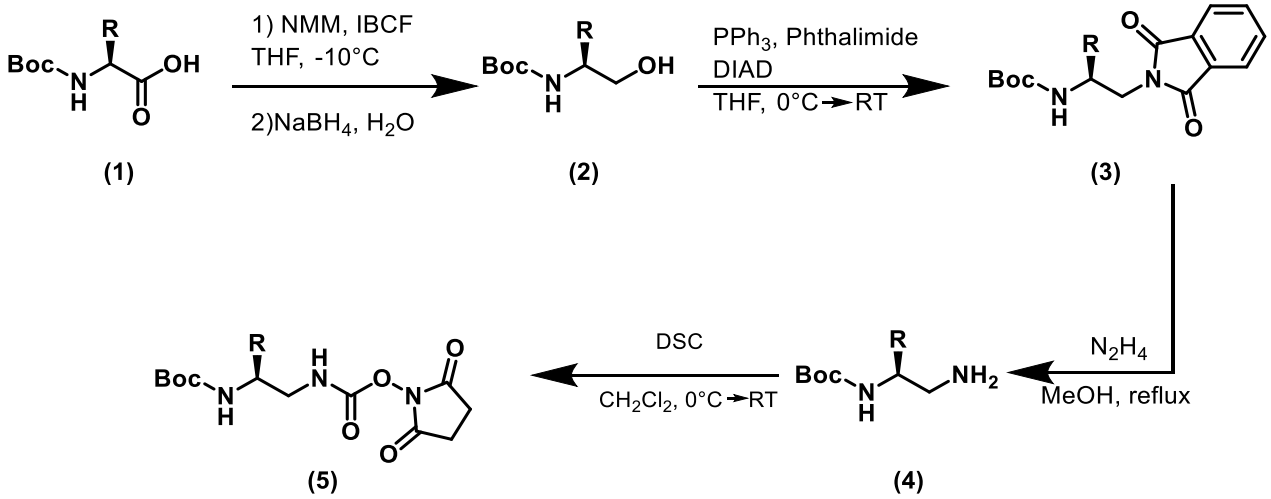

5a: R=Me r=34% (over 4 steps)
5b: R=*i*Pr r=34% (over 4 steps)
5c: R=*i*Bu r=31% (over 4 steps)

Scheme 2.1 *Synthesis of Boc-protected building blocks* ***5a, 5b, 5c***

The synthesis way described above, while affording the expected product at a multi-gram-scale, exhibited inconsistent and low yields compared to what would be expected for the continuation of this project. Upon further inspection during the synthesis, the yield inconsistency problems were isolated around the phthalimide product. Purification of **(3)** by column chromatography proved to be unfeasible due to the amount of crude product and the size of the column it would require. The inability to isolate this key species of this synthetic approach compelled the consideration of an alternative way to access the building blocks. The finalised pathway to access the building blocks **(5)** is described in **scheme 2.2** below. The initial step as well as the final two steps remain identical to the previous method, however installation of the phthalimide group was avoided altogether in two steps. Mesylation of alcohol **(2)** provided mesylate **(6)** which was subjected to sodium azide to substitute the mesyl group by an azide. Finally, reduction of azide **(7)** led back to monoprotected amine **(4).** While consisting of one more step than the initial synthesis, this pathway gave consistently higher and more repeatable yields (ranging from 49% to 58% over 5 steps) due to cleaner crude materials being obtained at every step.

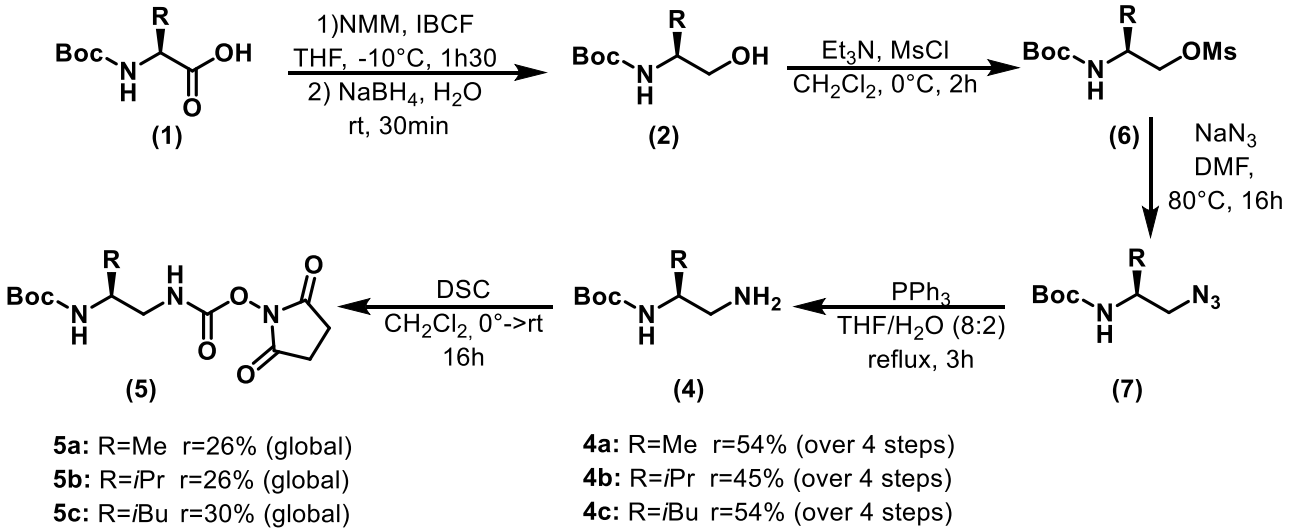

Scheme 2.2 *Alternative synthesis for Boc-protected building blocks* ***5a, 5b, 5c***

With the building blocks derived from natural amino-acids prepared, we turned our attention towards the preparation of new building blocks in order to integrate them into new catalyst sequences. One way to change the structure of the oligourea foldamers is through the side chains coming from the starting amino-acid from which the building block is derived. The nature of this side chain as well as its position along the backbone are key tunable elements during the synthesis of our foldamer catalysts **(Figure 2.5)**. These parameters do, however, require planning according to the structure they are expected to adopt once the helix is formed instead of a linear structure. It has been shown that the helix formed using canonical building blocks 5 derived from L-amino acids (side chain on the β-carbon) exclusively is right-handed. Interestingly, it was later found that this canonical helical conformation tolerates the introduction of non-canonical building blocks with alternative substitution patterns, i.e. with the side chain on the α carbon. However, the stereochemistry of the block substituted in the α-position needs to be inverted to still be compatible with helix formation (the synthesis of the block-

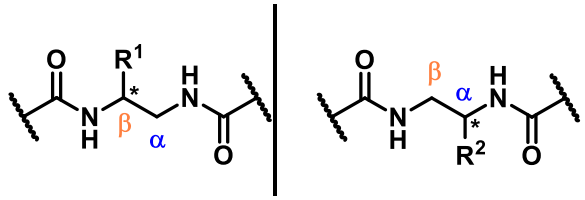

Figure 2.5 *Canonical monomeric units and alternative substitution patterns in oligoureas.*

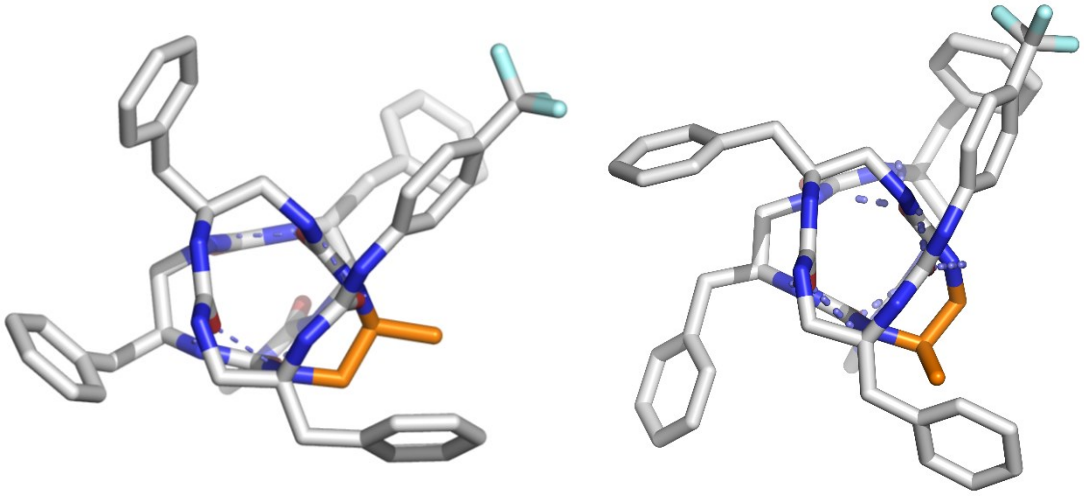

Figure 2.6 *X-ray structure of both the canonical oligourea helix and of a sequence containing a monomeric unit (orange) with the side chain shifted on the α-carbon with inversion of chirality.*[2]

-thus requests to start from a D-amino acid). It is worth noting that in this case the projection of the side of the inverted unit at the surface of the helical structure changes from equatorial to a more axial orientation (see Figure 2.6).

Following the structures we had envisioned at the start of this work, a way to access building blocks derived from (D)-amino-acids was put in place.

The seven-step synthesis starts with the reduction of the Cbz-protected (D)-amino-acid **(8)** into its alcohol **(9).** The alcohol was mesylated to afford **(10)** and the mesylate was treated with sodium azide to obtain **(11)**. The azide was reduced by a Staudinger reaction so as to avoid Cbz deprotection, leading to mono-protected amine **(12)**. The free amine was protected with a Boc group to give compound **(13)**. The Cbz group was removed by palladium-catalysed hydrogenation to reveal free amine **(14)**. Treatment of this amine with disuccinimidyl carbonate led to the Boc protected activated carbamate block **(15)**. To differentiate the two types of blocks, the (D)-amino-acid derived blocks are further referred as "inversed" (^{inv})

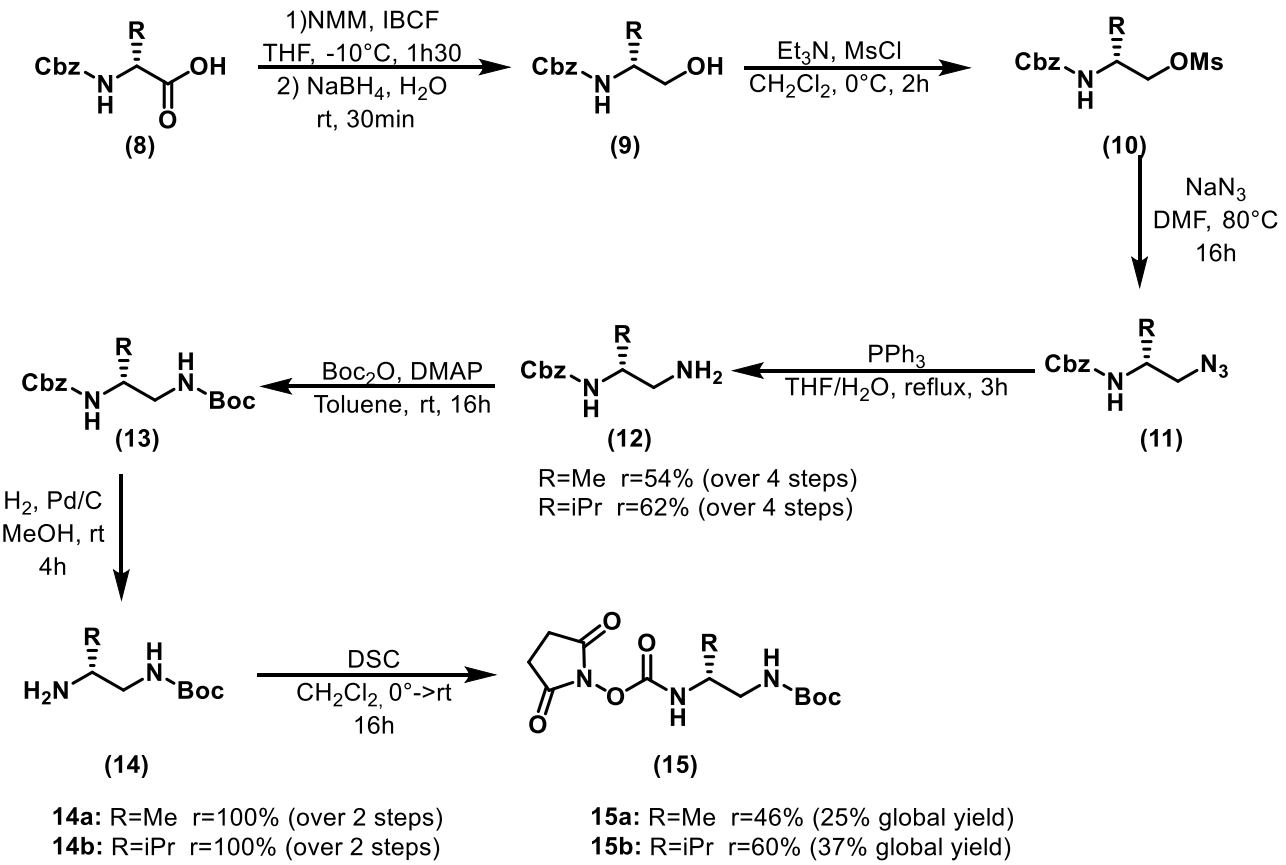

Scheme 2.3 *Synthesis of inversed building blocks* ***15a, 15b***

3) Synthesis of oligoureas

With a robust way of accessing the necessary building blocks, the synthesis of oligourea catalysts can be considered. One of the initial changes that we have considered has been a change of the ending at the C-terminus of the oligourea catalysts. While the group's previously syntheses of oligoureas in solution start with a small primary amine (e.g. N-methylamine) to generate a methylated urea[4] as an inert termination, a change of the C-terminus cap is a parameter that remains to be explored. Here we thought that it could be of particular interest to have a more modular synthesis approach authorizing a modification of this termination (corresponding to the negative pole of the helix macrodipole) once the chain elongation is completed. This would allow us to (i) study the impact on the nature of the terminal chain on the catalytic process (e.g. a longer hydrocarbon chain to favour a degree of aggregation or on the contrary more solubilizing side chains) without the need to resynthesize the whole oligomer and (ii) attach the foldamer catalyst on a solid-support at a late stage in the synthesis and generate a well-characterized solid-supported catalyst. We thus needed a relatively stable function that would remain untouched during the synthesis of the oligoureas but that would also allow for modification post-synthesis. With these considerations taken into account, we initially decided to synthesise the catalysts with an azide termination as a modular orthogonal protecting group for the terminal amine **(see Fig. 2.7)**.

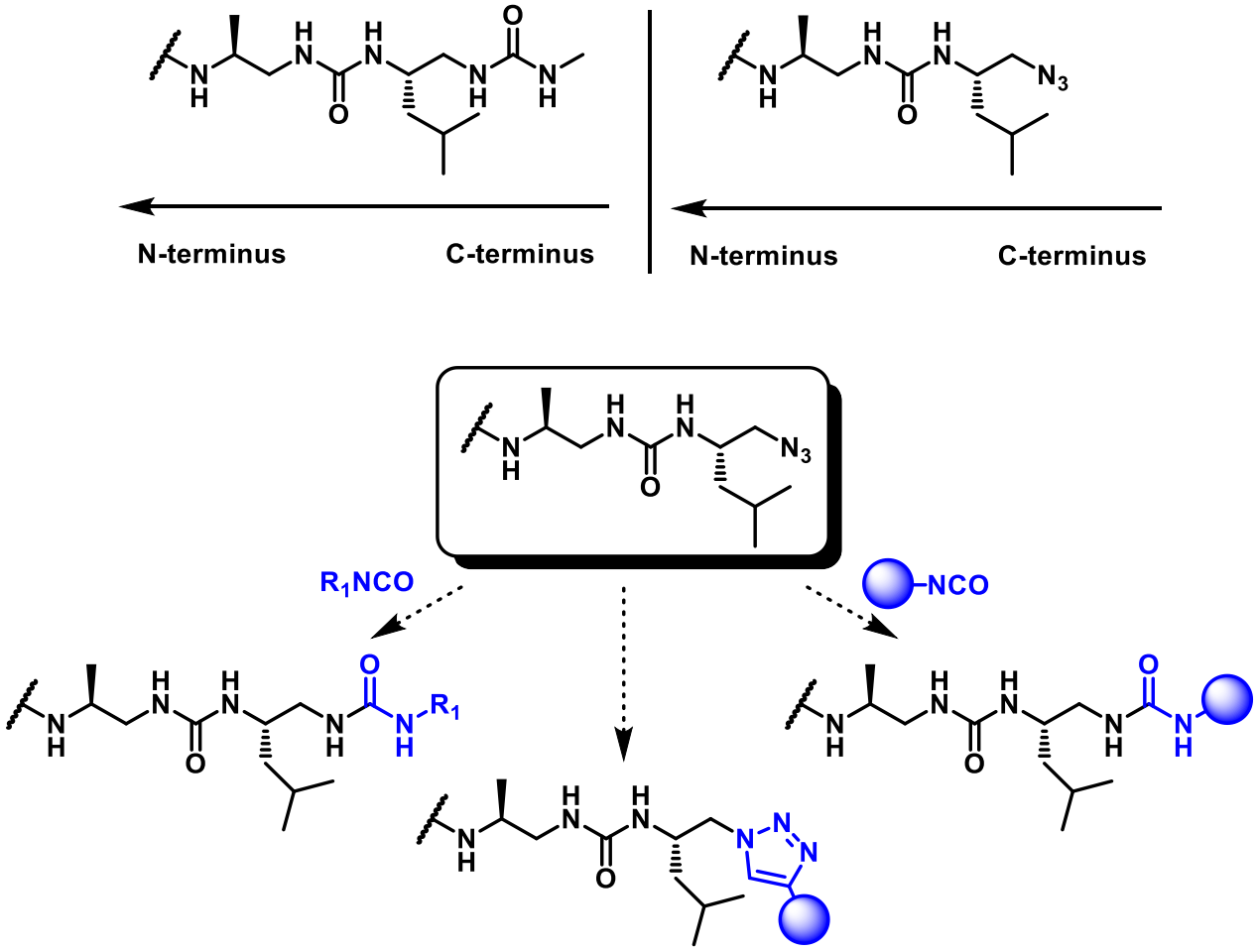

Figure 2.7 *Methyl urea vs azide C-terminus capping and further functionalisation of the catalyst including anchoring on a solid support*

Synthesis of hexaurea 22 bearing an azide termination:

As mentioned previously, the oligomers were synthesised by successive deprotection and coupling steps. In a typical synthetic stage, the Boc-protected *N*-mer is deprotected with trifluoroacetic acid before being coupled with the activated carbamate building block in basic conditions to afford the *(N+1)*-mer **(see Scheme 2.4)**.

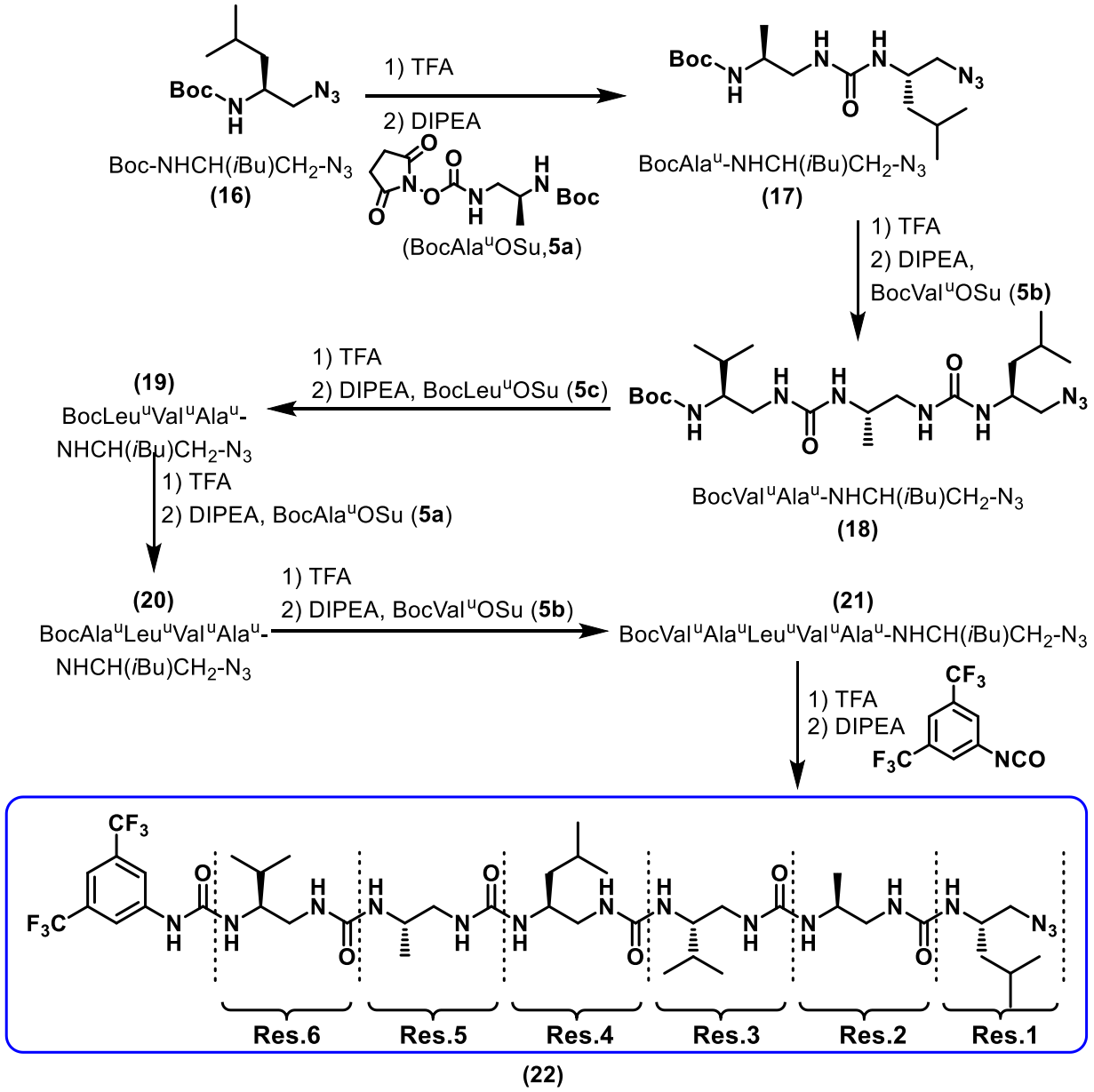

Scheme 2.4 *Synthesis of the azide hexamer catalyst (Ureido residues are denoted Xaa^{u} by analogy to the three letter code of α-amino acids they were derived from)*

Due to the fact that only the last two urea groups have the ability to interact with external substrates in the catalytic process, the rest of the residues being engaged in *intra*-helical H-bonding, tetramer **(19)** can be considered as a precursor to all catalyst variations that will be synthesised. It therefore needed to be accessed in significant quantities in order to have enough material for the synthesis of multiple hexamer sequences.

While the synthesis of the azide terminated hexamer catalyst **(22)** was successfully accomplished **(see Figure 2.8)** over six steps with a 10% global yield, some difficulties were encountered over repeating steps leading to shorter intermediates. Undesired coupling reactions were observed during reactions leading to trimer **(18)** and tetramer **(19)** resulting in unidentifiable oligourea structures. While the coupling reactions were investigated in order to determine the underlying cause of the observed misreactions, no single parameter could be tied to the phenomenon.

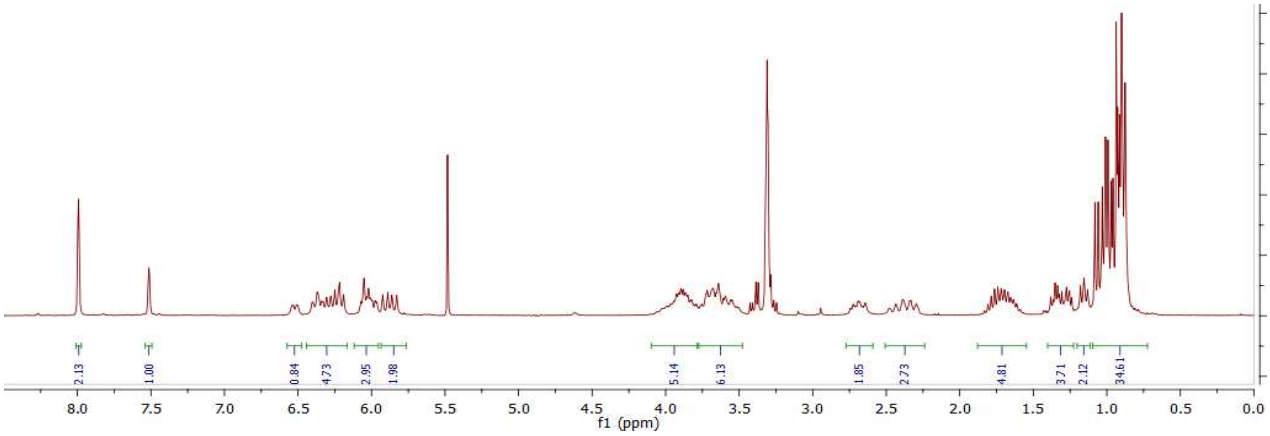

Figure 2.8 *^{1}H NMR spectrum of activated hexamer **(22)** bearing an azide termination (CD_3OH, 300MHz)*

With the oligourea foldamers usually adopting a helical conformation, a useful indicator of the geometry of these compounds is the signals corresponding to the backbone CH_2^{α}. The lengthening of the oligourea chain, accompanied by the adoption of the folded conformation leads to an increasing anisochronicity for these two protons, and therefore constitutes a measurable parameter. The difference of anisochronicity for the CH_2^{α} between azide terminated hexamer **(22)** and previously described[4] **(C44)** is presented in **Table 2.1.**

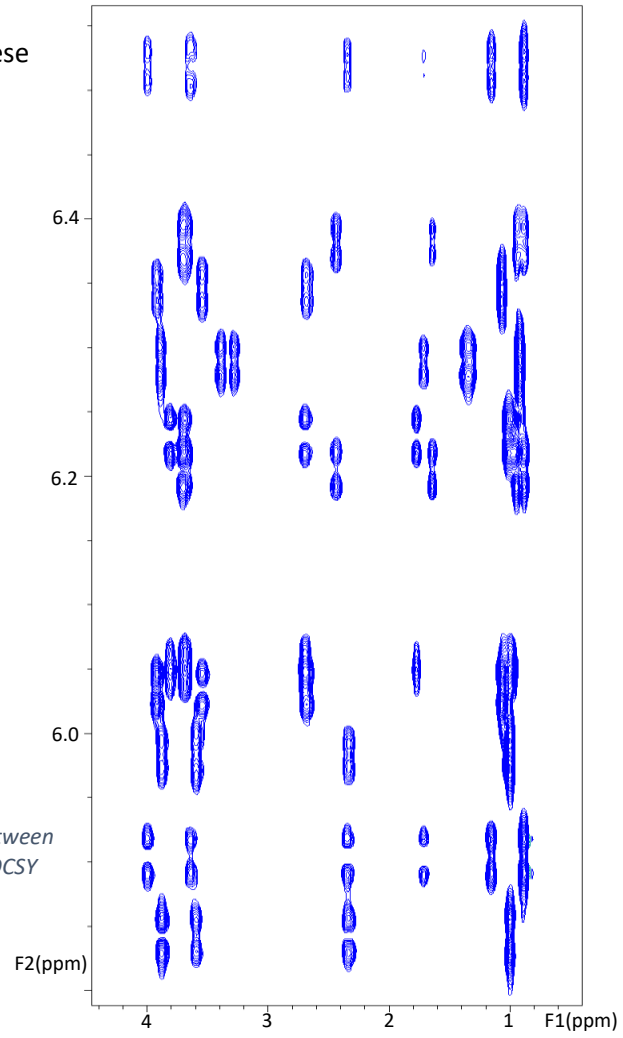

Residue type	Residue number	Δδ **(22)** (ppm)	Δδ **(C44)** (ppm)
Val	6	1.25	1.00
Ala	5	1.22	1.28
Leu	4	1.30	1.34
Val	3	1.25	1.27
Ala	2	1.26	1.20
NHCH(*i*Bu)CH_2N_3	1	0.12	0.95

Table 2.1 *Difference of anisochronicity for backbone CH_2^{α} hydrogens between hexamer **(22)** and reference catalyst **C44** calculated from COSY and TOCSY (right, fingerprint region) spectra (400MHz, CD_3OH)*

The azide termination and therefore lack of a *C*-terminal urea to provide a final anchoring site for the helix has a considerable impact on the first two residues of the oligourea while the rest of the sequence shows a slightly more stable helix conformation in comparison with reference catalyst **C44**.

Attempts to obtain (C44) from 22:

To obtain final catalyst **(C44)** used by the group in its previous works, the azide group of this precursor needs to be reduced to obtain the free amine which can then be transformed into the methyl urea by reaction with N-succinimidyl N-methylcarbamate. The free amine can also be coupled with a functionalised solid support (e.g. commercially available isocyanatomethyl polystyrene or aminomethyl-succinamic acid polystyrene) in order to get an easily separated and highly reusable catalyst system. To that effect, reduction of azide **(22)** was first conducted by classical hydrogenation over palladium on carbon.

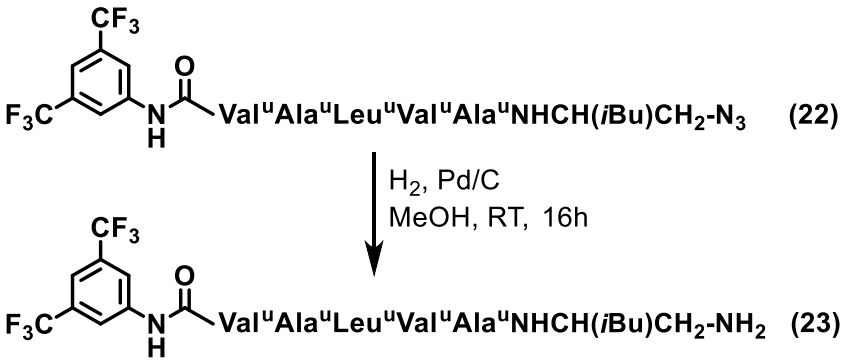

Scheme 2.5 *Reduction of the activated azide hexamer* ***(22)***

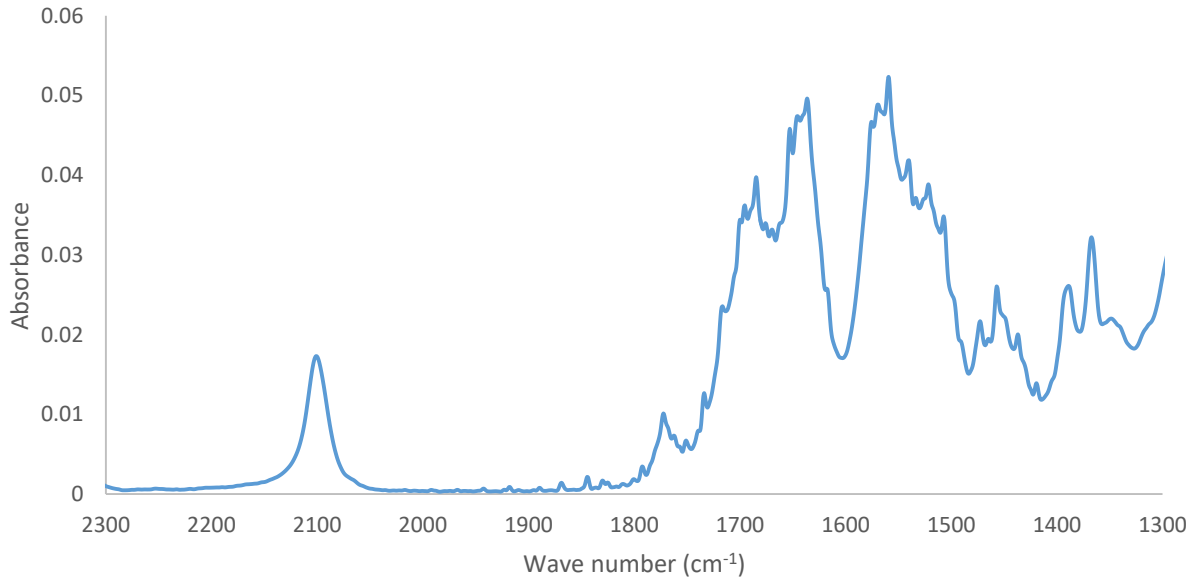

Figure 2.9 *Solid state infrared absorption spectrum of the isolated material after reduction attempt of* ***(22)***

As shown by the infrared absorption spectra of the isolated reaction material above **(Fig. 2.9)**, the signature signal of the azide termination can be seen at 2100cm^{-1}, thus indicating that the expected reduction reaction did not occur. It was previously shown using FT-IR that helically folded oligoureas exhibit two

characteristic bands[2] centered at 1635 cm^{-1} (Urea I) and 1570 cm^{-1} (Urea II). We clearly see after the reduction attempt that the signal is much more complex in this region suggesting unwanted reactions. This observation was also confirmed by ^{1}H NMR and mass spectrometry as no indication of the desired product could be found. The reduction step was attempted again with hexamer **(21)** that did not have the activating *N*-terminal cap but a –Boc group instead. The FT-IR absorption spectrum of the crude material **(Fig. 2.10)** still exhibits the azide signature at 2100cm^{-1}, however the desired reduction reaction was confirmed by mass spectrometry where the expected material was observed. The two main urea bands in the carbonyl region at 1638 and 1574 cm^{-1} also correspond to what is usually expected for folded oligoureas.[2] Attempted isolation of the free amine was ultimately unsuccessful.

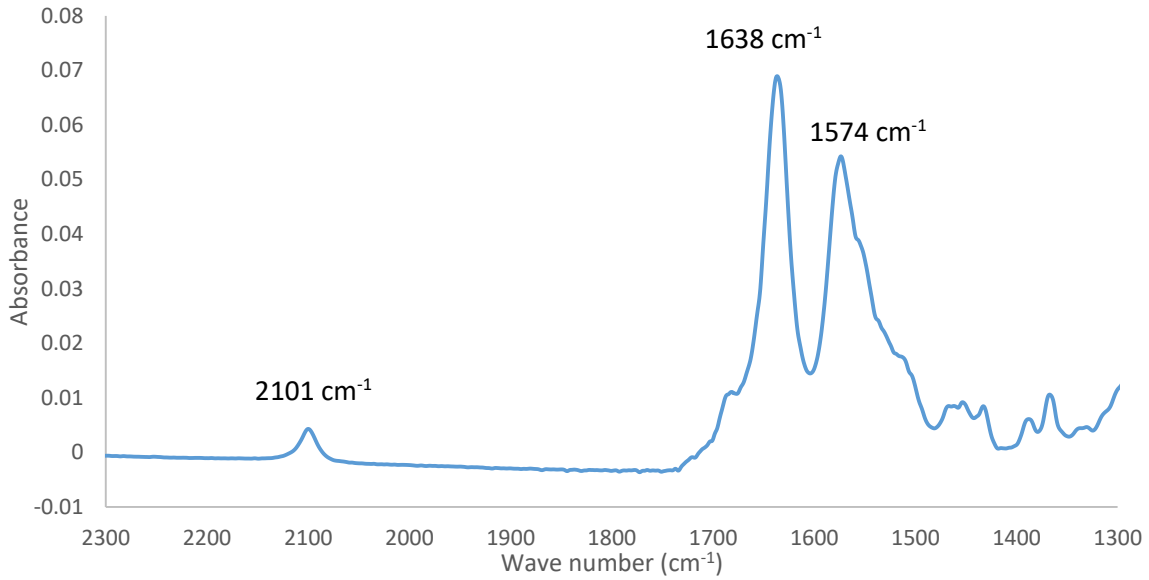

Figure 2.10 *Solid state infrared absorption spectrum of the crude material recovered after azide reduction attempt of* ***(21)***

Following the azide reduction, the obtained unpurified material was coupled with N-Succinimidyl-n-methylcarbamate in order to cap the *C*-terminus of the catalyst with a methyl- urea **(Scheme 2.6)**. The capping step however proved unsuccessful, most likely due to the low reactivity of the *C*-terminal end of the foldamer.

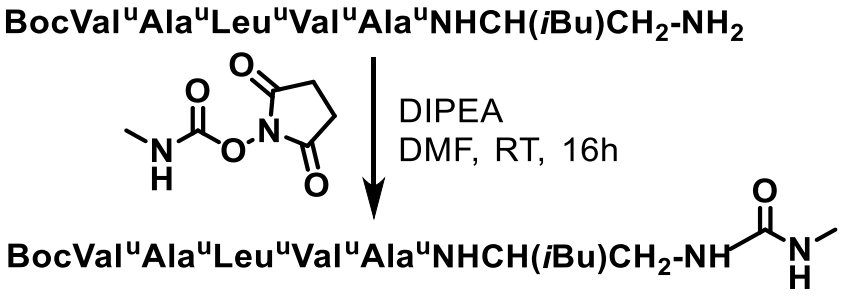

Scheme 2.6 *Reduced hexamer C-terminus capping reaction*

The azide reduction step would certainly require further optimisation and careful choice of the substrate (e.g. **21**) to access the amine-terminated oligourea in good yield and purity for optimal post-synthesis functionalization. However, access to hexamers **21** and **22** represents a substantial effort in terms of chain

extension steps as well as consumption of building blocks that need to be prepared beforehand. To save time and efforts to access **(C44)** and related analogues in sufficient yield for applications in catalysis, it was decided at that stage to temporarily abandon this strategy and move to the more traditional route.

Synthesis of catalysts (C44)-(C46):

Thus, all catalysts from this point have been synthesised with the previously reported N-methyl urea terminus introduced at an early stage to avoid complications stemming from the difficulties to transform the terminal azide. The same chain extension methodology was applied for the synthesis of all the hexamers with the first step of the synthesis being the installation of the N-methyl urea cap by reaction of building block **5c** with methylamine **(see scheme 2.7)**.

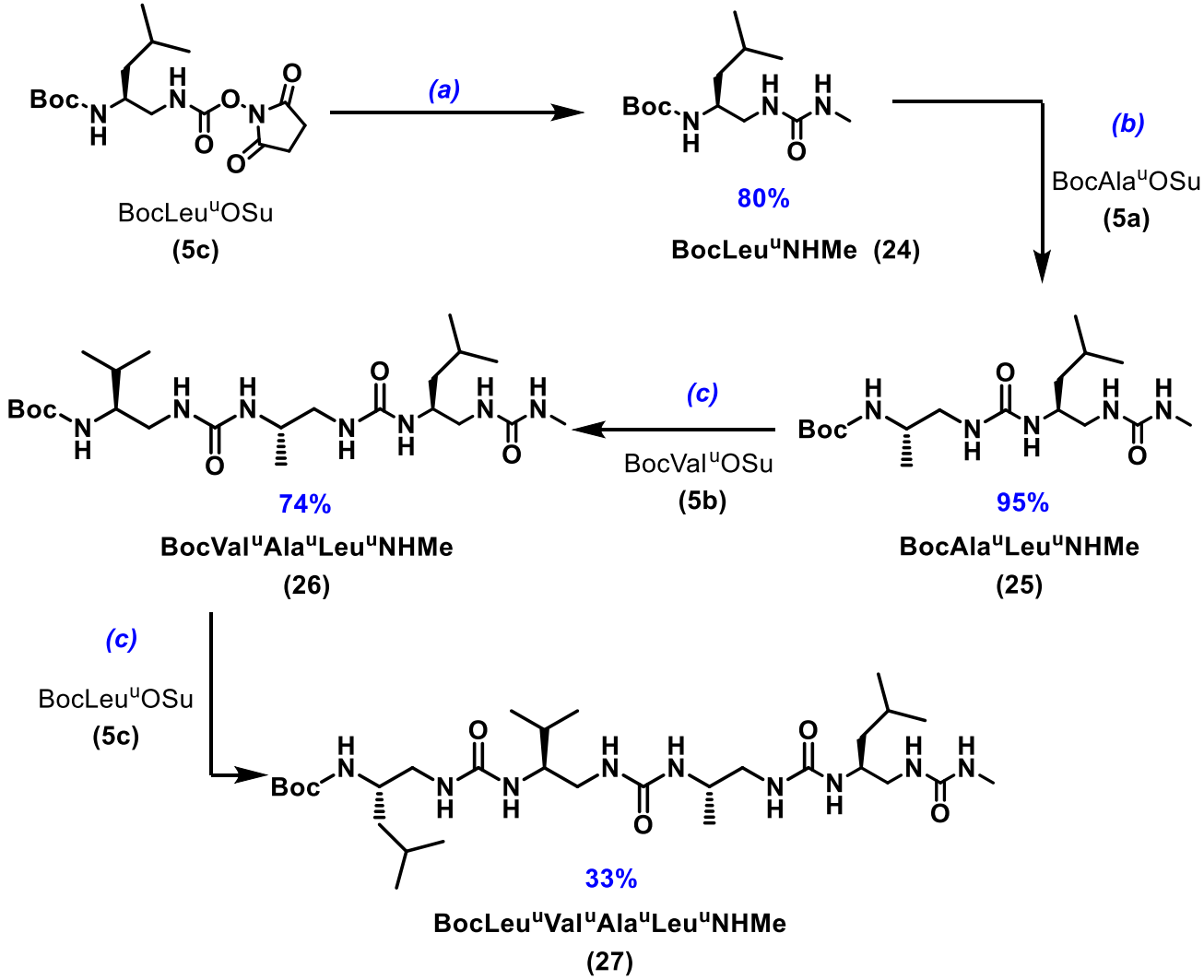

(a) 2.5eq $MeNH_2$ HCl, 5eq DIPEA, CH_3CN, RT, 4h
(b) (i) TFA, RT, 30min; (ii) 1.5eq building block, 3eq DIPEA, DMF, RT, 16h
(c) (i) TFA, RT, 30min; (ii) 1.2eq building block, 3eq DIPEA, DMF, RT, 16h

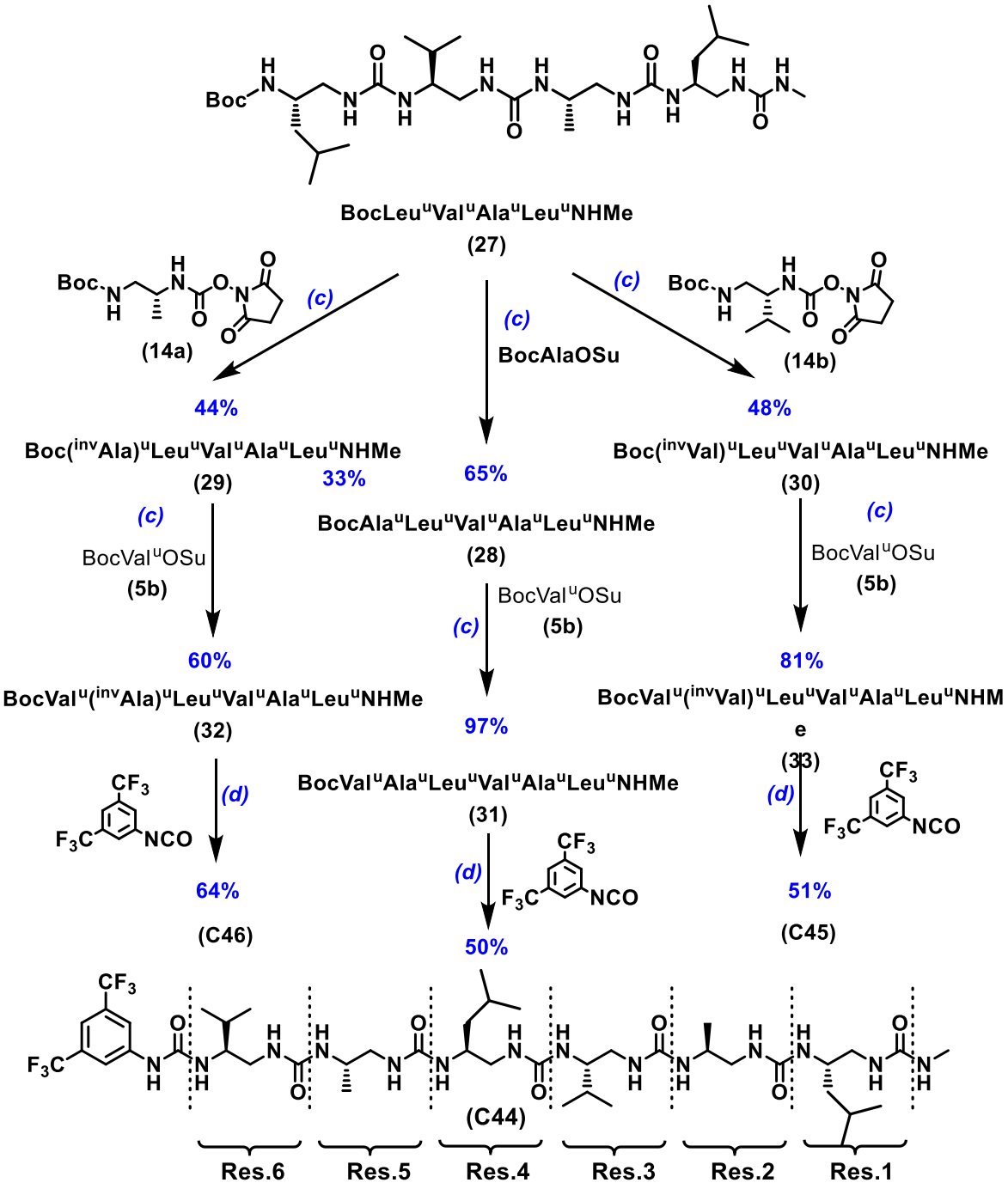

(a) 2.5eq $MeNH_2$ HCl, 5eq DIPEA, CH_3CN, RT, 4h
(b) (i) TFA, RT, 30min; (ii) 1.5eq building block, 3eq DIPEA, DMF, RT, 16h
(c) (i) TFA, RT, 30min; (ii) 1.2eq building block, 3eq DIPEA, DMF, RT, 16h
(d) (i) TFA, RT, 30min; (ii) 1.5eq $(CF_3)_2PhNCO$, 3eq DIPEA, DMF, RT, 16h

Scheme 2.7 *Synthesis of N-methyl urea terminated catalysts* ***C44-C46***

In addition to **(C44)** two new sequences were synthesised in which the nature of the side chain and the substitution pattern of the residue at the fifth position (Ala^{u}) have been modified. Catalyst **(C45)** and **(C46)** thus contain an inversed valine ($^{inv}Val^{u}$) residue and inversed alanine ($^{inv}Ala^{u}$) residue, respectively. In accordance with the previously reported results, the final residue of the catalyst was kept constant as a valine derived urea (Val^{u}) in these sequences. The modifications were introduced on the basis of the crystal

structures of the original catalyst **(C44)** and the possible impact that both side chain modification and orientation (from equatorial to axial position with respect to the helix axis) could have on the enantioselectivity of the reaction as illustrated in **Fig 2.3**. All three compounds have tetramer **27** as a common intermediate. Tetramer **27** was prepared in gram scale quantity and obtained with an 23% yield over three steps from BocLeu^{u}-NHMe **(24)**. Following Boc removal, the synthesis of **(C44)**-**(C46)** diverged with the coupling of the fifth residue. All syntheses were completed with essentially the same steps, namely the coupling of BocVal^{u}OSu **(5b)** as the sixth residue and terminal 3,5-bis-(trifluoromethyl)phenyl isocyanate.

Attempted synthesis of catalyst C47:

Concurrently, another type of modification was investigated in terms of catalyst structure that we thought could be accessible rapidly from segment condensation starting from tetramer **(27)**. The idea was to modify the H-bond properties of the catalyst **(C44)** by transforming one of the two H-bond donor sites into an H-bond acceptor site, thus introducing bifunctionality in the catalytic site (→ **C47**). In yet unpublished work, previous co-workers among the Guichard group have shown that urea groups in short oligoureas can be readily transformed into a 2,4,5-imidazolidinetrione moieties in the presence of oxalyl chloride. We anticipated that such a modification would not compromise helical folding of the main chain while changing the overall behaviour of the catalyst. When attempting to apply this reaction to our catalysts at a late stage, one possible complication was the regioselectivity. Which of the two terminal ureas would react preferentially? Could the reaction take place with one of the internal ureas, therefore breaking the helicity of the catalyst? In order to ensure control of the position of this H-bond acceptor function, the best approach was to use the common tetramer **(27)** and a dimer containing the last two residues connected by the imidazolidinetrione **(Scheme 2.8)**. The advantage of such a strategy would be to allow direct activation of the dimeric unit into the corresponding succinimidyl carbamate for subsequent fragment condensation, a strategy which is not possible with canonical oligoureas due to the formation of a biuret derivative upon activation[7].

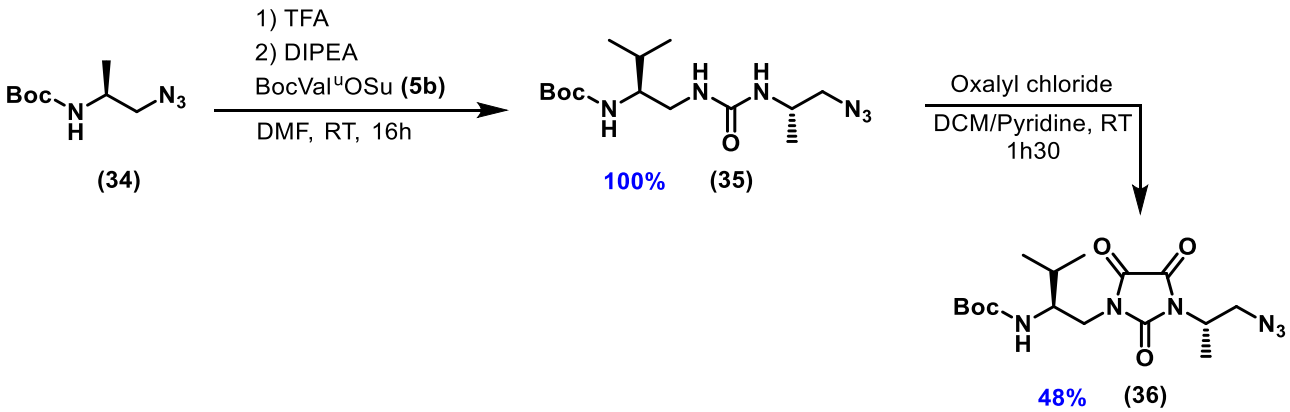

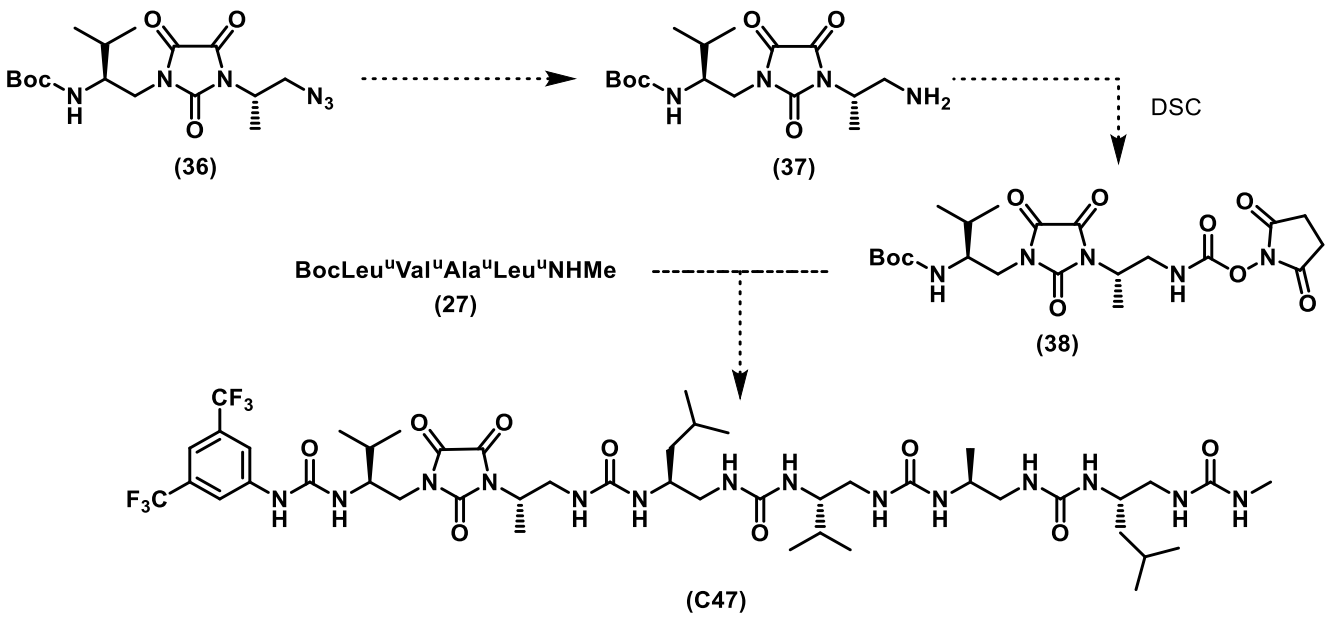

Scheme 2.8 *Planned synthesis to access oligourea* ***(C47)*** *bearing a 2,3,5-imidazolinetrione group to replace the second H-bond donor site of the catalyst* ***(C44)***.

To that effect, we used Boc-CH(Me)CH_2-N_3 **(34)** prepared from Boc-Ala-OH (in 32 % yield) as the starting point. After Boc removal, the block was coupled under standard conditions with Boc-Val^{u}-OSu to give the corresponding dimer **(35)** without difficulty. Treating the dimer with two equivalents of oxalyl chloride afforded the imidazolidine-trione motif **(36)** in fair yield (48%) **(see Figure 2.11)** which needed to be reduced and activated respectively to give compounds **(37)** and **(38)** prior to the fragment condensation with **(27)** and capping to access hexamer **(C47)**.

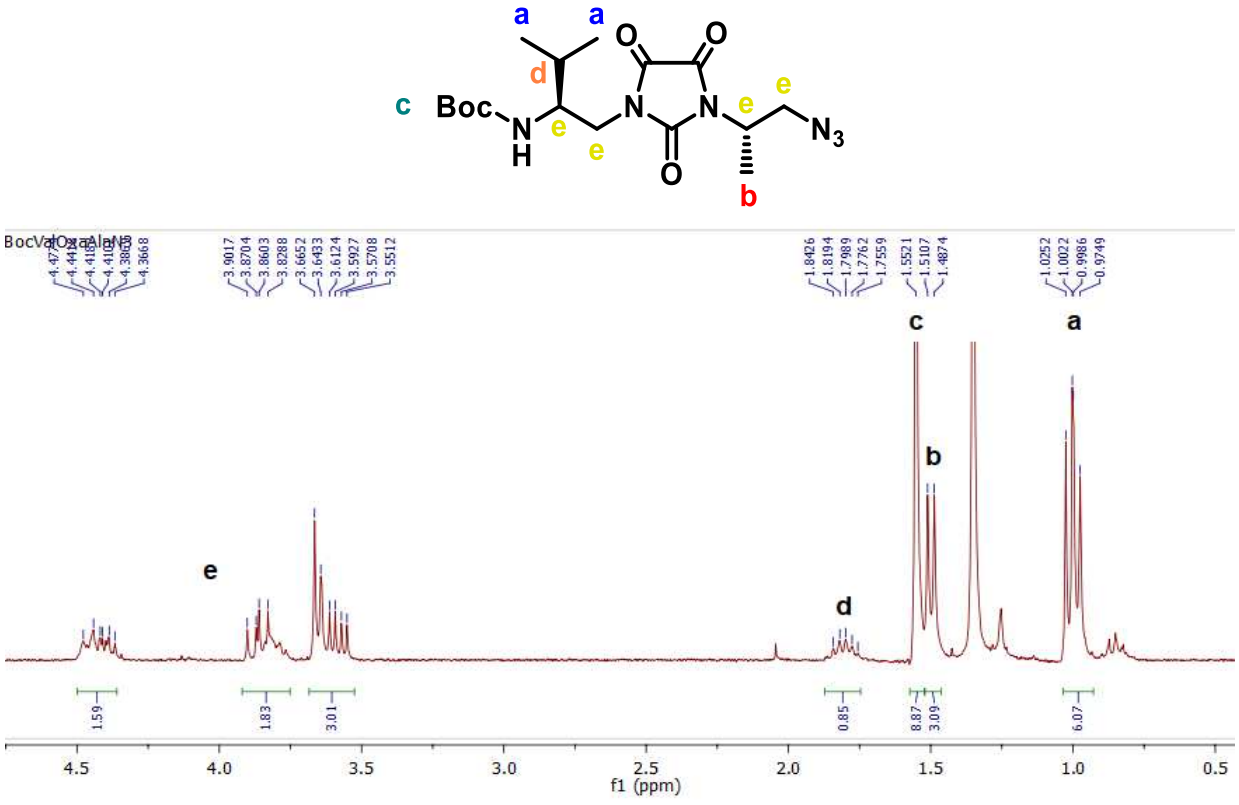

Figure 2.11 *1H NMR spectrum of the isolated* ***(36)*** *with signal attribution ($CDCl_3$, 300MHz)*

However, once again, the reduction of the azide function of this compound proved to be the most challenging step on this synthesis. As shown in **Fig. 2.12**, although several reduction methods were tried, none of the attempts were completely successful with palladium catalysed hydrogenation and triphenylphosphine reduction successfully reducing the azide (no signal at 2100 cm^{-1}) but exhibiting signs of oligourea degradation (bands at 1635 cm^{-1} and 1570 cm^{-1}) while reduction with iron (III) chloride and sodium iodide proving unsuccessful to yield the amine.

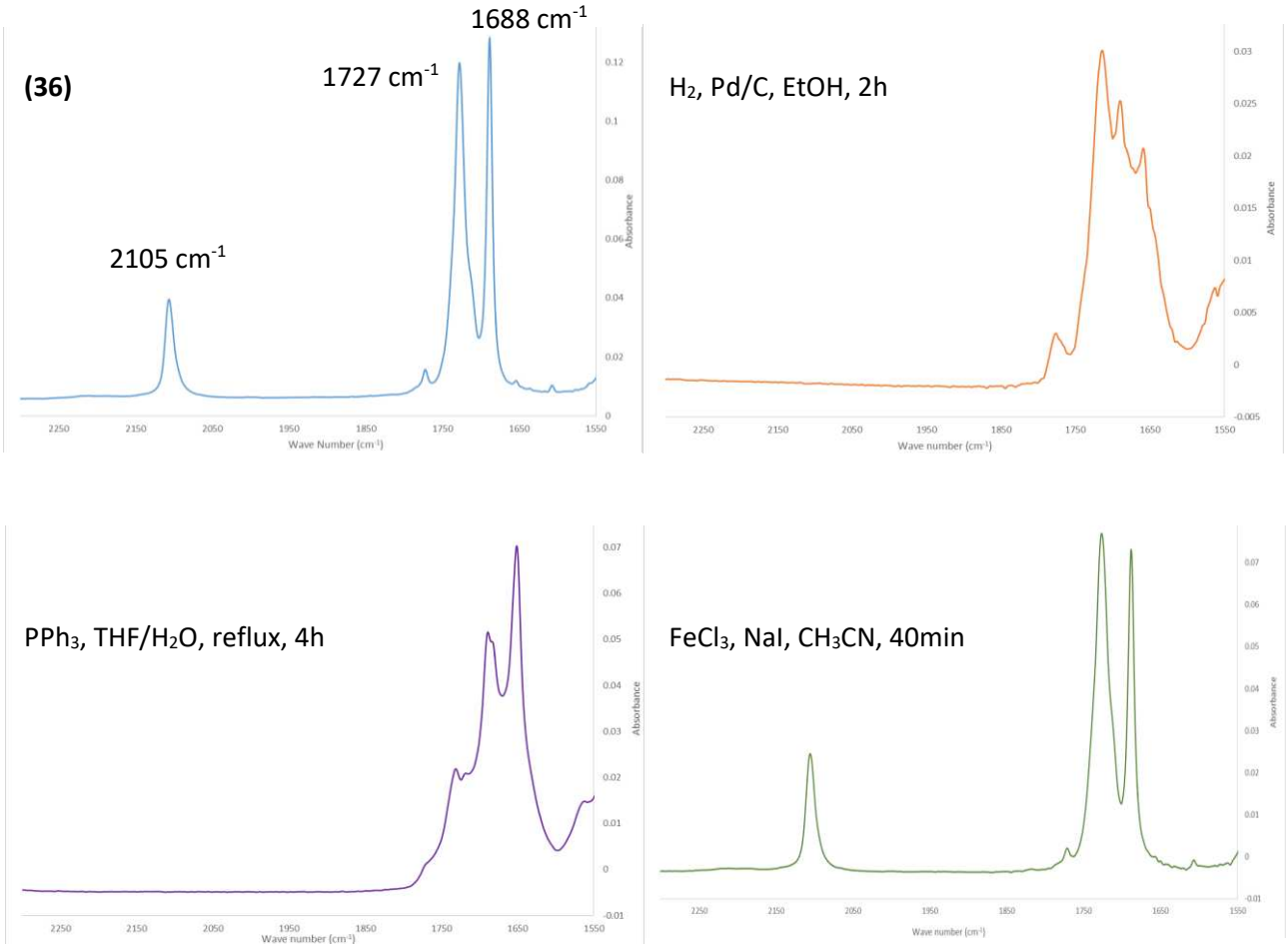

Figure 2.12 *Solid state infrared absorption spectra (1550-2300 cm^{-1}) of **36** and various azide reduction reaction crude mixtures*

Although the [M+H] signal corresponding to the desired product was observed by mass spectrometry, the free amine could not be isolated or obtained cleanly enough for carbamate activation using the reduction methods presented above. These results have caused reasonable doubt about the feasibility of the synthesis pathway that was considered for this fragment and shown that another approach is necessary in order to obtain the desired dimer with the imidazolidine-trione motif.

Synthesis of C48

Finally to evaluate the effect of reinforcing the helical conformation of the catalyst **(C44)** through the installation of more acidic NHs at the extremity distal from the catalytic site, we prepared oligomer **(C48)** bearing two consecutive thiourea linkages. Oligo(thio)urea **(C48)** was prepared in two steps from the corresponding Boc-protected hexamer previously prepared in the laboratory and whose X-ray structure was been published in 2015 **(Fig. 2.13)**. The introduction of two thiourea moieties at one extremity of the

foldamer was also expected to modulate the solubility properties of the resulting oligomer in organic solvents. Increasing the solubility of the catalysts while preserving their efficiency could help expanding their potential utility.

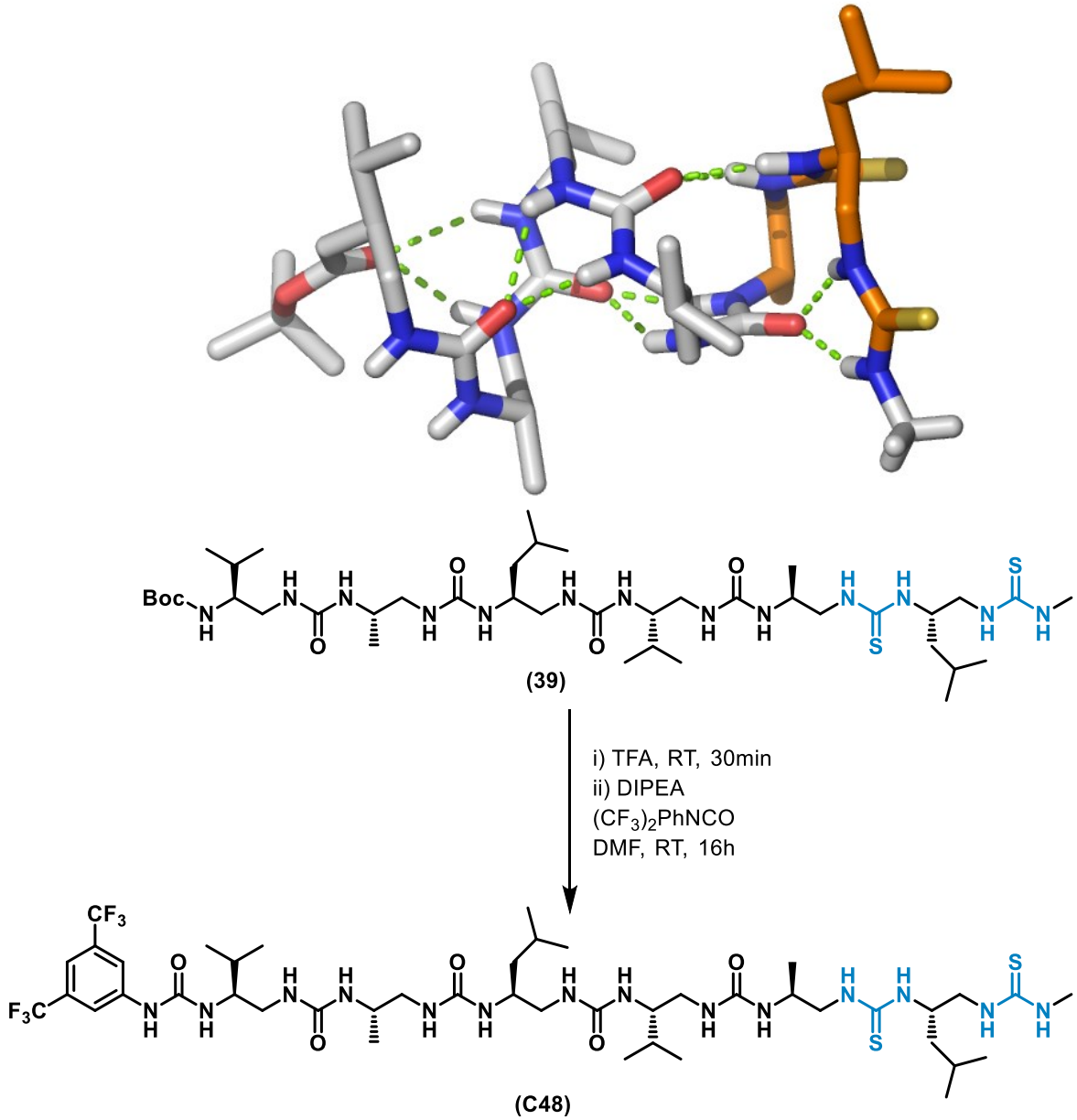

Figure 2.13 *X-ray crystal structure of precursor* ***(39)***[5] *and synthesis of catalyst* ***(C48)***

III- Catalysis tests:

Michael addition reaction of carbonyl pronucleophiles to nitroalkenes : A structure-activity relationship study.

With the new catalyst structures in hand and sequences already available in the group, one of our first objectives was to investigate whether the already excellent results obtained previously by the team could be improved even further. Should no improvement be possible, some insight could be gained from the modification of one of the active site's residues due to the nature and position of the side chain.

In an effort to gain better insight into the relationship between the structure of our oligourea catalysts and the obtained reactivity, the new sequences were compared to the original catalyst. Foldamer **C44** was the most active catalyst in the group's published work with an isolated yield of Michael addition adduct of 86% and 95% *ee* at a 0.1 mol% catalyst loading in the presence of 10 mol % Et_3N) and was thus taken as reference during the entirety of our studies **(see Table 2.2)**.

Influence of the termini:

The impact of the *C*-terminus modification of the oligourea catalysts was studied by replacing the two ultimate ureas of reference catalyst **C44** moieties by their thiourea counterpart in catalyst **C48**. As this change is taking place away from the catalytic site and should therefore have a limited influence on reactivity and enantioselectivity themselves but the stability of the helix as well as its solubility in apolar solvents could be improved owing to the terminal thioureas.

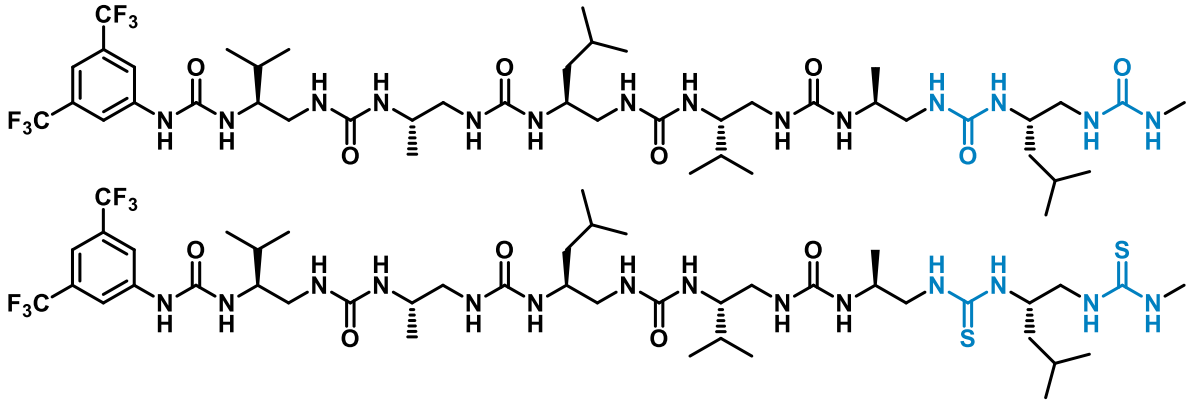

Entry	Catalyst	Conversion (%)	Yield (%)	*ee (%)*
1	**C44**	100	86	95
2	**C48**	100	80	87

Table 2.2 *Influence of the C-terminus modification of* ***C44***

Using both catalysts, full conversion was achieved after 48h and isolated yields were within experimental error range. However, a slight reduction of the enantiomeric excess was observed when using catalyst **C48,** indicating that the *C*-terminus of the catalyst did have a measurable influence.

The influence of the N-terminus of the catalysts was studied through two types of modifications: the *p*-methoxyphenyl activating group (**C49**) was compared to the previously studied capping groups (**C44** and **C50**)[4] and the function between the N-terminus cap and the terminal residue (**C52**, **C53**) was also probed.

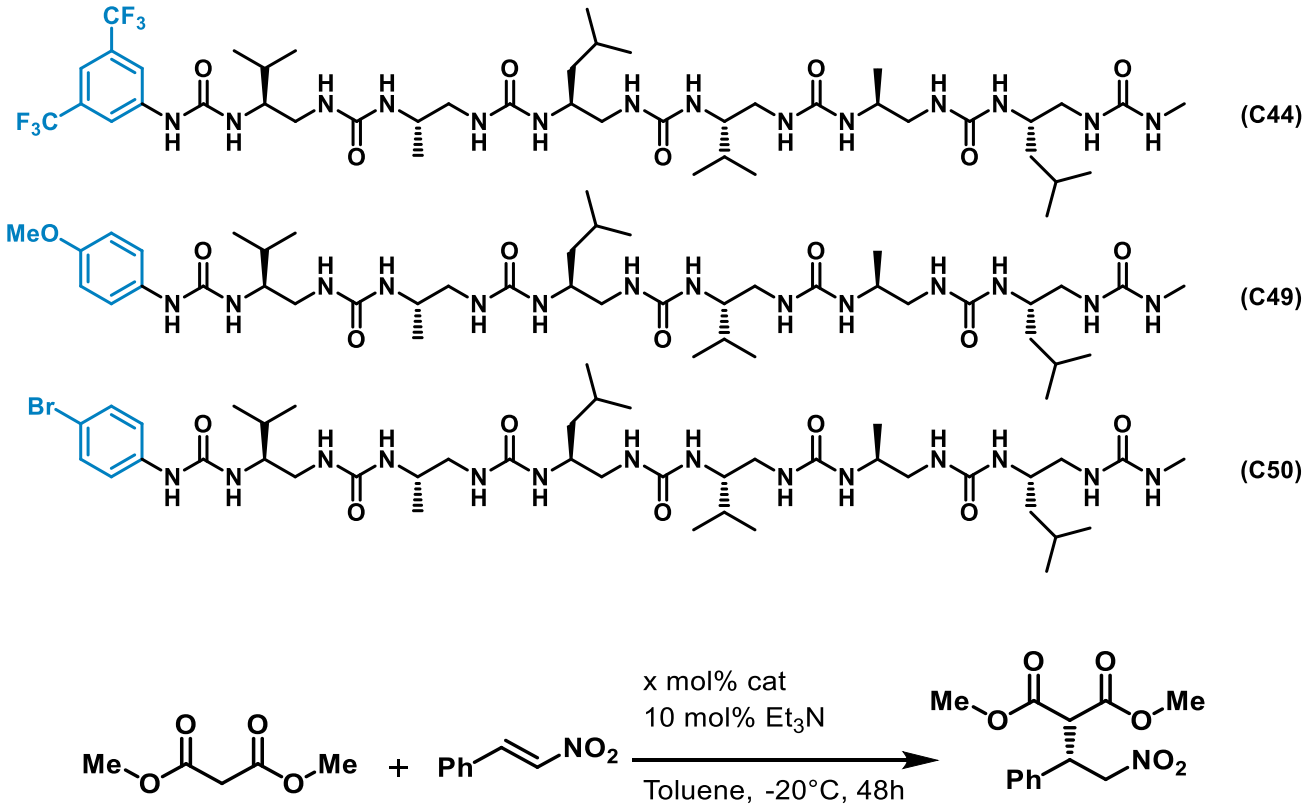

Entry	Catalyst	Loading (mol%)	Conversion (%)	*ee (%)*
1	**C44**	0.1	100	95
2	**C49**	0.1	60	65
3	**C50**	0.1	62	68
4	**C44**	0.001	67	74
5	**C49**	0.001	32	29
6	**C50**	0.001	27	18

Table 2.3 *Influence of the N-terminus cap*

Three different *N*-terminus cappings with an increasing electron withdrawing effect have now been compared: most usually employed 3,5-bis-(trifluoromethyl)phenyl **(C44)** was compared against less electroattractive groups *p*-bromo-**(C50)** and *p*-methoxy- **(C49)**. Starting with a 0.1 mol% loading, catalysts **C49** and **C50** resulted in a similar reduction of selectivity, respectively leading to a 30% and 27% loss *ee*. Lowering the catalyst loading to 0.001 mol% led to a drastical loss of enantioselectivity with both catalysts while also showing some differentiation between the two capping groups. Combining the results that were obtained, the nature of the N-terminal capping unit has a profound effect on the selectivity of the reaction which is more apparent at lower loadings. The finding that the highest enantiocontrol is obtained with the

most electron withdrawing termination can be attributed either to an increase of the acidity of the first two ureas responsible for the catalysis resulting in an increased interaction with the substrate, to the electron withdrawing effect causing a stronger differentiation of these two urea functions or to a combination of these effects.

Another factor that should have a major impact on the activity of the catalyst is the nature of the H-bonding groups at the active site. To that end, previously synthesised tetramer catalyst **C52** containing a squaramide and **C53** containing a sulfamide at the catalytic site was compared to its urea counterpart **C51.**

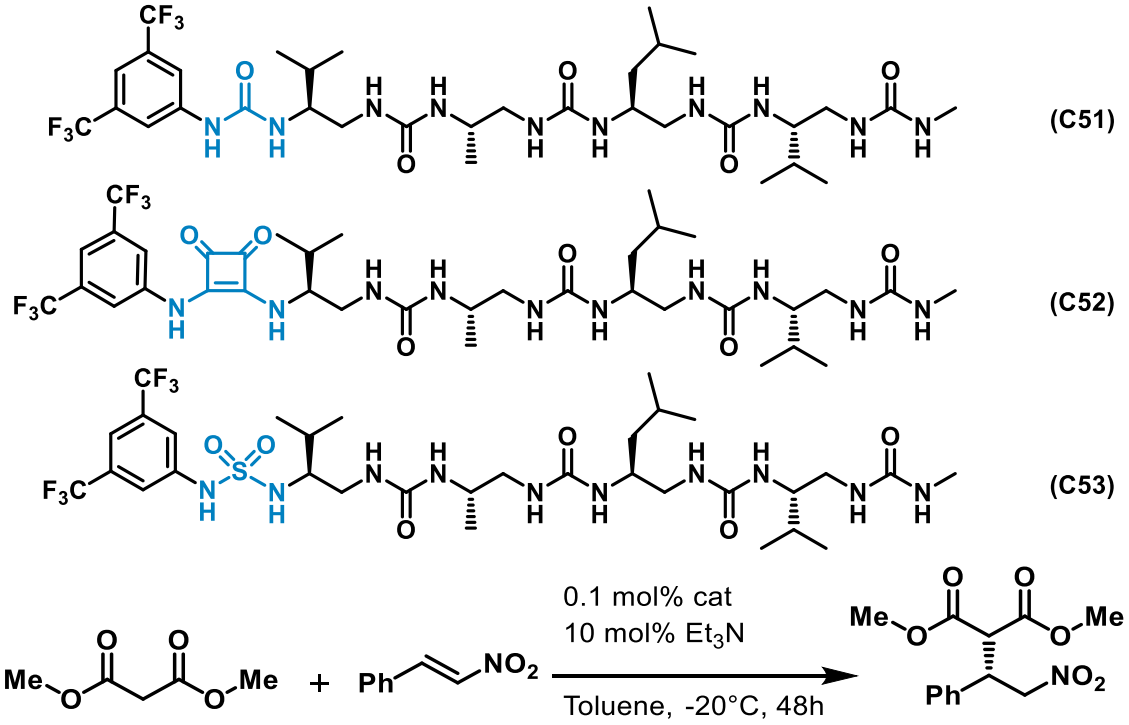

Entry	Catalyst	H-bond donor	Conversion (%)	*ee (%)*
1	**C51**	Urea	57	36
2	**C52**	Squaramide	21	12
3	**C53**	Sulfamide	19	16

Table 2.4 *Influence of the terminal H-bond donor*

As evidenced by the results presented in the table above, the nature of the H-bond donor at the *N*-terminus of the catalyst does indeed have a severe influence on the reaction as both the reactivity and the selectivity were impacted by the modification of the final urea function. This result is in line with the previous experience of the group as blocking one of the two –NH groups of the ultimate or penultimate urea resulted in reduced reactivity and almost complete loss of enantioselectivity **(Scheme 2.9)**[4]. Another aspect that may play a role independently of the different H-bonding donor properties of the new group introduced at the last position is the orientation of the terminal H-bonding group with respect to the rest of the helix. This parameter may indeed be affected by the different nature of the building block and its different ability of the H-bonding acceptor groups to be engaged in the intramolecular network. X-ray crystallography of these catalysts could be particularly useful to gain additional insight into lack of reactivity and enantiocontrol of these catalysts.

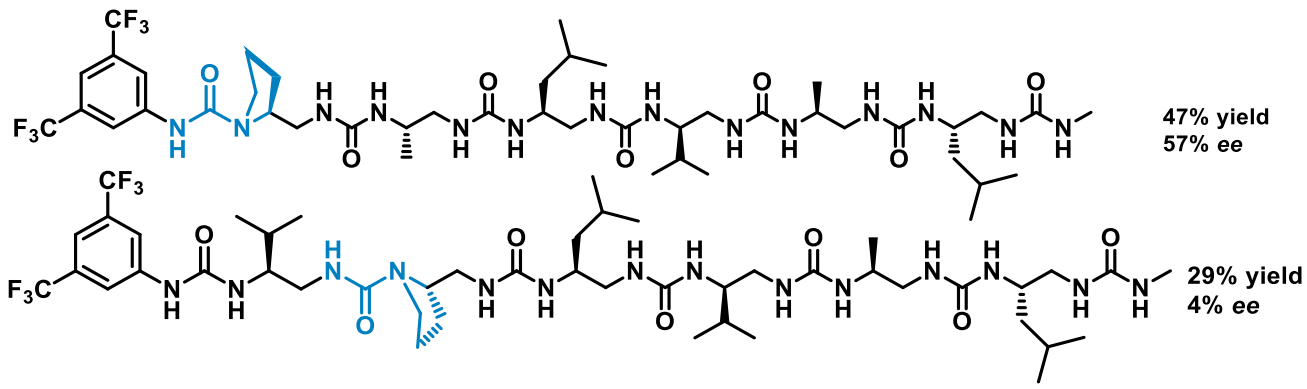

Scheme 2.9 *Effect of blocking one or the other H-bonding donor site on catalysis* [4]

Influence of the side chains

Studies on the influence of the side chain have previously been initiated by the group in the first report on oligourea-based catalysis[4]. These initial studies focused on two modifications of the final residue. Substituting the isopropyl side chain with a benzyl group **(Table 2.5, entry 4)** or completely removing the side chain **(Table 2.5, entry 5)** had little impact on the conversion and only slightly reduced the selectivity. Here we asked whether introducing a bulkier side chain such as a *tert*-butyl group instead of the isopropyl side chain could have a more substantial effect. This modification was introduced in the sequence of oligourea catalyst **C44' (Figure 2.14)** bearing a thiourea termination. As can been seen in **Table 2.5**, this modification has little effect on the conversion and *ee*. Surprisingly, the introduction of both the side chain (*i*Pr → *i*Bu) and a variation in the substitution pattern, i.e. shifting the side chain of the first residue to the α carbon with an inversion of stereochemistry, resulted in a drastical loss of stereoselectivity while the conversion remained at comparable levels to the other catalyst **(Table 2.5, entry 6)**.

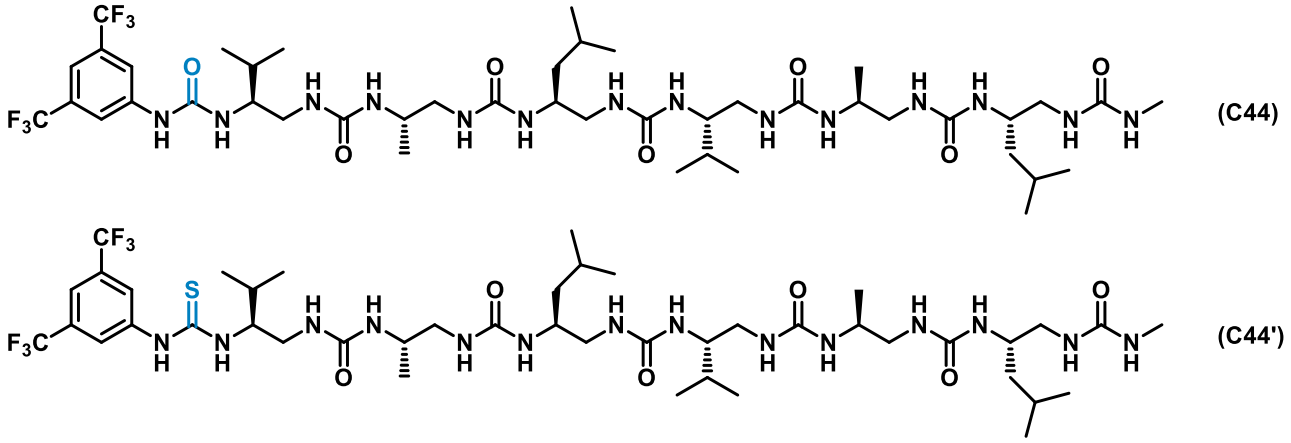

Figure 2.14 *Reference catalyst* ***C44*** *and thiourea variation* ***C44'*** *used in previous published works*

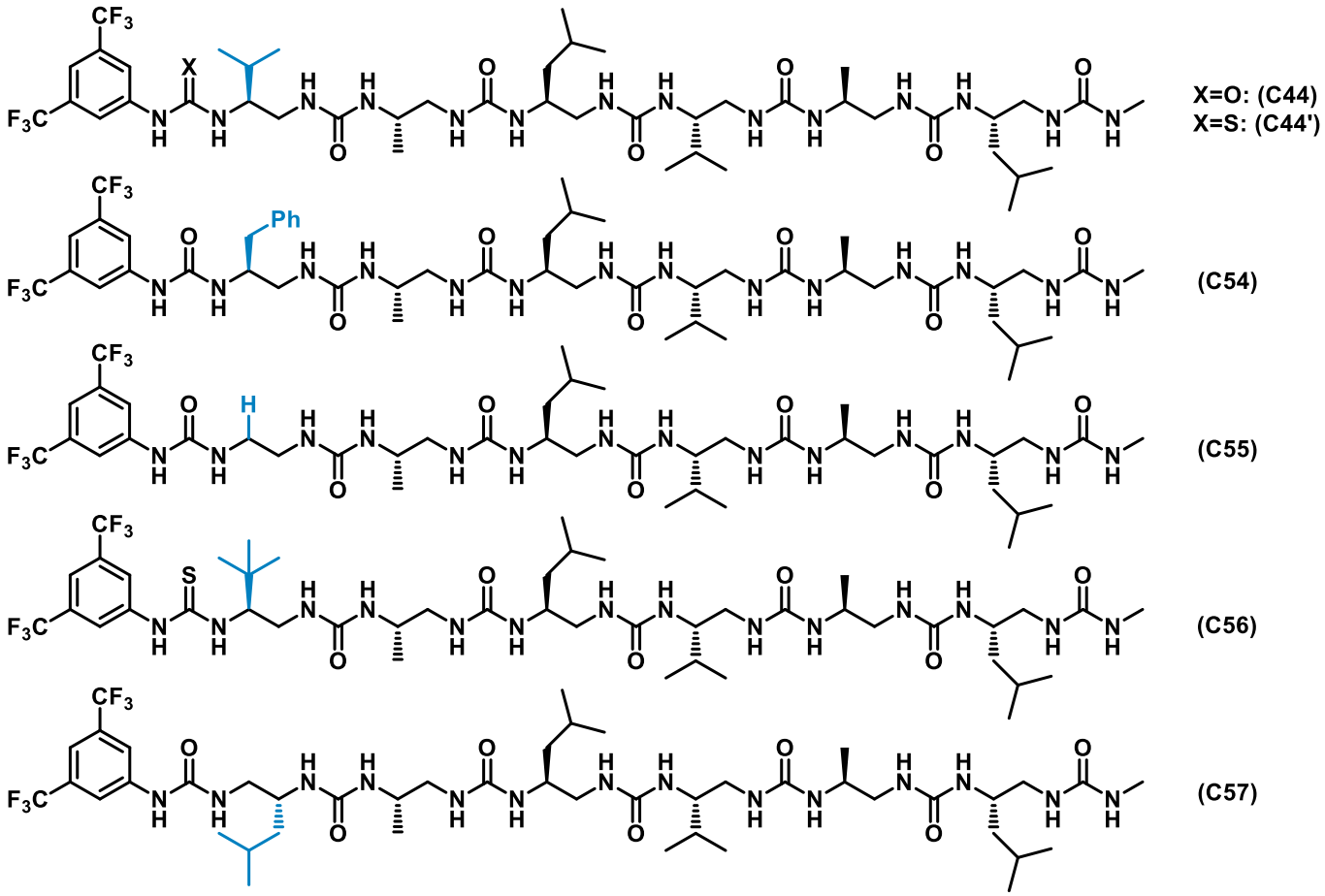

*Catalysts **C44**, **C44'**, **C54** and **C55** have been used by the team in the works published in 2017* [4]

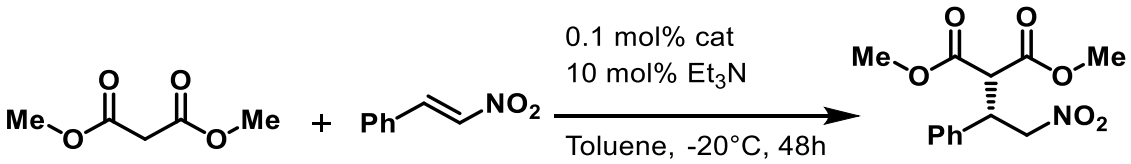

Entry	Catalyst	Conversion (%)	*ee (%)*
1	**C44**	100	95
2	**C44'**	98	93
3	**C56**	100	86
4	**C54**	92	83
5	**C55**	94	88
6	**C57**	89	8

***Table 2.5** Influence of the side chain from residue 6*

Modification of the side chain of the penultimate residue was then determined as the most logical way to continue this structure-function study. For catalysts **C45**, **C46** and **C58**, the residue in second position was once again displaced one carbon further as well as using a monomer derived from the non-natural amino acid of (D) configuration. This set of modifications was decided after examination of the crystal structures from previously synthesised oligoureas, with the idea that this modification could orient the side chain in an axial position and would point towards the catalytic sites. This change was predicted to modify the steric

hindrance that is present at the second urea and possibly improve the enantioselectivity of the reaction. Together, these catalytic tests will come to complement the previous results obtained by the team with the objective to better understand the origin of the high selectivity exhibited by the oligourea foldamers in this reaction.

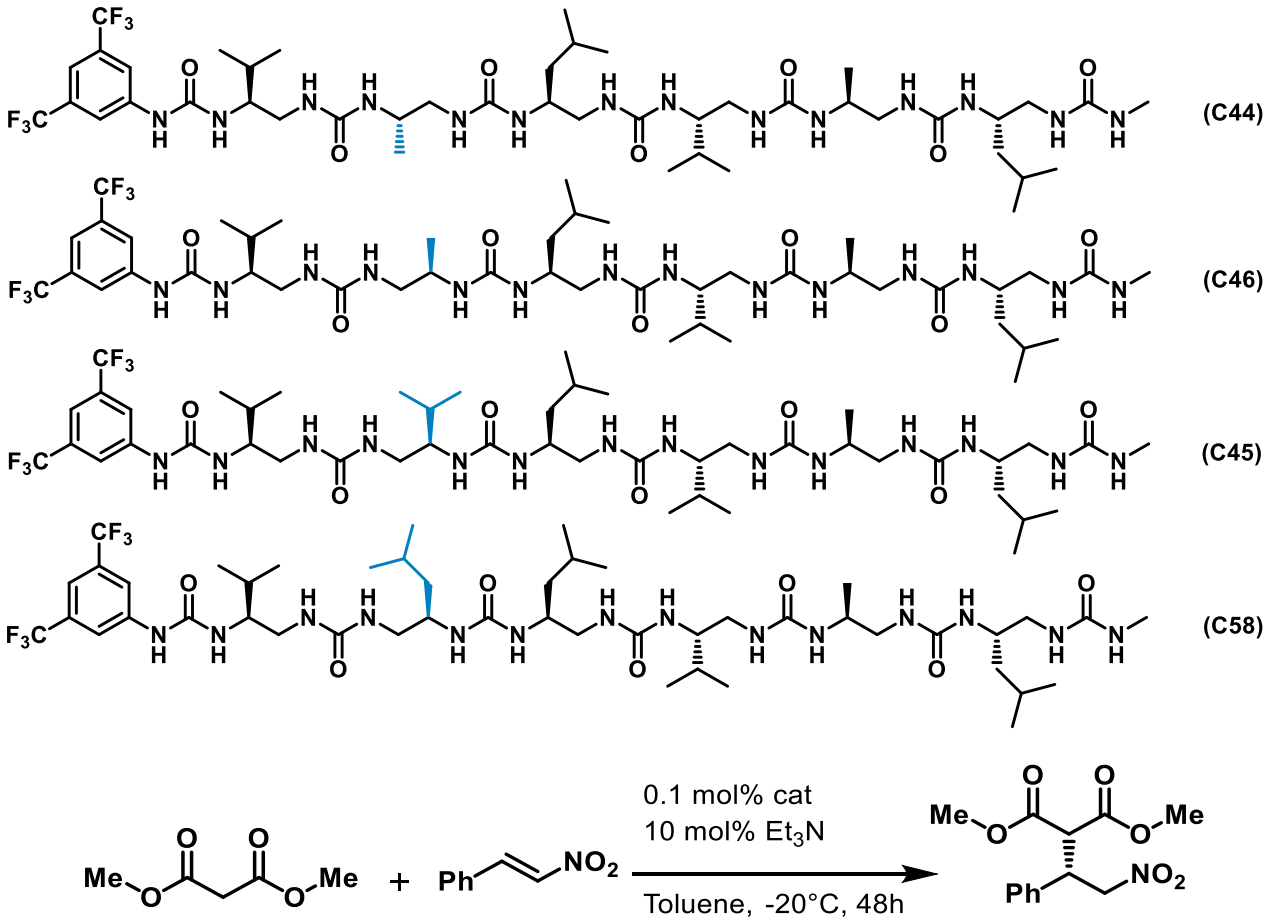

Entry	Catalyst	Conversion (%)	Yield (%)	*ee (%)*
1	**C44**	100	86	95
2	**C45**	100	78	78
3	**C46**	100	77	84
4	**C58**	100	90	70

Table 2.6 *Michael addition results with different foldamer catalysts*

From these results, we can see that shifting the side chain of the penultimate residue from the α- to the β-position and simultaneously reversing the chirality of the residue is tolerated but none of the newly tested catalysts could actually outperform the previously obtained optimal catalyst sequence **C44** for the tested reaction. The conversion was not affected although in two cases the isolated yields were slightly lower. As for enantioselectivity, the catalyst that gave the highest *ee* remained catalyst **C44**. Out of the newly tested catalyst structures, **C46** with a methyl side chain led to a 10% lower *ee*. Changing the side chain from a methyl to an isopropyl group (**C45**) led to a 17% lower *ee* and sequence **C58** gave the lowest selectivity with a 25% lower *ee*. This difference in enantioselectivity shows that the modification of the substitution pattern

(shift from α to β position) with the association of a bulkier side chain in second position in the hexamer seems to decrease the selectivity of the reaction. Still the use of alternate α-substituted residues is much better tolerated at this position than at the terminal position where enantiocontrol was almost completely lost, probably due to unwanted conformational reorganisation at the helix terminus.

While the catalysts tested in this work certainly gives some insight into the requirements to design successful oligourea catalysts, they however show no specific improvement over catalyst **C44** at least in the tested reaction and by using Et_3N as the Brønsted base co-catalyst. Our current understanding of the exact workings of this type of catalyst in the addition of malonates to nitro-olefins remains quite insufficient and while the process of iteration through different catalyst structures does allow us to gain insight into the important parameters of the catalyst structure, it appears to be a slower approach resembling the slow improvement of enzymes observed in Nature. This process could be accelerated by a better understanding of the exact way the catalyst interacts with the different reaction partners and the structure of the transition state during the enantiodetermining step. Such an understanding can be obtained from theoretical modelling which could help with better catalyst structure prediction for an accelerated optimisation. Initial theoretical studies concerning the interactions between the reaction partners and energy optimisations are ongoing in partnership with the CAPT group (IPREM, Université de Pau et des Pays de l'Adour). Current results have been obtained after a global optimisation search with a C44 analogue pentamer oligourea, (1*E*)-3-Methyl-1-nitro-1-butene as the electrophile, the deprotonated diethylmalonate as the nucleophile and triethylamine as the base. Probing the possible binding modes of the two reactants with the catalyst individually has revealed that the site [2] is favoured by the electrophilic species, leading to a stabilisation of 18 kcal/mol. As for the nucleophilic species, the most favourable binding mode was obtained when the malonate was astride on the two sites resulting in a stabilisation of 25 kcal/mol. However, considering the two reactants simultaneously, optimal stabilisation resulted from the nucleophile binding exclusively to site [1], thus clearly indicating a bifunctional activation by the catalyst. Additionally, this most energetically favoured structure promotes the formation of the C-C bond between the two reactants as the optimised C-C distance was calculated at 3.69Å. **(Fig.2.15)** (All calculations by Yaidel Toledo-González and Philippe Carbonniere)

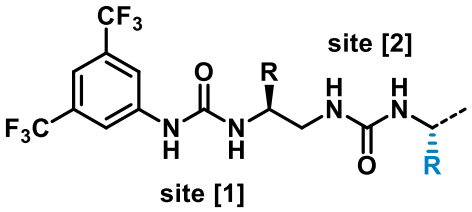

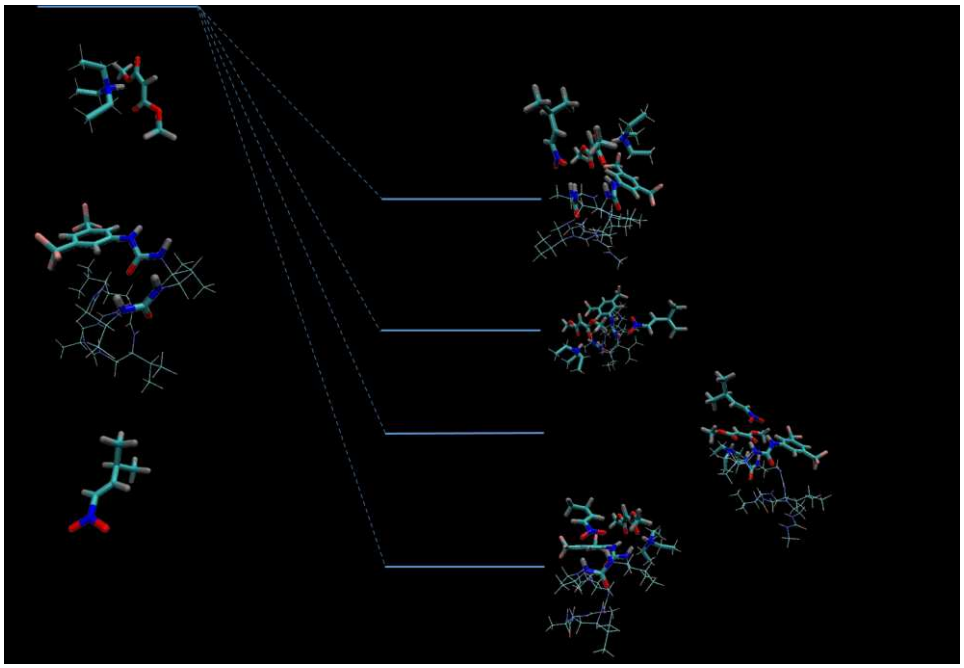

Figure 2.15 *Binding energies (kcal/mol) for the deprotonated malonate as the nucleophile and the nitroalkene as the electrophile on the oligourea catalyst and calculated C-C bond length between reactants. (B3LYP-D3/6-31+G(d,p) (diffuse functions for N, O, F and carbonyl group of the malonate) level of theory, SMD model for the toluene)*

Extension of reactivity

Beside structure-activity relationship studies and attempts to further optimize catalysts in the Michael addition of malonates to nitro-olefins, one of the ideas of the current project was to evaluate whether we can expand the scope of such catalysts. Extending the already tried reactivity seemed to be the next step in this new field for the team. Following the report in 2017 by Palomo *et al* in which the group presented a bifunctional squaramide catalysed Michael addition of β, γ-unsaturated ketones to nitro-olefins with excellent site-, diastereo- and enantioselectivities[8] **(Scheme 2.10)**, we thought the application of oligourea foldamer catalysts to this reaction could prove interesting.

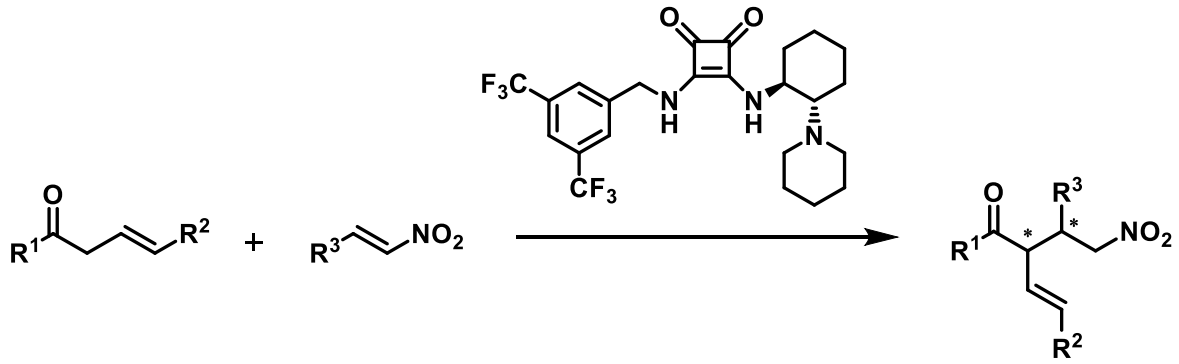

Scheme 2.10 *Bifunctional squaramide catalysed β, γ-unsaturated ketone Michael addition to nitro-olefins*

With the Palomo group reporting the exclusive formation of the α-addition product as well as diastereomeric ratios up to 20:1 and 97% *ee*, the application of our catalysts to this reaction could answer a number questions in comparison with a bifunctional H-bond/Brønsted base catalyst. Some of the points of interest would be the suitability of the combination of the foldamer catalyst with an external base instead of the two coming from the same catalyst and would this new system also present some parallel α/γ selective addition? Should the reaction give promising results, would the optimal catalyst structure be the same as in the previous Michael addition reaction? Could conjugated enoyl nucleophiles become viable candidates instead of their skipped counterparts in this type of reaction by using a stronger base in combination with the foldamer catalyst? **(See scheme 2.11)**

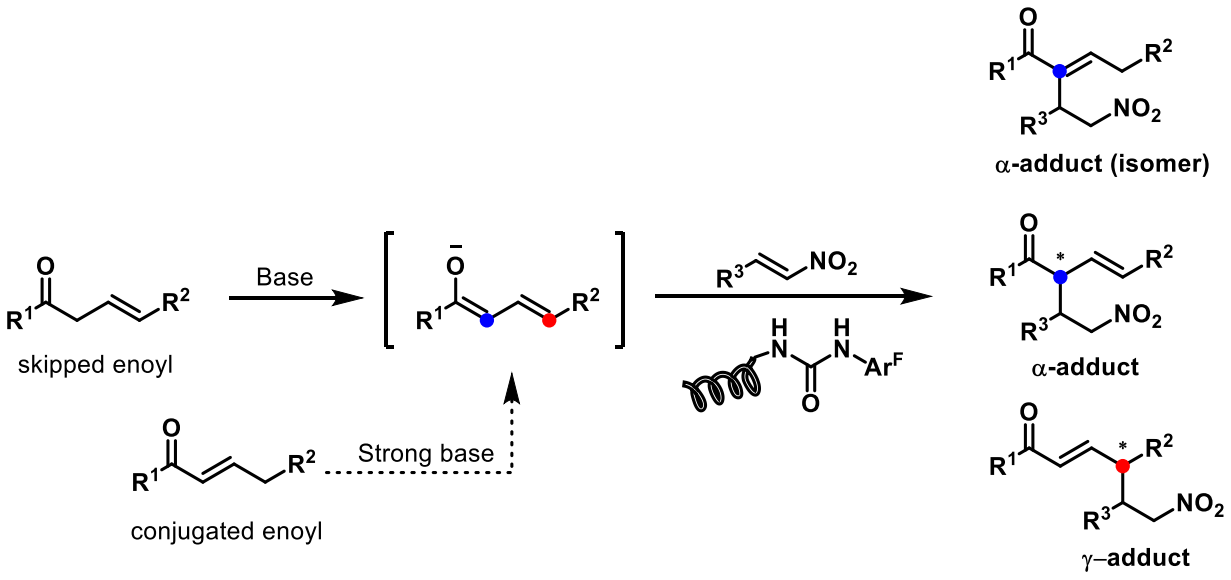

Scheme 2.11 *Foldamer catalysed Michael addition of β, γ-unsaturated ketones to nitro-olefins*

The reaction was tested using commercial nitrostyrene as the electrophile while a simple electrophile was synthesised. β,γ- unsaturated ketone **(40)** was obtained cleanly and in one step by cross-coupling between methyl vinyl ketone and benzaldehyde according to the procedure described by Palomo *et al*[8]. **(Scheme 2.12)**

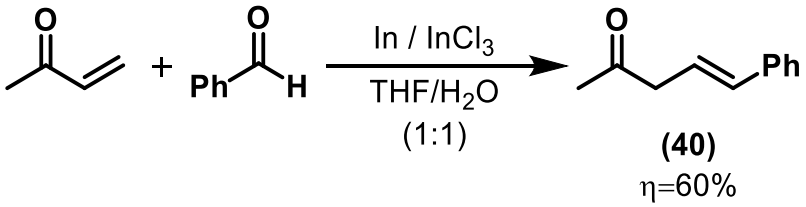

Scheme 2.12 *Synthesis of the testing nucleophile*

With both reaction partners available, initial testing was launched between the skipped enone and nitrostyrene only to ensure no background reaction was taking place. After 6 hours at ambient temperature, no reaction was detected and 0.5 mol% of catalyst **C44** was added to the reaction mixture and stirred for an additional 16h. Again, no reaction has taken place, thus proving that the foldamer catalyst alone cannot promote the reaction. As a result, 30 mol% triethylamine were added and after stirring for 6 hours at room temperature, 63.2% conversion was obtained by ^{1}H NMR spectroscopy. In a second experiment, nitrostyrene and the enone were treated with only 30 mol% of triethylamine at room temperature for 6 hours resulting in 73% conversion taking place. These two results taken into account, the base seems to be the key part for any reactivity to take place while the catalyst could serve as the source of stereoselectivity.

Influence of the solvent:

Oftentimes in catalytic reactions, the solvent plays an important role in either the reaction rates or selectivity or both. The solvent that was used for the exploratory reactions was the same as the one that was used by the Palomo group in their report. Indeed, dichloromethane was used in all catalytic experiments involving this reaction under their bifunctional catalyst. However, in order to determine whether the foldamer catalyst had an influence on this reaction, its rate had to be reduced in order for the catalyst to have any possibility of useful interaction. To that end, the first parameter that was investigated was the nature of the solvent.

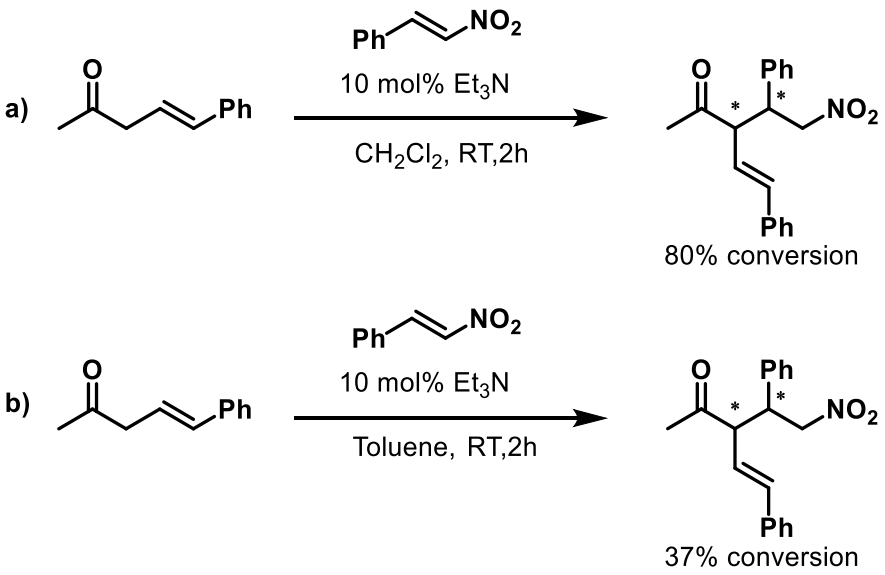

Scheme 2.13 *Testing the influence of the solvent*

As H-bonding catalysts are usually not compatible with protic solvents, ethers or aromatic solvents are often preferred for this type of reactions. In the case of our oligourea foldamers, the optimal solvent to minimize racemic background reaction for the Michael addition was identified as toluene. As shown by **scheme 2.13**, going from dichloromethane to toluene as a solvent has reduced the conversion of the addition reaction from 80% to 37% in two hours at room temperature, more than a 2x reduction over the same amount of time. However, the speed of the racemic reaction was possibly too high for the catalyst to have a useful impact on selectivity, therefore, tweaking other parameters of the reaction to slow it down even more was necessary

Influence of the temperature:

Another important parameter in asymmetric, and more generally, catalytic reactions is temperature. As it has a crucial impact on kinetics, changing the temperature of the reaction could allow for a sufficient reduction of the rate of the background racemic reaction resulting in a set of optimal reaction parameters for the evaluation of the foldamer catalyst's activity.

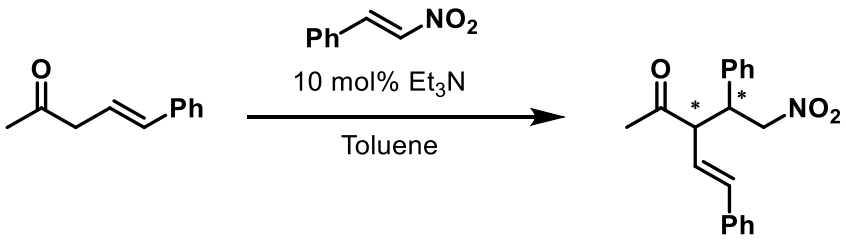

Entry	Temperature	Time	Conversion
1	24°C	2h	37%
2	24°C	4h	51%
3	-20°C	2h	24%
4	-20°C	4h	32%

Table 2.7 *Influence of the temperature of the reaction*

To determine the influence of the temperature, the reaction was ran under identical time and base loading conditions with one tube being kept in a controlled ambient temperature room while the second was immersed in a bath kept at a constant -20°C. After two hours, the ambient temperature reaction had reached 37% conversion while the low temperature reaction showed 24% conversion. After four hours, the ambient temperature reaction reached 51% conversion whereas the cold temperature only achieved 32% conversion. Thus, while the initial reaction rate remains steep, the overall speed of the reaction was greatly reduced by changing the solvent and temperature parameters in order to have any observable catalyst activity.

Influence of the base:

The initial parameters that were chosen to test this new reaction have been based on the optimal conditions that were previously obtained during the addition of 1,3-dicarbonyl compounds to nitro-olefins. Therefore, a 30 mol% loading for the base was carried over. As well as the loading, the nature of the base was also kept the same as the one that generally gave the best results for the abovementioned reaction. After optimisation of the solvent and temperature parameters, we turned to investigating the last parameter before evaluating the oligourea foldamer catalysed reaction.

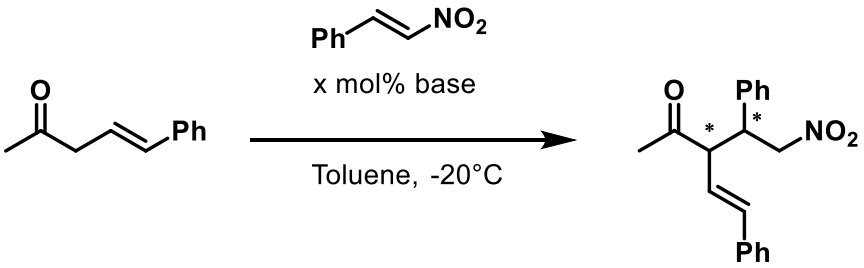

Entry	Base	Loading	Time	Conversion
1	Et_3N	10 mol%	2h	24%
2	Et_3N	10 mol%	4h	32%
3	Et_3N	5 mol%	2h	18%
4	Et_3N	5 mol%	4h	22%
5	Et_3N	1 mol%	2h	8%
6	Et_3N	1 mol%	4h	13%
7	DIPEA	5 mol%	2h	< 1%
8	DIPEA	5 mol%	4h	12%

Table 2.8 *Influence of the base on the addition reaction*

After the preliminary tests that were conducted, the loading of triethylamine was lowered to 10 mol% to mimic the loading described by Palomo *et al*. This value was taken as reference instead of the 30 mol% that was used initially. In an attempt to slow the base mediated reaction further, lowering the loading of the base to 5 mol% reduced the conversion by 25% in two hours and 31% in four hours **(Table 2.8 entries 1&3; 2&4)**. Going down to 1 mol% triethylamine resulted in a 66% reduction of the conversion in two hours and a 60% reduction of conversion in four hours. These reaction rates were deemed as optimal to proceed with the oligourea catalyst and obtain some amount of effect from it.

In order to test if the nature of the base that was used had an impact on the reaction, triethylamine was substituted with diisopropylethylamine (DIPEA) as it was another base that gave excellent results in the

previous Michael addition reaction. Using 5 mol% DIPEA resulted in less than 1% conversion in two hours and only 12% conversion in four hours, therefore proving that the nature of the base had an important role on the kinetics of the reaction.

Evaluating foldamer catalyst activity:

With the previous experiments, the base mediated undesired reaction was able to be reduced enough for our oligourea foldamer catalyst to show potential activity. With these parameters fixed, the reaction was investigated using a 1 mol% loading of oligourea **C44** and monitored by ^{1}H NMR. By observing the signals in the 6.55-6.40ppm region (in $CDCl_3$), we can see a chemical shift change between the H_γ of the starting enone **(Fig 2.15a&b, red)** and that of the addition product **(Fig 2.15b, blue)**. The conversion of the reaction can be obtained by the ratio of the integrals for the starting material and the addition product. As well as the conversion, another information that can be gained by this method is the α/γ selectivity that results from the presence of the catalyst.

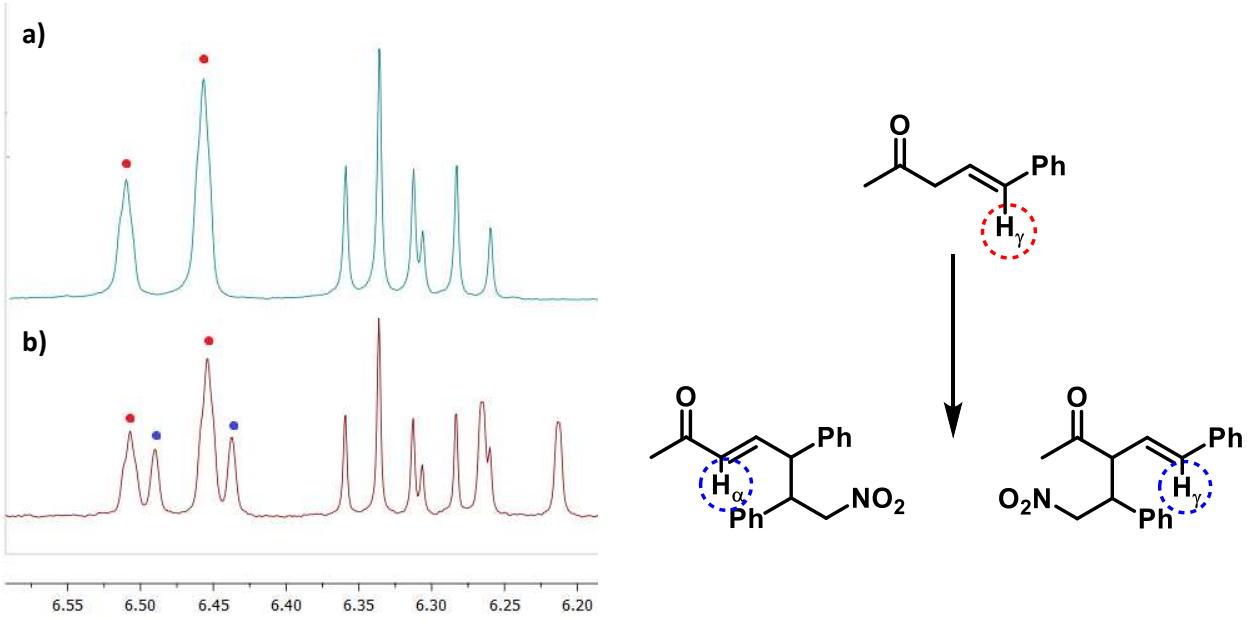

Figure 2.15 *Determination of the reaction conversion by ^{1}H NMR analysis of respective signals of the expected products*

Figure 2.16a shows the double triplet signals corresponding to the alkenyl proton H_β of the starting material surrounded in red while **Figure 2.16b** shows the area of interest for the interpretation of the reaction results. Shown in green is the doublet corresponding to the alkenyl proton H_β of the γ-addition product and in blue, the set of signals corresponding to the H_β protons for the two α-addition product epimers (attributions shown by Palomo *et al*[8]). In the case of **Figure 2.16b**, an α/γ gamma addition ratio of 3:1 was observed. From these observations, direct comparison of the reaction mixture between the foldamer catalysed and uncatalysed reactions can be established by sampling an aliquot from both of the reaction vessels and analysing it without further purification.

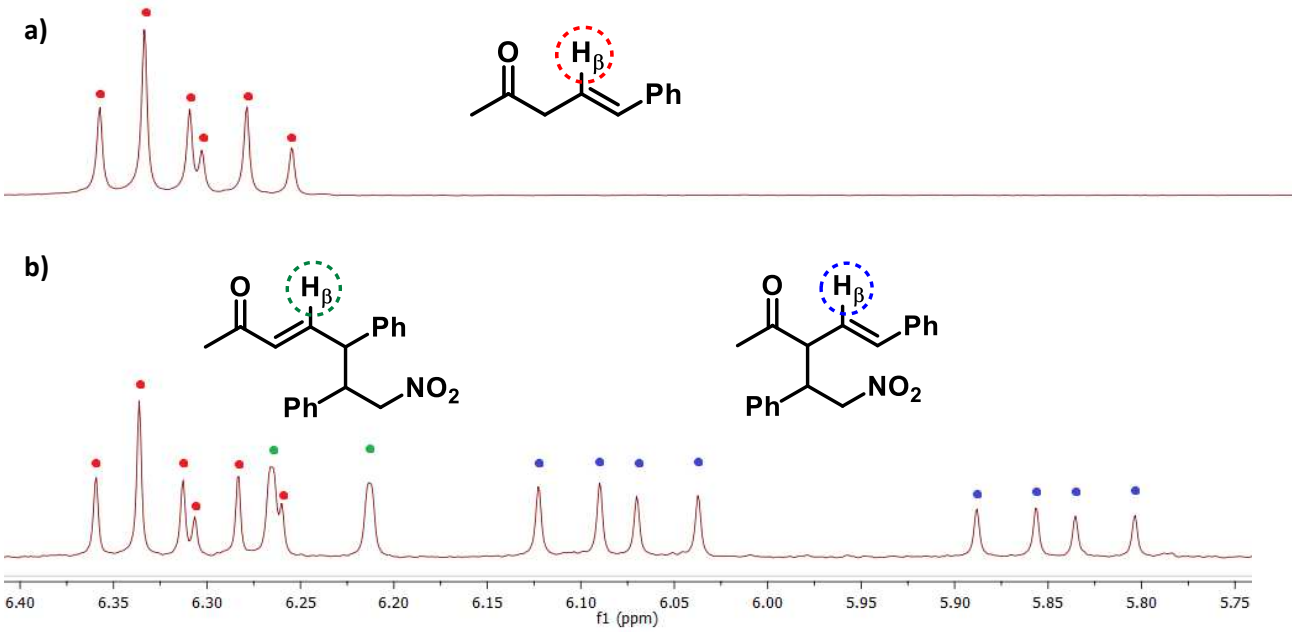

Figure 2.16 ^{1}H NMR analysis of selectivity (Reaction conditions: Table 2.8 entry 1, NMR conditions:$CDCl_3$, 300MHz)

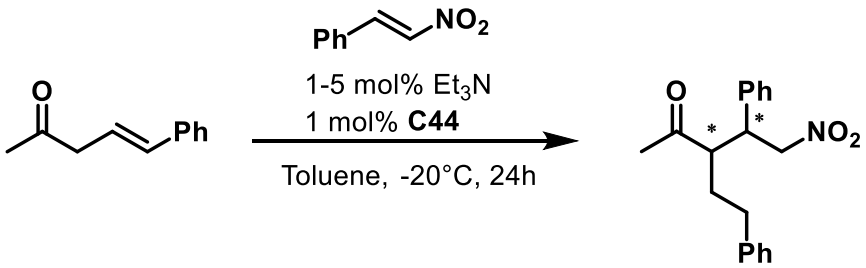

Entry	Et_3N loading	Time	Cat. Conversion	Uncat. Conversion
1	5 mol%	2h	23%	18%
2	5 mol%	4h	28%	22%
3	5 mol%	24h	29.5%	40%
4	1 mol%	2h	12%	8%
5	1 mol%	4h	15%	13%
6	1 mol%	24h	28.6%	27.6%

Table 2.9 *Vinylogous enolate addition to nitro-olefins using foldamer catalyst*

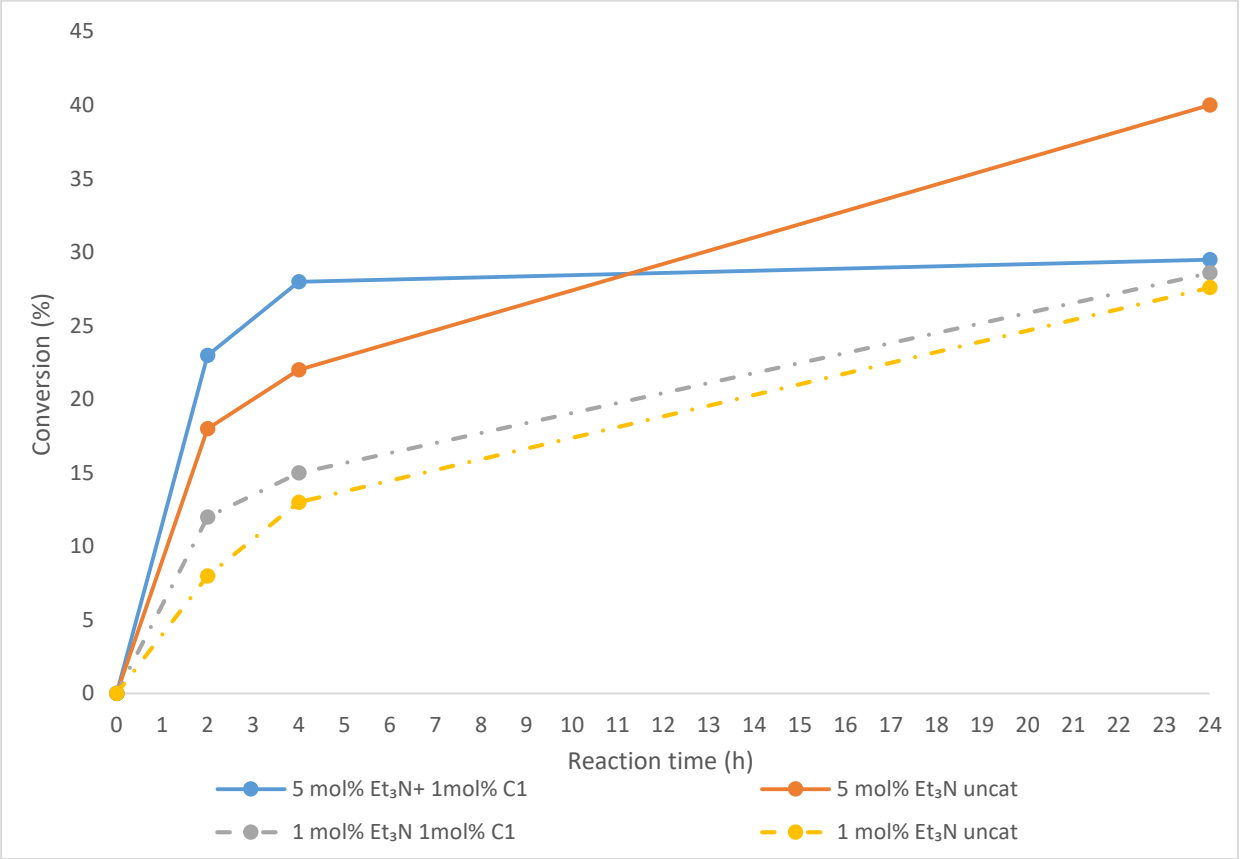

Figure 2.17 *Monitoring of conversion (determined by starting material signal consumption by ^{1}H NMR)*

Two series of reactions, catalysed and uncatalysed, were ran in parallel for 24 hours at -20°C with 5 mol% and 1 mol% Et_3N respectively. An aliquot taken from the reaction at an interval of 2h, 4h and 24h was analysed by ^{1}H NMR according to the process explained above. The obtained data, plotted in **Figure 2.17**, indicates that while the initial reaction rate (0h to 2h) of the foldamer catalysed reaction is slightly higher, some inhibition seems to take place after the 2h mark. The observed inhibition appears to be much more important with a 5 mol% base loading than a 1 mol% base loading indicating that the inhibition mechanism involves the base.

These results taken together point out that although they are extremely active when all the parameters are ideal, oligourea foldamer catalysts cannot simply be used in a broader range of reactions without preliminary studies on the mode of action for these species. Although we had hoped to discover a broader application to our catalysts, the latest results prove that this class of catalyst acts in a highly substrate selective manner, thus not showing the excellent results obtained in the case of 1,3-dicarbonyl compound additions to nitro-olefins.

References

[1] V.Semetey, C. Didierjean, J.P. Briand, A. Aubry, G. Guichard, *Angew. Chem. Int. Ed.* **2002**, *41*, 1895-1898

[2] N. Pendem, C. Douat, P. Claudon, M. Laguerre, S. Castano, B. Desbat, D. Cavagnat, E. Ennifar, B. Kauffmann, G. Guichard, *J. Am. Chem. Soc.* **2013,** *135*, 4884-92.

[3] V. Diemer, L. Fischer, B. Kauffmann, G. Guichard, *Chem. Eur. J.* **2016,** *22*, 15684-15692; R. Wechsel, J. Raftery, D. Cavagnat, G. Guichard, J. Clayden, *Angew. Chem. Int. Ed.*, **2016**, *55*, 9657-9661; R. Wechsel, M. Zabka, J.W. Ward, J. Clayden, *J. Am. Chem. Soc.*, **2018**, *140*, 3528-3531

[4] D. Becart, V. Diemer, A. Salaün, M. Oiarbide, Y. R. Nelli, B. Kauffmann, L. Fischer, C. Palomo, G. Guichard, *J. Am. Chem. Soc*,. **2017**, *139*, 12524−12532

[5] Y. Reddy Nelli, S. Antunes, A. Salaun, E. Thinon, S. Massip, B. Kauffmann, C. Douat, G. Guichard, *Chem. Eur. J.*, **2015**, *21*, 2870-2880

[6] G. Guichard, V. Semetey, C. Didierjean, A. Aubry, J.P. Briand, M. Rodriguez, *J. Org. Chem.*, **1999**, *64*, 8702-8705

[7] V. Semetey; C. Didierjean; J.P. Briand; A. Aubry; G. Guichard, *Angew. Chem. Int. Ed.***, 2002**, *41*, 1895-1898

[8] I. Iriarte, O. Olaizola, S. Vera, I. Gamboa, M. Oiarbide, C. Palomo, *Angew. Chem. Int. Ed.*, **2017**, *56*, 8860 –8864

Chapter 3

I- Anion binding:

The covalent bond and its formation is a topic that has been at the centre stage of synthetic chemistry, the presence and importance of charged species in all manners of transformations should not be forgotten. When learning from Nature and enzymes and the tremendous work they accomplish, it should be underlined that many of their substructures and the cofactors that take part in enzymatic processes are, in fact, ionic species.[1] It stands to reason that for these processes involving charged substrates to take place, a way to recognise and interact with them is a necessity. While both positively and negatively charged species can be involved, we will focus more specifically on anions and their interactions with larger structures. Noncovalent modes of interaction with anions have been extensively studied[2], spanning from the demonstration that in addition to cation-π interaction, certain aromatic surfaces can also interact with anions through their π* orbitals. This type of interaction between electron deficient aromatic rings and anions was demonstrated to be theoretically favourable by Bartberger and co-workers[3] as well as the Elguero group[4] and supported by crystal structures studied by Deyà and co-workers[5].

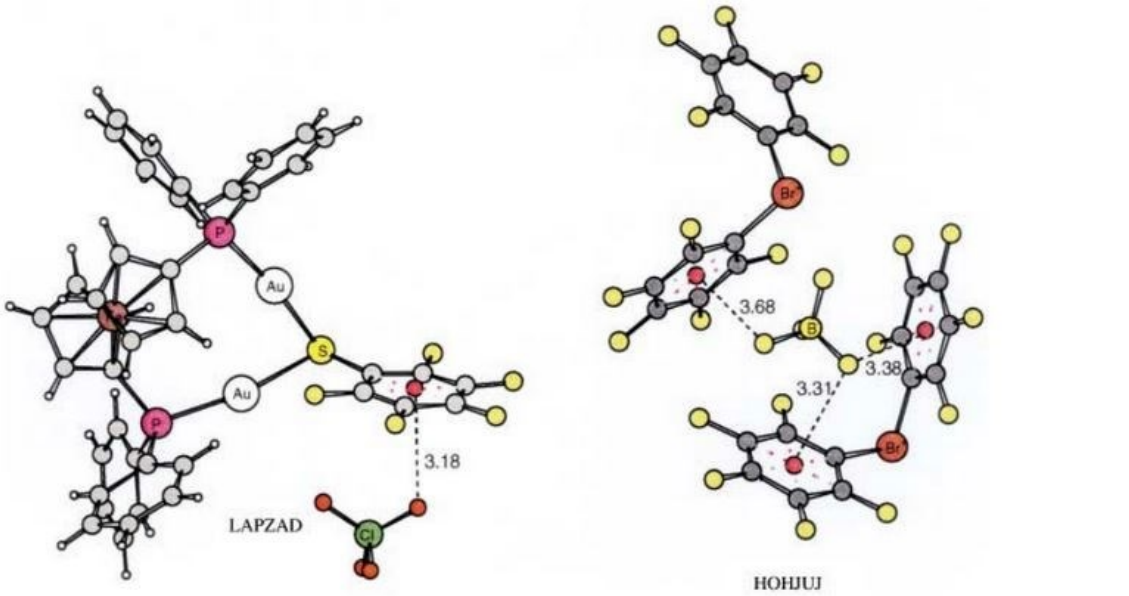

X-ray crystal structures of $[(Ph_2PC_5H_4)_2FeAu_2SC_6F_5][ClO_4]$ (LAPZAD)[31] and $[(C_6F_5)_2Br][BF_4]$ (HOHJUJ); distances in Å.

Figure 3.1 *X-ray crystal structures demonstrating anion-π interaction[5]*

Although this novel type of binding charged species was demonstrated both theoretically as well as through studies of older x-ray structures, it has remained fairly scarce until recently. Recent research[6] has shown that this overlooked non-covalent interaction may also find some applications in catalysis[7] The interaction mode that has seen the highest amount of use and success in the field of noncovalent interactions is the H-bond. Many structures containing H-bond donating motifs have been described interacting with neutral and charged species.[2,8] Hydrazone-based receptors such as the ones presented in **Fig. 3.2a** have been show to bind dihydrogen phosphate[9] while (thio)urea and squaramide unit containing structures have been used in the recognition or binding of halides and oxoanions such as HSO_4^-, OAc^- and NO_3^- **(Fig. 3.2b)**[10] or other charged species of interest such as cyanide.[11]

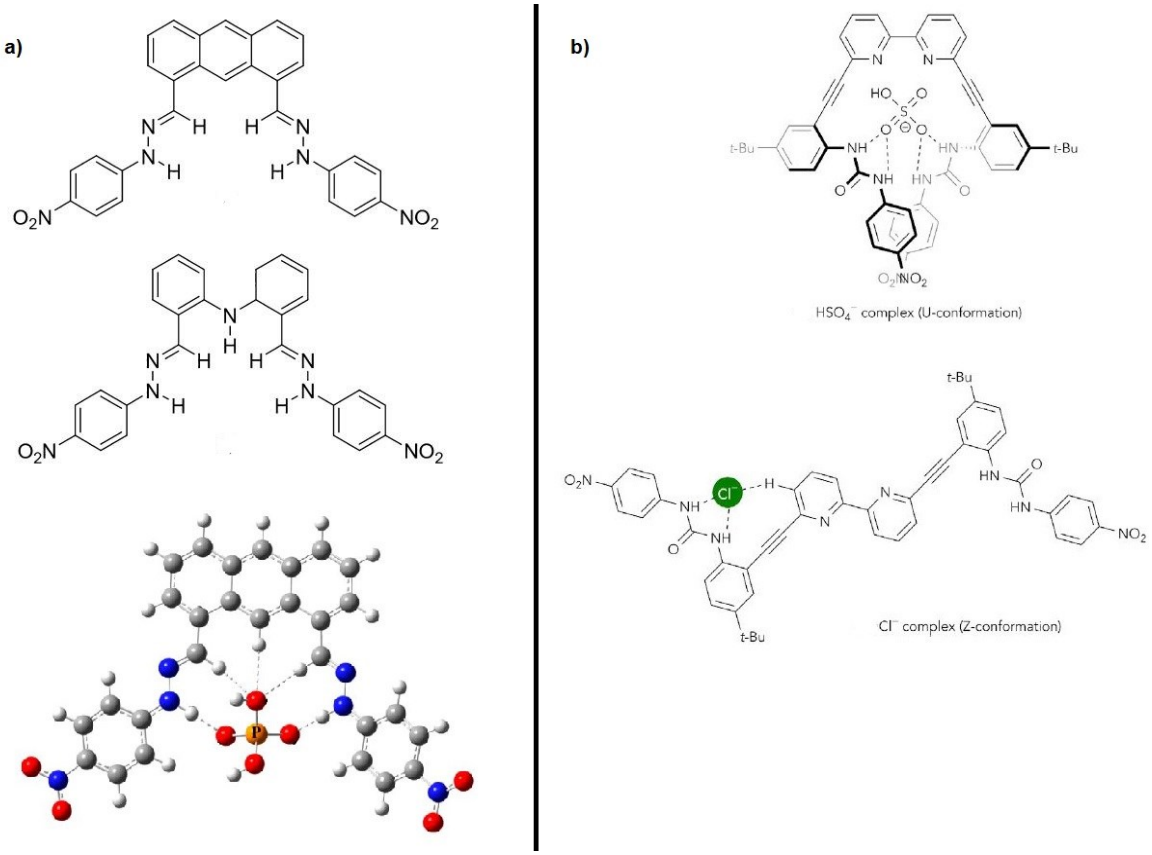

Figure 3.2 *Examples of H-bond anion receptors*

The field of noncovalent interactions with anions is, of course, not limited to the previously mentioned types of bonds. Other interactions such as halogen[12] or chalcogen bonding[13] have also been described, although less frequently.

The discovery and study of macromolecular structures able to recognise or bind anions has allowed for a deeper understanding of the complex active sites in enzymes and underlined some important parameters in the recognition process: the directionality of the H-bonds implicated in the interaction as well as the geometry of the binding site and its compatibility with the geometry of the targeted anion. These considerations resulting from extensive investigation into noncovalent interactions have provided tools for the application of these principles to other fields, such as catalysis.

II- Applications in catalysis:

While most chemical reactions require some degree of polarisation, not all of them implicate discretely charged species. Catalytic systems involving neutral or transiently charged substrates have been described for a large library of transformations (see Chapter 1 for some examples) involving H-bond catalysis.

One domain that has gained interest in recent research has been the usage of ion-pairing and its potential applications in the field of catalysis. Like H-bonding or π-π interactions, ion-pairing is worthy of consideration as yet another noncovalent type of interaction in synthetic chemists' toolboxes.

The anion-binding capabilities of H-bond donor groups such as (thio)ureas[14] or guanidines[15] has been well-documented. Unlike previous examples, this catalysis method does not directly activate the neutral substrate with a neutral catalyst, but instead, employ the neutral H-bonding group or groups of said catalyst to generate the discretely charged active reaction partner.

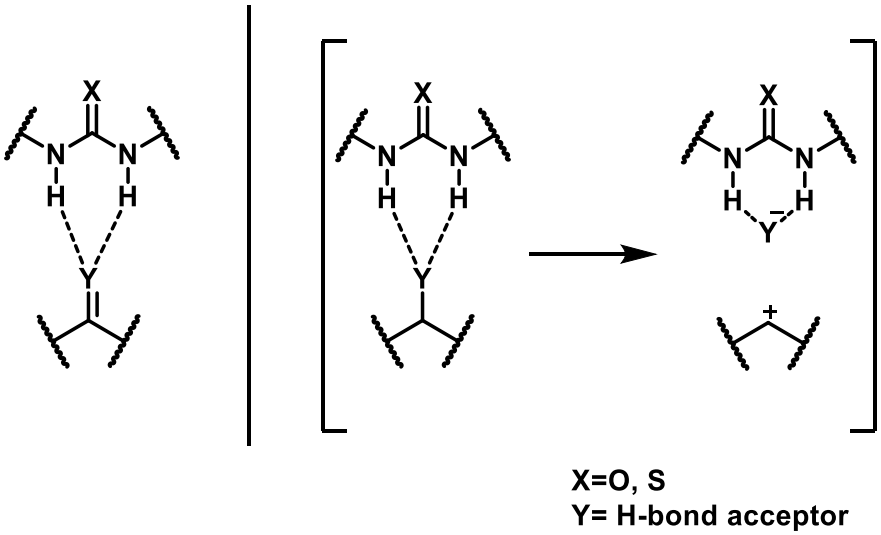

Figure 3.3 *Neutral H-bonding vs. Anion abstraction activation*

The formation of acetals by the reaction between alcohols and carbonyl groups has been described under both Lewis and Brønsted acid catalysis[16] as well as under N-bromo succinimide (NBS) catalysis.[17] However, these methods present issues preventing their broader application to substrates that are incompatible with acids for example. In an effort to circumvent these problems, the Schreiner group developed a thiourea catalysed acetalisation of aldehydes and ketones involving orthoesters.[18]

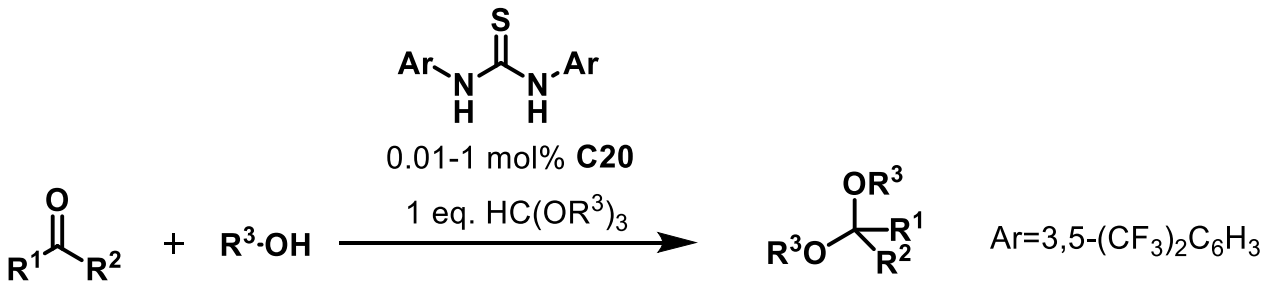

Scheme 3.1 *Schreiner's thiourea catalysed acetalisation*

Under catalysed conditions, the reaction proceeded with good to excellent yields with catalyst loadings as low as 0.01-1 mol%, whereas the uncatalysed reaction yielded less that 1% transformation in the same amount of time. The authors explained the observed reactivity through the abstraction of an alkoxy- group from the orthoester in order to reveal the active species **(see Scheme 3.2)**

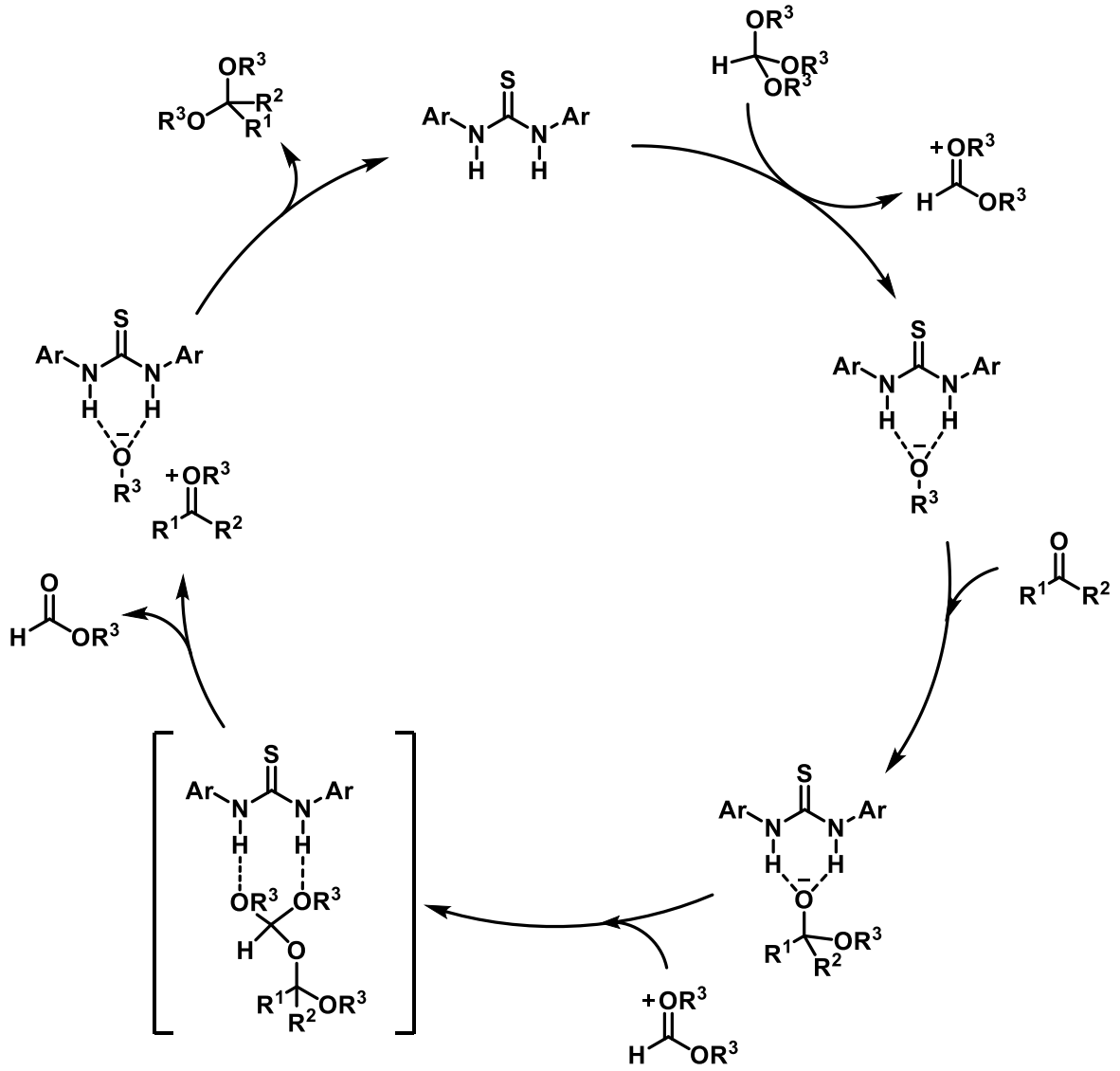

Scheme 3.2 *Proposed mechanism for the thiourea catalysed acetalisation by anion binding*

The Strecker reaction is a transformation that has received much interest due to it providing precious precursors for the synthesis of α-amino acids. One of the main drawbacks of this reaction is employment of highly hazardous cyanide sources such as HCN or TMSCN.

In 2008, Pan and List presented the acylcyanation of imines catalysed by thioureas.[19] Using Schreiner's achiral thiourea catalyst, the reaction proceeded with a loading of 2 mol%, leading to good yields with aromatic imines and moderate to good yields in the case of aliphatic imines.

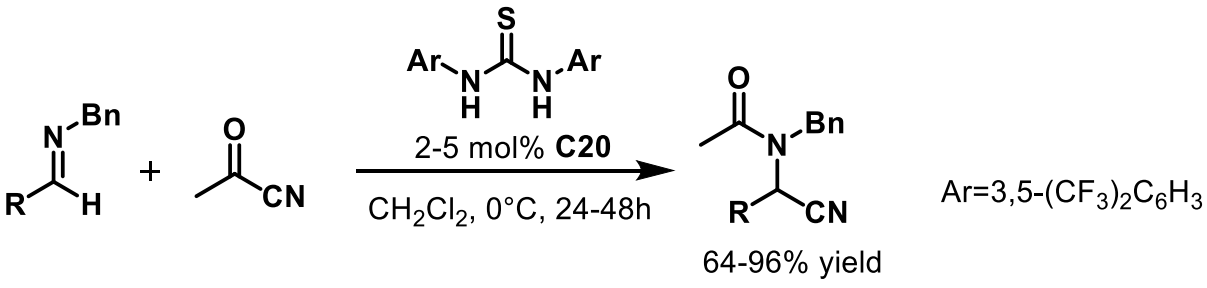

Scheme 3.3 *Thiourea catalysed acylcyanation*

From this initial success, the team probed an asymmetric version of the reaction. While BINOL derived phosphoric acids have been shown to catalyse the reaction[20], they did not provide useful enantioselectivity. However, the thioureas developed by Jacobsen *et al* have been shown to afford the expected product with high yields and selectivities.[21]

In an effort to shed light on the reaction mechanism, hydrocyanation of the starting imine followed by an acylation provided the expected product, although with a halved yield, thus discarding a mechanism involving the *in-situ* formation of HCN. The group consequently proposed a mechanism in with the formation of an N-acyliminium species leads to an ion-pair with the cyanide counter anion being bound by the thiourea catalyst **(see Scheme 3.4)**

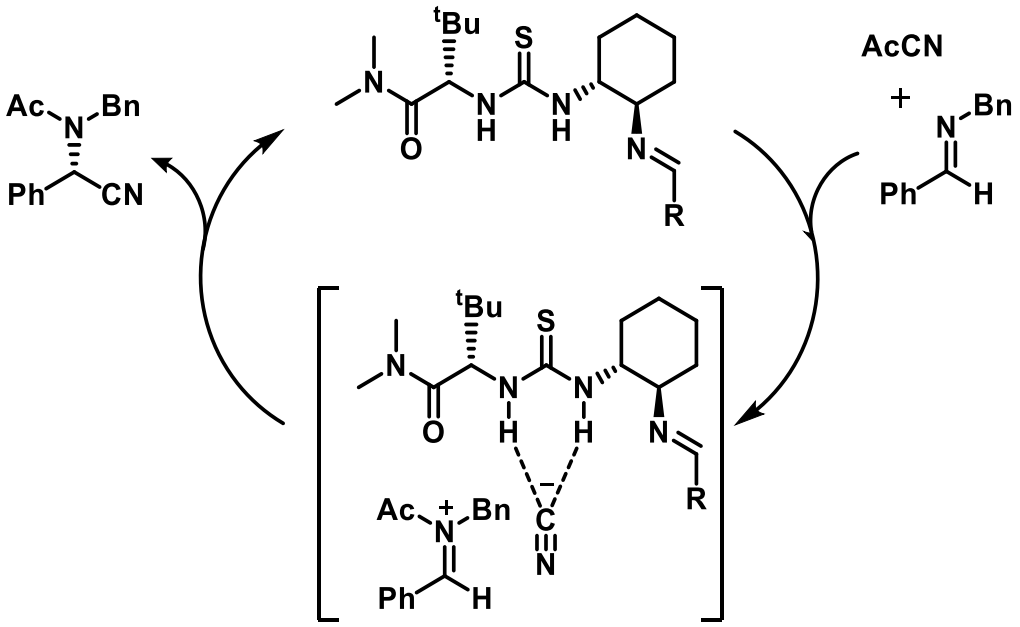

Scheme 3.4 *Proposed mechanism for the asymmetric acylcyanation of imines*

With H-bonding interactions with nitronate anions being reported in receptors incorporating amidinium and guanidinium moieties[22], the applicability of thiourea derivatives in a catalysed reaction involving the abovementioned anions was theorised. The Hiemstra group successfully applied this type of catalysis for the Henry addition of nitromethane to aromatic aldehydes.[23]

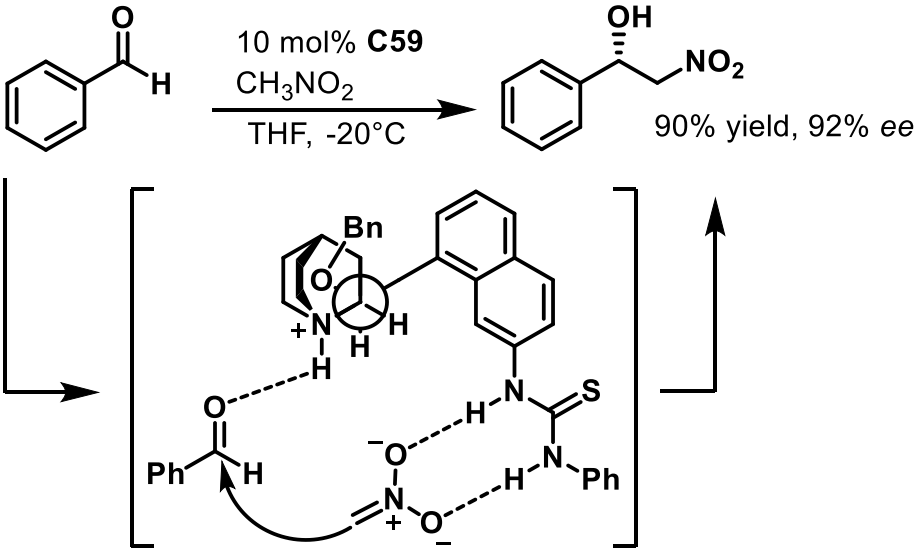

Scheme 3.5 *Thiourea catalysed Henry addition of nitromethane*

Ureas and thioureas have been recognised as powerful anion and especially halide recognition and binding agents.[24] The application of compounds integrating these functions as catalysts can nowadays be considered as inevitable due to their properties and the previous successes they have enjoyed in the field of organocatalysis (see Chapter 1).

Important work in the field of (thio)urea catalysed anion-binding chemistry has been reported by Jacobsen and his co-workers.
A pioneering report by the group described the usage of a thiourea catalyst for a Pictet-Spengler type cyclisation.[25] Because previous work on this type of reactivity involved strong Brønsted acids or high reaction temperatures[26], activation of imine species through the formation of N-acyliminium ions was envisioned as a potential solution and gave encouraging results in the initial tests. Through catalyst structure optimisation, the team discovered that the chiral diamine moiety had a drastic impact on enantioselectivity.

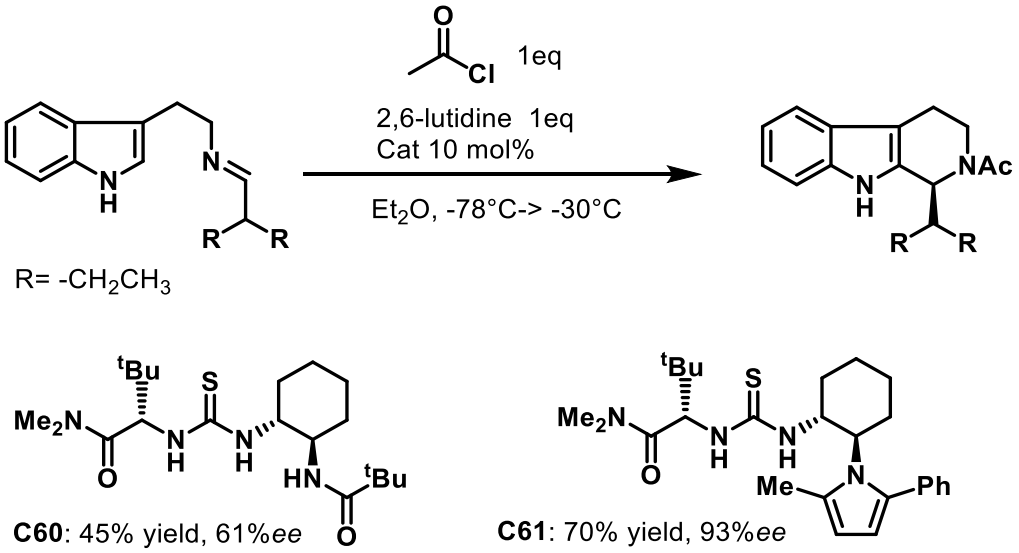

Scheme 3.6 Thiourea catalysed Pictet-Spengler cyclisation by anion-abstraction

While no mechanistic insight could be given as part of the original report, this type of catalysis was applied by the group in the total synthesis of the alkaloid (+)-Yohimbine.[27]

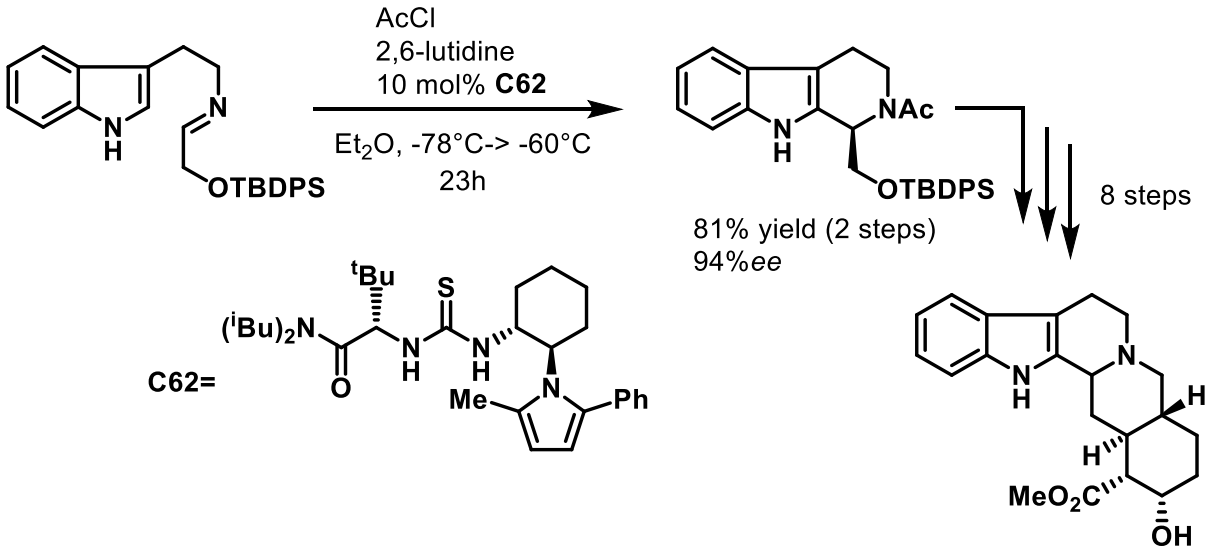

Scheme 3.7 Total synthesis of (+)-Yohimbine by the Jacobsen group

This methodology was expanded by the team to the cyclisation of hydroxylactams.[28] By forming a halolactam *in-situ*, the team demonstrated excellent reactivity and selectivity **(Scheme 3.8)**.

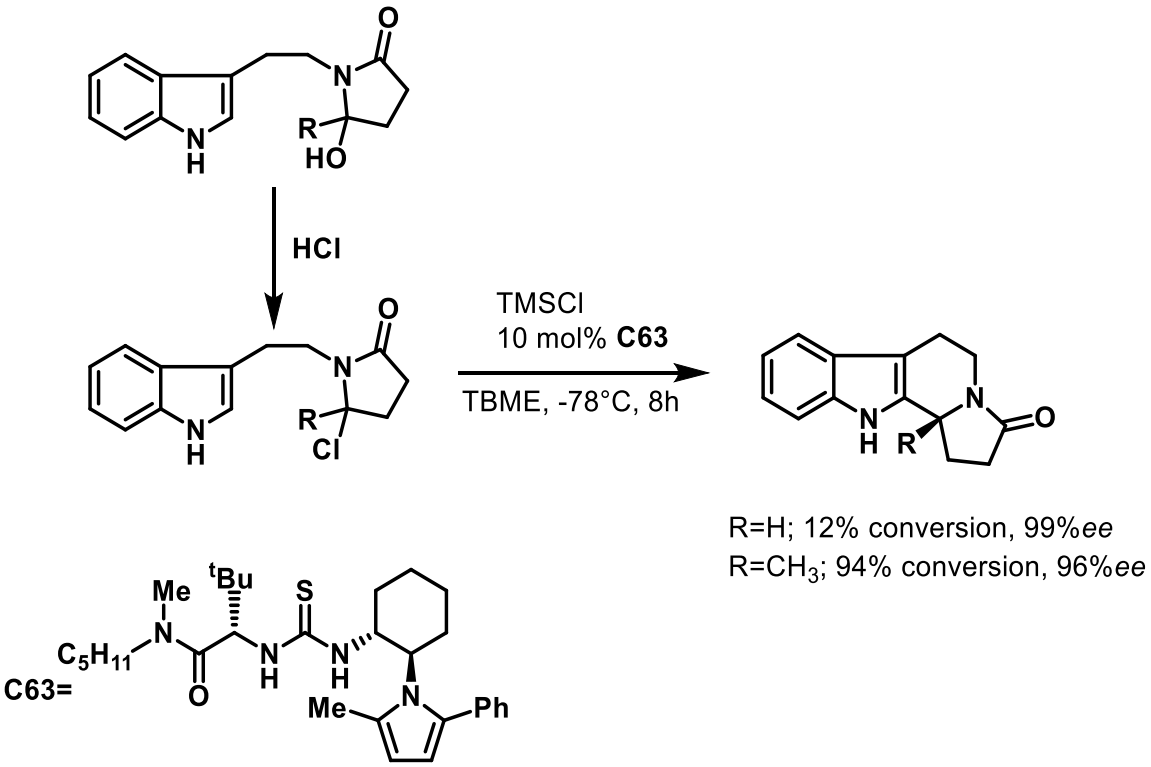

Scheme 3.8 *Thiourea catalysed hydroxylactam cyclisation by anion-abstraction*

This work also allowed better insight as to the workings of this type of catalysis. Firstly, through the substitution on the lactam, an S_N1 reaction mechanism was suggested as increased substitution led to high reactivity. Secondly, it was noted that both the nature of the halide and the employed solvent had a tremendous impact on the selectivity of the reaction **(see Table 3.1)**

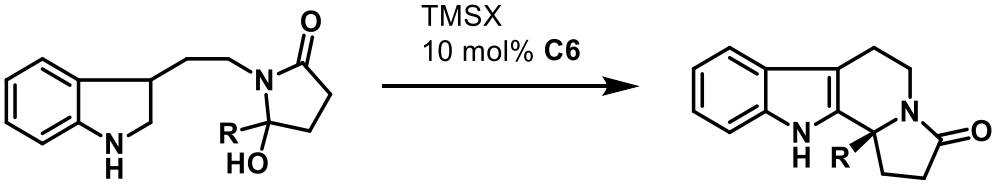

Entry	Solvent	X	T (°C)	t (h)	Conversion	ee
1	TBME	Cl	-55	23	80%	97%
2	TBME	Br	-55	23	82%	68%
3	TBME	I	-55	23	75%	<5%
4	TBME	Cl	-55	8	65%	97%
5	CH_2Cl_2	Cl	-55	8	>95%	<5%

Table 3.1 *Study of the hydroxylactam cyclisation reaction parameters*

The general applicability of this catalysis method was demonstrated by the intramolecular cyclisation of pyrroles with hydroxylactams[29] but also intermolecular addition of indoles to hydroxylactam derivatives.[30]

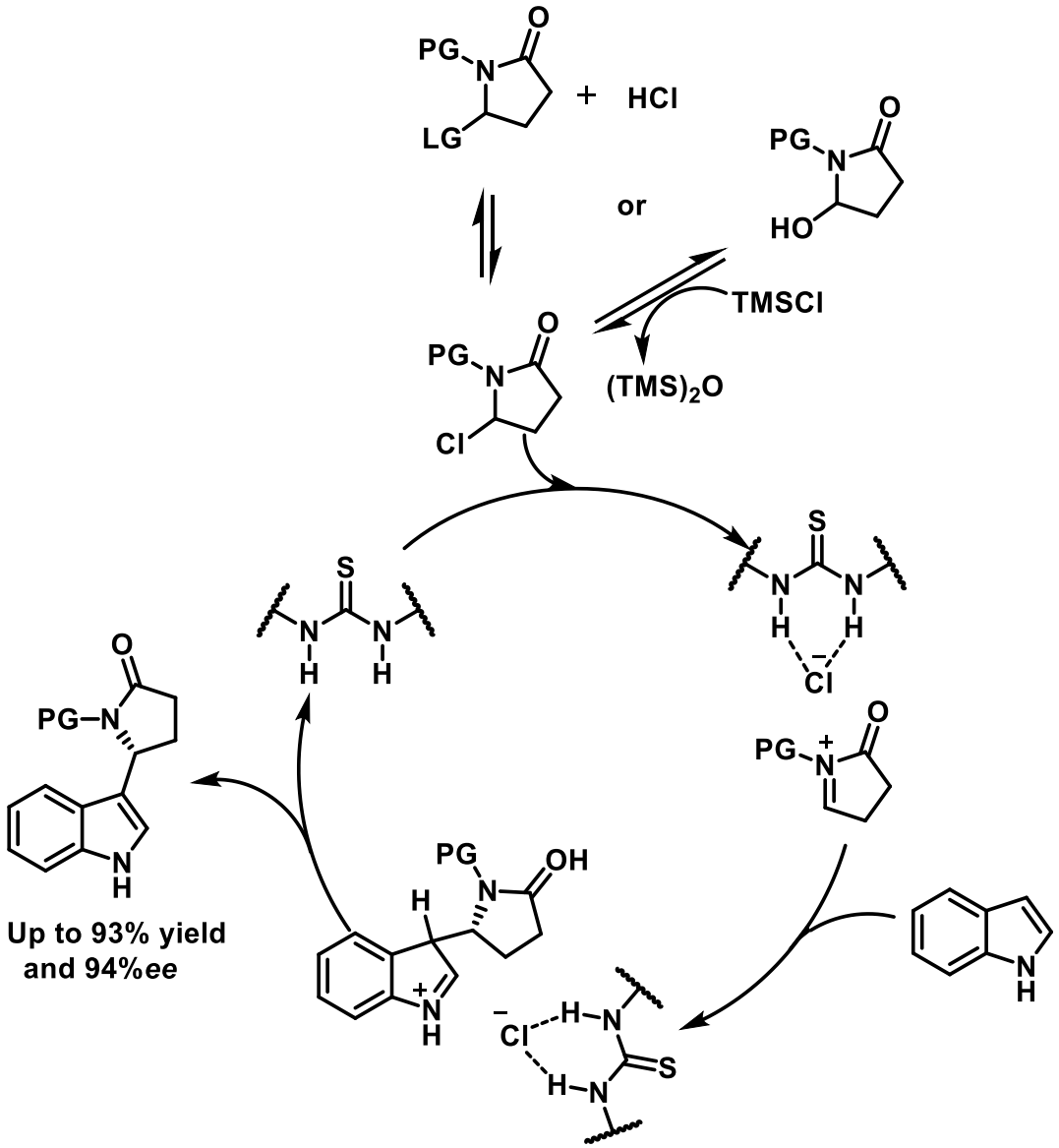

Scheme 3.9 *Proposed mechanism for the addition of Indoles to N-acyliminium intermediates*

A major contribution to the field came in 2016 from Jacobsen *et al* who noted while studying the thiourea catalysed alkylation of α-chloroisochroman with silyl ketene acetals that these compounds tended to aggregate as **[cat•cat]** dimeric complexes under typical reaction conditions.[31] After a kinetics study to better understand the transformation mechanism, the group concluded that two catalyst molecules are involved in the interaction with the chloride anion and proposed two interaction structures that could correspond to this description. **(Fig 3.4)**

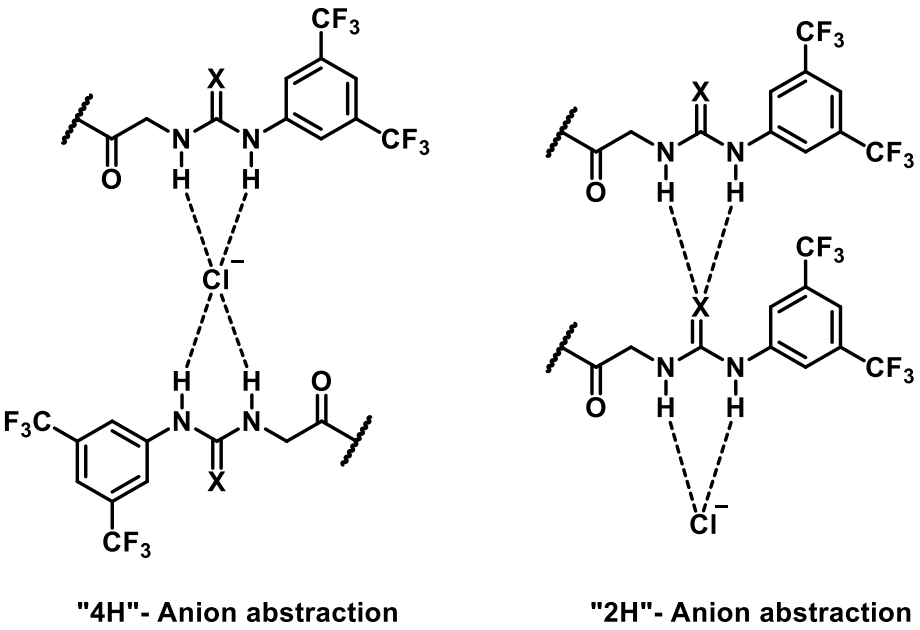

Figure 3.4 Possible double catalyst activation structures

In the "4H" dual interaction complex, the thiourea motifs of the two involved catalyst molecules act as H-bond donors towards the chloride for the abstraction step whereas the "2H" mode involves the activation of the catalyst by intermolecular H-bonding from a second molecule. While the 2H mode of activation has been described in the case of designed linked H-bond donor catalysts by Smith *et al*[32] **(Scheme 3.10)** Jacobsen *et al* demonstrated that their catalysts adopted a 4H complex geometry in the solid state[33]

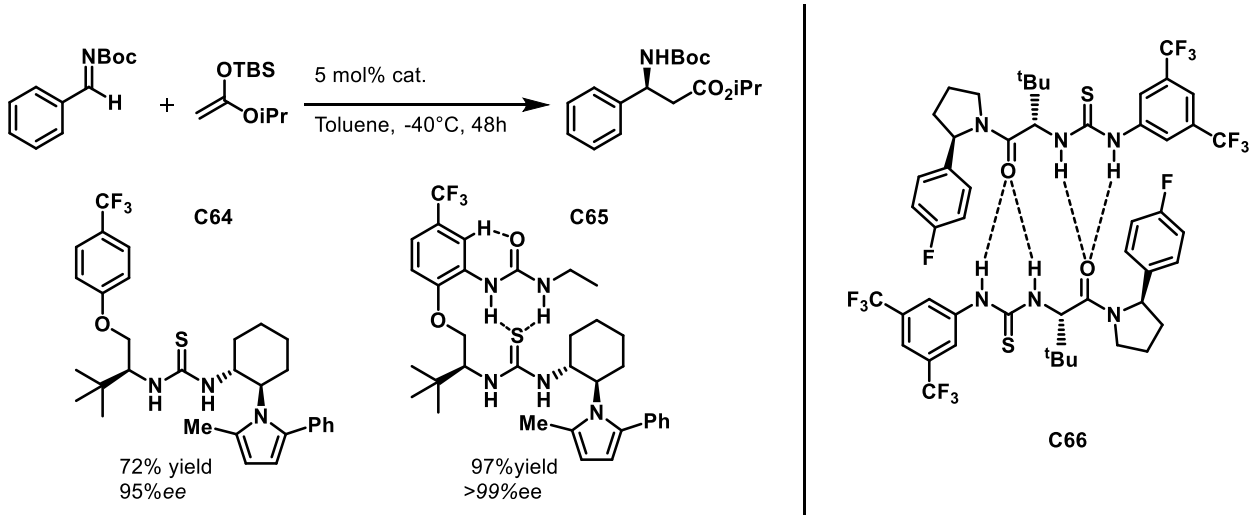

Scheme 3.10 Reported examples of dual activation structures

With no way to kinetically distinguish the two interaction pathways, DFT calculations of the two models were attempted, however, the theoretical study indicated that the two transition states occupied similar energy levels and a preferential mechanism could therefore not be confirmed. Following the results the group had published, Jacobsen and co-workers synthesised linked bis-thiourea catalysts in order to elucidate the activation method.[34] These dual H-bond donor catalysts were designed to favour the 4H mode of interaction while inhibiting potential aggregation.

Although this approach required some optimisation, it proved highly successful as the reaction was able to be carried out with a catalyst loading lowered by a factor of 100 with a reaction time shortened by a factor of 8. **(Scheme 3.11)**

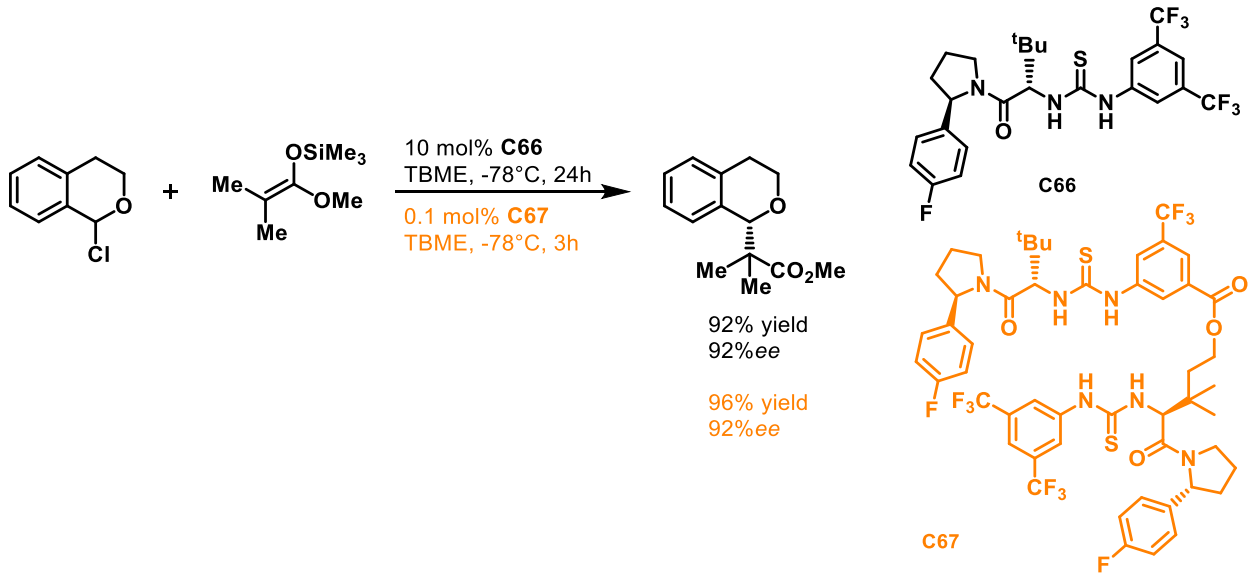

Scheme 3.11 *Single vs. dual H-bond donor catalysts for anion abstraction*

This reactivity was revisited in 2016 when the group published the results of a long-term study aimed at understanding and improving the previous system. The exact mode of interaction between the catalyst and the chlorinated substrate during the reaction was subsequently investigated[35]. NMR studies revealed two essential informations: in the presence of the catalyst, the chloride bearing center went through epimerisation but also that the addition of an external source of chloride completely hindered any reactivity. These results taken together pointed the group towards an S_N1 type mechanism where the chloride anion is abstracted by 2 catalyst molecules leading to an ion-pair with the catalyst system heavily shielding one side of the electrophile **(see Scheme 3.12)**

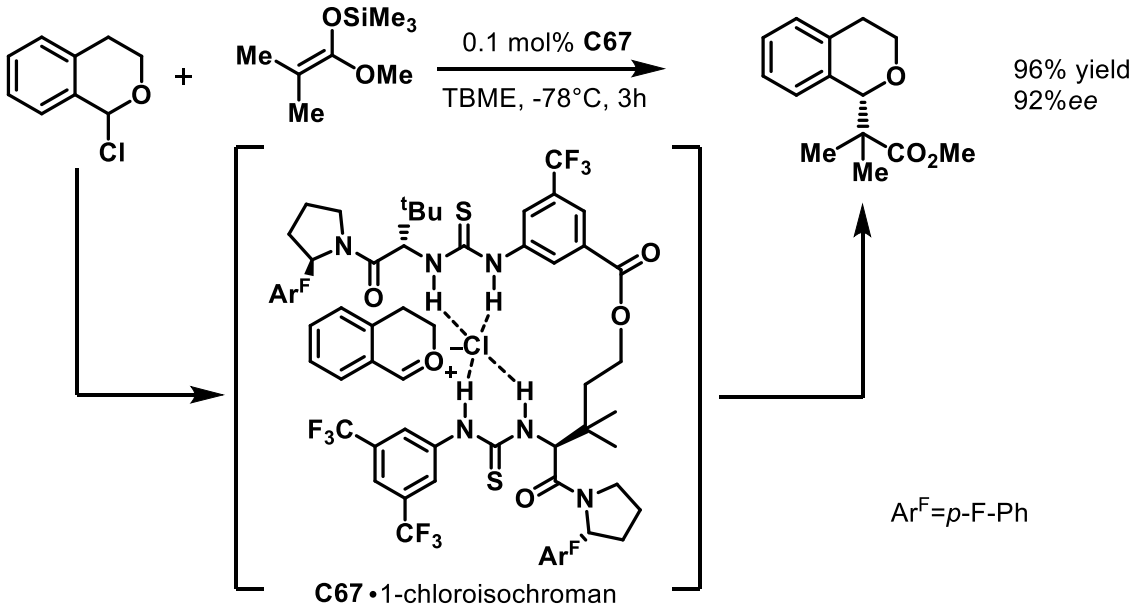

Scheme 3.12 *Proposed transition state for the bis-thiourea catalysed anion abstraction pathway*

The Jacobsen group expanded this bis-thiourea chemistry in 2017 by describing stereospecific glycosylation reactions of chlorides with alcohols.[36]
The authors demonstrate that neither single nor the previously presented bis-thiourea catalyst were able to promote the glycosylation reaction with satisfying yields or selectivity (although the bis-thiourea managed to reverse the selectivity trend of the reaction) **(Scheme 3.13, catalysts C66 and C67)**. Useful reactivity could only be observed when using certain macro cyclic bis-thioureas **(Scheme 3.13, catalysts C68 and C69)**. These catalysts were able to promote the glycosylation of chloride derivatives with simple alcohols and various sugars with good to excellent yields and enantioselectivities.

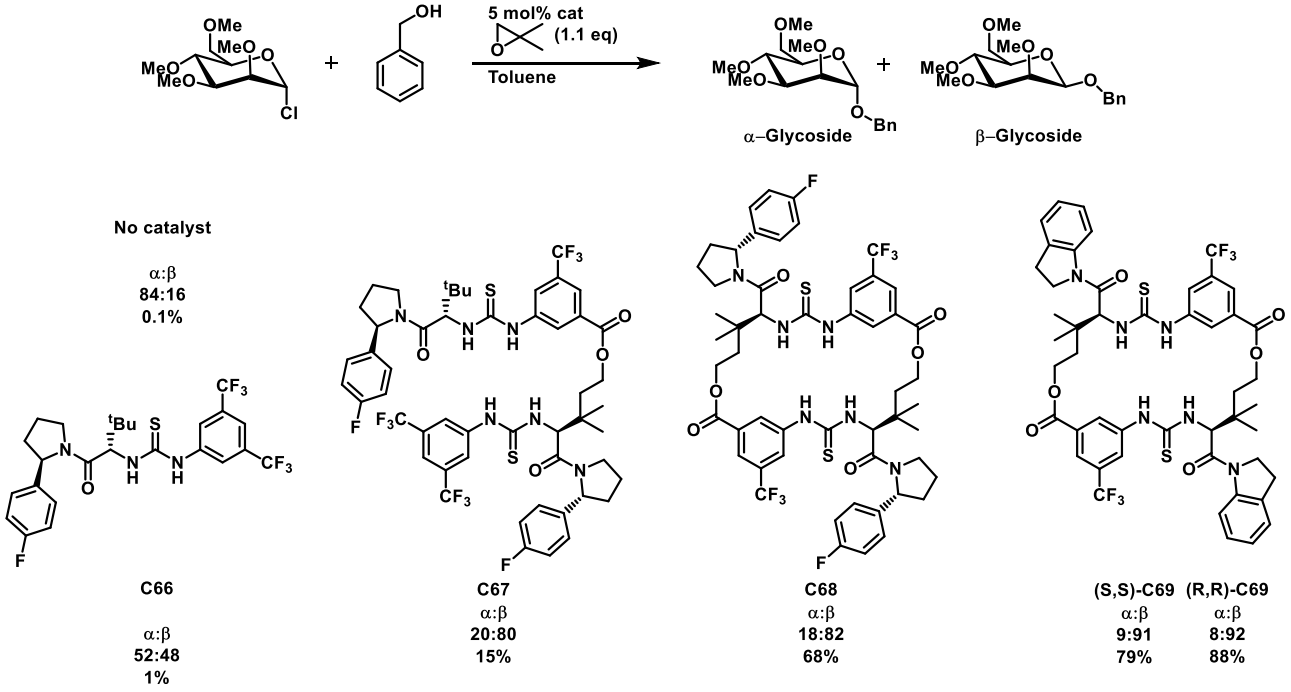

Scheme 3.13 *Stereoselective glycosylation dual HBD catalyst screening*

While the works that have been presented above have focused on H-bonding catalysts applied in the context of anion binding, other types of interactions have also been described. The works of the Mancheño group make use of helical macromolecular receptors incorporating the triazole motif.[37]

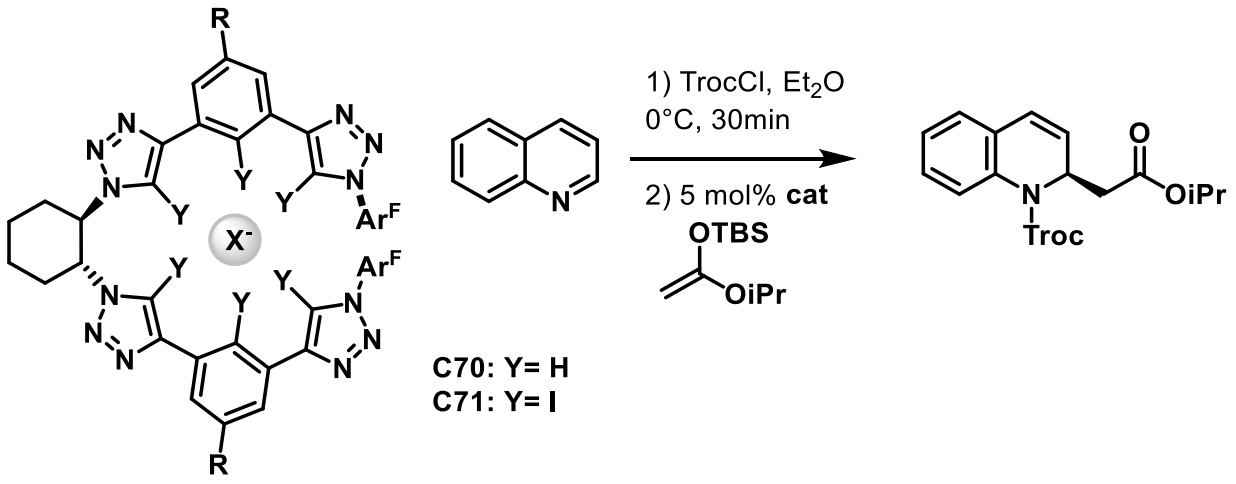

Scheme 3.14 *Helical triazole receptors for anion binding catalysis*

Other examples of non H-bonding anion binding catalysts that have been described include imidophosphorimidiate catalysed synthesis of oxygenated Heterocycles from lactol acetates[38] **(Scheme 3.15, a)** or pyridinium cations catalysing the coupling reaction of isochromans to silyl ketene acetals through Coulombic interaction with the anion[39] **(Scheme 3.15, b)**

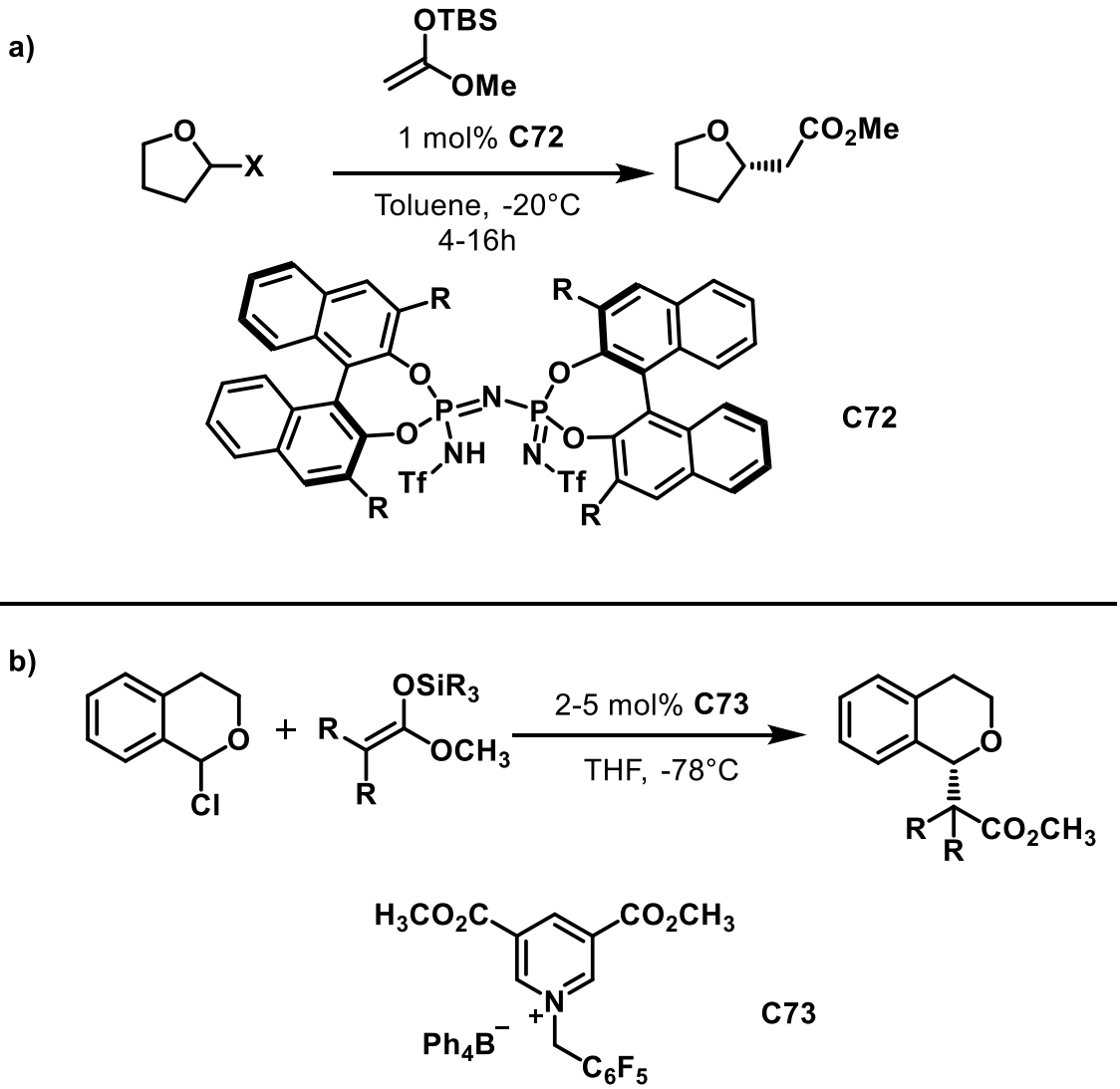

Scheme 3.15 *Examples of non H-bonding anion binding catalysts*

With these reports taken into account, the question of the applicability of oligourea foldamer catalysts in the field of anion abstraction can be justified by the previous successes that H-bonding catalysts have enjoyed in this type of catalysis.

References

[1] S. Mangani, M. Ferraroni, *Supramolecular Chemistry of Anions*, Wiley, New York, **1997**
[2] M. Breugst, D. von der Heiden, J. Schmauck, *Synthesis*, **2017**, *49*, 3224-3236; P.A. Gale, E.N.W. Howe, X. Wu, *Chem*, **2016**, *1*, 351-422
[3] M. Mascal, A. Armstrong, M.D. Bartberger, *J. Am. Chem. Soc.* **2002**, *124*, 6274-6276
[4] I. Alkorta, I. Rozas, J. Elguero, *J. Am. Chem. Soc.* **2002**, *124*, 8593-8598
[5] D. Quiñonero, C. Garau, C. Rotger, A. Frontera, P. Ballester, A. Costa, P.M. Deyà, *Angew. Chem. Int. Ed.* **2002**, *41*, 3389-3392
[6] R.E. Dawson, A. Hennig, D.P. Weimann, D. Emery, V. Ravikumar, J. Montenegro, T. Takeuchi, S. Gabutti, M. Mayor, J. Mareda, C.A. Schalley, S. Matile, *Nat. Chem.*, **2010**, *2*, 533-538
[7] Y. Zhao, Y. Cotelle, L. Liu, J. Lopez-Andarias, A.B. Bornhoff, M. Akamatsu, N. Sakai, S. Matile, *Acc. Chem. Res.*, **2018**, *51*, 2255-2263
[8] D. Bulfield, S.M. Huber, *Chem. Eur. J.*, **2016**, *22*, 14434 – 14450
[9] J. Jo, R. Putikam, M.C. Lin, J. Kang, *Tetrahedron Lett.*, **2016**, *57*, 3208–3214
[10] J.V. Gavette, N.S. Mills, L.N. Zakharov, C.A. Johnson, D.W. Johnson, M.M. Haley, *Angew. Chem. Int. Ed.*, **2013**, *52*, 10270–10274
[11] H.J. Mo, Y. Shen, Y., B.H. Ye, *Inorg. Chem.*, **2012**, *51*, 7174−7184
[12] G.R. Desiraju, P.S. Ho, L. Kloo, A.C. Legon, R. Marquardt, P. Metrangolo, P. Politzer, G. Resnati, K. Rissanen, *Pure Appl. Chem.* **2013**, *85*, 1711-1713
[13] K.S.C. Reid, P.F. Lindley, J.M. Thornton, *FEBS Lett.*, **1985**, *190*, 209-213; S. Benz, M. Macchione, Q. Verolet, J. Mareda, N. Sakai, S. Matile, *J. Am. Chem. Soc,*. **2016**, *138*, 9093-9096
[14] Z. Zhang, P.R. Schreiner, *Chem. Soc. Rev.***, 2009**, *38*, 1187-1198
[15] F.P. Schmidtchen, M. Berger, *Chem. Rev.*, **1997**, *97*, 1609-1646
[16] H. Firouzabadi, N. Iranpoor, B. Karimi, *Synlett.*, **1999**, 321-323; D. J. Cox, M. D. Smith, A. J. Fairbanks, *Org. Lett.*, **2010**, *12*, 1452-1455
[17] B. Karimi, H. Hazarkhani, J. Maleki, *Syntheis*, **2005**, 279-285
[18] M. Kotke, P. R. Schreiner, *Tetrahedron*, **2006**, *62*, 434-439
[19] C.S. Pan, B. List, *Chem. Asian. J*, **2008**, *3*, 430-437
[20] M.Rueping, E.Sugiono, C.Azap, *Angew. Chem. Int. Ed.*, **2006**, *45*, 2617 –2619
[21] M.S. Sigman, E.N. Jacobsen, *J. Am. Chem. Soc.*, **1998**, *120*, 4901-4902
[22] P. H. Boyle, M. A. Convery, A. P. Davis, G. D. Hosken, B. A. Murray, *J. Chem. Soc., Chem. Commun.*, **1992**, *239*; E. Vanaken, H. Wynberg and F. Vanbolhuis, *J. Chem. Soc.,Chem. Commun.*, **1992**, *629*
[23] T. Marcelli, R. N. S. van der Haas, J. H. van Maarseveen, H. Hiemstra, *Angew. Chem., Int. Ed.*, **2006**, *45*, 929-931
[24] V.B Bregovic, N. Basaric, K. Mlinaric-Majerski, *Coord. Chem. Rev.*, **2015**, *295*, 80-124; D.A. Jose, D.K. Kumar, B. Ganguly, A. Das, *Org. Lett.*, **2004**, *6*, 3445-3448; J.N. Babu, V. Bhalla, M. Kumar, R.K. Puri, R.K. Mahajan, *New J. Chem.*, **2009**, *33*, 675-681
[25] M.S. Taylor, E.N. Jacobsen, *J. Am. Chem. Soc.*, **2004**, *126*, 10558-10559
[26] R. Tsuji, M. Yamanaka, A. Nishida, M. Nakagawa, *Chem. Lett.*, **2002**, *31*, 428-429; H. Yamada, T. Kawate, M. Matsumizu, A. Nishida, K. Yamaguchi, N. Nakagawa, *J. Org. Chem.*, **1998**, *63*, 6348-6354
[27] D.J. Margott, S.J. Zuend, E.N. Jacobsen, *Org. Lett.*, **2008**, *10*, 745-748
[28] I.T. Raheem, P.S. Thiara, E.A. Peterson, E.N. Jacobsen, *J. Am. Chem. Soc.*, **2007**, *129*, 13404-13405
[29] I.T. Raheem, P.S. Thiara, E.N. Jacobsen, *Org. Lett.*, **2008**, *10*, 1577-1580
[30] E.A. Peterson, E.N. Jacobsen, *Angew. Chem. Int. Ed.*, **2009**, *48*, 6328-6331
[31] D. D. Ford, D. Lehnherr, C. R. Kennedy, E. N. Jacobsen, *ACS. Catal.*, **2016**, *6*, 4616-4620
[32] C. R. Jones, G. D. Pantos, A. J. Morrison, M. D. Smith, *Angew. Chem. Int. Ed.*, **2009**, *48*, 7391-7394
[33] D. D. Ford, D. Lehnherr, C. R. Kennedy, E. N. Jacobsen, *J. Am. Chem. Soc.*, **2016**, *138*, 7860-7863
[34] C.R. Kenndey, D. Lehnherr, N. S. Rajapaksa, D. D. Ford, Y. Park, E. N. Jacobsen, *J. Am. Chem. Soc.*, **2016**, *138*, 13525-13528
[35] D.D. Ford, D. Lehnherr, C.R. Kennedy, E.N. Jacobsen, *ACS Catal.*, **2016**, *6*, 4616-4620
[36] Y. Park, K. C. Harper, N. Kuhl, E. E. Kwan, R. Y. Liu, E. N. Jacobsen, *Science*, **2017**, *355*, 162-166
[37] D.G. Piekarski, P. Steinforth, M. Gomez-Martinez, J. Bamberger, F. Ostler, M. Schonhoff, O.G. Mancheño, *Chem. Eur. J.*, **2020**, *26*, 17598 – 17603; F. Ostler, D.G. Piekarski, T. Danelzik, M.S. Taylor, O.G. Mancheño, *Chem. Eur. J.*, **2021**, *27*, 2315 – 2320
[38] S. Lee, P.S.J Kaib, B. List, *J. Am. Chem. Soc.*, **2017**, *139*, 2156-2159
[39] A. Berkessel, S. Das, D. Pekel, J.M. Neudorfl, *Angew. Chem. Int. Ed.*, **2014**, *53*, 11660-11664

III- Objectives:

The oligourea foldamers that have been developed in the Guichard group have shown the capacity to recognise and bind certain anions such as AcO^-, $H_2PO_4^-$ and Cl^- owing to the two free urea functions that are found at the N-terminus of the helix.[1]

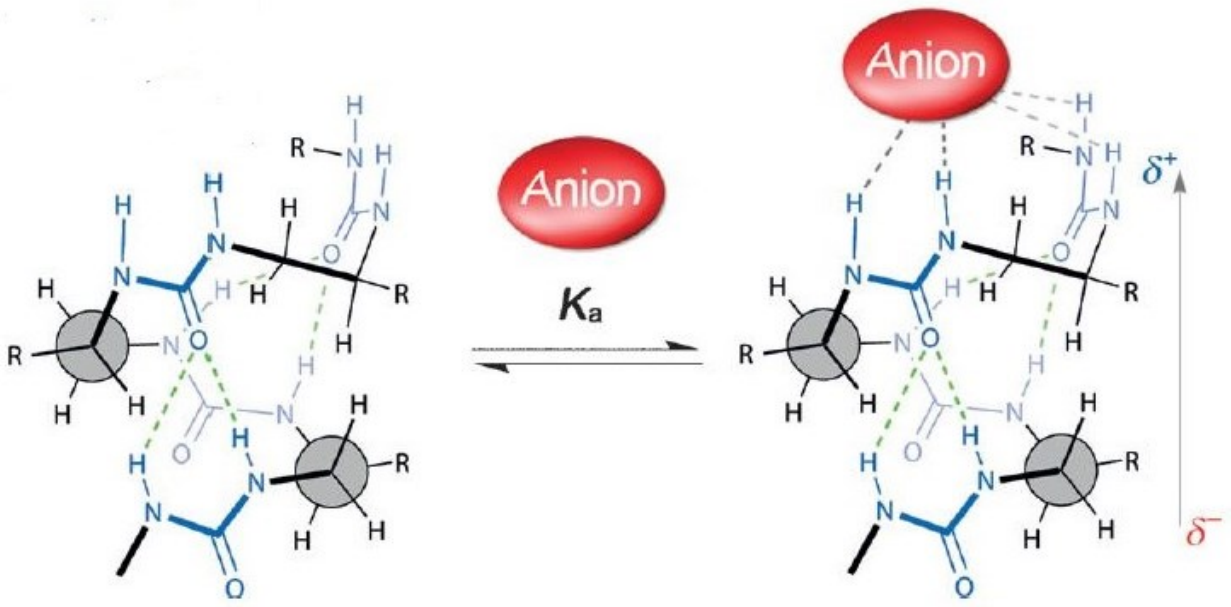

Figure 3.5 *Oligourea foldamer anion binding scheme*[1]

With the strong development of anion binding catalysis and the success that H-bonding motifs have demonstrated in this field, we believed the sequences that we have synthesised could have interesting applications in yet untested reactions. Much like the examples described above, the oligourea foldamers designed by our group present two H-bond donating free urea units that are covalently linked, reminiscent of the bis-thiourea catalysts developed and successfully applied by the Jacobsen group.

Thus, our objective will be the identification of new reactivity that is suitable to the application of oligourea foldamer catalysts following an anion abstraction pathway.

Initial considerations:

The objective of our work being the identification of new and previously untested reactions, two main approaches are to be considered. The first one consists in focusing on one reaction and optimising the parameters to obtain satisfying results while the second one would be based on screening a large panel of different reactions in order to identify the ones that appear as promising. Both approaches present advantages as well as drawbacks. In the case of the focus on one reaction, the risk consists of the chosen transformation not providing satisfying results but this method would be less intensive on catalyst usage. The multiple reaction screening has a higher chance of resulting in a promising transformation but comes at the cost of high amounts of catalyst consumption, as initial screenings usually require high loadings.

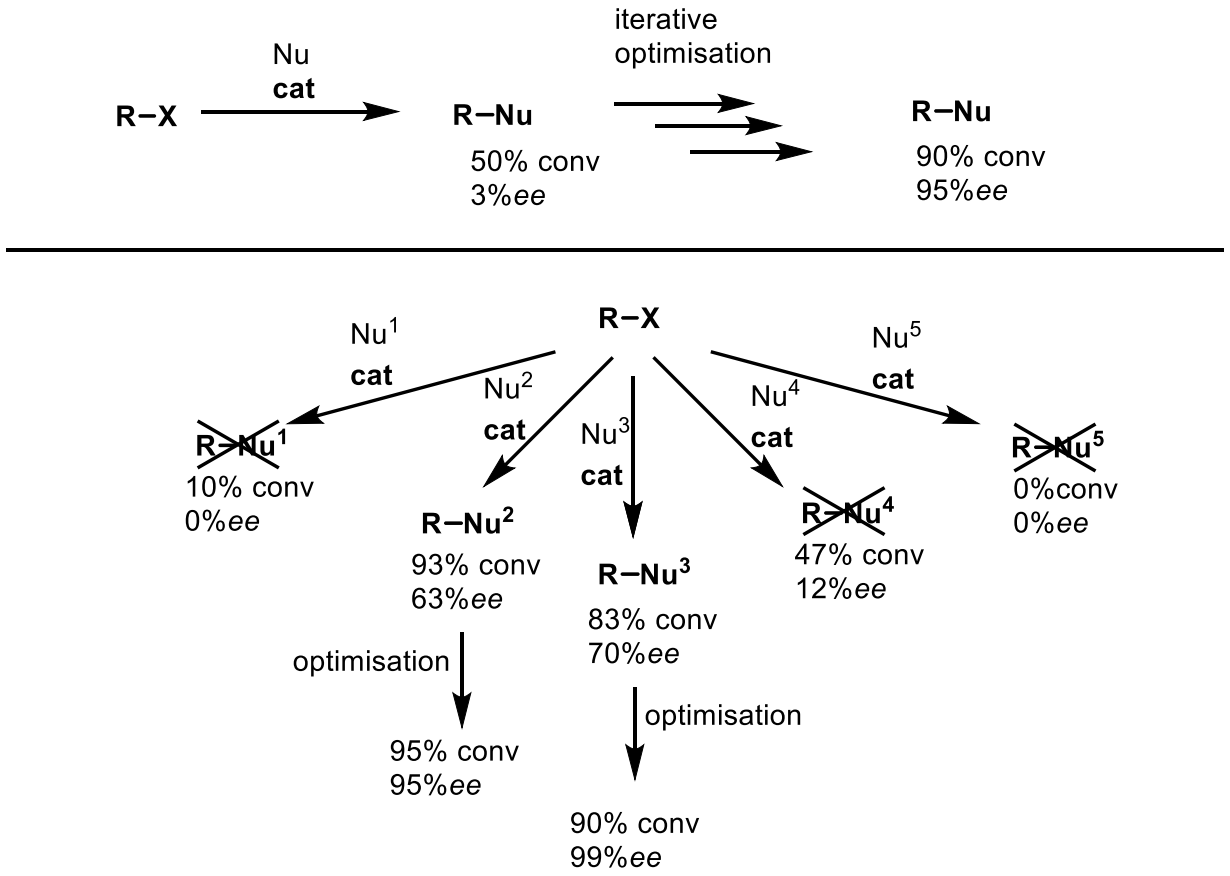

Figure 3.6 *General approaches for implementing new catalytic reactions*

As presented above, the exploration of multiple reactions is more likely to lead to exploitable reactivity, however, due to the nature of our catalysts, the relative difficulty of access limiting the scales that can be practically synthesised and the low loadings required by these factors, the first method focusing on a single reaction and iterative optimisation of its parameters was chosen for this study.

With the exploratory approach selected, the next choice concerns the reaction to be investigated. While the oligourea catalysts have demonstrated a propensity to bind halides (chloride in particular) as well as oxyanions such as acetate, initial reactivity probing involving chloride anion abstraction was deemed more realistically feasible for the initial attempts.

The amount of examples of anion binding catalysis have multiplied over the last 20 years, encompassing many different types of reactions. A simplified representative scheme for this type of catalysis is presented below in **scheme 3.16**.

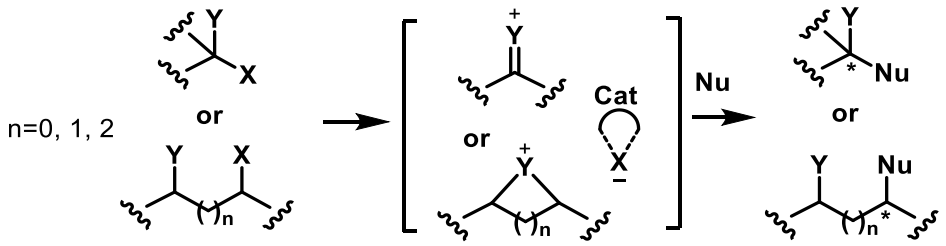

Scheme 3.16 *Representation of described anion binding catalysis examples*

As shown in the depiction above, most of the described anion-binding catalysed reactions go through a heteroatom cation stabilised transition state after abstraction of the anion. A study in literature shows that while a majority of anion binding examples deal with iminium (Y= -NR)[2, 2a] or oxocarbenium intermediates (Y=O)[2, 2b], very few descriptions of reactions implicating sulfenium intermediates (Y=S, n=0)[3] and no report of reactions proceeding through thiocarbenium intermediates could be found.
Thus, nucleophile addition reactions to α-chlorosulfides were selected for initial studies of anion binding catalysis with our oligourea foldamers.

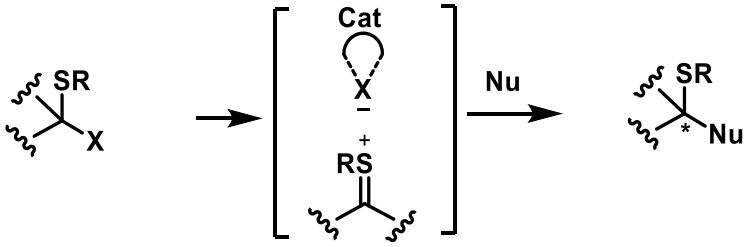

Scheme 3.17 *Expected reaction pathway for the foldamer catalysed addition reaction to α-chlorosulfides*

In fact, to the best of our knowledge the only catalytic approaches to this type of reaction before our studies were initiated have mostly involved heteronucleophiles and silylated carbon based nucleophiles and I_2 or $TiCl_4$ and related strong Lewis acids as catalysts/promoters, with no enantioselective examples described.[4]

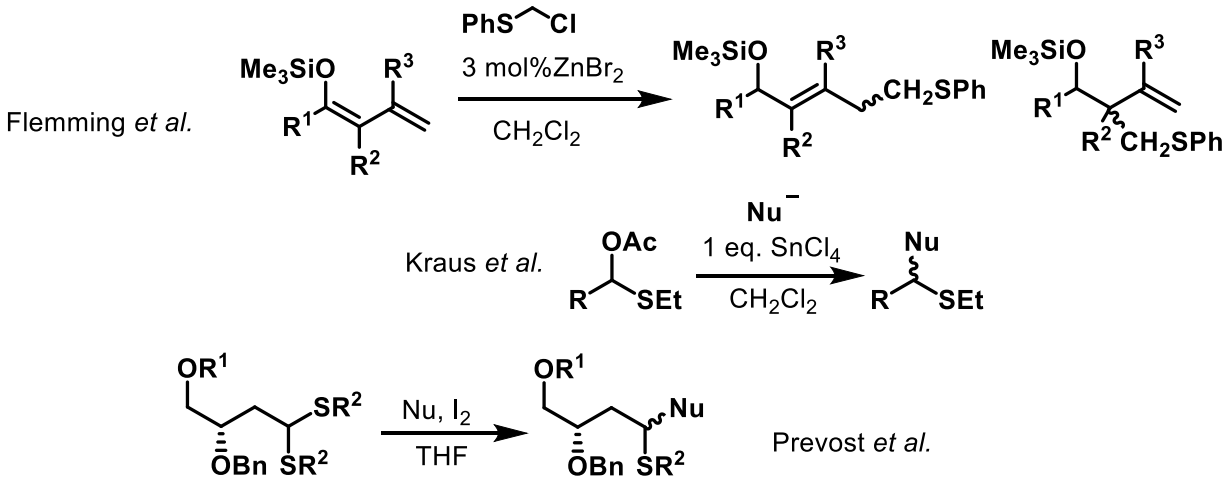

Scheme 3.18 *Examples of reactions involving S-stabilised cationic intermediates*

Synthesis of chlorides:

For the initial test substrate, the following synthesis path leading to ethyl-chlorobenzyl sulfide **(43)** was considered. Ethyl-benzyl sulfide **(42)** was obtained by a substitution reaction between benzyl bromide **(41)** and ethanethiol. Subsequent chlorination of the benzylic position should afford the desired α-chlorosulfide **(43)**.

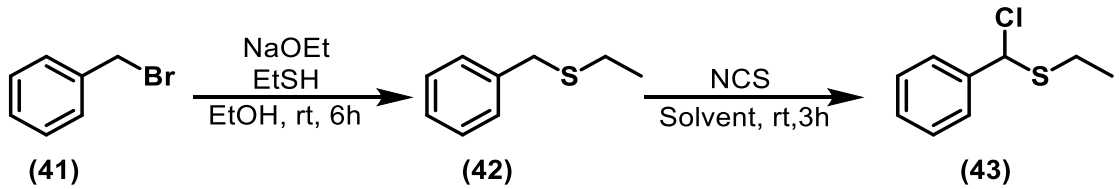

Scheme 3.19 *Synthesis scheme for ethyl-chlorobenzyl sulfide* ***(3)***

While ethyl-benzyl sulfide **(42)** was obtained cleanly, chlorination of the benzylic position in α of the sulphur proved more difficult. **Figure 3.7** shows the ^{1}H NMR spectra of **(42)** and the product obtained after purification by column chromatography for the different chlorination conditions that were attempted.

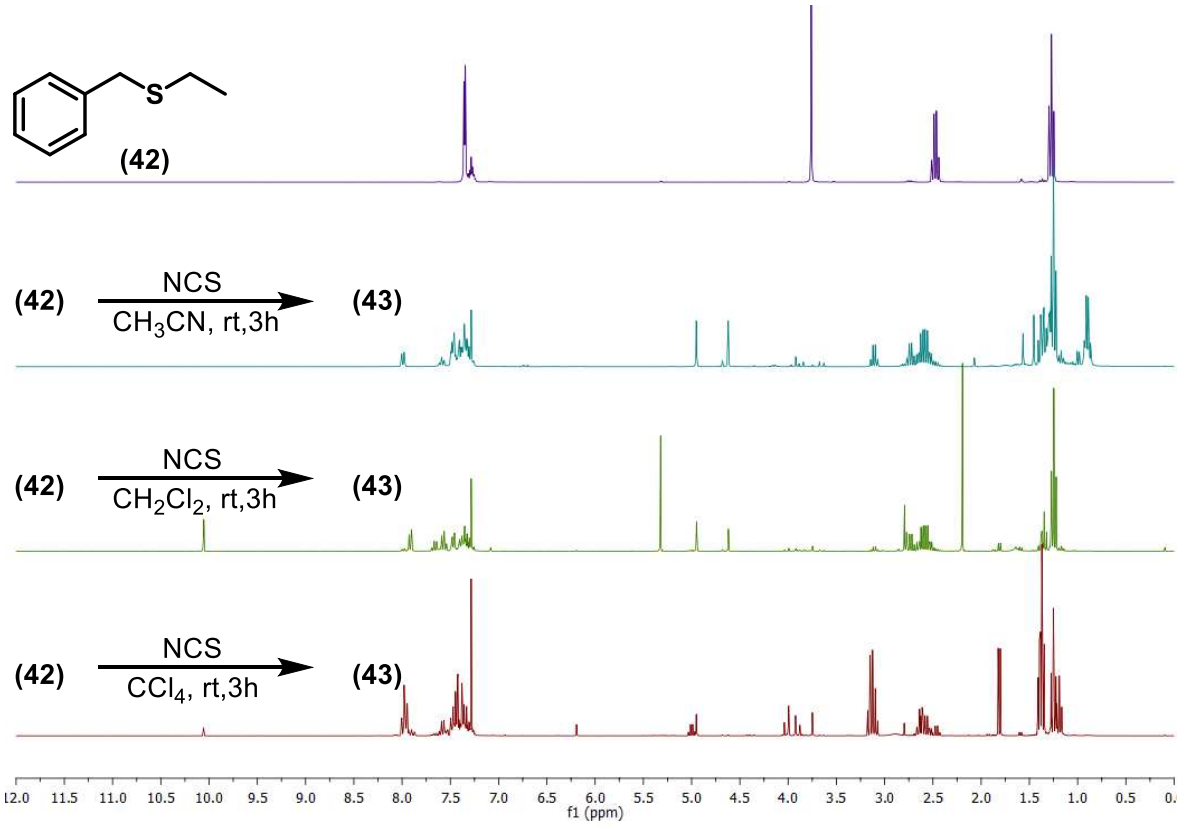

Figure 3.7 *^{1}H NMR spectra of crude materials from chlorination attempts of* ***2*** *using NCS*

Chlorination attempts on the benzylic position using N-chlorosuccinimide (NCS) under conditions described by Tuleen and co-workers[5] proved unsuccessful as the analysis of the crude mixture indicated important degradation occurring during the reaction. With few precedents covering the halogenation of the benzylic position in α of a sulfide group, a different approach using sulfuryl chloride following reports by McBee and Pitt[6] was attempted but remained unsuccessful as no reaction occurred under these conditions.

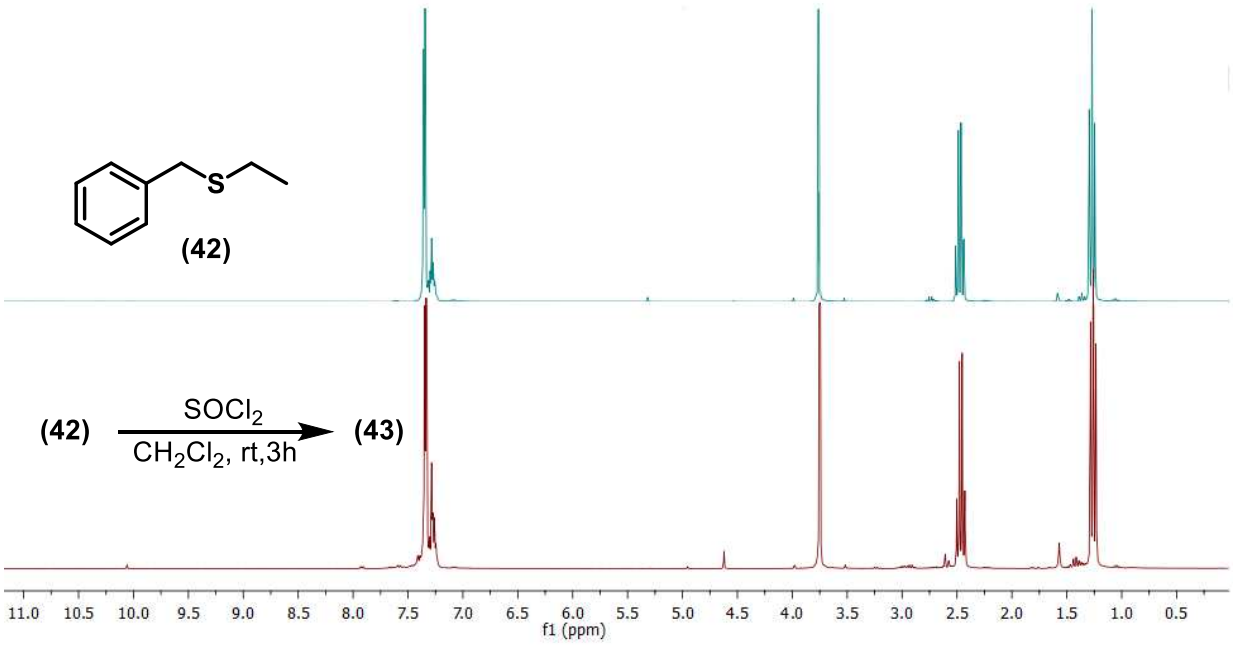

Figure 3.8 *^{1}H NMR ($CDCl_3$, 300MHz) spectra of the chlorination attempts using NCS*

Due to the inaccessibility of desired compound **(43)**, a new chlorinated substrate had to be synthesised in order to start catalytic tests. Observing the structure ethyl-chlorobenzyl sulfide **(43)**, we can see that two α to the sulfur positions are available for chlorination. While the **α** benzylic position could not be chlorinated cleanly, the **α'** position in the ethyl chain should prove to be a better candidate for clean introduction of chloride **(Scheme 3.20)**.

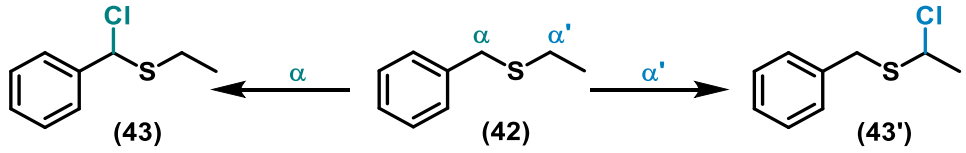

Scheme 3.20 *Chlorination of available a positions*

In order to avoid any regioselectivity issues, sulfide **(45)** was synthesised from phenyl mercaptan so as to eliminate the possibility of chlorination of the **α** benzylic position. Thioanisole **(47)** was used to assess the chlorination conditions before moving to ethylphenyl sulfide **(45)**.

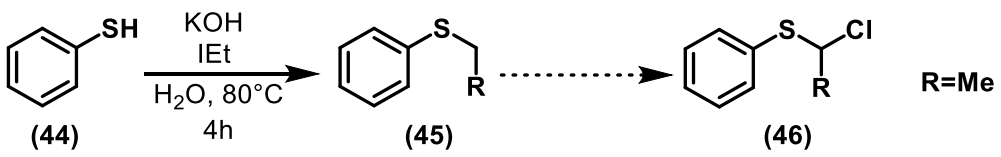

Scheme 3.21 *Synthesis of 1-chloroethylphenyl sulfide*

Using NCS in dichloromethane at 0°C for 16h, the signals corresponding to the desired product were observed in the crude mixture, however purification by column chromatography proved impossible due to the degradation of the product. Before attempting other purification methods, a simpler change to the reaction conditions was attempted. Dichloromethane was substituted with carbon tetrachloride following

procedures described by Tuleen *et al.* [5] and resulted in a much cleaner reaction, thus affording the crude product without needing further purification.

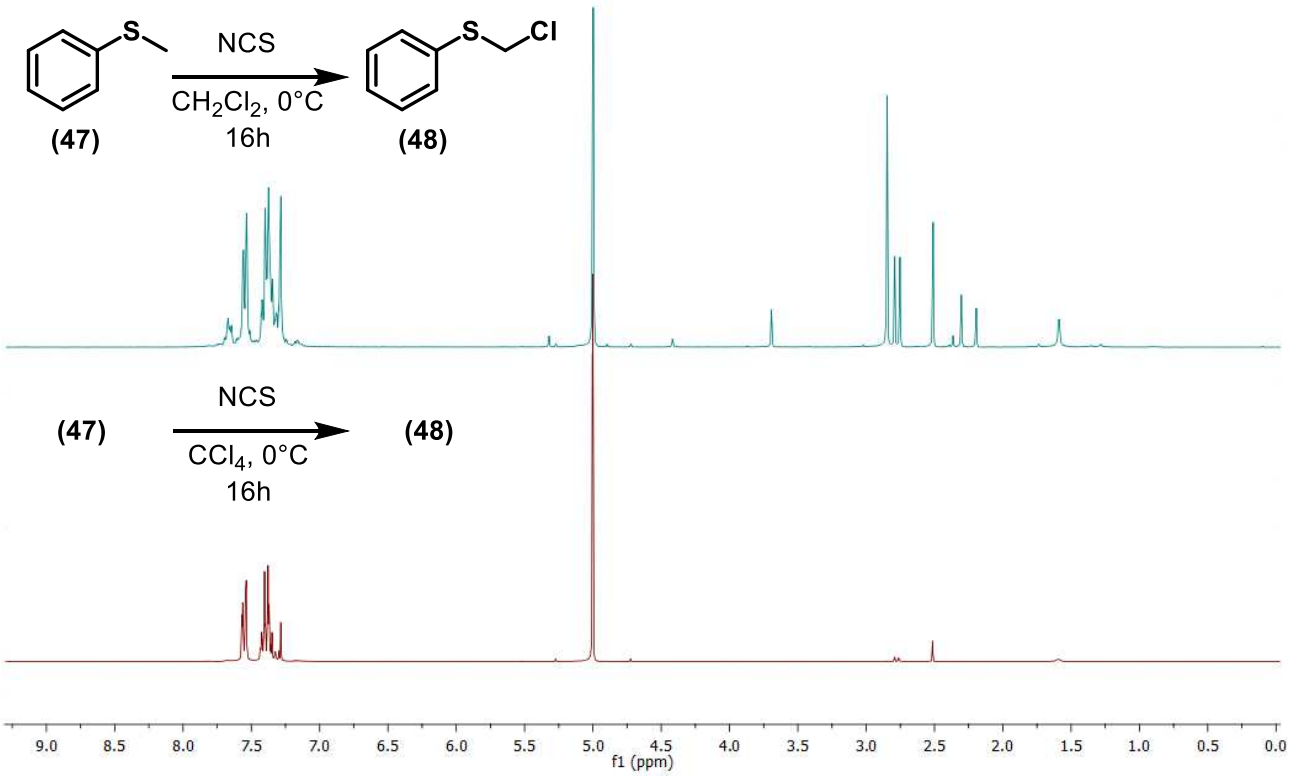

Figure 3.9 *^{1}H NMR ($CDCl_3$, 300MHz) spectra of the chlorination attempts in CH_2Cl_2 and CCl_4*

The same conditions were used for the chlorination of ethylphenyl sulfide **(45)** and led to the desired product cleanly as well.

Exploration of reactivity:

With the chlorinated substrates prepared, reactivity probing was initiated using simple achiral catalysts to explore promising nucleophiles for the addition reaction. The reaction progression was monitored by ^{1}H NMR analysis of aliquots taken from the reaction mixture by monitoring the consumption of the quadruplet signal corresponding to the proton of the chloride bearing carbon circled in purple **(Fig 3.10)**.

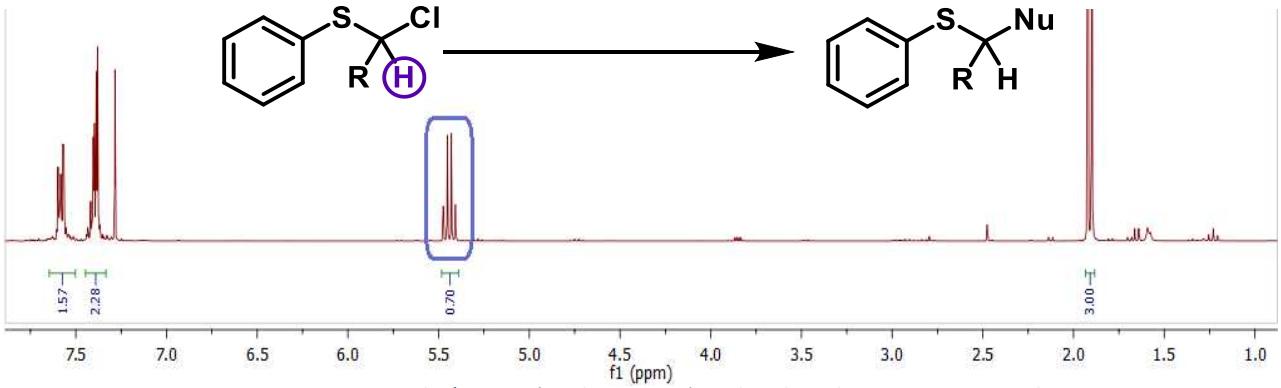

Figure 3.10 *Reaction monitoring by ^{1}H NMR ($CDCl_3$, 300MHz) analysis based on starting material consumption.*

Tetralones and derivatives:

The first selected candidate nucleophiles were tetralones **(9), (10)** and silyl enol ether **(11)**, derived from α-tetralone. While the initial two would require an external base for nucleophilic substrate activiation, and hence the reaction to take place, the latter was considered for the possibility of running the reaction without any base.

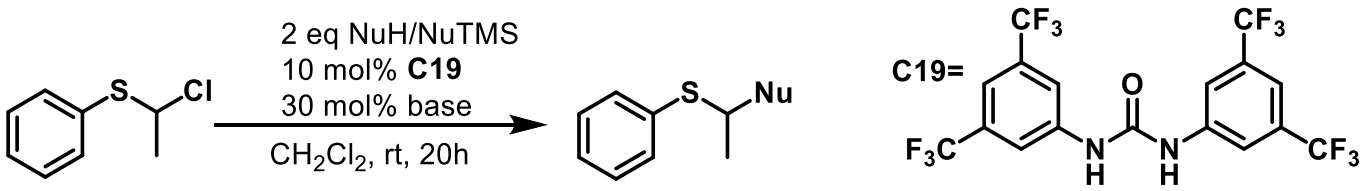

Entry	Nucleophile	Base	Conversion	Entry	Nucleophile	Base	Conversion
1	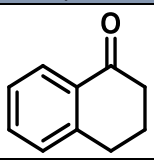 **(49)**	Et_3N	0%	3	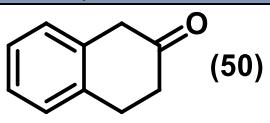 **(50)**	Et_3N	0%
2	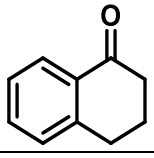 **(49)**	DBU	0%	4	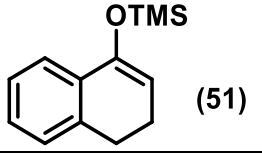 **(51)**	-	100%*

Table 3.2 *Nucleophile probing with chlorosulfide **46**: tetralones and derivatives*

As presented in **Table 3.2**, neither α-tetralone nor β-tetralone gave any reaction with our chlorinated substrate and the starting materials were able to be isolated and recovered. In the case of the α-tetralone derivative silyl enol ether, complete consumption of the quadruplet signal corresponding to the hydrogen on the chloride bearing carbon was observed by ^{1}H NMR. Although the general aspect of the crude mixture's ^{1}H NMR spectrum seemed promising, the expected product was not obtained after purification by column chromatography.

Activated heterocycles:

With this first batch of reaction partners proving inadequate, we believed that more reactive pronucleophiles might prove necessary to obtain some reactivity. Thus, the activated heterocycles 1H-thiazol-4(5H)-one **(52)** and Imidazol-4(5H)-one **(53)**, which would be easily deprotonated *in situ* in the presence of a weak base to provide the required enolate, were selected to verify our hypothesis.

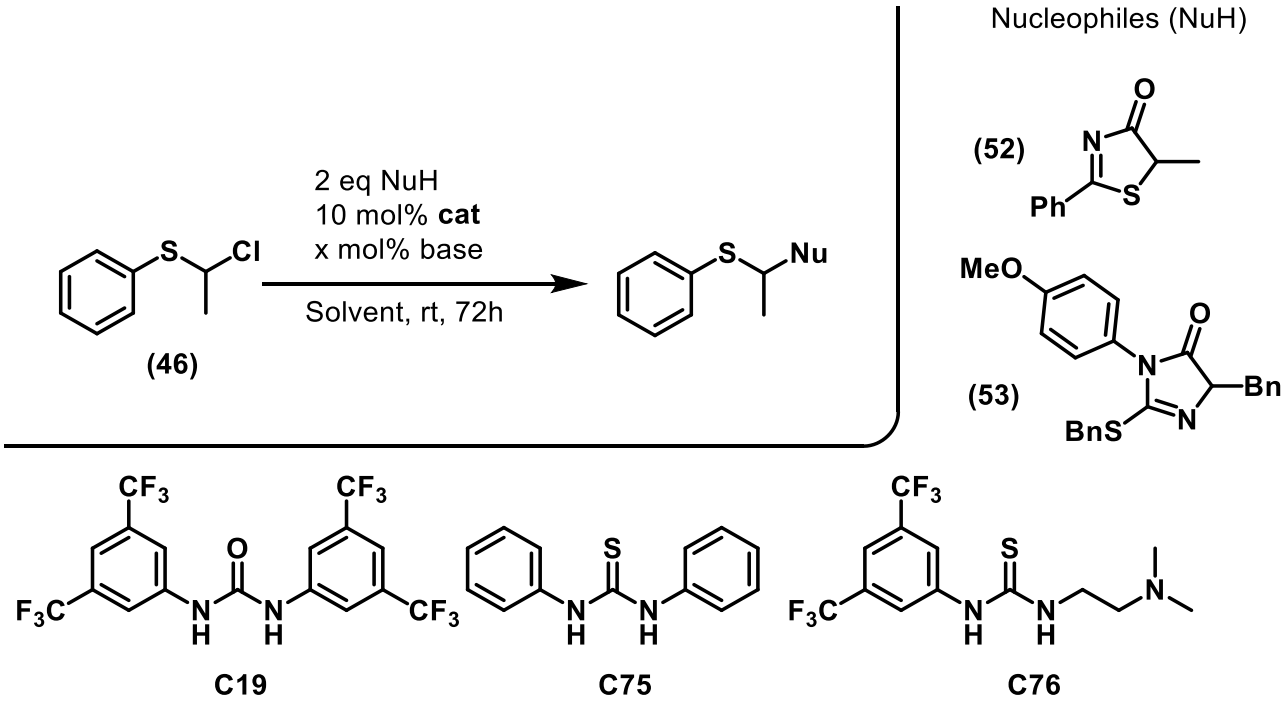

Entry	Nucleophile	Catalyst	Solvent	Base	Conversion
1	**(52)**	**C19**	CH_2Cl_2	Et_3N (110 mol%)	0% [a]
2	**(52)**	**C75**	CH_2Cl_2	Et_3N (110 mol%)	0% [a]
3	**(53)**	**C76**	CH_2Cl_2	Et_3N (110 mol%)	100% [b]
4	**(53)**	**C76**	CH_2Cl_2	DIPEA (110 mol%)	100% [b]
5	**(53)**	**C19**	MTBE	Et_3N (110 mol%)	100% [b]

[a] Degradation of starting material observed; [b] Undesired reaction observed

Table 3.3 *Nucleophile probing: activated heterocycles*

As reported in **Table 3.3**, thiazole derivative **(52)** did not react with starting chloride **(46)** with either of the tested catalysts. While the starting materials could be partially recovered, some degradation was observed in the ^{1}H NMR spectra of the crude mixture. In the case of imidazoline derivative **(53)**, complete consumption of the starting chloride was observed with catalyst **C76** and 1.1 equivalents of triethylamine. However, no signals corresponding to the expected material could be detected in the crude mixture. In order to test if the conditions used were too harsh for the reaction, the base was changed to DIPEA, however the same undesired reactivity was observed **(Table 3.3, entry 4)**. As this pronucleophile appeared to be excessively active, a change of solvent was attempted to reduce the reaction rate and possibly establish control over the reactivity. To that end, dichloromethane was substituted with methyl-tertbutyl ether (MTBE), however, the undesired reaction could not be inhibited and the expected reactivity did not take place under these conditions.

Thiols:

With carbon-carbon bond formation often being more challenging than its carbon-heteroatom bond counterpart, we decided to investigate the addition of thiols to our chlorides. This reactivity would result in the obtention of asymmetric dithioacetals with different substitutents if desired.

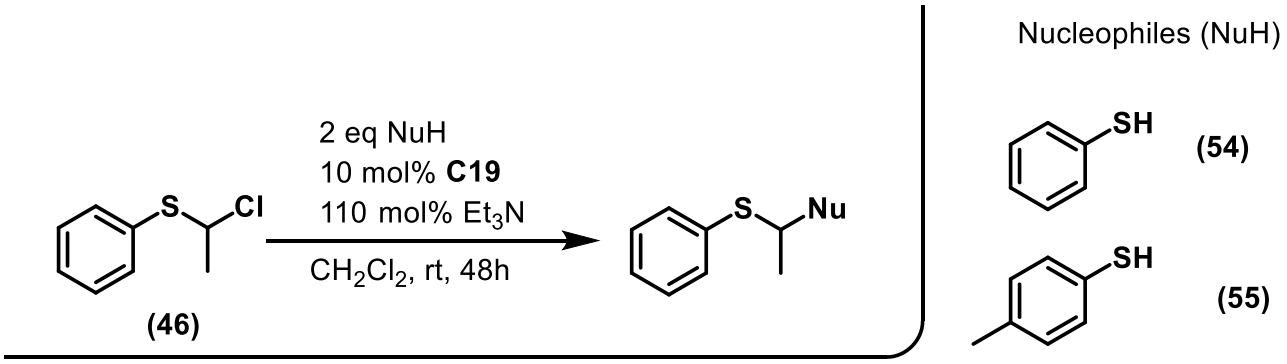

Entry	Nucleophile	Conversion
1	**(54)**	0%
2	**(55)**	0%

Table 3.4 *Nucleophile probing: thiols*

The reaction was attempted with simple and commercially available thiophenol **(54)** and *p*-thiocresol **(55)**. As presented in **Table 3.4**, no reaction was observed with either of the tested thiols and the starting materials were recovered without any observable degradation.

Other nucleophiles:

With the nucleophiles that have been tested up to this point not leading to successful reactivity, two other commonly used pronucleophiles with higher carbon acidities, nitroethane **(56)** and diethylmalonate **(57b)** were probed.

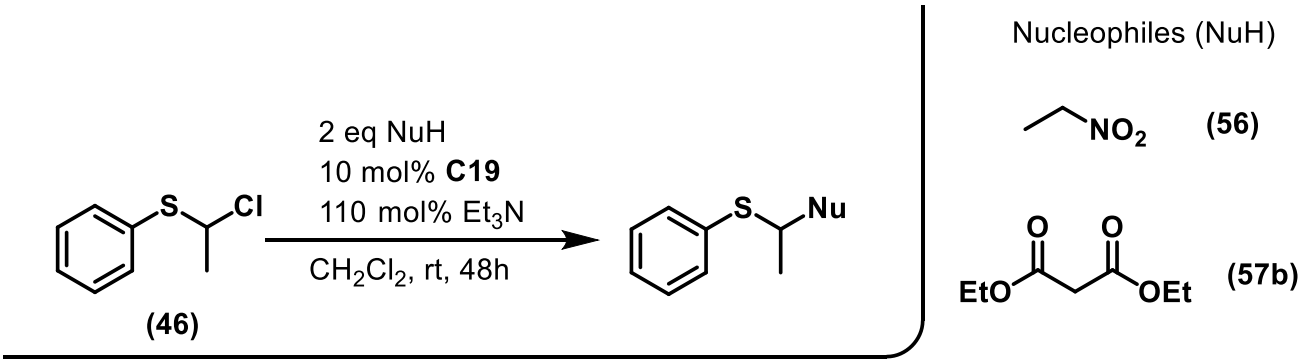

Entry	Nucleophile	Conversion
1	**(56)**	0%[a]
2	**(57b)**	90%[b]

[a] *Starting material degradation observed;* [b] *Crude mixture not purified*

Table 3.5 *Nucleophile probing: common pronucleophiles*

While no reaction takes place between the starting chloride **(46)** and nitroethane **(56)**, some transformation is observed with diethylmalonate **(57b)**. As presented in **Figure 3.11**, the reaction was monitored by ^{1}H NMR analysis of aliquots taken over time.

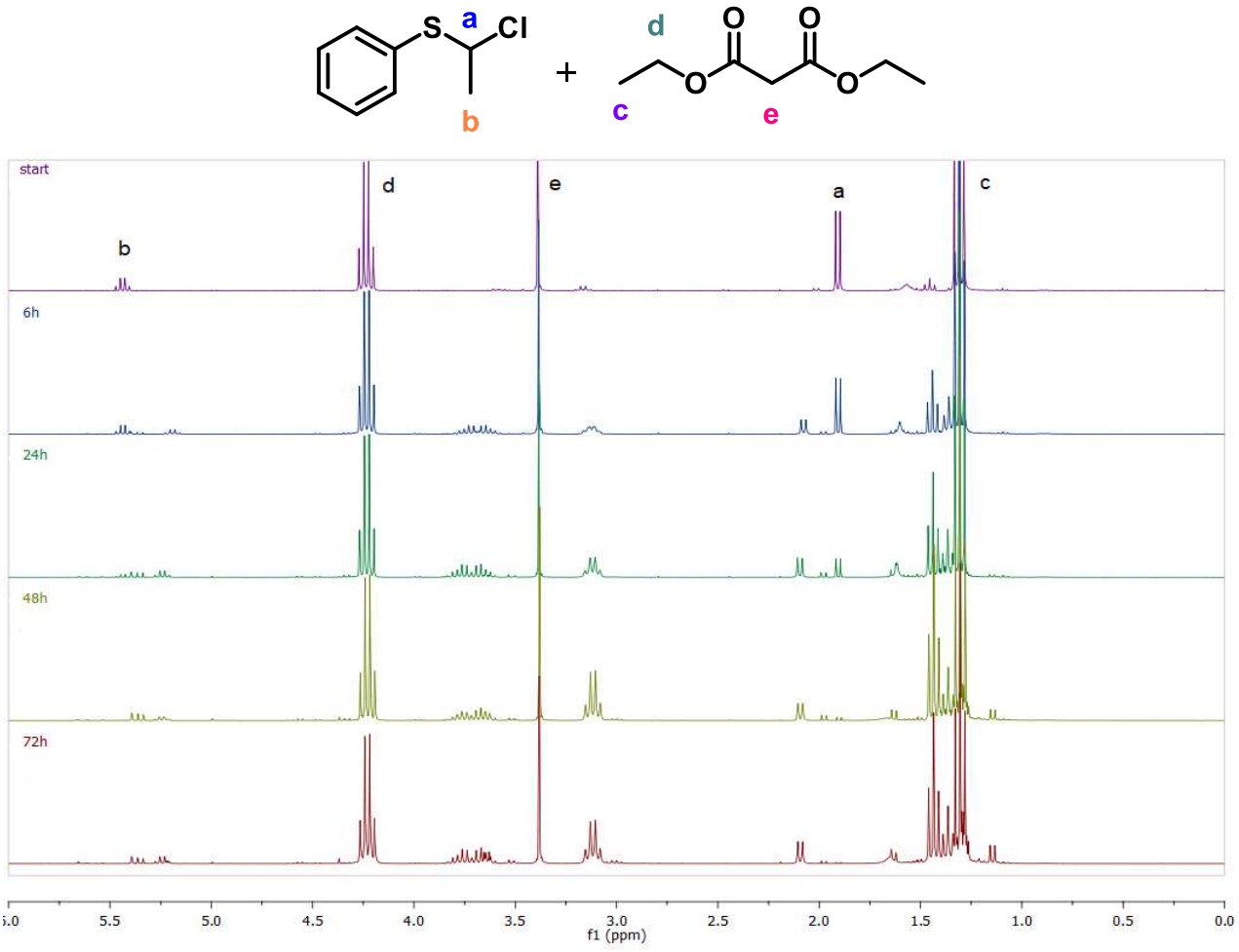

Figure 3.11 *Monitoring of the reaction between* ***46*** *and* ***57b*** *in the presence of* ***C19*** *by ^{1}H NMR ($CDCl_3$, 300MHz)*

While the signals corresponding to the starting material at 5.43ppm (quadruplet) and 1.90ppm (doublet) are consumed along the reaction, the formation of new signals can be observed, most notably the doublet at 2.09ppm and the signals in the 5.45-5.15ppm seem promising concerning the nature of the reactivity taking place. This type of compounds are little described in literature, however a report of similar product **(59)** obtained from Michael addition of thiophenol to 1,3-Dimethyl 2-ethylidenepropanedioate **(58)** could be found **(Scheme 3.22)**.[7]

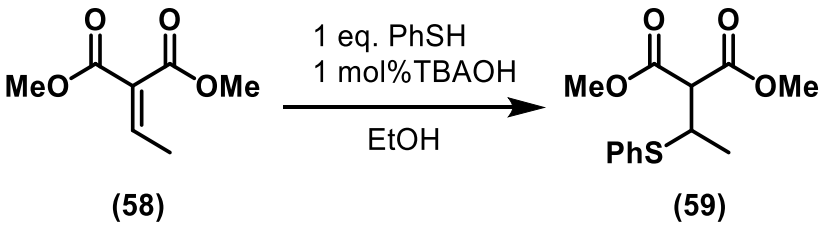

(58) **(59)**

Scheme 3.22 *Synthesis of dimethyl 2-[1-(phenylthio)ethyl]malonate* [7]

The comparison of the signals described by Marchi *et al* and those from our crude mixture comforted the hypothesis that the desired reaction has taken place, although not cleanly. Purification attempts using both column chromatography and vacuum distillation did not allow for the isolation of the addition product with both methods leading to partial or complete degradation of the material.

Conclusions and perspectives: α-chlorides

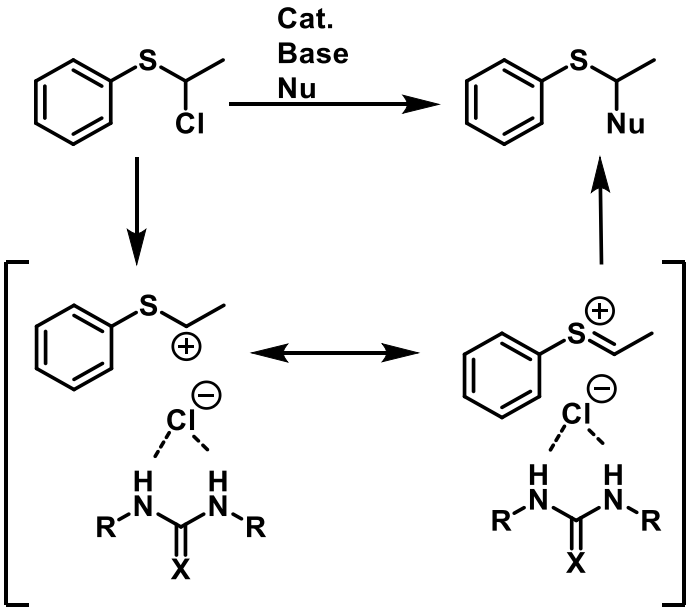

Scheme 3.23 *Nucleophile addition to α-chlorosulfides by anion abstraction*

The nucleophilic addition reaction to α-chlorosulfides by chloride anion abstraction **(Scheme 3.23)** was explored with nine different partners. Out of all tested nucleophiles, the only type that gave promising results was the malonates as the others led to no reaction taking place or complete degradation of the starting material.

Although promising results were obtained with dimethylmalonate judging from the analysis of the crude material, the isolation of the final product proved more challenging than originally anticipated.

As well as the purification difficulties that were faced, a second issue that was not forecasted has been the stability of the synthesised α-chlorosulfides. While chloromethyl-phenyl sulfide **(48)** remained stable at room temperature for a few months, our main reactant **(46)** showed signs of quick degradation at room temperature and slightly slower breakdown at -20°C, constituting another roadblock in the investigation of this reactivity.

Due to time restraints, our efforts had to be refocused on alternative electrophile candidates, however the reactivity between malonates and α-chlorosulfides could be improved upon with more stable starting chlorides and final products in order to allow for purification and isolation.

New electrophilic substrates:

Due to the difficulties faced when using our previously synthesised α-chlorosulfides, the necessity to find a new electrophile candidate for our catalytic system became evident. A recent report by Gouverneur *et al* involving the fluorination of β-bromosulfides under a phase transfer catalyst system attracted our attention **(Scheme 3.24)**.[8]

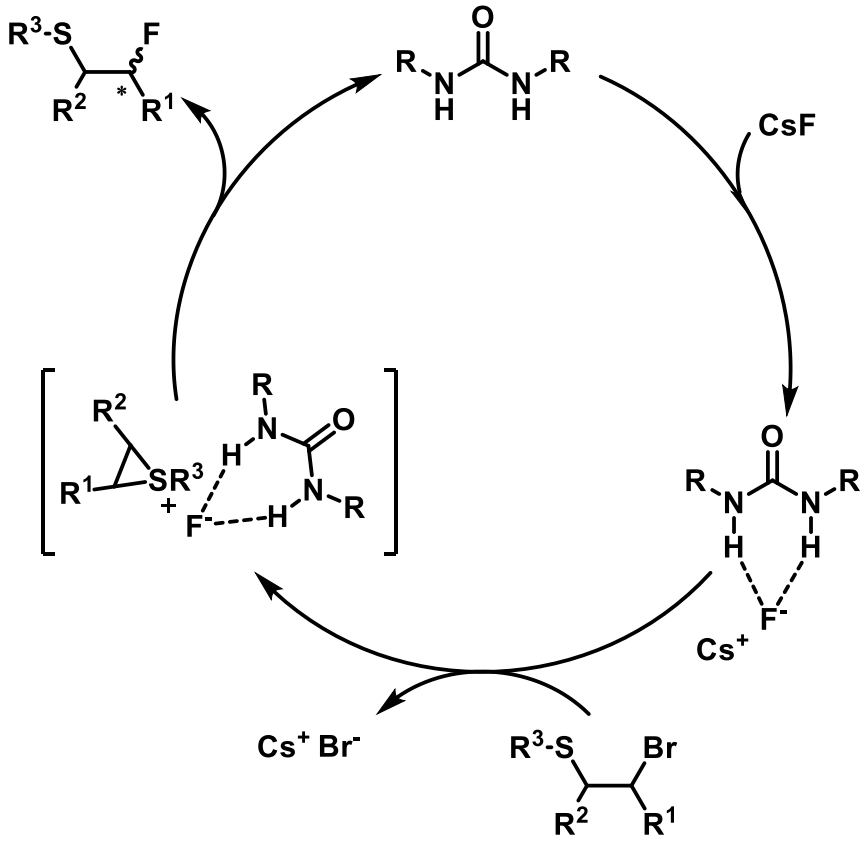

Scheme 3.24 *Asymmetric fluorination with phase transfer catalyst* [8]

This reaction has multiple points of interest for us as it implicates a substrate that is analogous to our chlorinated sulfides with the clear advantage of being more stable, because it involves a H-bonding catalyst for the transformation, but also because it was described to proceed through the formation of an episulfonium intermediate.

β-chlorosulfides were therefore selected as the alternative electrophilic substrates for our exploratory reaction.

Synthesis of β-chlorosulfides:

For our initial approach to synthesise the desired β-chlorosulfides, a single step direct sulfenylchlorination of alkenes employing a mixture of oxalyl chloride and DMSO was attempted according to a procedure described by Tian and co-workers[9] **(Scheme 3.25)**.

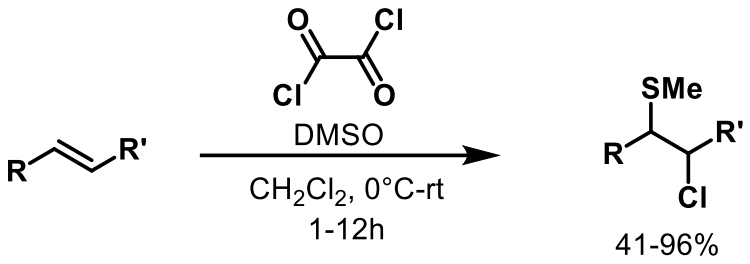

Scheme 3.25 *Single step sulfenylchlorination of alkenes by Tian et al*

This method was initially tested with *trans*-stilbene **(60).** Treatment of **(61)** with a (2:1) mixture of DMSO and oxalyl chloride at 0°C for 4h resulted in an extremely low conversion of 9% (determined by ^{1}H NMR). As this exact alkene was not described by the Tian group, the procedure was attempted once more with cyclopentene **(62)** to have comparable results. After 16h of reaction time and treatment, the obtained crude material essentially consisted of the unreacted starting material.**(Scheme 3.26)**

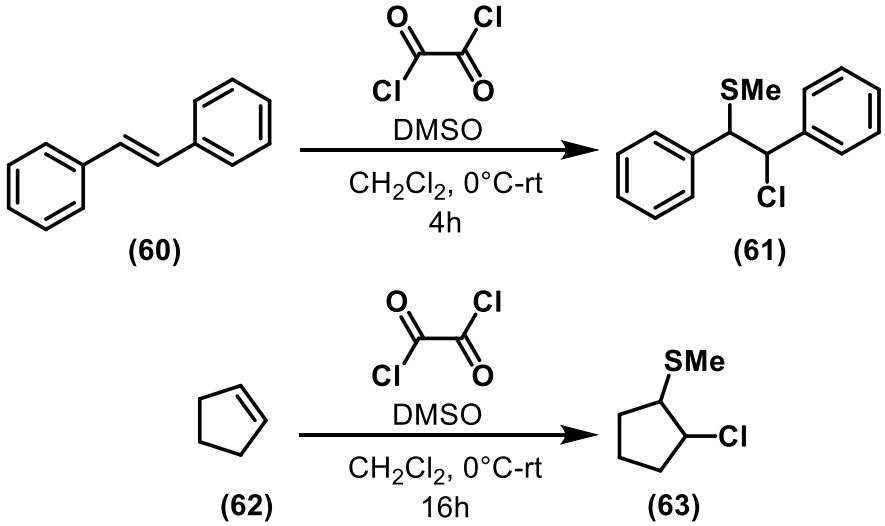

Scheme 3.26 *Sulfenylchlorination attempt with trans-stilbene and cyclopentene*

As this method of accessing the desired β-chlorosulfides could not be repeated, an alternative synthetic approach was taken. Since the desired substrates are very close to the ones used and described by Gouverneur *et al*, their reported synthesis[8] was used to supply our candidates.

Initial substrate (2-chloro-1,2-diphenylethyl)(ethyl)sulfide **(66)** was obtained in two steps. *Trans*-stilbene oxide **(64)** was opened with ethanethiol under basic conditions to yield racemic β-hydroxysulfide **(65)**. The –hydroxy group was subsequently substituted with chlorine using thionyl chloride with excellent yield and no additional purification being needed.

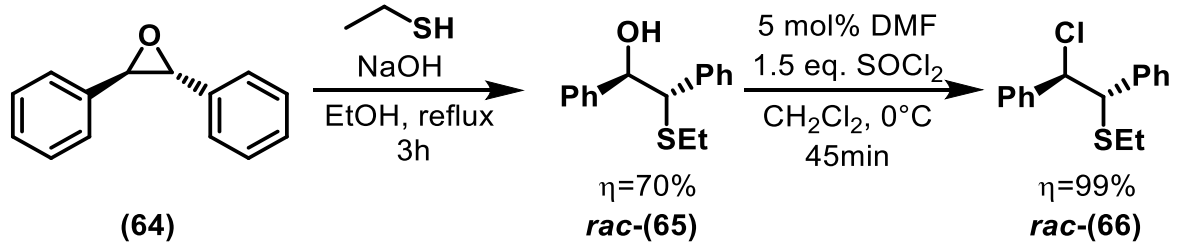

Scheme 3.27 *Synthesis of (2-chloro-1,2-diphenylethyl)(ethyl)sulfide* ***(66)***

As well as chloride **(66)**, racemic chlorosulfides **(69)** derived from cyclopentene and **(71)** bearing a phenylethyl- substituent on the sulfur as a more directly comparable substrate to that employed by Gouverneur *et al* **(Scheme 3.28)** were synthesised using the same strategy in order to have a substrate variation in the case where one would not behave as expected during our reactivity exploration.

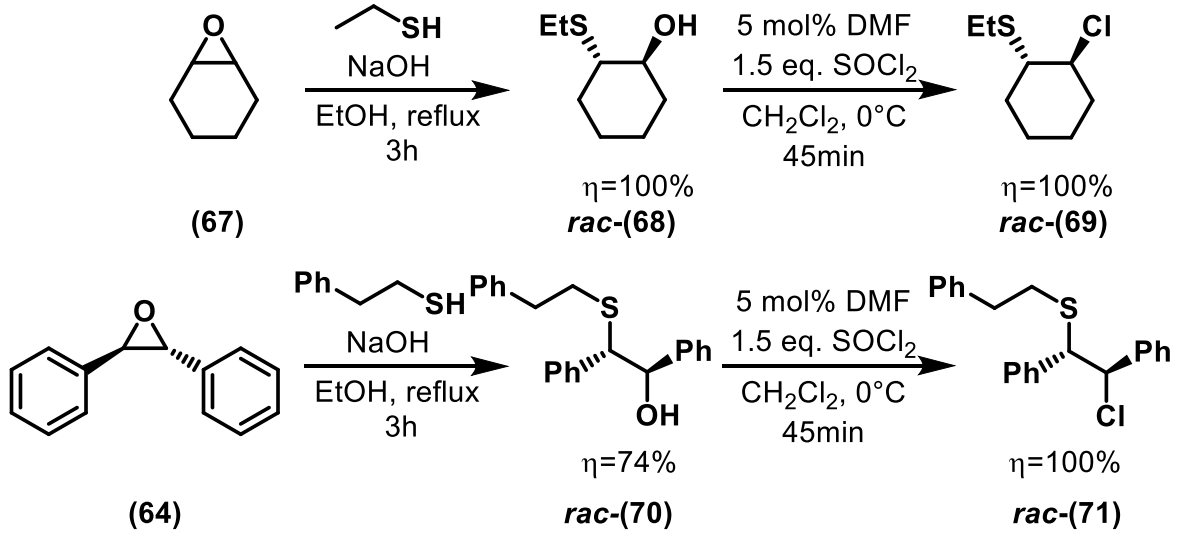

Scheme 3.28 *Synthesis of additional chlorosulfides*

With the new β-chlorinated substrates successfully obtained, the reactivity exploration was started once more with the simple achiral catalysts to probe potentially interesting nucleophiles before involving the oligourea catalysts.

Reactivity exploration

Carbon-based nucleophiles and pronucleophiles:

Initial reactivity probing efforts have been concentrated on finding new reactions for the formation of carbon-carbon bonds. As such, three partners were tested, including nitroethane **(56)** and dimethylmalonate **(57a)**, which were evaluated with our previous α-chlorinated substrates, and silyl ketene acetal **(72)**. As for their α-chlorinated counterparts, the reactivity of the β-chlorosulfides was evaluated by the consumption of the characteristic signals of the starting material by ^{1}H NMR.

It should be noted that in the reactions that follow involving several distinct nucleophiles, the C-Cl substitution process is assumed to occur with retention of configuration at the C-X carbon center, as a result of two consecutive S_N2-type inversions.

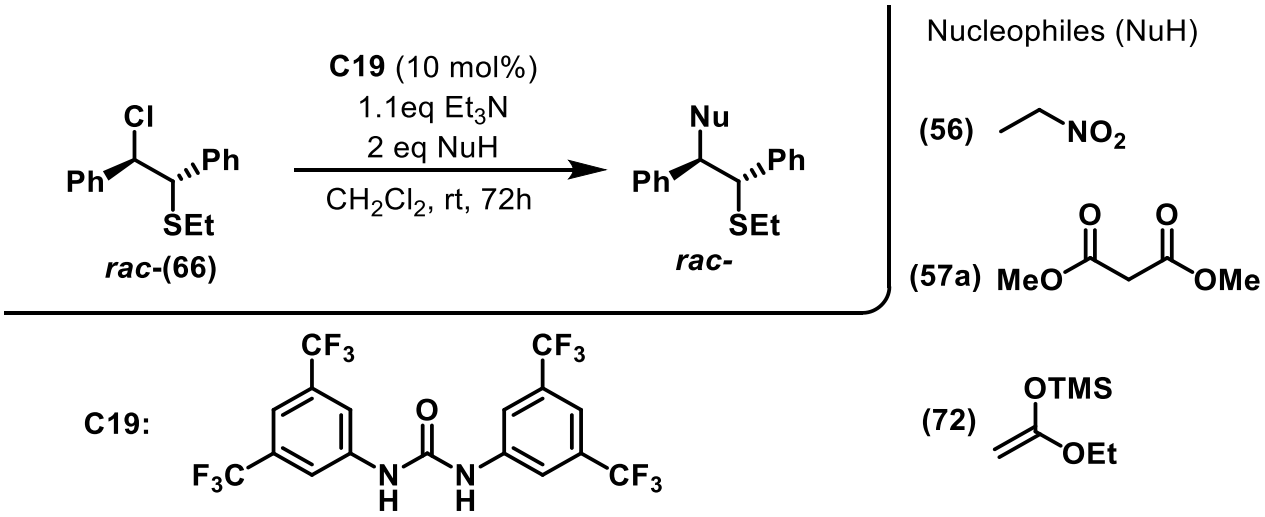

Entry	Nucleophile	Conversion[a]
1	**(56)**	100%
2	**(57a)**	95%
3	**(72)**	0%

[a] Conversion determined by ^{1}H NMR

Table 3.6 *Carbon based nucleophiles*

As presented in **Table 3.6**, for our initial experiments, excellent conversions were observed with nitroethane **(56)** and dimethylmalonate **(57a)**, whereas no reaction was obtained with silyl ketene acetal **(72)**.

In order to understand the obtained results, the reaction mixtures were successfully purified by column chromatography and the isolated fractions were characterised by NMR spectroscopy. The obtained spectra are presented below **(Figure 3.12).**

Surprisingly, in the case of the reaction with nitroethane **(56)**, the main product that was recovered after purification was unsubstituted *trans*-stilbene **(Figure 3.12 a)**.

More unexpectedly, purification of the reaction mixture with dimethylmalonate **(57a)** revealed that while an almost complete conversion being observed, the desired reaction had not taken place. Instead of the expected result, three different products were recovered.

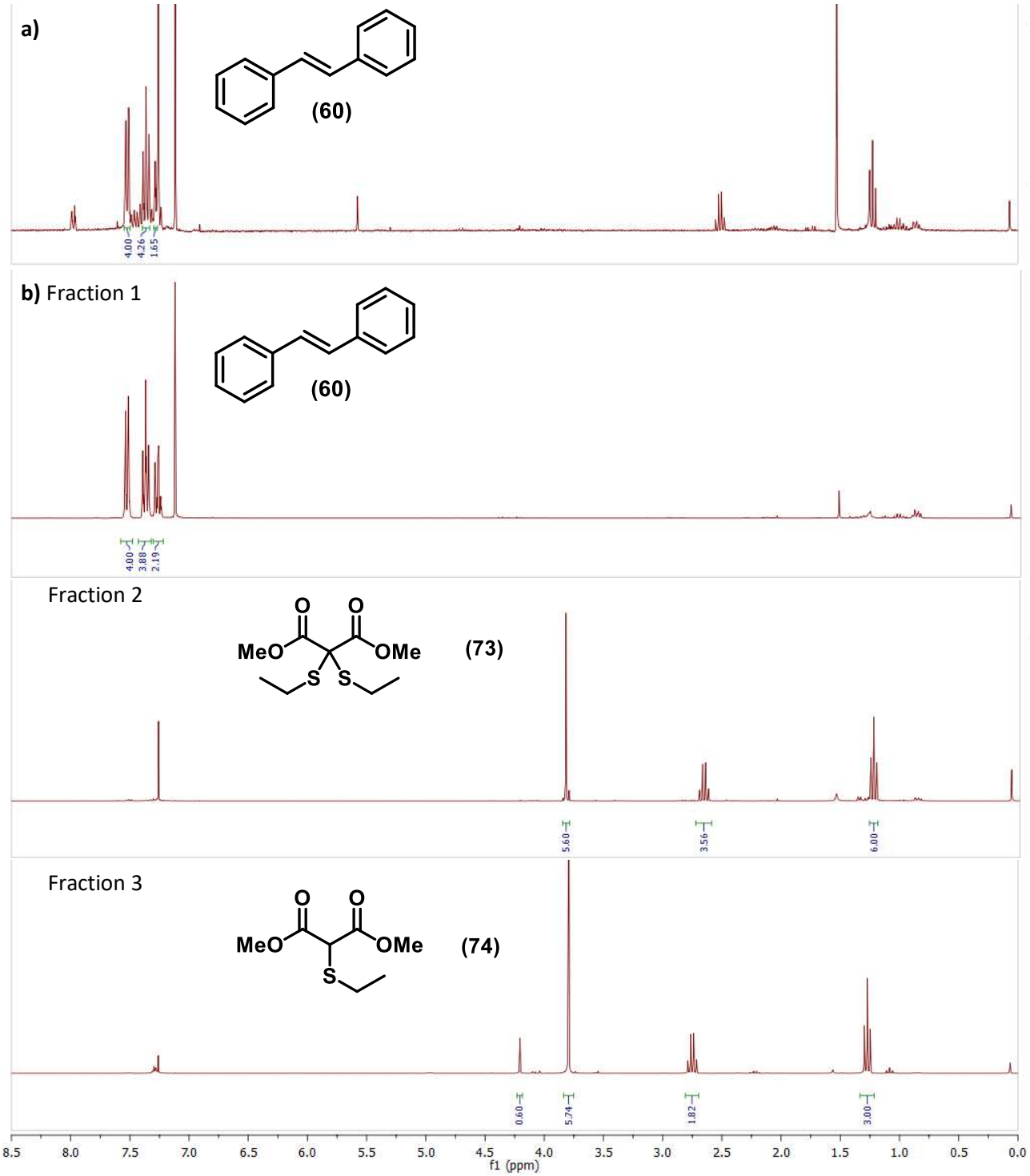

Figure 3.12 *^{1}H NMR of isolated reaction products*

The first fraction was determined to be unsubstituted *trans*-stilbene **(Figure 3.12b, Fraction 1)**. The second and third fractions, however gave important information concerning the observed transformation as they

were determined to correspond to the *bis*- **(Figure 3.12b, Fraction 2)** and *mono*-sulfenylated **(Figure 3.12b, Fraction 3)** malonate respectively.

Taken together, the results from these two reactions provide a clearer picture as to the transformation taking place. Thus, a hypothetical mechanism explaining how stilbene and malonate sulfenylation are obtained is proposed below **(Scheme 3.29)**.

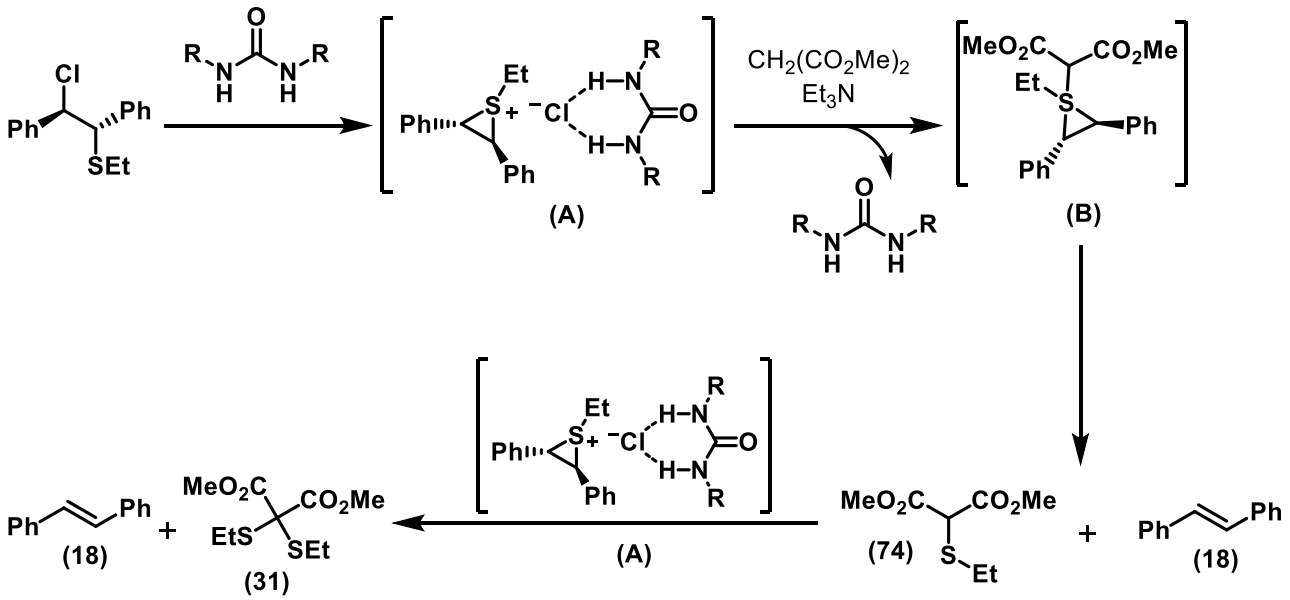

Scheme 3.29 *Proposed mechanism for the formation of* ***(73), (74)*** *and stilbene* ***(60)***

The reaction is initiated by the interaction between the catalyst and the starting chloride leading to anion pair **(A)**. While the formation of episulfonium ions through abstraction of a leaving group has been demonstrated by Jacobsen *et al* [10], the formation of intermediate **(B),** featuring a tetravalent organosulfur species, is only a conjecture as it was not isolated nor detected by any means. Thus, the possibility that the malonate attack and sulfide dissociation take place simultaneously, leading to **(74)** should also be considered.

These observations show that the nucleophile attack does not occur on a carbon centre as expected, but rather on the sulfur atom, thus leading to mono- and bis-sulfenylation of the nucleophile instead of the desired addition product. Indeed, more in-depth literature research uncovered that this behaviour for C-centered nucleophiles was not completely unanticipated as shown by studies from the Helmkamp group[11]

Under the hypothesis that this behaviour is coming from the usage of carbon-based nucleophiles, the reaction was attempted using heteroatom-based nucleophiles.

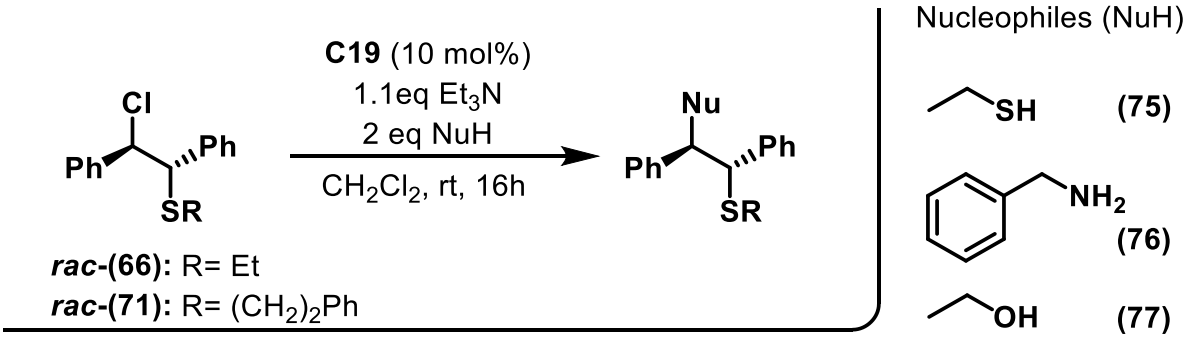

Entry	Substrate	Nucleophile	Conversion
1	**(66)**	**(75)**	86%
2	**(66)**	**(76)**	100%
3	**(71)**	**(77)**	50% [a]

[a] *Degradation was observed*

Table 3.7 *Heteroatom-based nucleophile screening*

As shown in **Table 3.7**, heteroatom-based nucleophiles demonstrated fairly successful reactivity compared to their carbon-based counterparts. Clean reactions were obtained using ethanethiol **(75)** and benzylamine **(76)** while partial reaction and slight degradation was observed using ethanol **(77)**, proving that heteroatom-based nucleophiles showed better compatibility with our expected reaction.

Following initial screening with nucleophiles **(75), (76)** and **(77)**, we decided to focus on thiols as partners for the addition reaction, partly to avoid potential complications with amines and alcohols, but also for the products that would be obtained in a reaction with thiols. Usage of the latter as nucleophilic reaction partners gives access to asymmetric α,β-bis-thiols, which are targets of interest due to being mustard derivatives.

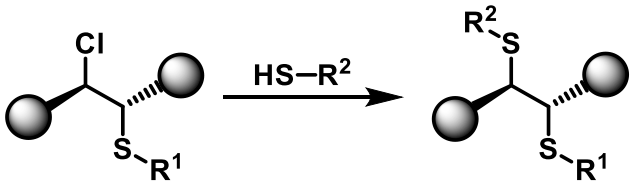

Scheme 3.30 *Synthesis of α,β-bis-thiols*

Thiols

With a promising initial result having been obtained using ethanethiol **(75)** as the nucleophile for our model reaction, we continued probing thiols as well as initiating an optimisation study of the reaction conditions.

- **Additional thiol screening:**

After successful ethanethiol **(75)** addition, nucleophile compatibility was tested with additional thiols.

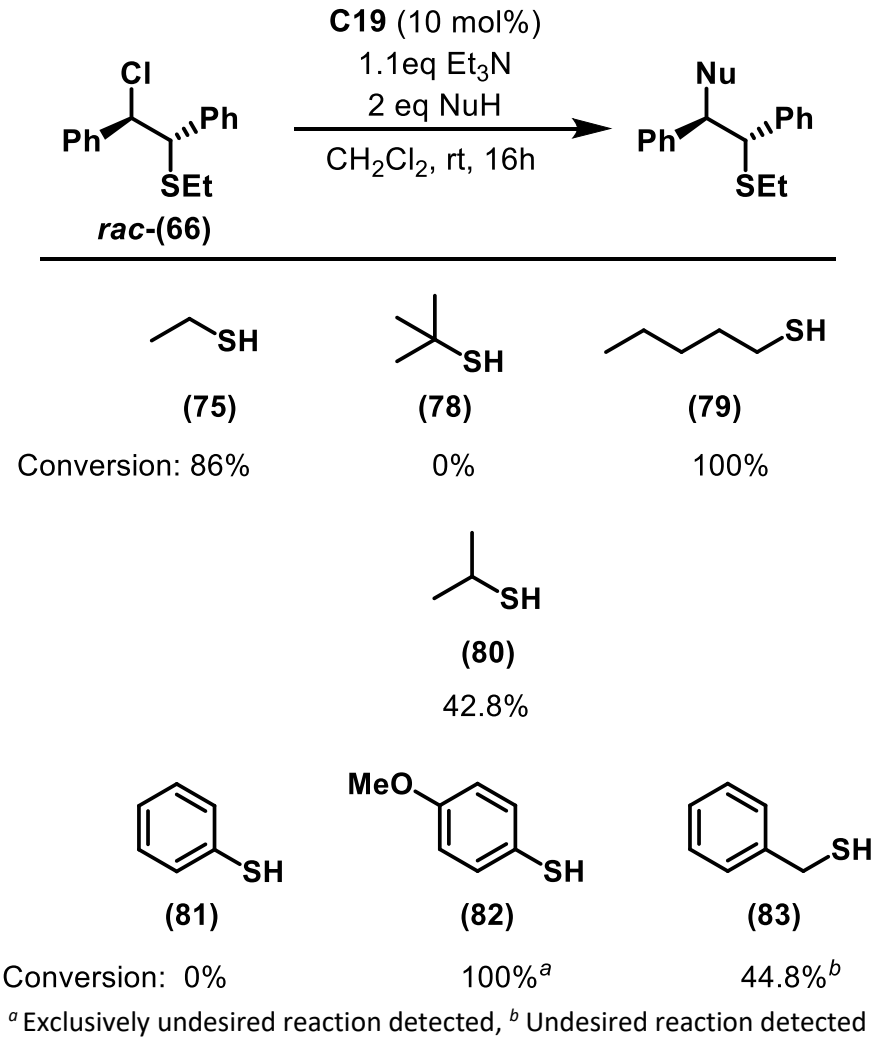

Scheme 3.31 *Thiol scope screening*

As shown in **Scheme 3.31**, linear thiols such as ethanethiol **(75)** and pentanethiol **(79)** demonstrated good reactivity, leading to high conversions in our model reaction at room temperature using achiral catalyst **C19**. Branched chained thio-alkanes demonstrated the sensitivity of the reaction to steric hindrance as isopropylthiol **(80)** led to middling conversion while no reaction could be obtained with *tert*-butylthiol **(78)**. Arylthiols were also probed with thiophenol **(81)** not reacting and *p*-methoxythiophenol **(82)** leading to undesired attack on the sulfur atom instead of the expected attack on a carbon center as evidenced by the identification of stilbene signals by ^{1}H NMR of the crude mixture. Finally, benzylthiol was tested, leading to moderate conversion but uncontrolled reactivity as signals corresponding to both the expected product and stilbene were identified, indicating that both competing reactions take place in the case of this nucleophile.

At this stage of our probe into the model reaction, the question of enantiomer separation needed to be studied. While no chiral catalyst was used, preliminary identification of separation conditions for the enantiomers with a racemic mixture is necessary for the continuation of our works. To that end, **(84)**

resulting from the addition of pentanethiol **(79)** to chlorosulfide **(66)** was used as reference for enantiomer separation by chiral HPLC.

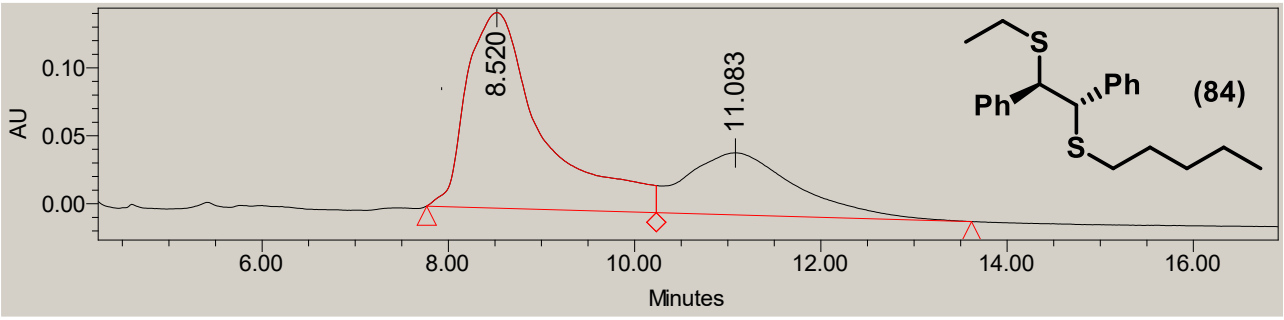

Figure 3.13 *Chiral HPLC enantiomer separation attempt for* ***(84)*** *(Chiralpak AD-H, 100% Hexane, flow: 1mL/min)*

Unfortunately, as shown by the shouldering observed in **figure 3.13** no separation conditions could be found to completely separate the two enantiomers, indicating that the enantiodifferentiation of the quasi-symmetrical bis-sulfide **(84)** remains an unanticipated challenge. In an attempt to resolve this issue, a batch of functionalised thiols were reacted with our β-chlorosulfides, hopefully leading to differentiable substituents and successful enantiomer separation.

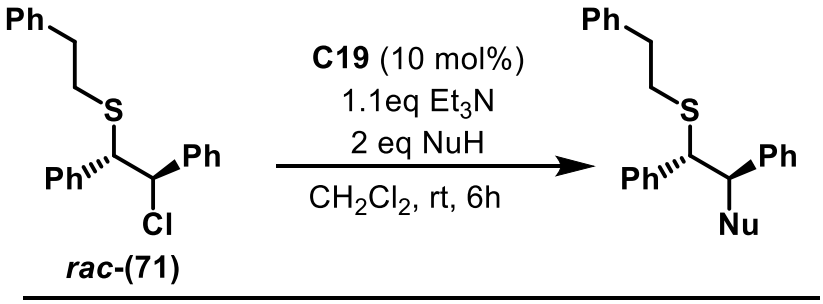

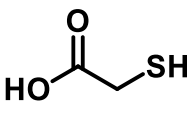

(85)

N.D.[a]

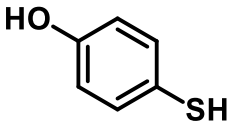

(86)

100%[b]

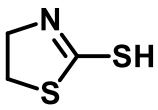

(87)

100%

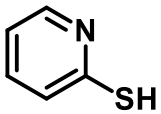

(88)

100%

[a] Extensive degradation, conversion could not be determined, [b] Exclusively undesired reaction detected

Scheme 3.32 *Functionalised thiol screening*

Out of the four test functionalised thiols, 2-mercapto-2thiazoline **(87)** and 2-pyridinethiol **(88),** exclusively and extremely cleanly, led to the respective desired products while mercaptoacetic acid **(85)** led to extensive degradation rendering interpretation of the results by ^{1}H NMR and TLC impossible. Finally, *p*-mercaptophenol **(86)** led to complete conversion of the starting chloride, however attack on the sulfur center was exclusively observed as stilbene was mainly recovered after purification. Thus, thiols **(87)** and **(88)** were retained as the best model candidates for the asymmetric reaction as both enantiomers of the corresponding adducts from **87** and **88** could be discerned conveniently by chiral HPLC analysis **(Figure 3.14)**.

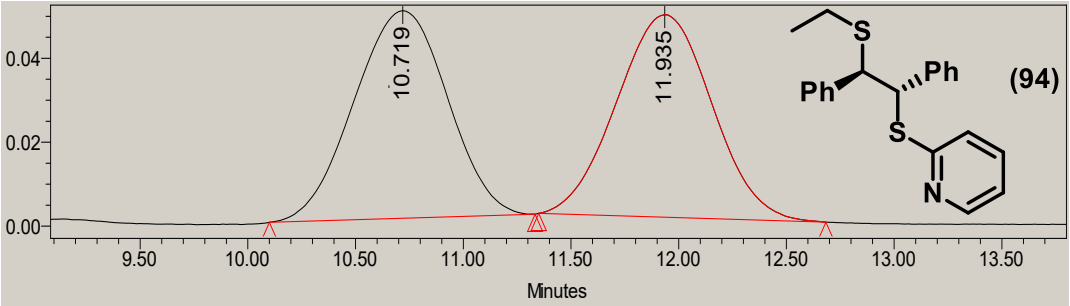

Figure 3.14 *Chiral HPLC enantiomer separation for* ***94*** *(Chiralpak AD-H, 99% Hexane-1%iPrOH, flow: 1mL/min)*

- **Influence of the solvent:**

While dichloromethane was used in all previous experiments, the solvent of the reaction should have an important effect on the reaction as the catalyst interaction as well as the formation of ion pairs are parameters that can be influenced by such modification. To that end, the reaction solvent was varied and its effect on conversion reported below in **Table 3.8**.

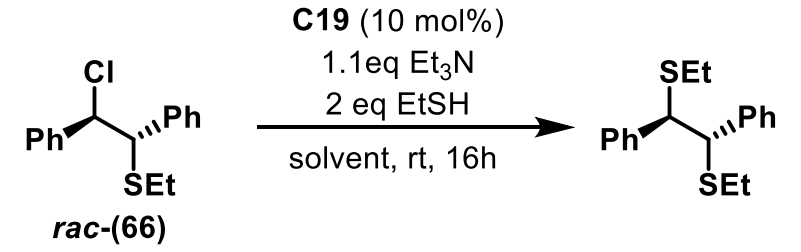

Entry	Solvent	Conversion
1	CH_2Cl_2	86%
2	Toluene	22%
3	MTBE	14%

Table 3.8 *Influence of the solvent*

As expected, the nature of the solvent that was used had tremendous impact on conversion with the reaction in dichloromethane leading to 86% conversion of the chloride into the expected product in 16h. Changing the solvent to toluene led to a reduction of the conversion by 74% for a 22% conversion after 16h

at room temperature **(Table 3.8, entry 2)** while reaction in MTBE led to an 83% reduction of the conversion or a final conversion of 14% after 16h **(Table 3.8, entry 3)**.

- **Influence of the base:**

After studying the influence of the solvent on our model reaction, the opportunity was taken to change the base in order to determine the impact it has on reactivity.

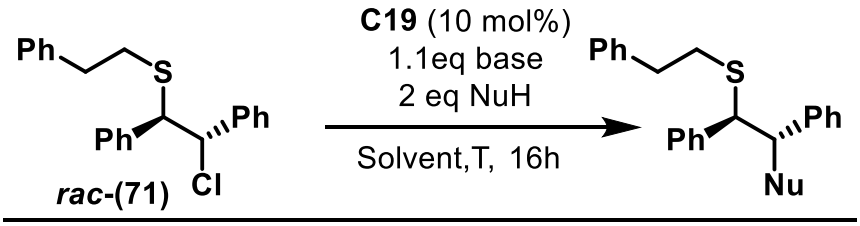

Entry	Nucleophile	Solvent	T	Base	Conversion
1	**(88)**	Toluene	0°C	Cs_2CO_3	33%
2	**(88)**	Toluene	0°C	NaOH	0%
3	**(88)**	Toluene	RT	Et_3N	100%
4	**(88)**	Toluene	RT	Cs_2CO_3	100%
5	**(87)**	Toluene	0°C	Cs_2CO_3	33%
6	**(87)**	Toluene	0°C	NaOH	0%
7	**(87)**	Toluene	RT	Et_3N	100%
8	**(87)**	Toluene	RT	Cs_2CO_3	100%
9	**(75)**	CH_2Cl_2	RT	Et_3N	69%
10	**(75)**	CH_2Cl_2	RT	DBU	0%
11	**(75)**	CH_2Cl_2	RT	NaOH	63%

Table 3.9 *Base variation results*

The results that were obtained by changing the nature of the base have been compiled in **Table 3.9**. The base that has been taken as reference in all our experiments has been triethylamine due to it giving the best results with all previous oligourea foldamer catalysed reactions. Two inorganic bases were tested in sodium hydroxide and caesium carbonate. The former did not lead to any reactivity at low temperatures **(entries 2 & 6)** but did lead to 63% conversion at room temperature **(entry 11)**, while the latter led to full conversion at room temperature **(entries 4 & 8)** and 33% conversion at 0°C in 16h **(entries 1 & 5)**. Thus, mineral bases were shown to be compatible with this reaction, albeit dependent on the temperature at which it is conducted. Replacing triethylamine with DBU did not result in any conversion at room temperature **(entry 10)**, showing that not all organic bases are compatible with the reaction. Upon inspection of the gathered data, while the nature of the base did have an impact in one case **(entry 10)**, the main factor of influence in these experiments appears to be the temperature.

- **Influence of the temperature:**

As observed in the previous section, during our investigation into the influence of the reaction parameters, the importance of the temperature parameter was indicated during our previous experiments. This is

expected, as temperature usually plays an important role in catalysed and especially asymmetric transformations.[12] The influence of the temperature was investigated with nucleophiles **(87)** and **(88)** by starting the reaction at -30°C and gradually allowing the temperature to rise back up to ambient.

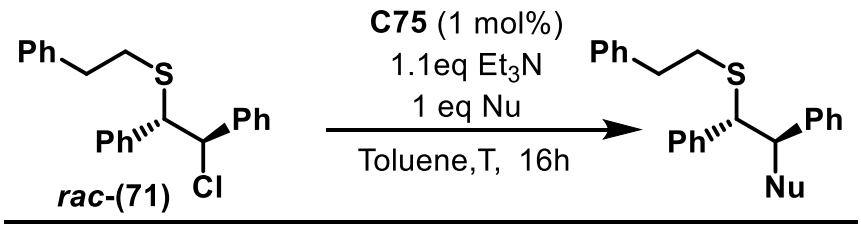

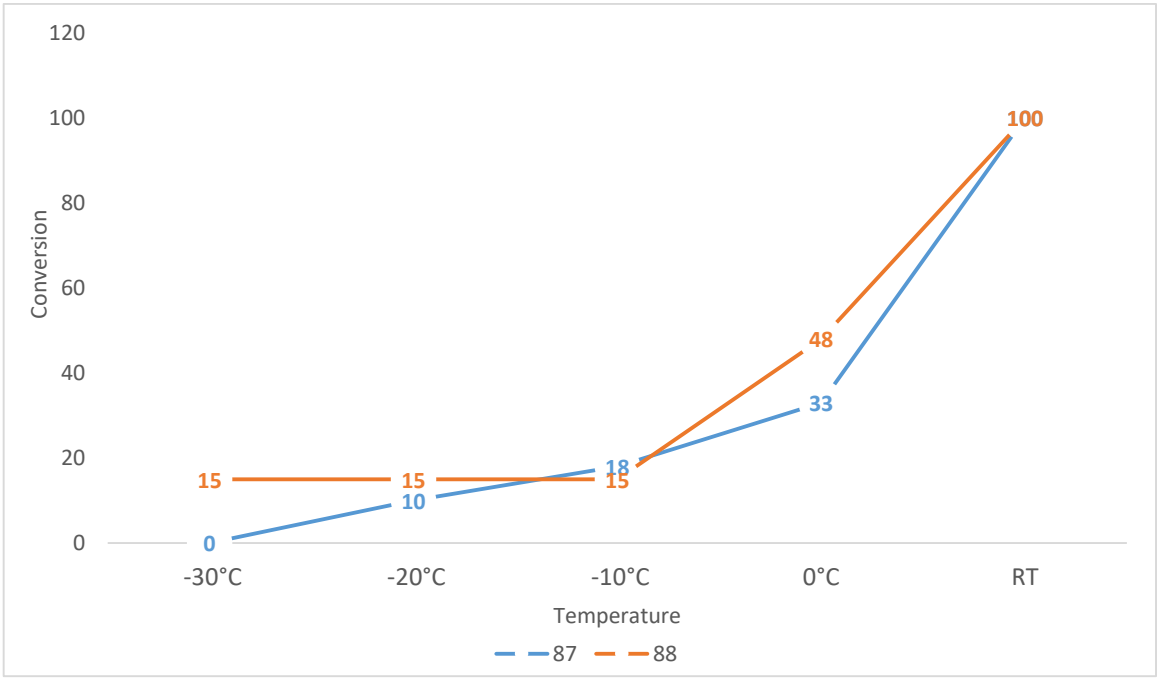

Figure 3.15 *Investigation of the influence of temperature*

Measurements of the reaction were taken every 16h after a temperature change to have regular intervals where data is comparable and the results were plotted on the chart shown in **Figure 3.15**. As expected, the temperature plays an important role in the observed reactivity. In the case of 2-mercapto-2-thiazoline **(87)**, no reaction was observed at -30°C, whereas the reaction showed low conversion starting from -20°C with a noticeable rate acceleration at 0°C. Interestingly, in the case of 2-pyridinethiol **(88),** while an initial conversion of 15% was observed at -30°C, the resulting signals obtained by ^{1}H NMR, although closely resembling, did not correspond to the expected product. These signals remained identical all the way until the temperature reaction reached -10°C, at which point, they were replaced with the characteristic signals of the usual addition product. The most likely hypothesis would be the formation of an intermediate at the start of the reaction that is stable enough at a temperature range of -30°C to -20°C for the reaction not to proceed further, while reaching -10°C allows for the energy barrier to be crossed and the reaction to pursue. This species could not be trapped or isolated in order to determine its structure. However, we speculated this intermediate may be the N-addition adduct as the kinetic reaction product **K** which subsequently rearranges into the more stable S-addition product **T (Scheme 3.33)**.

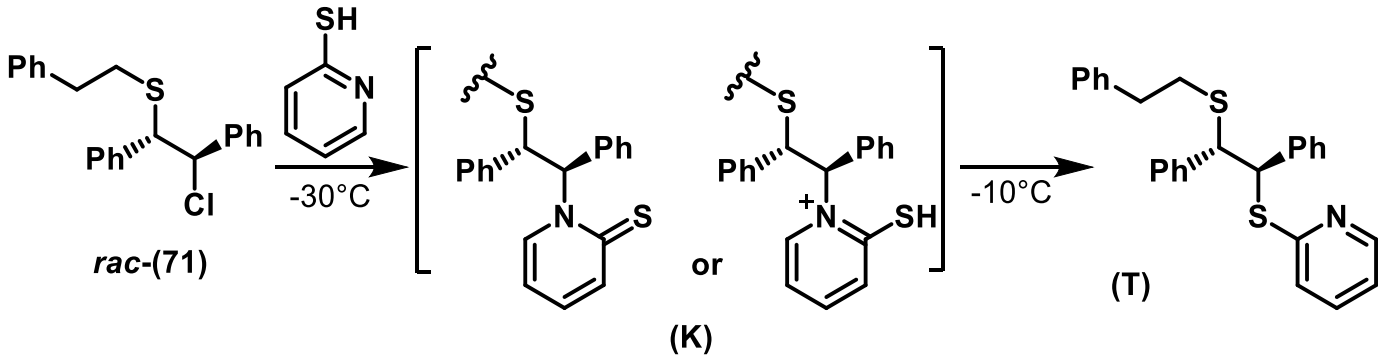

Scheme 3.33 kinetic N-addition product **(K)** and rearrangement into thermodynamic S-addition product **(T)**

- **Cis/trans configuration of the intermediate sulfenium**

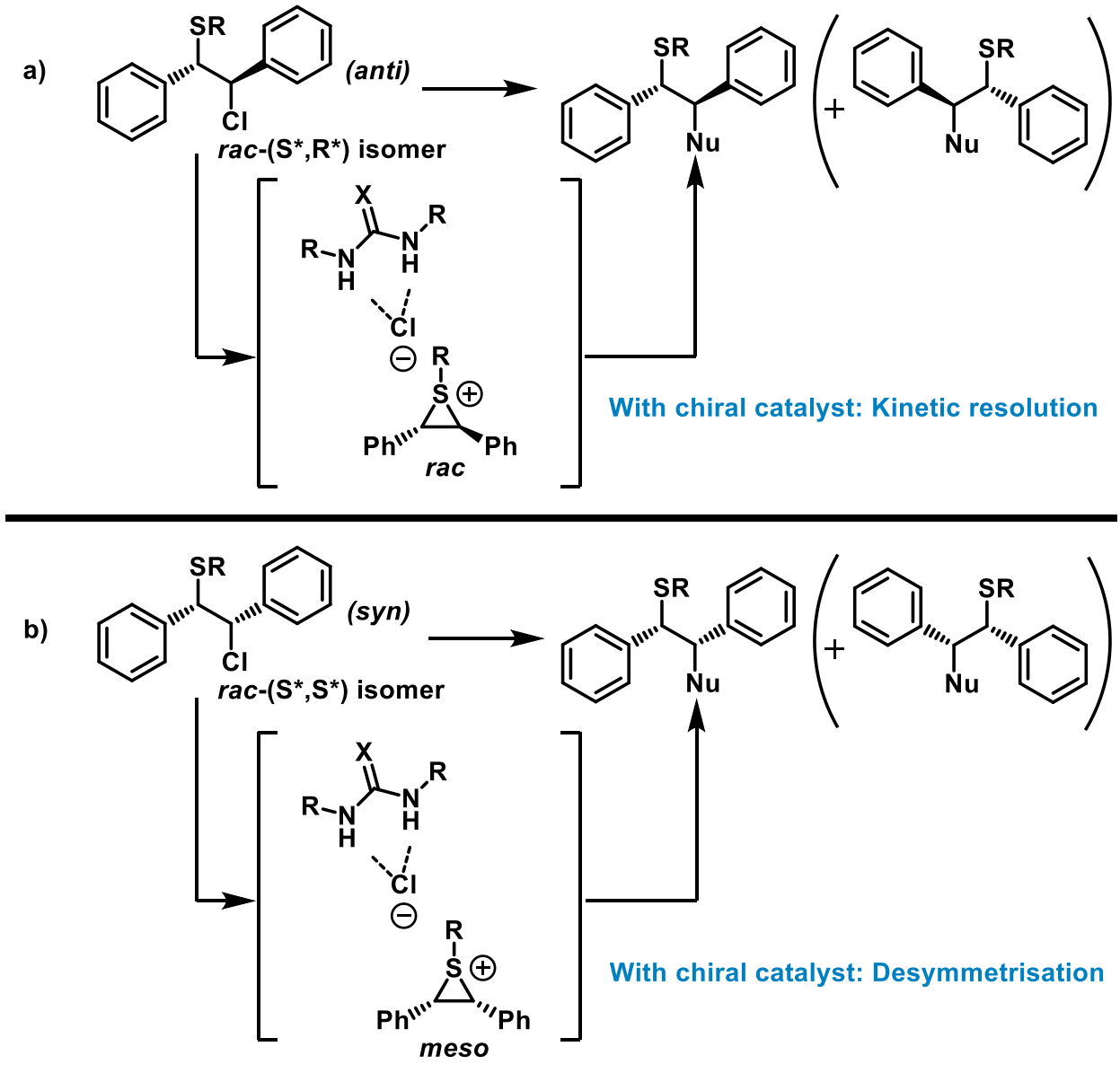

Scheme 3.34 addition reaction according to β-chlorosulfide configuration

The β-chlorosulfides that were synthesised have been derived from *trans*-stilbene oxide, thus displaying a (S*,R*) or *syn* relative configuration **(Scheme 3.34, a)**. During the reaction, after anion abstraction, these β-chlorosulfides would give way to chiral C_2-symmetrical sulfenium species as a racemic mixture. Thus, in the absence of a chiral reagent or catalyst, both enantiomers would react at same rate leading to either enantiomeric product at equal proportions. Note that, because of the C2-symmetry of the sulfenium intermediate, nucleophilic attacks at either carbon site would generate the same final product. However, in the presence of a chiral reagent or catalyst, a kinetic resolution may take place. On the contrary, using *cis*-stilbene as the starting material, the corresponding β-chlorosulfides with a (S*,S*) or *anti* relative configuration will be obtained. In that case, after the chloride abstraction step, the resulting *meso*-episulfonium ion could be desymmetrised in the presence of a chiral reagent or catalyst to obtain one enantiomer in excess of the other. In order to evaluate the impact of the relative configuration of the substrates on their general reactivity, and particularly their behaviour under the present catalytic conditions, a new β-chlorosulfide derived from *cis*-stilbene was synthesised according to the pathway presented in **(Scheme 3.35)**

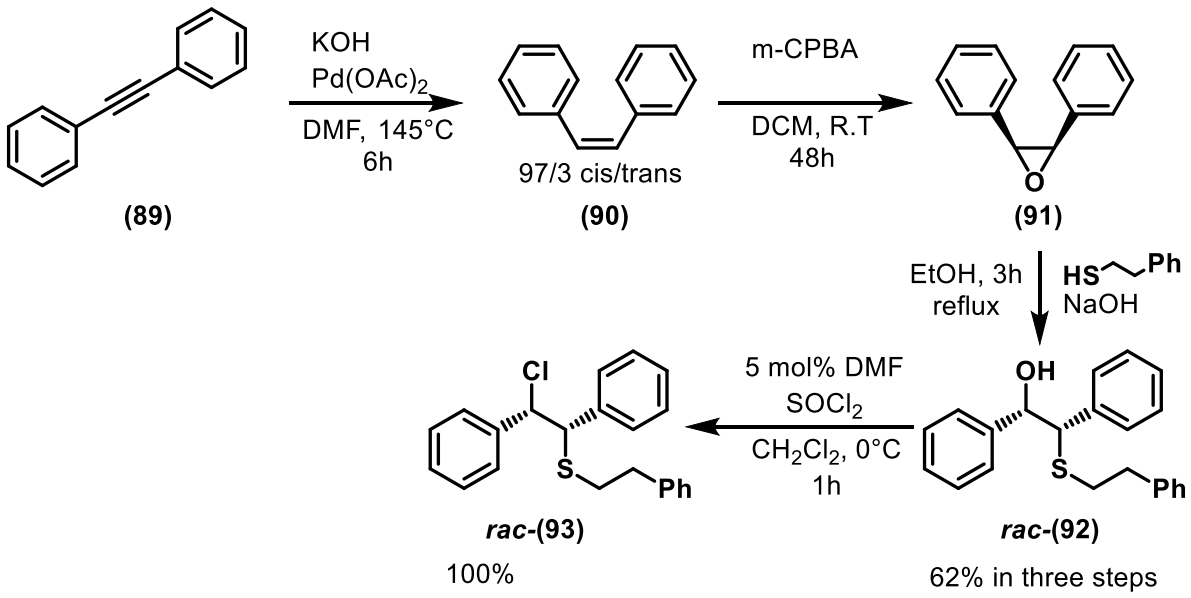

Scheme 3.35** Synthesis of syn-β-chlorosulfide **(51)

Phenylacetylene **(89)** was reduced into *cis*-stilbene **(90)** with a 97/3 *cis*/*trans* ratio using palladium acetate and potassium hydroxide according to a previously described procedure [13]. *Cis*-stilbene oxide **(91)** was obtained by treatment of **(90)** with m-CPBA. Finally, the epoxide was opened with the desired thiol and sodium hydroxide and the alcohol was substituted with the chloride using thionyl chloride using the same procedure as for the (S*,R*)-β-chlorosulfides that were previously synthesised. Thus, chlorosulfide **(93)** was obtained as a 97/3 mixture of the (S*,S*)/(S*,R*) isomers with a global yield of 62%.

The diastereoisomers were subsequently compared to each other.

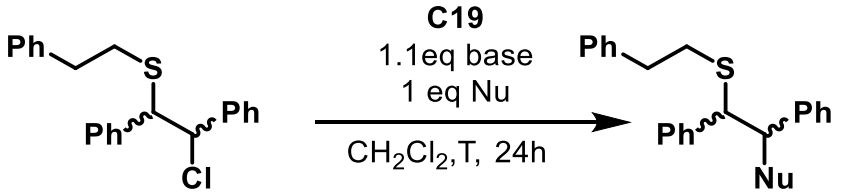

(71): *(S*,R*)*
(93): *(S*,S*)*

Entry	Substrate	Nucleophile	Base	Temperature	Conversion
1	**(71)**	EtSH **(75)**	Et_3N	RT	86%
2	**(93)**	EtSH **(75)**	Et_3N	RT	3%[a]
3	**(71)**	$C_5H_{11}SH$ **(79)**	Et_3N	RT	100%
4	**(93)**	$C_5H_{11}SH$ **(79)**	Et_3N	RT	3%[a]
5	**(71)**	**(88)**	Et_3N	RT	100%
6	**(93)**	**(88)**	Et_3N	RT	100%
7	**(71)**	**(88)**	Et_3N	-30°C	35%
8	**(93)**	**(88)**	Et_3N	-30°C	18%[b]

[a] Only *(S*,R*)* isomer reacts; [b] *(S*,R*)* and *(S*,S*)* isomers react

Table 3.10 *Reactivity comparison of β-chlorosulfide stereoisomers*

Some useful information can be gained from the results compiled in **Table 3.10**. Indeed, at all temperature ranges and with all tested nucleophiles, the *anti*-configured isomer appears to be the more reactive of the two. More importantly, using less reactive nucleophiles such as ethylthiol **(75)** or pentanethiol **(79)** show that the *syn*-configured isomer does not react at all whereas the *anti*-isomer shows usual reactivity **(entries 2 & 4)**. Only when using stronger nucleophiles such as 2-mercaptopyridine **(88)**, was any reaction with the *syn*-isomer observed **(entries 6 & 8)**. This difference in reactivity between the two isomers comes unexpectedly as other examples of episulfonium opening found in literature have mostly employed *syn*-configured isomers [3,8], rendering such an issue rather unforeseeable.

- **Influence of the catalyst:**

After studying the tuneable reaction conditions, the effect of the catalyst has been the final point of our probe into this model reaction. While initial testing has been done using the achiral urea catalyst **C19,** the final objective has been the evaluation of our oligourea foldamer catalysts for reactions involving anion binding.

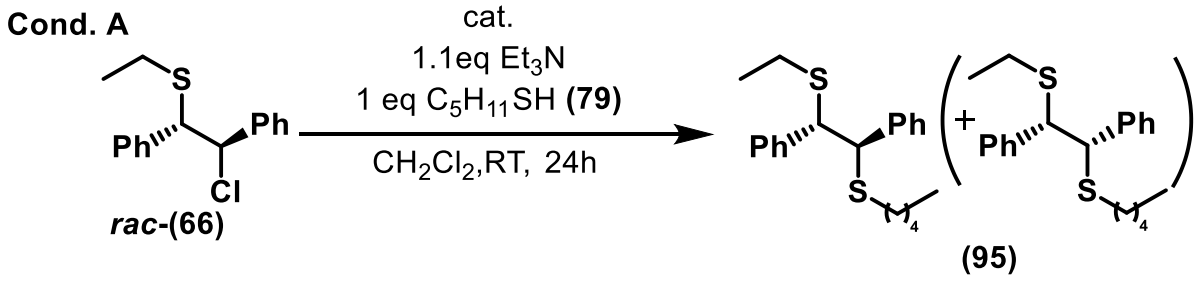

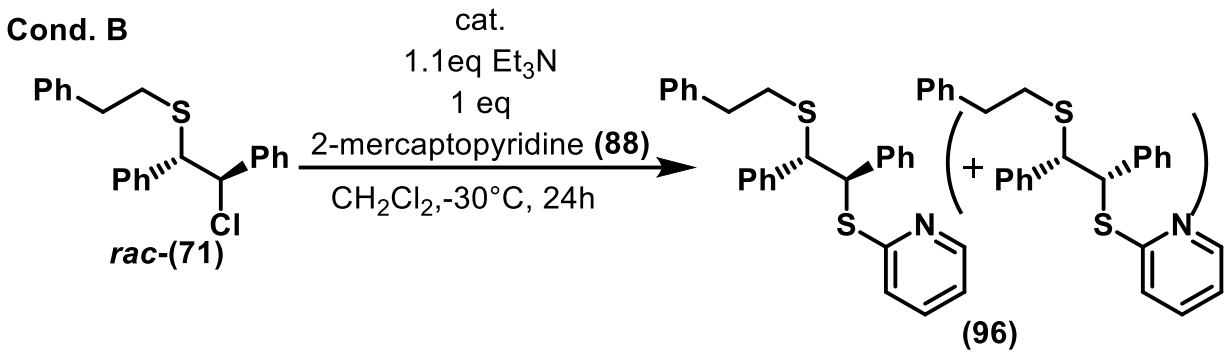

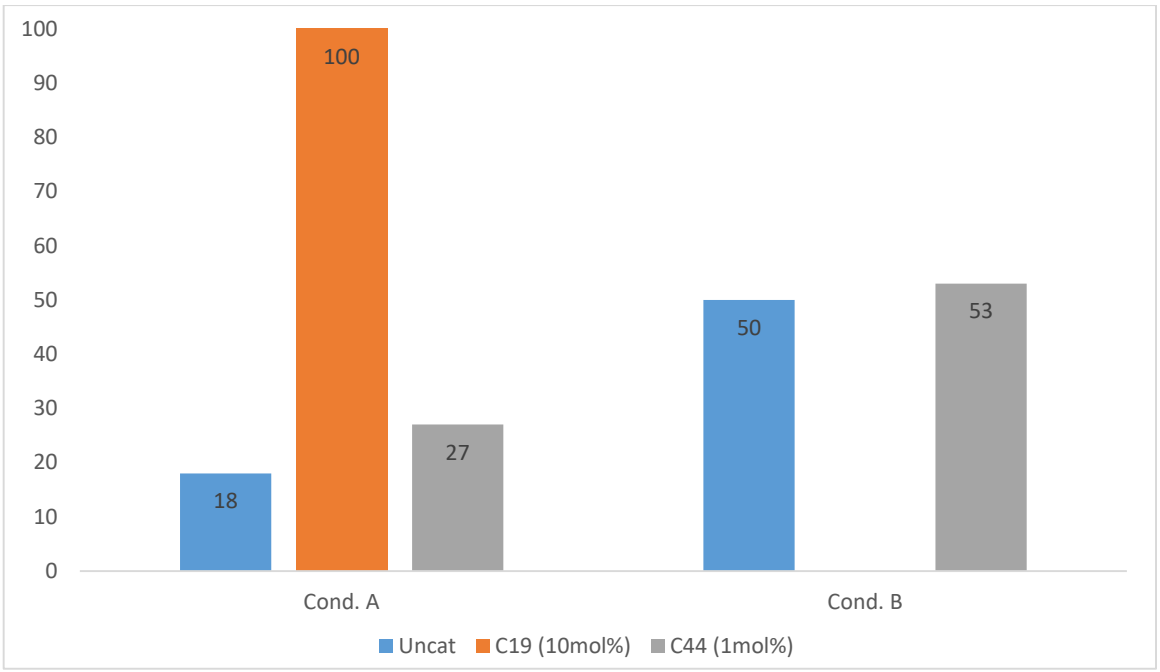

Figure 3.16 Catalyst effect study on conversion

In order to determine the activity of the catalyst, two sets of conditions were employed, one for pentanethiol **(79)** and another for 2-mercaptopyridine **(88)**. In each case, the background reactivity in the absence of catalyst was measured in a period of 24h. The same reaction was then ran with our oligourea catalyst **C44** and the conversion was compared. The results of this study are compiled in the chart presented above in **Figure 3.16**. At room temperature, the uncatalysed reaction between chlorosulfide **(66)** and pentanethiol **(79)** resulted in 18% conversion in 24h. In the presence of achiral catalyst **C19**, total conversion was obtained in the same time period while using oligourea catalyst **C44** resulted in a conversion of 27%. This result indicates very low catalyst activity for these conditions and due to the low difference between the ethyl- and pentyl- side chain, no separation could be obtained by HPLC to evaluate whether the catalyst had any asymmetric induction. To that end, the second set of conditions gave us some answers. At -30°C, the uncatalysed reaction between chlorosulfide **(71)** and 2-mercaptopyridine **(88)** resulted in 50% conversion while a comparable conversion of 53% was obtained in the presence of oligourea catalyst **C44**. It should also be noted that quite surprisingly, when attempted with chlorosulfide **(93)** under condition set B, no reactivity was observed using catalyst **C44.**

This set of data once again demonstrates little if no effect of the oligourea catalyst on the transformation. Purification of the crude material followed by analysis by chiral HPLC confirms this hypothesis with a 1:1 ratio of both enantiomers being separated **(Figure 3.17)**, thus showing no asymmetric induction from the part of the catalyst.

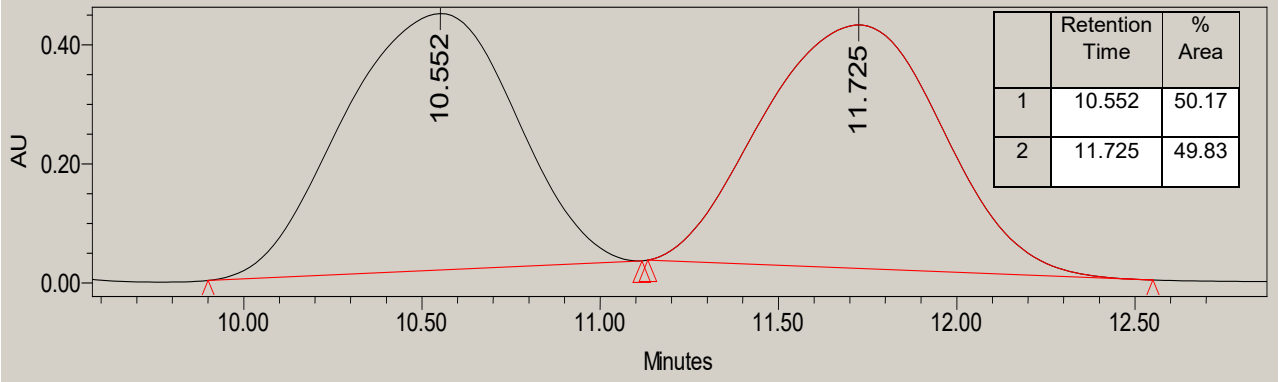

Figure 3.17 *Chiral HPLC chromatogram of enantiomer mixture* ***(96)*** *(Lux Amylose 1, 99% hexane, 1%iPrOH, flow 1mL/min)*

References

[1] V. Diemer, L. Fischer, B. Kauffmann, G. Guichard, *Chem. Eur. J.*, **2016**, *22*, 15684-15692

[2] For reviews on anion binding catalysis: S. Beckendorf, S. Asmus, O.G. Mancheño, *ChemCatChem*, **2012**, *4*, 926-936; K. Brak, E.N. Jacobsen, *Angew. Chem. Int. Ed.*, **2013**, *57*, 534-561

a) For examples of anion abstraction catalysis involving iminium cations: I.T. Raheem, P.S. Thiara, E.A. Peterson, E.N. Jacobsen, *J. Am. Chem. Soc.*, **2007**, *129*, 13404-13405; C.S. Pan, B. List, *Chem. Asian J.*, **2008**, *3*, 430-437

b) For examples of anion binding catalysis involving oxocarbenium intermediates: S. E. Reisman, A. G. Doyle, E. N. Jacobsen, *J. Am. Chem. Soc.*, **2008**, *130*, 7198 – 7199; N. Z. Burns, M. R. Witten, E. N. Jacobsen, *J. Am. Chem. Soc.* **2011**, *133*, 14578 – 14581

[3] G.L. Hamilton, T. Kanai, F.D. Toste, *J. Am. Chem. Soc.*, **2008**, *130*, 14984-14986; S. Lin, E.N. Jacobsen, *Nat. Chem.*, **2012**, *4*, 817-824

[4] I. Fleming, J. Goldhill, I. Paterson, *Tetrahedron Lett.*, **1979**, *34*, 3209-3212 ; G.A. Kraus, H. Maeda, *Tetrahedron Lett.*, **1995** , *36*, 2599-2602 ; Groth, *Liebigs Ann. Chem*. **1993**, 49; Guindon *Org Lett* **2002**, *4*, 241; Prévost, *J. Org. Chem*. **2014**, *79*, 10504

[5] D.L. Tuleen, V.C. Marcum, *J. Org. Chem.* **1967**, *32*, 204–206; D.L. Tuleen, T.B. Stephens, *J. Org. Chem.* **1969**, *34*, 31–35

[6] W.E. Truce, G.H. Birum, E.T. McBee, *J. Am. Chem. Soc.* **1952**, *74*, 3594–3599; F.G. Bordwell, B.M. Pitt, *J. Am. Chem. Soc.* **1955**, *77*, 572–577

[7] D.R. Nicponski, J.M. Marchi, *Synthesis*, **2014**, *46*, 1725-1730

[8] G. Pupo, F. Ibba, D.M.H. Ascough, A.C. Vicini, P. Ricci, K.E. Christensen, L. Pfeifer, J.R. Morphy, J.M. Brown, R.S. Paton, V. Gouverneur, *Science*, **2018**, *360*, 638-642

[9] L. Lan, Y. Gao, T. Zhang, Y. Liu, B. Sun, H. Tian, *Synth. Commun.*, **2019**, *Vol 49 (4)*, 539-549

[10] S. Lin, E.N. Jacobsen, *Nat. Chem.*, **2012**, *4*, 817-824

[11] D.C. Owsley, G.K. Helmkamp, S.N. Spurlock, *J. Am. Chem. Soc.*, **1969**, *91*, 3606-3609

[12] S. Ikeda, T. Yamagishi, M. Yamaguchi, M. Hida, *Bull. Chem. Soc. Jpn.*, **1989**, *62*, 3508-3512; J. Xu, T. Wei, Q. Zhang, *J. Org. Chem.* **2003**, *68*, 10146–10151

[13] J. Li, R. Hua, T. Liu, *J. Org. Chem.*, **2010**, *75(9)*, 2966-2970

Conclusions and perspectives:

After a very successful application of oligourea catalysts to the Michael addition reaction of malonates to nitro-olefins, the objective of our group has been the exploration of additional reaction that could benefit from this family of catalysts.
Two investigation axles were identified for the continuation of the previous works: the modification of the reference catalyst **C44** in an effort to better understand the role of the oligourea backbone on the activity and the exploration of new reactivity.
Through the modifications such as side chain nature, activating cap and terminal H-bond donor functions that were brought to the most active catalyst **C44**, none of the new structures managed to surpass the conversion and stereoselectivity demonstrated by the reference compound. This highlights the need to obtain more intricate information as to the way our catalyst interacts with the target substrates and the transition state of the reaction in order to improve the catalytic system. To that end, the collaboration between our group and the theoretical chemistry team at the UPPA (Université de Pau et des Pays de l'Adour) plays a major role in filling the information gaps that still remain and will allow for a faster iteration of the catalytic system.

Our group's studies of the application of these catalysts has shown that while they are capable of recognising and binding anions, their application to ion pair catalysis is not as straightforward as initially believed. Our first efforts were directed towards the development of a yet unexplored asymmetric thioalkylation reaction involving thiocarbenium species as reactive intermediates from α-chlorinated sulphides as substrates. Unexpected challenges in the synthesis of the α-chlorinated sulfides as well as the encountered incompatibility of most carbon-based nucleophiles with the tested reaction have forced the consideration of alternative reaction substrates and nucleophiles.
In a second phase, the asymmetric catalytic transformation of β-chlorinated sulphides via intermediate episulfenium species was explored. While promising results were obtained with thiols as nucleophiles, some challenges such as HPLC enantioseparation, reactivity at low temperature and the lack of activity observed with our oligourea foldamer catalysts did not allow us to reach the desired reactivity as we had set out to achieve.
A more thorough investigation on the influence of the various reaction conditions has brought us to the conclusion that the application of our oligomeric catalysts to other reactions may not be as straightforward as we believed at the beginning of our project. Much like enzymes showing high substrate and reaction specificity, similar increases in specificity may arise from the size and locked geometry of the catalysts brought by the structural backbone.

Therefore, a different approach towards the application of oligourea foldamer catalysis to promote reactions (enantio)selectively to new reactions could prove judicious. As we have learned from this endeavour, focusing on one reaction and its optimisation may not bring the desired results. Thus, the simultaneous exploration of multiple new types reactions followed by a focus on the ones giving promising results may be a better option.

To that end however, some improvements to the method of catalyst synthesis seems to be necessary in order to access the final hexamers, the oligomers showing optimal reactivity and selectivity so far, at scales permitting such a screening study. One way to easily simplify the overall synthesis would be to use a

single monomer for main chain elongation (only one block to prepare). For example, it has been shown that residues with branched side chains (e.g. Val^u) increase helix propensity of oligoureas (results from the group), similar to what has been found for β-peptides.[1] One could thus focus on the synthesis of short $(Val^u)_n$ oligomers (e.g. n = 5) which in principle could be produced more readily on large (> 1 g) scale. Alternatively, catalysts on solid-support which are potentially reusable could eventually be used more readily to screen a larger number of reactions.

[1] T.L. Raguse, J.R. Lai, S.H. Gellman, *Helv. Chim. Acta*, **2002**, *Vol.85*, p4154-4164

Methods and data:

General Methods:

Unless specified otherwise, all used reagents were acquired from commercial sources (Fluorochem, Alfa Aesar, Merck, TCI, Sigma-Aldrich) and used as is without further purification. The employed solvents such as dichloromethane, toluene and tetrahydrofuran have been dried by filtration over activated alumina. Hygroscopic bases (triethylamine, N,N-diisopropylethylamine) were purified by distillation and kept over 3Å molecular sieves.

Reaction monitoring was typically performed by thin layer chromatography on plates coated with silica gel 60 F254 by Merck. Compounds were detected by direct UV light revelation in relevant cases or by charring with the suitable revealing agent.

Purification by column chromatography was carried out on silica gel with a particle size of 40-63µm purchased from Merck. Automated purification was performed on a Teledyne CombiFlash Rf system with silica gel columns from the same provider.

High resolution electrospray ionization time-of-flight (ESI-TOF) mass spectra were measured in the positive ion mode on a Waters/Micromass Q-Tof Ultima.
^{1}H NMR spectra were recorder using a Bruker Avance II spectrometer operating at 300MHz or 400MHz when needed. ^{13}C NMR spectra were recorded using a Bruker Avance II spectrometer operating at 75MHz. The chemical shifts (δ) were reported in parts per million (ppm) relative to the residual signal of the deuterated solvent that was used in the experiment.
The obtained spectra were processed using MestReNova 6.0.2 and Bruker TopSpin 3.6.1 and use the following designation for signal multiplicity: s, singlet; d, doublet; t, triplet; q, quartet, m, multiplet. The reported coupling constants (J) are given in Hertz (Hz).

For asymmetric reactions, the enantiomeric excesses were determined using high performance liquid chromatography performed on a Waters-600E equipped with a 2996 and 2998 photodiode array UV detector using Daicel Chiralpak AD-H and AY-H or Phenomenex Lux Amylose-1 columns

Syntheses concerning chapter 2:

Synthesis of building blocks:

-Regular blocks:

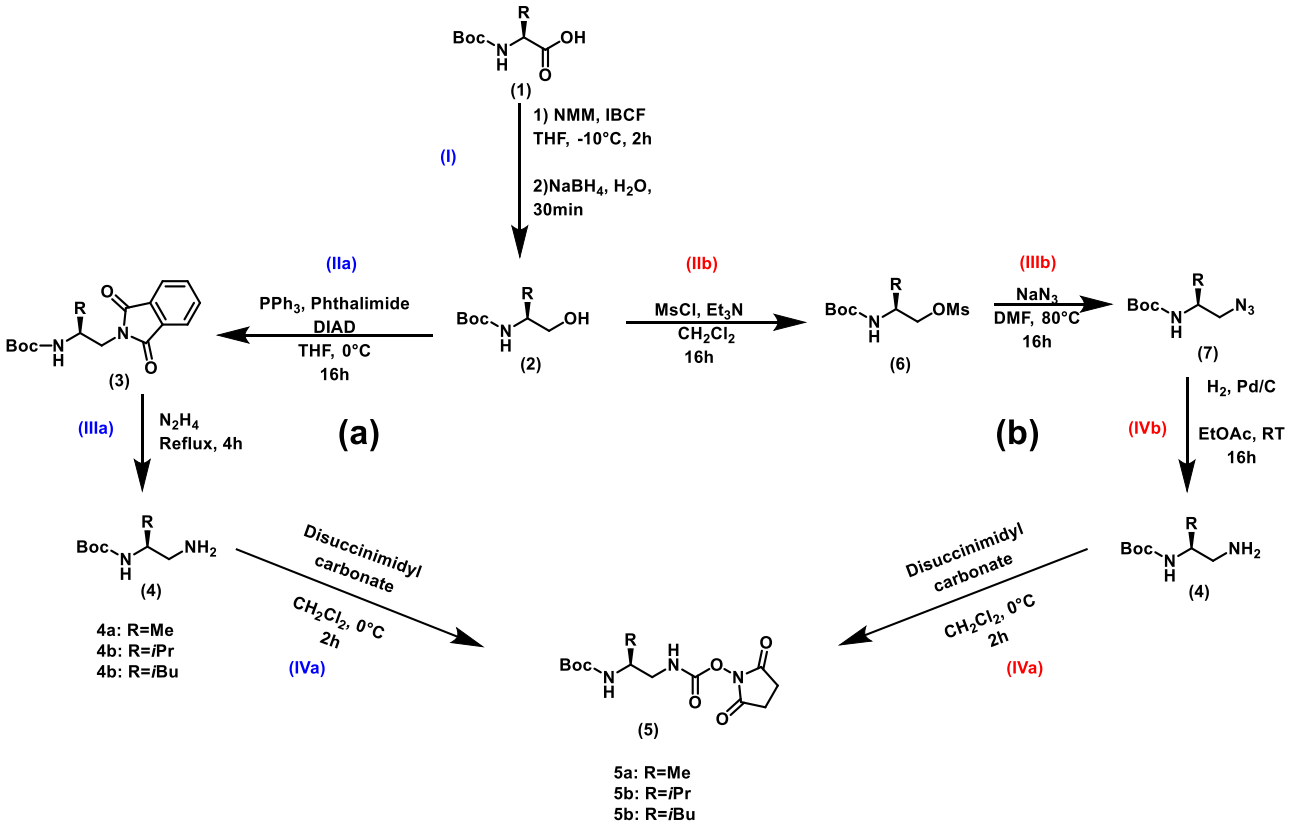

Scheme 1 *General block synthesis*

Amino-acid reduction **(I)**:

The Boc protected aminoacid was dissolved in dry THF and cooled to -10°C. N-Methylmorpholine (1.1eq) and Isobutylchloroformate (1.1eq) were subsequently added and the reaction was stirred at -10°C for 1.5h (TLC in cyclohexane/EtOAc 50:50). The reaction mixture was filtered to remove the white precipitate formed during reaction. The filtrate was slowly and carefully poured over a solution of $NaBH_4$ (2.1eq) in H_2O (5mL). The resulting mixture was left to stir and degas for 30min at room temperature after which the THF was evaporated under reduced pressure and EtOAc (1.5mL/mmol aminoacid) was added. The remaining $NaBH_4$ was quenched by adding aqueous $KHSO_4$ (1N) until degassing was complete. The organic layer was washed with a saturated solution of $NaHCO_3$ and brine before being dried over $MgSO_4$ and concentrated *in vacuo* to afford the crude product as a colorless liquid.

No further purification was employed and the crude amino-alcohols were engaged directly in the next step.

Mitsunobu reaction **(IIa)**:

PPh_3 (1.2eq) and the Phthalimide were suspended in dry THF (1mL/mmol) and cooled to 0°C.After the mixture was cooled, DIAD (1.2eq) was added slowly, leading to a thick precipitate forming and stopping the magnetic stirrer. The previously obtained alcohol was dissolved in THF and added to the mixture. The

reaction was stirred at room temperature overnight. The solvent was evaporated under reduced pressure and the crude product was engaged in the next step without further purification.

Phthalimide hydrazinolysis **(IIIa)**:

The previously obtained phthalimidation product was dissolved in MeOH (4mL/mmol), Hydrazine hydrate (3eq) was added and the solution was refluxed for 4 hours leading to a lot of precipitate appearing.
After cooling, the precipitate was filtered on fritted glass and washed with Ethyl Acetate. The filtrate was concentrated thus leading to more precipitate forming. The filtration/evaporation step was repeated until no more precipitate appears.
The crude product was purified by column chromatography by separating the impurities using Ethyl Acetate as the sole eluent and flushing the amine out of the column with a DCM/MeOH/Et_3N (85:10:5) mixture.The amine was extracted in DCM, dried over $MgSO_4$ and concentrated *in vacuo*.

tert-butyl (*S*)-(1-aminopropan-2-yl)carbamate **(4a)**: Synthesised from **(3a)** according to general procedure given above.

Global yield over three steps: 34%

tert-butyl (*S*)-(1-amino-3-methylbutan-2-yl)carbamate **(4b)**: Synthesised from **(3b)** according to general procedure given above.

Global yield over three steps: 34%

tert-butyl (*S*)-(1-amino-4-methylpentan-2-yl)carbamate **(4c)**: Synthesised from **(3c)** according to general procedure given above.

Global yield over three steps: 31%

NMR data presented further down (procedure IVb)

Alcohol mesylation **(IIb)**:

In a two necked round bottom flask fitted with a dropping funnel, the alcohol was dissolved in DCM (1mL/mmol) and cooled to 0°C. Triethylamine (3eq) was added in one portion while MsCl (1.5eq) was added dropwise over 10min. The reaction was stirred at 0°C for 2h (TLC monitoring Cyclohexane/EtOAc 80:20)

The dichloromethane was evaporated under reduced pressure and EtOAc was added to dissolve the residue. The organic layer was washed with a saturated $NaHCO_3$ solution (2 x 0.5mL/mmol), brine (2 x 0.5mL/mmol), dried over $MgSO_4$ and concentrated *in vacuo*

The obtained crude material was engaged in the next step without further purification.

Azide formation **(IIIb)**:

The mesylated alcohol was dissolved in DMF (1mL/mmol). NaN_3 (3eq) was added to the mixture and after fitting a condenser, the reaction was stirred at 80°C overnight.

Ethyl acetate was added to the reaction mixture. The organic layer was washed with a saturated $NaHCO_3$ solution (2 x 0.5mL/mmol), brine (2 x 0.5mL/mmol), dried over $MgSO_4$ and concentrated *in vacuo*.

The crude product was engaged in the next step without further purification.

Azide reduction **(IVb)**:

The azide was dissolved in a THF/H_2O mixture (8:2, 2mL/mmol). Triphenylphosphine (1.2 eq) was added and the reaction was refluxed for 3h (TLC monitoring: 100% EtOAc)

Ethyl acetate was added to the reaction mixture and the organic layer was washed with brine (2 x 0.5mL/mmol), dried over $MgSO_4$ and concentrated *in vacuo*.

The amine was purified by column chromatography. The impurities were flushed using 50:50 CH_2Cl_2/EtOAc. The product was recovered using CH_2Cl_2/MeOH/Et_3N (85:10:5) as eluent.

tert-butyl (*S*)-(1-aminopropan-2-yl)carbamate **(4a)**: Synthesised from **(7a)** according to general procedure given above.

Global yield over four steps: 53.8%

tert-butyl (*S*)-(1-amino-3-methylbutan-2-yl)carbamate **(4b)**: Synthesised from **(7b)** according to general procedure given above.

Global yield over four steps: 45%

tert-butyl (*S*)-(1-amino-4-methylpentan-2-yl)carbamate **(4c)**: Synthesised from **(7c)** according to general procedure given above.

Global yield over four steps: 53.8%

DSC activation of amines **(IVa):**

N,N'-Disuccinimidyl carbonate (DSC) (1.1eq) was suspended in DCM (0.5mL/mmol) and the resulting suspension was cooled to 0°C. The previously obtained hydrazinolysis product was dissolved in DCM (0.5mL/mmol) and added to the DSC suspension. After checking that pH>8 the reaction was stirred at 0°C for 45min and at room temperature for a further 45min.

The solvent was evaporated and the residue was dissolved in EtOAc. A 1N $KHSO_4$ solution (0.5mL/mmol) was added to the reaction mixture. The two layers were separated and the organic layer was washed with brine (3 x 0.5mL/mmol) before being dried over $MgSO_4$ and concentrated *in vacuo*.

The DSC activated building blocks were obtained after trituration in Et_2O.

***tert*-butyl (2,5-dioxopyrrolidin-1-yl) propane-1,2-diyl(*S*)-dicarbamate (5a)**

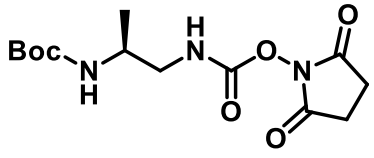

^{1}H NMR (300 MHz, $CDCl_3$) δ 6.13 (s, 1H), 4.52 (s, 1H), 3.84 (s, 1H), 3.47 – 3.31 (m, 1H), 3.29 – 3.14 (m, 1H), 2.81 (s, 4H), 1.45 (s, 9H), 1.18 (d, *J* = 6.8 Hz, 3H).

η= 49%

***tert*-butyl (2,5-dioxopyrrolidin-1-yl) (3-methylbutane-1,2-diyl)(*S*)-dicarbamate (5b)**

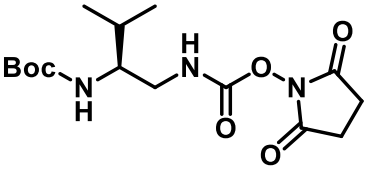

^{1}H NMR (300 MHz, $CDCl_3$) δ 6.04 (s, 1H), 4.53 (s, 1H), 3.39 (s, 1H), 3.26 (s, 1H), 2.81 (s, 4H), 1.78 (s, 1H), 1.46 (s, 9H), 0.96 (t, 6H).

η= 58%

tert-butyl (2,5-dioxopyrrolidin-1-yl) (4-methylpentane-1,2-diyl)(S)-dicarbamate **(5c)**

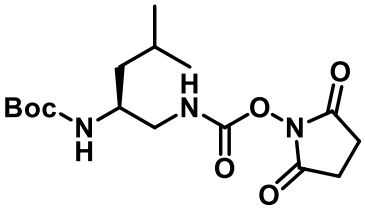

^{1}H NMR (300 MHz, $CDCl_3$) δ 6.13 (s, 1H), 4.47 (d, *J* = 7.8 Hz, 1H), 3.41 – 3.31 (m, 1H), 3.27 – 3.08 (m, 1H), 1.76 – 1.61 (m, *J* = 17.7, 5.6 Hz, 2H), 1.47 (s, 9H), 0.90 (dd, 6H).

η= 55%

-Inversed blocks:

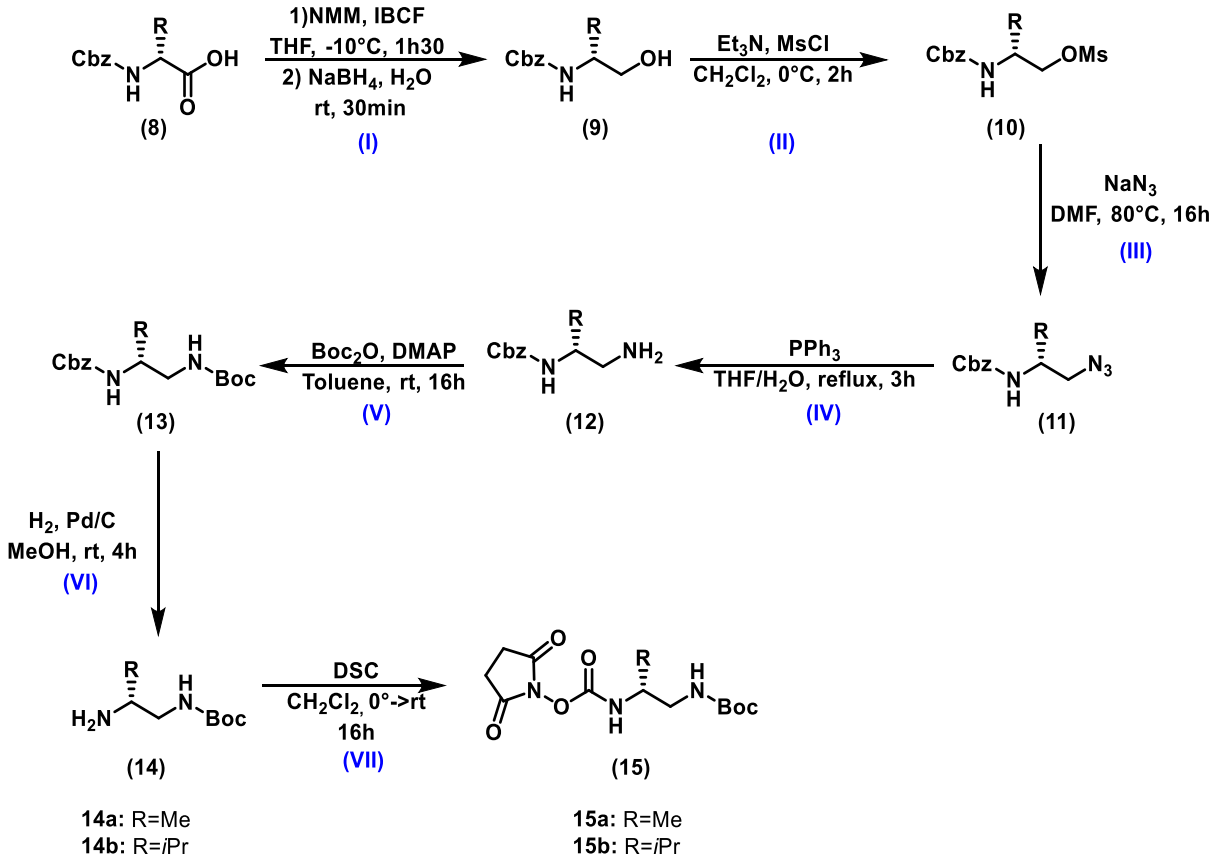

***Scheme 2** General synthesis plan for inversed blocks*

Amino acid reduction **(I)**:

The Boc protected aminoacid was dissolved in dry THF and cooled to -10°C. N-Methylmorpholine (1.1eq) and Isobutylchloroformate (1.1eq) were subsequently added and the reaction was stirred at -10°C for 1.5h (TLC in cyclohexane/EtOAc 50:50). The reaction mixture was filtered to remove the white precipitate formed during reaction. The filtrate was slowly and carefully poured over a solution of $NaBH_4$ (2.1eq) in H_2O (5mL). The resulting mixture was left to stir and degas for 30min at room temperature after which the THF

was evaporated under reduced pressure and EtOAc (1.5mL/mmol aminoacid) was added. The remaining $NaBH_4$ was quenched by adding aqueous $KHSO_4$ (1N) until degassing was complete. The organic layer was washed with a saturated solution of $NaHCO_3$ and brine before being dried over $MgSO_4$ and concentrated *in vacuo* to afford the crude product as a colorless liquid.

No further purification was employed and the crude amino-alcohols were engaged directly in the next step.

Alcohol mesylation **(II)**:

In a two necked round bottom flask fitted with a dropping funnel, the alcohol was dissolved in DCM (1mL/mmol) and cooled to 0°C. Triethylamine (3eq) was added in one portion while MsCl (1.5eq) was added dropwise over 10min. The reaction was stirred at 0°C for 2h (TLC monitoring Cyclohexane/EtOAc 80:20)

The dichloromethane was evaporated under reduced pressure and EtOAc was added to dissolve the residue. The organic layer was washed with a saturated $NaHCO_3$ solution (2 x 0.5mL/mmol), brine (2 x 0.5mL/mmol), dried over $MgSO_4$ and concentrated *in vacuo*

The obtained crude material was engaged in the next step without further purification.

Azide formation **(III)**:

The mesylated alcohol was dissolved in DMF (1mL/mmol). NaN_3 (3eq) was added to the mixture and after fitting a condenser, the reaction was stirred at 80°C overnight.

Ethyl acetate was added to the reaction mixture. The organic layer was washed with a saturated $NaHCO_3$ solution (2 x 0.5mL/mmol), brine (2 x 0.5mL/mmol), dried over $MgSO_4$ and concentrated *in vacuo*.

The crude product was engaged in the next step without further purification.

Azide reduction **(IV)**:

The azide was dissolved in a THF/H_2O mixture (8:2, 2mL/mmol). Triphenylphosphine (1.2 eq) was added and the reaction was refluxed for 3h (TLC monitoring: 100% EtOAc)

Ethyl acetate was added to the reaction mixture and the organic layer was washed with brine (2 x 0.5mL/mmol), dried over $MgSO_4$ and concentrated *in vacuo*.

The amine was purified by column chromatography. The impurities were flushed using 50:50 CH_2Cl_2/EtOAc. The product was recovered using CH_2Cl_2/MeOH/Et_3N (85:10:5) as eluent.

Boc protection **(V)**:

The amine was dissolved in Toluene (1mL/mmol). DMAP (1.2eq) and Boc_2O (1.2eq) were added and the mixture was stirred at room temperature overnight.

EtOAc was added to the reaction mixture and washed it with $KHSO_4$ (1N solution) and brine. The organic layer was dried over $MgSO_4$ and concentrated *in vacuo*.

The crude product was used without further purification.

Cbz deprotection **(VI)**:

The Boc protected amine was dissolved in EtOAc (3mL/mmol) and Pd/C (15% weight) was added. The flask was subjected to three vacuum/ argon flush cycles before the reaction was stirred under H_2 atmosphere overnight.

The Palladium was filtered over a celite bed and the solvent was removed under reduced pressure to recover the crude product.

The crude product was purified by column chromatography using EtOAc (100%) to flush the impurities and DCM/MeOH/Et_3N (85/10/5%) to recover the product.

***tert*-butyl (*R*)-(2-aminopropyl)carbamate (14a)**: Synthesised from **(13a)** according to general procedure given above.

Global yield over three steps: 36.5%

***tert*-butyl (*R*)-(2-amino-3-methylbutyl)carbamate (14b)**: Synthesised from **(13b)** according to general procedure given above.

Global yield over three steps: 33.2%

Carbamate activation **(VII)**:

N,N'-Disuccinimidyl carbonate (DSC) (1.1eq) was suspended in DCM (0.5mL/mmol) and the resulting suspension was cooled to 0°C. The previously obtained hydrazinolysis product was dissolved in DCM (0.5mL/mmol) and added to the DSC suspension. After checking that pH>8 the reaction was stirred at 0°C for 45min and at room temperature for a further 45min.

The solvent was evaporated and the residue was dissolved in EtOAc. A 1N $KHSO_4$ solution (0.5mL/mmol) was added to the reaction mixture. The two layers were separated and the organic layer was washed with brine (3 x 0.5mL/mmol) before being dried over $MgSO_4$ and concentrated *in vacuo*.

The DSC activated building blocks were obtained after trituration in Et_2O.

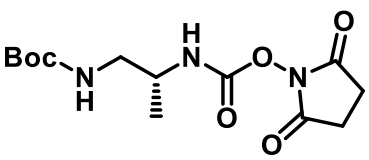

Boc^{inv}AlaOSu (15a): Synthesised according to general procedure given above.

η= 16.9% over 7 steps

^{1}H NMR (300 MHz, $CDCl_3$) δ 6.19 (s, 1H), 4.96 (s, 1H), 3.81 (s, 1H), 3.26 (s, 2H), 2.84 (s, 4H), 1.48 (s, 9H), 1.25 (d, *J* = 6.6 Hz, 3H).

^{13}C NMR (75 MHz, $CDCl_3$) δ 169.94, 169.86, 157.14, 151.22, 80.17, 50.00, 45.10, 28.32, 25.49, 17.89.

HRMS: m/z calculated for $C_{13}H_{22}N_3O_6$ $[M+H]^+$ 316.1503, found 316.1556.

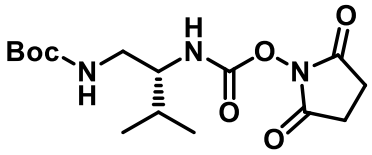

Boc^{inv}ValOSu (15b): Synthesised according to general procedure given above.

η= 14.6% over 7 steps

^{1}H NMR (300 MHz, $CDCl_3$) δ 6.06 (s, 1H), 4.55 (d, *J* = 7.7 Hz, 1H), 3.63 – 3.49 (m, *J* = 8.1, 4.7 Hz, 1H), 3.47 – 3.34 (m, 1H), 3.32 – 3.15 (m, 1H), 2.81 (s, 4H), 1.87 – 1.72 (m, 1H), 1.46 (s, 9H), 0.95 (t, *J* = 6.9 Hz, 6H).

^{13}C NMR (75 MHz, $CDCl_3$) δ 170.05, 156.93, 152.14, 79.87, 53.92, 47.05, 28.33, 25.49, 19.14, 18.04, 17.54.

HRMS: m/z calculated for $C_{15}H_{26}N_3O_6$ $[M+H]^+$ 344.1816, found 344.1873.

Synthesis of oligoureas:

- **BocLeu^{u}NHMe (24):**

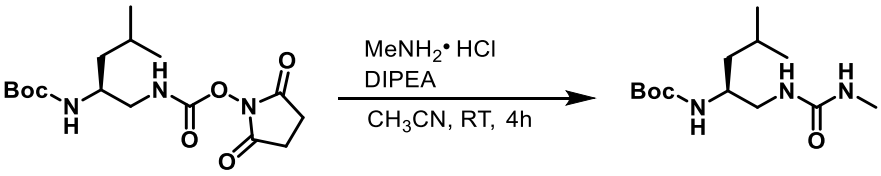

Methylamine hydrochloride (2.5 eq) was suspended in acetonitrile (2mL/mmol) and the mixture was cooled 0°C. DIPEA (5 eq) and BocLeu^{U}OSu were subsequently added and the mixture was stirred for 4 hours while allowing for the temperature to rise to RT. (Reaction progress tracked by TLC using DCM/MeOH 9:1 as eluent). After verifying for the completion of the reaction, the solvent was removed and the residue was dissolved in ethyl acetate (3 mL/mmol). The organic layer was washed with a 1N $KHSO_4$ solution (2mL/mmol) and a saturated $NaHCO_3$ solution (2mL/mmol). The organic layer was separated and dried over $MgSO_4$ and concentrated *in vacuo* to yield the crude product as a yellow oil.

The crude oil was purified by flash chromatography using a CH_2Cl_2/MeOH 100:0 ➡ 90:10 gradient system as eluent. The purified product was obtained as a white solid.

η =80%

^{1}H NMR (400 MHz, $CDCl_3$) δ 5.06 (s, 1H), 4.73 – 4.45 (m, 2H), 3.75 – 3.57 (m, 1H), 3.19 (d, *J* = 15.5 Hz, 2H), 2.76 (d, *J* = 4.7 Hz, 2H), 1.43 (s, 9H), 0.91 (t, *J* = 6.9 Hz, 6H).

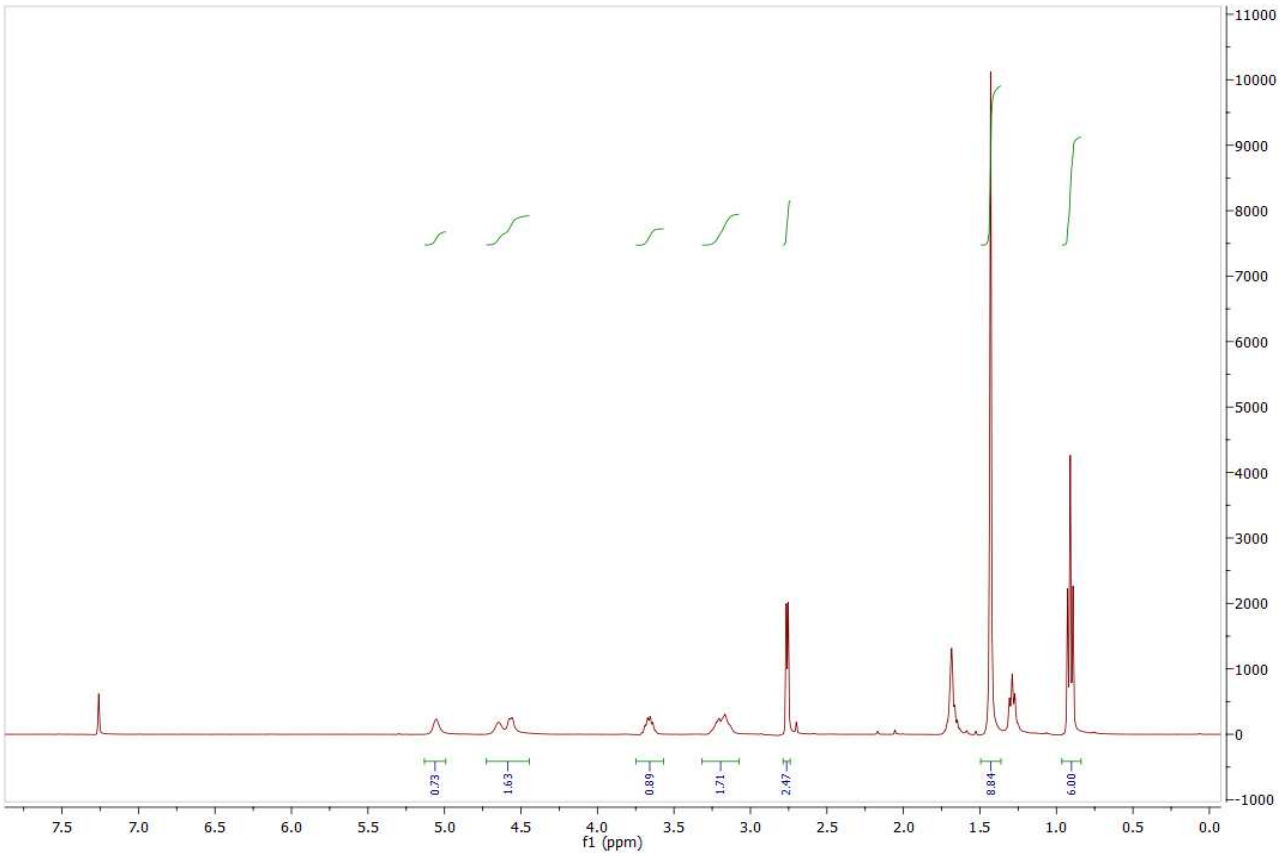

- **BocAla^{u}Leu^{u}NHMe (25):**

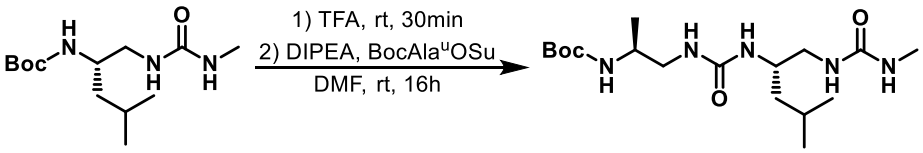

BocLeu^{u}NHMe was dissolved in TFA and stirred at room temperature for 30 min. The acid was removed by three successive co-evaporations with Toluene. The residue was dried under high vacuum for 5h30.

The resulting oil was dissolved in acetonitrile (3mL/mmol) and stirred. DIPEA (3eq) was added to the reaction mixture and the pH was checked to be above 9 after which BocAlaOSu (1.5eq) was dissolved in acetonitrile and added to the TFA salt mixture. The reaction was left to stir overnight.

The acetonitrile was evaporated under reduced pressure and the residue was dissolved in Ethyl Acetate. The mixture was washed with $KHSO_4$ (3x1mL/mmol, 1M solution), $NaHCO_3$ (3x1mL/mmol, sat. solution) and brine (2x1mL/mmol, sat. solution). The combined organic layers were dried and concentrated *in vacuo* to afford the crude product as a pale yellow oil.

The product was obtained by precipitation in cold Et_2O as a white solid.

η: 95%

^{1}H NMR (400 MHz, CD_3OH) δ 6.49 (d, *J* = 7.1 Hz, 1H), 6.05 – 5.75 (m, 1H), 3.68 (t, *J* = 29.7 Hz, 2H), 3.01 – 2.85 (m, *J* = 23.8 Hz, 2H), 2.68 (t, *J* = 5.3 Hz, 3H), 1.75 – 1.58 (m, 1H), 1.08 (t, *J* = 8.2 Hz, 3H), 0.98 – 0.85 (m, 6H).

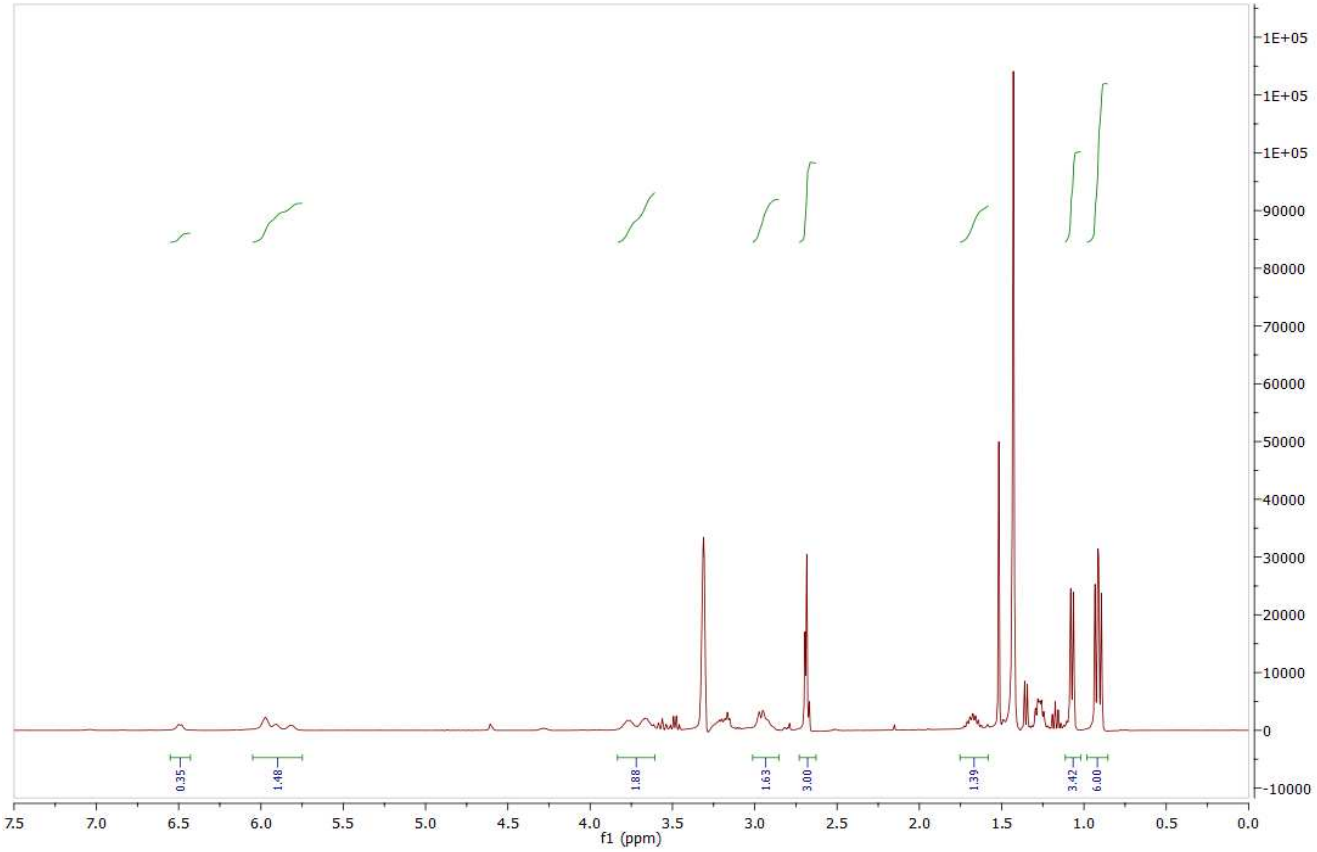

- **BocVal^{u}Ala^{u}Leu^{u}NHMe (26):**

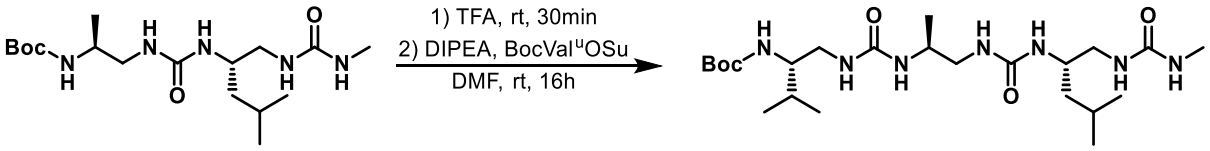

BocAla^{u}Leu^{u}NHMe was dissolved in TFA and stirred at room temperature for 30 min. The acid was removed by three successive co-evaporations with Toluene. The residue was dried under high vacuum for 4h.

The resulting oil was dissolved in DMF (3mL/mmol) and stirred. DIPEA (3eq) was added to the reaction mixture and the pH was checked to be above 9 after which BocValOSu (1.2eq) was added to the TFA salt mixture. The reaction was left to stir overnight.

The acetonitrile was evaporated under reduced pressure and the residue was dissolved in Ethyl Acetate. The mixture was washed with $KHSO_4$ (3x1.5mL, 1M solution), $NaHCO_3$ (3x1.5mL, sat. solution) and brine (2x1.5mL, sat. solution). After the first washing with $NaHCO_3$, a precipitate was formed and filtered off. The combined organic layers were dried and concentrated *in vacuo* to afford the crude product as a yellow oil

The crude product was triturated in cold Et_2O to afford the pure compound as an off-white solid

η =74.3%

^{1}H NMR (400 MHz, CD_3OH) δ 6.49 (d, *J* = 9.7 Hz, 1H), 6.33 (s, 1H), 6.07 (s, 1H), 5.86 (dd, *J* = 27.0, 8.8 Hz, 3H), 3.88 (d, *J* = 39.1 Hz, 2H), 3.56 – 3.35 (m, 4H), 2.68 (d, *J* = 4.3 Hz, 3H), 1.79 – 1.53 (m, 3H), 1.44 (s, 9H), 1.22 (t, *J* = 7.1 Hz, 2H), 1.03 (d, *J* = 6.8 Hz, 3H), 0.89 (dd, *J* = 11.5, 6.8 Hz, 14H).

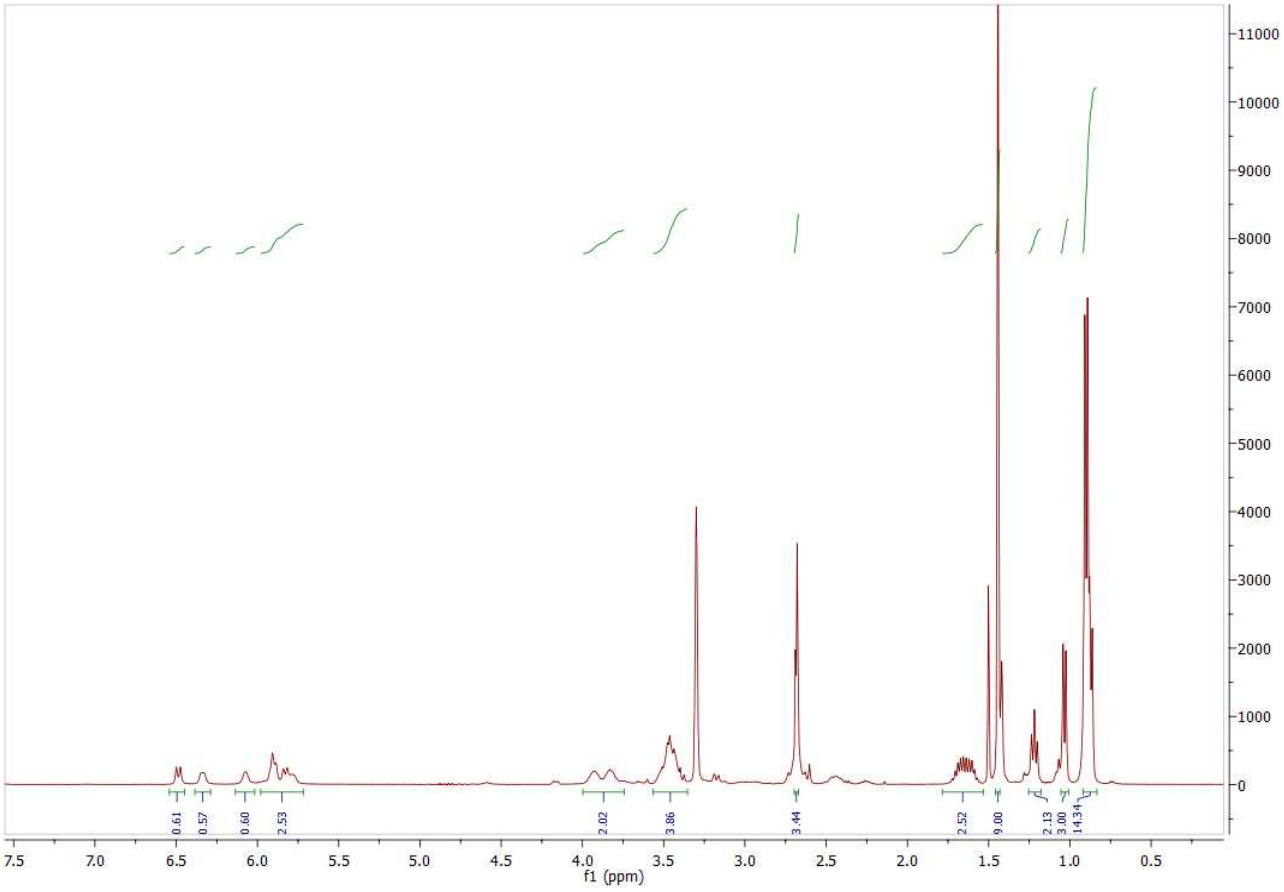

- **BocLeu^{u}Val^{u}Ala^{u}Leu^{u}NHMe (27):**

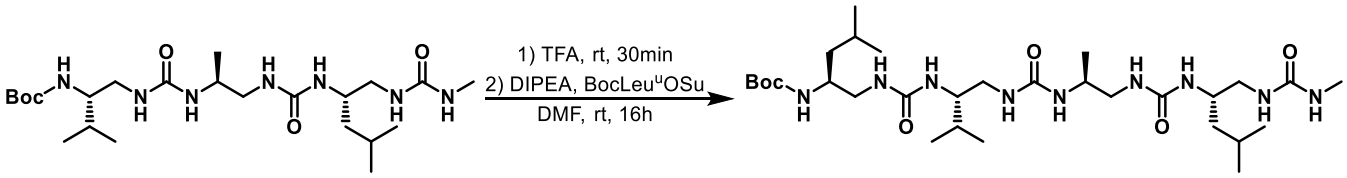

BocVal^{u}Ala^{u}Leu^{u}NHMe was dissolved in TFA and stirred at room temperature for 30 min. The acid was removed by three successive co-evaporations with Toluene. The residue was dried under high vacuum for 5h.

The resulting oil was dissolved in DMF (3mL/mmol) and stirred. DIPEA (3eq) was added to the reaction mixture and the pH was checked to be above 9 after which BocLeuOSu (1.2eq) was added to the TFA salt mixture. The reaction was left to stir overnight.

Ethyl Acetate was added to the reaction mixture. The mixture was washed with $KHSO_4$ (3x1.5mL, 1M solution), $NaHCO_3$ (3x1.5mL, sat. solution) and brine (2x1mL, sat. solution). After the first washing with $NaHCO_3$ a precipitate was formed. After filtration, the precipitated was determined to be the expected tetramer.

The aqueous layer was re-extracted with EtOAc (2x10mL). The combined organic layers were dried and concentrated *in vacuo* to afford the crude product as a yellow oil.

The crude product was triturated in cold Et_2O to recover the remaining product as an off-white solid.

η =33.7%

^{1}H NMR (300 MHz, CD_3OH) δ 6.66 (d, *J* = 9.7 Hz, 1H), 6.38 (s, 2H), 6.20 (d, *J* = 4.6 Hz, 1H), 6.16 – 6.07 (m, 1H), 6.03 (d, *J* = 9.4 Hz, 1H), 5.83 (d, *J* = 10.0 Hz, 3H), 4.05 (s, 1H), 3.98 – 3.75 (m, 2H), 3.75 – 3.41 (m, 5H), 2.73 (d, *J* = 4.7 Hz, 3H), 1.87 – 1.56 (m, 4H), 1.49 (s, 9H), 1.33 – 1.17 (m, 5H), 1.04 (d, *J* = 6.8 Hz, 3H), 1.01 – 0.85 (m, *J* = 13.8, 5.8 Hz, 21H).

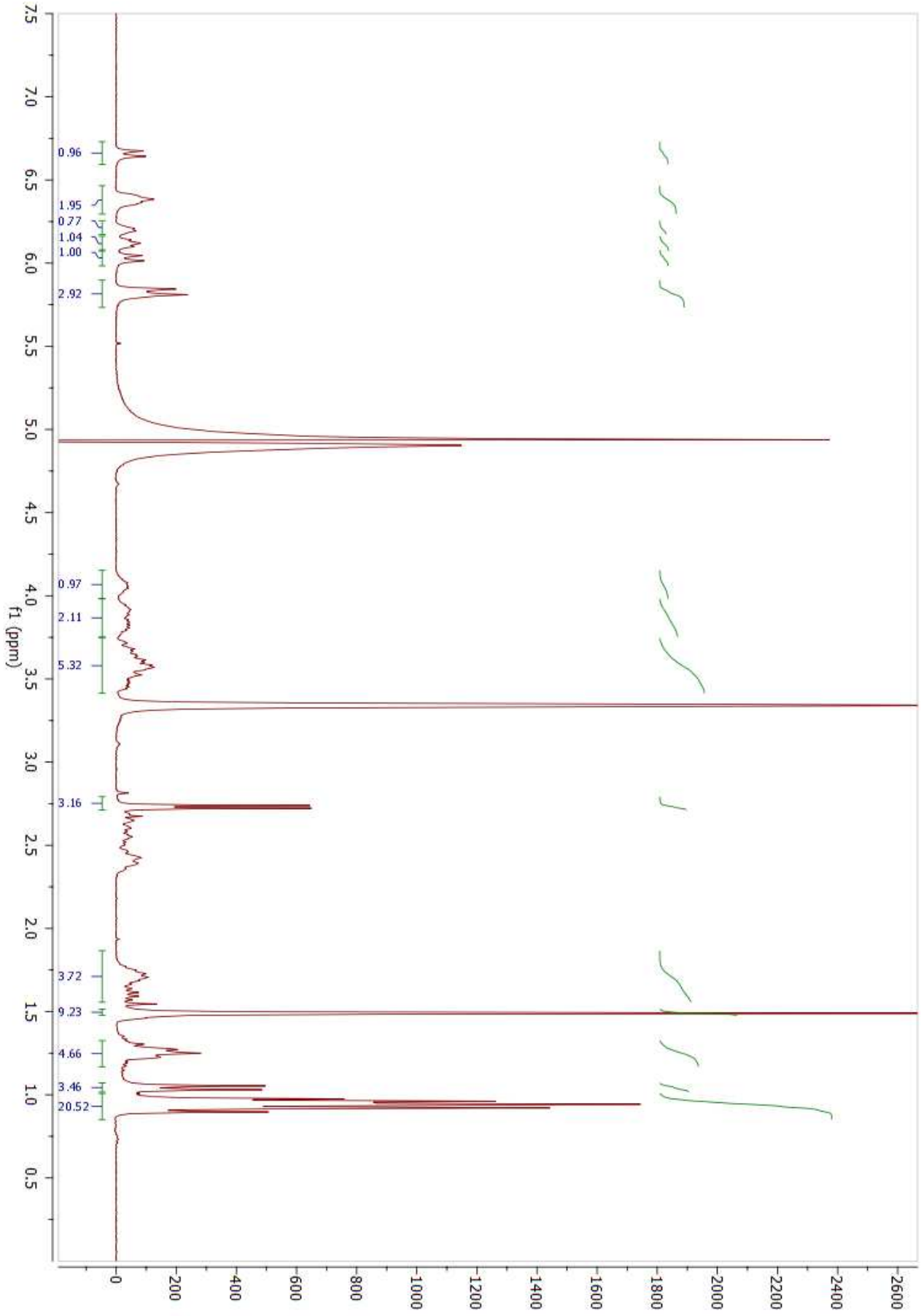
0.96
1.95
0.77
1.04
1.00
2.92
0.97
2.11
5.32
3.16
3.72
9.23
4.66
3.46
20.52
f1 (ppm)

- **BocAla^{u}Leu^{u}Val^{u}Ala^{u}Leu^{u}NHMe (28):**

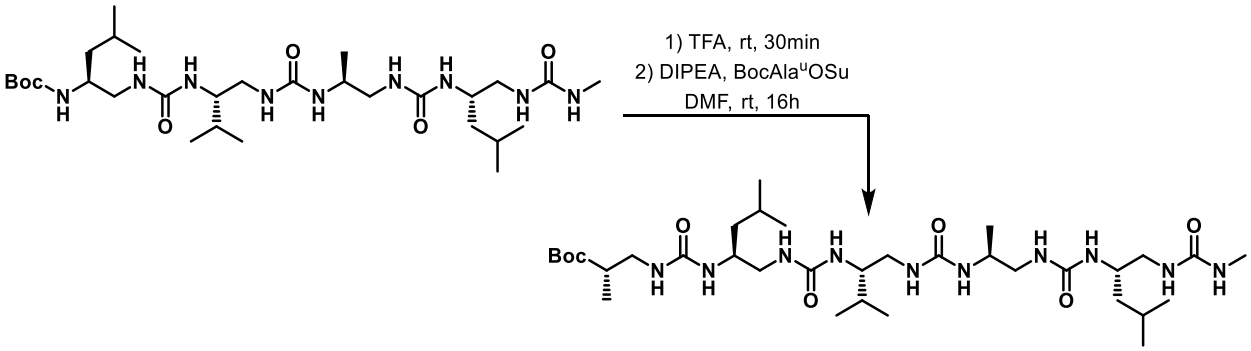

BocLeu^{u}Val^{u}Ala^{u}Leu^{u}NHMe was dissolved in TFA and stirred at room temperature for 30 min. The acid was removed by three successive co-evaporations with Toluene. The residue was dried under high vacuum for 5h.

The resulting oil was dissolved in DMF (3mL/mmol) and stirred. DIPEA (3eq) was added to the reaction mixture and the pH was checked to be above 9 after which BocAlaOSu (1.2eq) was added to the TFA salt mixture. The reaction was left to stir overnight.

Ethyl Acetate was added to the reaction mixture. The mixture was washed with $KHSO_4$ (3x1.5mL, 1M solution), $NaHCO_3$ (3x1.5mL, sat. solution) and brine (2x1mL, sat. solution). After the first washing with $NaHCO_3$ a precipitate was formed. After filtration, the precipitated was determined to be the expected tetramer.

The aqueous layer was re-extracted with EtOAc (2x10mL). The combined organic layers were dried and concentrated *in vacuo* to afford the crude product as a yellow oil.

The crude product was triturated in cold Et_2O to recover the remaining product as a white solid.

η = 65.5%

^{1}H NMR (300 MHz, CD_3OH) δ 6.72 (d, *J* = 9.6 Hz, 1H), 6.51 (s, 1H), 6.38 (d, *J* = 8.3 Hz, 2H), 6.20 (d, *J* = 4.5 Hz, 1H), 6.10 (s, 1H), 6.07 – 5.97 (m, 2H), 5.89 (d, *J* = 10.4 Hz, 2H), 5.79 (d, *J* = 10.1 Hz, 1H), 4.16 – 3.51 (m, 10H), 2.70 (d, *J* = 4.7 Hz, 3H), 1.80 – 1.53 (m, 4H), 1.45 (S, 9H), 1.31 – 1.17 (m, 6H), 1.07 (ddd, *J* = 20.5, 10.2, 4.5 Hz, 9H), 0.97 – 0.81 (m, 19H).

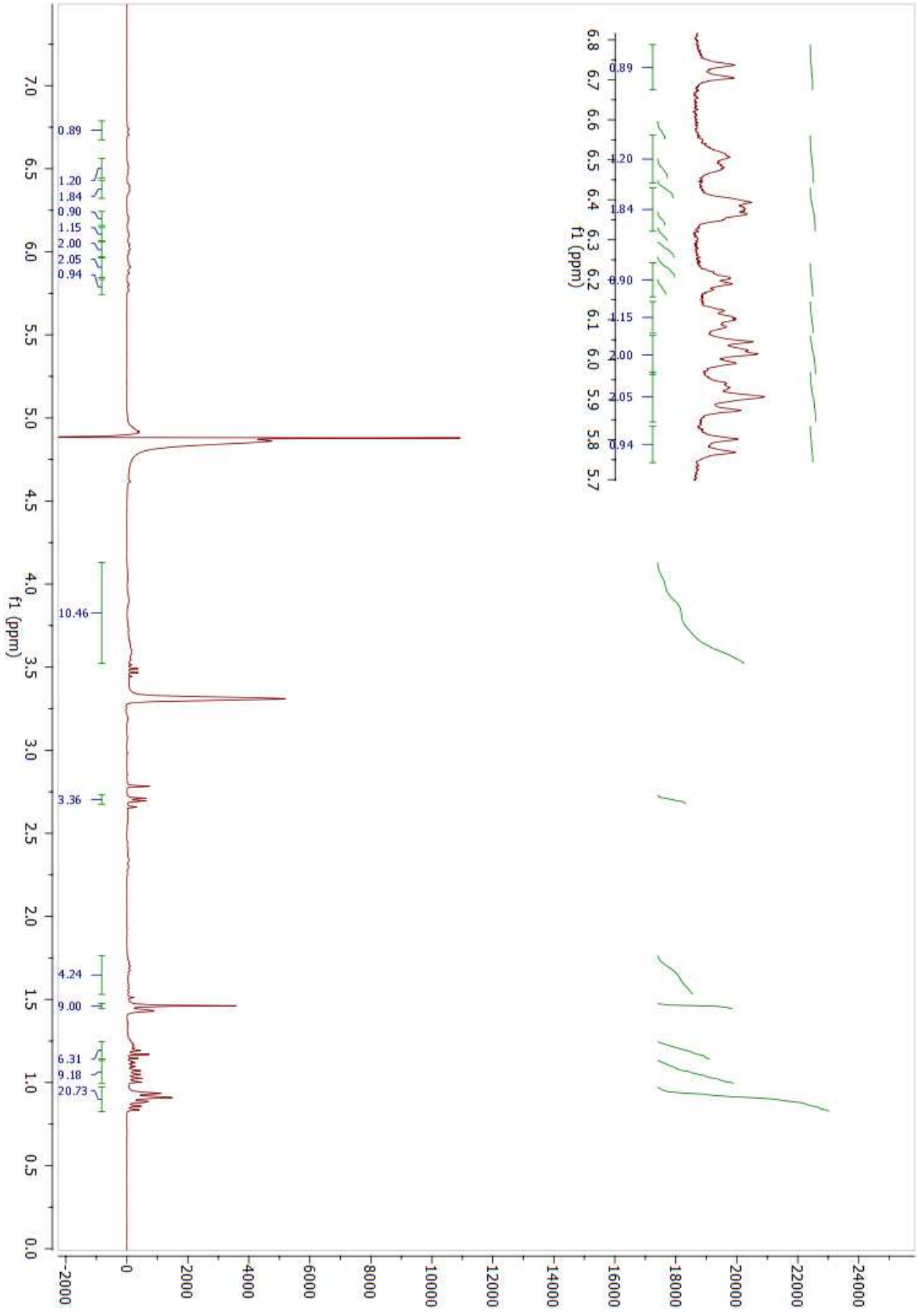
f1 (ppm)
0.89
1.20
1.84
0.90
1.15
2.00
2.05
0.94
10.46
3.36
4.24
9.00
6.31
9.18
20.73

- **Boc^{u}Val^{u}Ala^{u}Leu^{u}Val^{u}Ala^{u}Leu^{u}NHMe (31):**

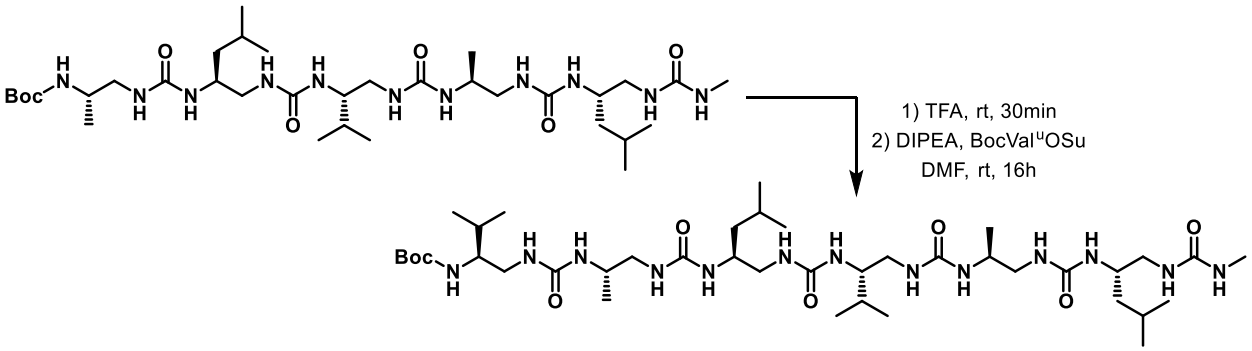

Boc^{u}Ala^{u}Leu^{u}Val^{u}Ala^{u}Leu^{u}NHMe was dissolved in TFA and stirred at room temperature for 30 min. The acid was removed by three successive co-evaporations with Toluene. The residue was dried under high vacuum for 5h.

The resulting oil was dissolved in DMF (3mL/mmol) and stirred. DIPEA (3eq) was added to the reaction mixture and the pH was checked to be above 9 after which BocValOSu (1.2eq) was added to the TFA salt mixture. The reaction was left to stir overnight.

Ethyl Acetate was added to the reaction mixture. The mixture was washed with $KHSO_4$ (3x1.5mL, 1M solution), $NaHCO_3$ (3x1.5mL, sat. solution) and brine (2x1mL, sat. solution). After the first washing with $NaHCO_3$ a precipitate was formed. After filtration, the precipitated was determined to be the expected tetramer.

The aqueous layer was re-extracted with EtOAc (2x10mL). The combined organic layers were dried and concentrated *in vacuo* to afford the crude product as a yellow oil.

The crude product was triturated in cold Et_2O to recover the remaining product as a white solid.

η =97%

^{1}H NMR (300 MHz, CD_3OH) δ 6.65 (d, *J* = 10.2 Hz, 1H), 6.60 – 6.34 (m, 5H), 6.22 (d, *J* = 10.3 Hz, 2H), 6.09 – 5.79 (m, 6H), 4.13 – 3.79 (m, 5H), 3.75 – 3.53 (m, 7H), 2.70 (d, *J* = 4.7 Hz, 3H), 1.84 – 1.53 (m, 6H), 1.46 (S, 9H), 1.31 – 1.18 (m, 5H), 1.03 (t, *J* = 6.3 Hz, 6H), 0.94 – 0.87 (m, 27H).

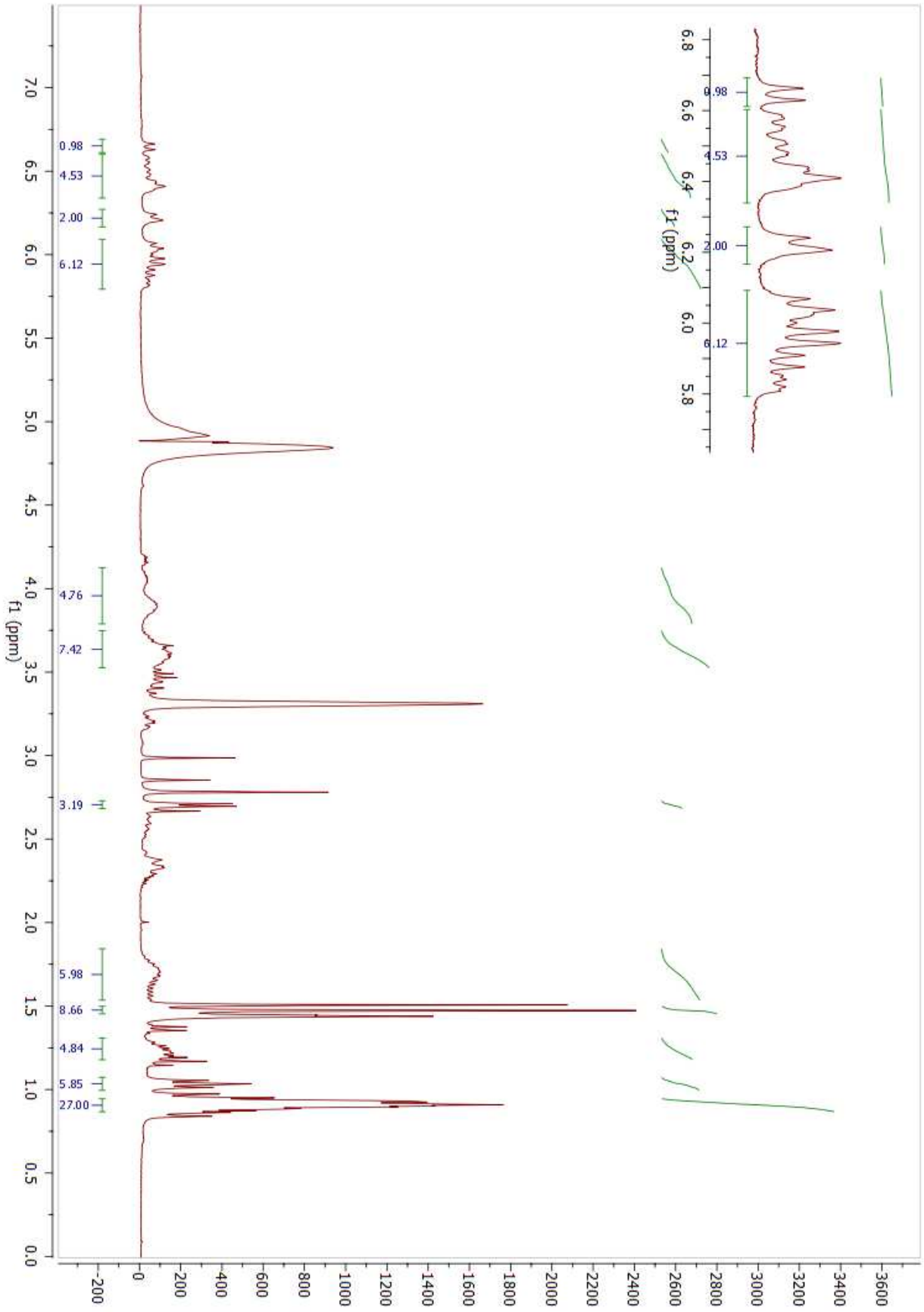
f1 (ppm)
0.98
4.53
2.00
6.12
4.76
7.42
3.19
5.98
8.66
4.84
5.85
27.00

- **$(CF_3)_2$PhNHCO-Val^{u}Ala^{u}Leu^{u}Val^{u}Ala^{u}Leu^{u}NHMe (C44):**

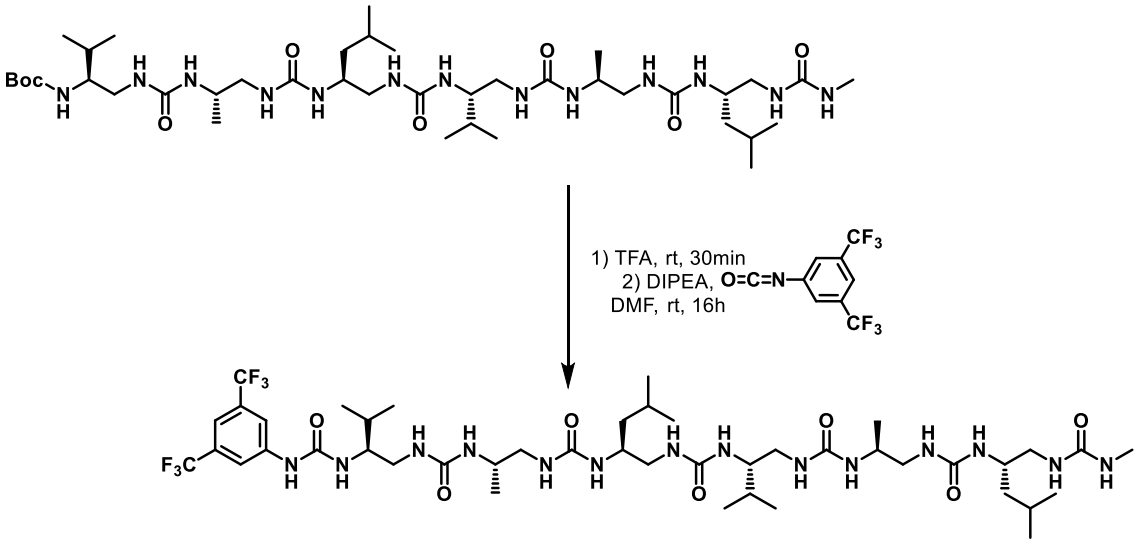

BocVal^{u}Ala^{u}Leu^{u}Val^{u}Ala^{u}Leu^{u}NHMe was dissolved in TFA and stirred at room temperature for 30 min. The acid was removed by three successive co-evaporations with Toluene. The residue was dried under high vacuum for 5h.

The resulting oil was dissolved in DMF (3mL/mmol) and stirred. DIPEA (3eq) was added to the reaction mixture and the pH was checked to be above 9 after which 3,5-Bis(trifluoromethyl)phenyl isocyanate (1.5eq) was added to the TFA salt mixture. The reaction was left to stir overnight.

Ethyl Acetate was added to the reaction mixture. The mixture was washed with $KHSO_4$ (3x1.5mL, 1M solution), $NaHCO_3$ (3x1.5mL, sat. solution) and brine (2x1mL, sat. solution). After the first washing with $NaHCO_3$ a precipitate was formed. After filtration, the precipitated was determined to be the expected tetramer.

The aqueous layer was re-extracted with EtOAc (2x10mL). The combined organic layers were dried and concentrated *in vacuo* to afford the crude product as a yellow oil.

The crude product was purified by flash chromatography using a CH_2Cl_2/MeOH 100:0 ➡ 90:10 gradient system as eluent.

η = 50.4%

^{1}H NMR (300 MHz, CD_3OH) δ 8.00 (s, 2H), 7.52 (s, 1H), 6.62 – 6.35 (m, 4H), 6.25 (d, *J* = 10.2 Hz, 3H), 6.13 – 5.80 (m, 7H), 4.13 – 3.45 (m, 10H), 2.71 (d, *J* = 4.8 Hz, 4H), 2.49 – 2.23 (m, 4H), 1.86 – 1.49 (m, 5H), 1.36 – 1.11 (m, 7H), 1.08 – 0.79 (m, 35H).

HRMS: m/z calculated for $C_{44}H_{77}F_6N_{14}O_7^+$ $[M+H]^+$ 1027.5998, found 1027.5973.

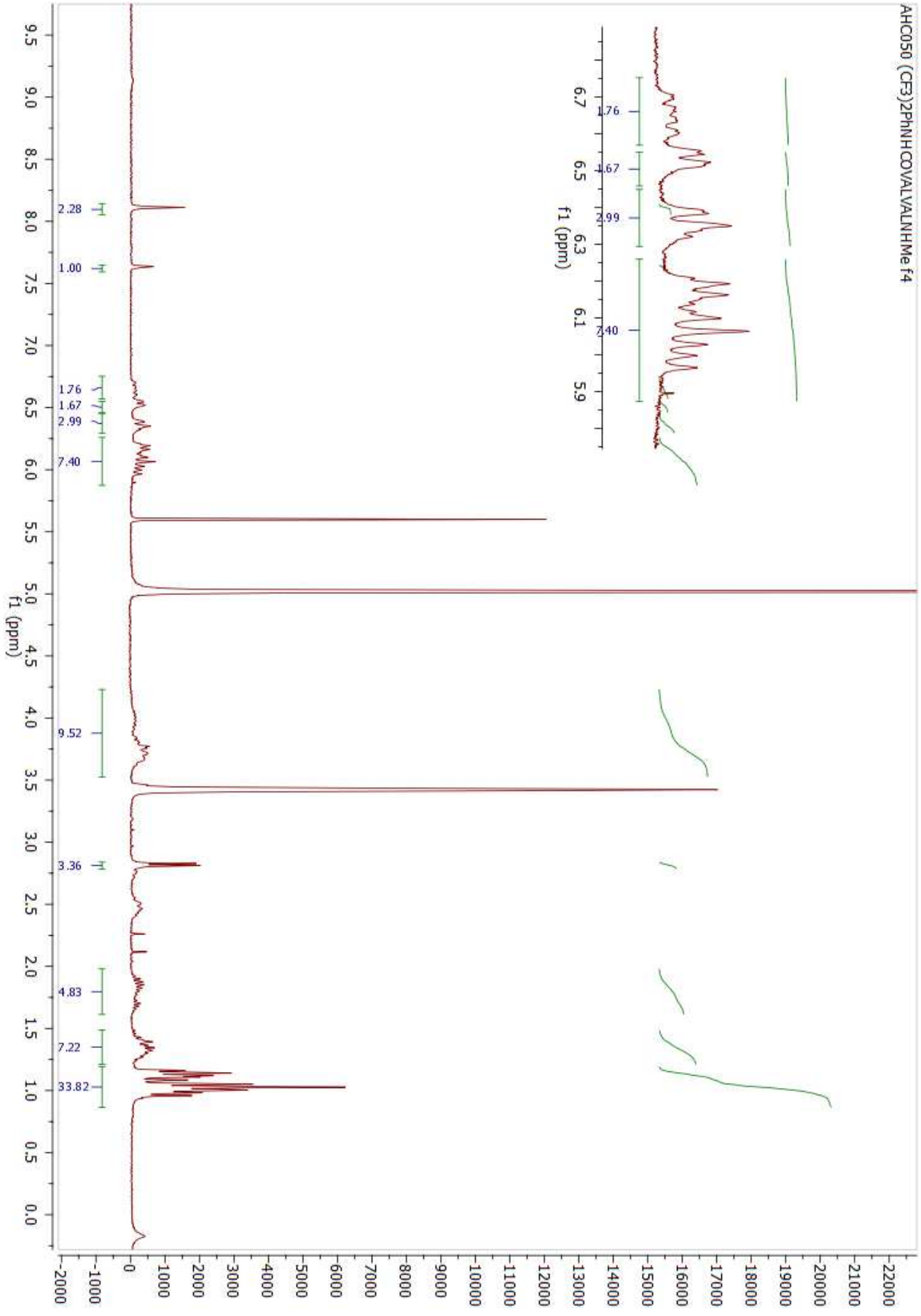
AHC050 (CF3)2PhNHCOVALVALNHMe f4
f1 (ppm)
2.28
1.00
1.76
1.67
2.99
7.40
9.52
3.36
4.83
7.22
33.82

- **Boc(^{inv}Ala)^{u}Leu^{u}Val^{u}Ala^{u}Leu^{u}NHMe (29):**

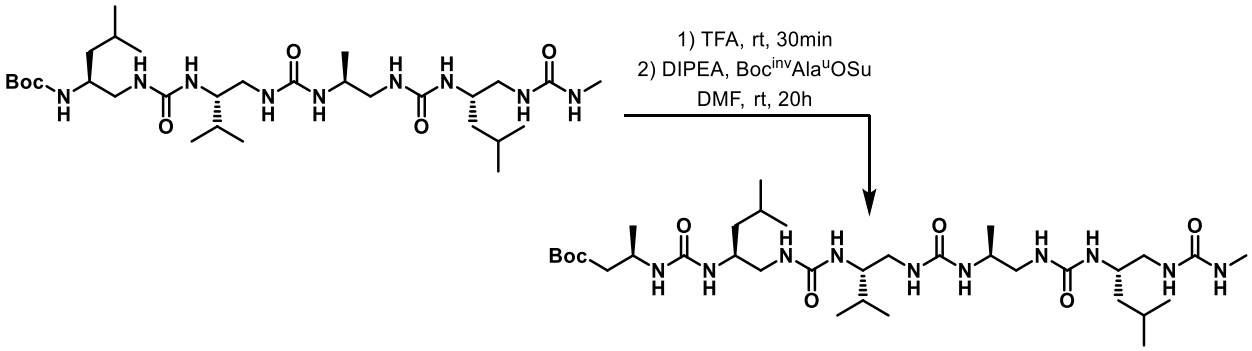

Boc-Leu^{u}-Val^{u}-Ala^{u}-Leu^{u}-NHMe was dissolved in TFA and stirred at room temperature for 30 min. The acid was removed by three successive co-evaporations with Toluene. The residue was dried under high vacuum for 5h.

The resulting oil was dissolved in DMF (1.5mL/mmol) and stirred. DIPEA (3eq) was added to the reaction mixture and the pH was checked to be above 9. Boc^{inv}AlaOSu (1.2eq) was dissolved in DMF (1.5mL/mmol) and added to the TFA salt mixture using a syringe pump set at 125µL/h. The reaction was left to stir for 20h (addition and reaction time combined) at room temperature.

Ethyl Acetate was added to the reaction mixture. The mixture was washed with $KHSO_4$ (3x1.5mL, 1M solution), $NaHCO_3$ (3x1.5mL, sat. solution) and brine (2x1mL, sat. solution). After the first washing with $NaHCO_3$ a precipitate was formed. After filtration, the precipitated was determined to be the expected tetramer.

The aqueous layer was re-extracted with EtOAc (2x10mL). The combined organic layers were dried and concentrated *in vacuo* to afford the crude product as a white solid.

The crude product was purified by flash chromatography using a CH_2Cl_2/MeOH 100:0 ➡ 90:10 gradient system as eluent.

η= 44%

^{1}H NMR (400 MHz, CD_3OH) δ 7.00 (s, 1H), 6.54 – 6.26 (m, 3H), 6.18 (s, 1H), 6.04 (d, *J* = 9.3 Hz, 2H), 5.88 (dd, *J* = 16.4, 10.2 Hz, 2H), 5.75 (d, *J* = 7.8 Hz, 1H), 5.59 (d, *J* = 9.8 Hz, 1H), 4.15 – 3.97 (m, 1H), 3.96 – 3.71 (m, 3H), 3.71 – 3.45 (m, 6H), 2.79 (d, *J* = 11.8 Hz, 1H), 2.70 (d, *J* = 4.7 Hz, 3H), 2.68 – 2.57 (m, 1H), 2.52 – 2.22 (m, 2H), 1.80 – 1.51 (m, 4H), 1.47 (s, 9H), 1.33 – 1.17 (m, 4H), 1.10 (d, *J* = 7.0 Hz, 3H), 1.01 (d, *J* = 6.9 Hz, 3H), 0.98 – 0.82 (m, 19H).

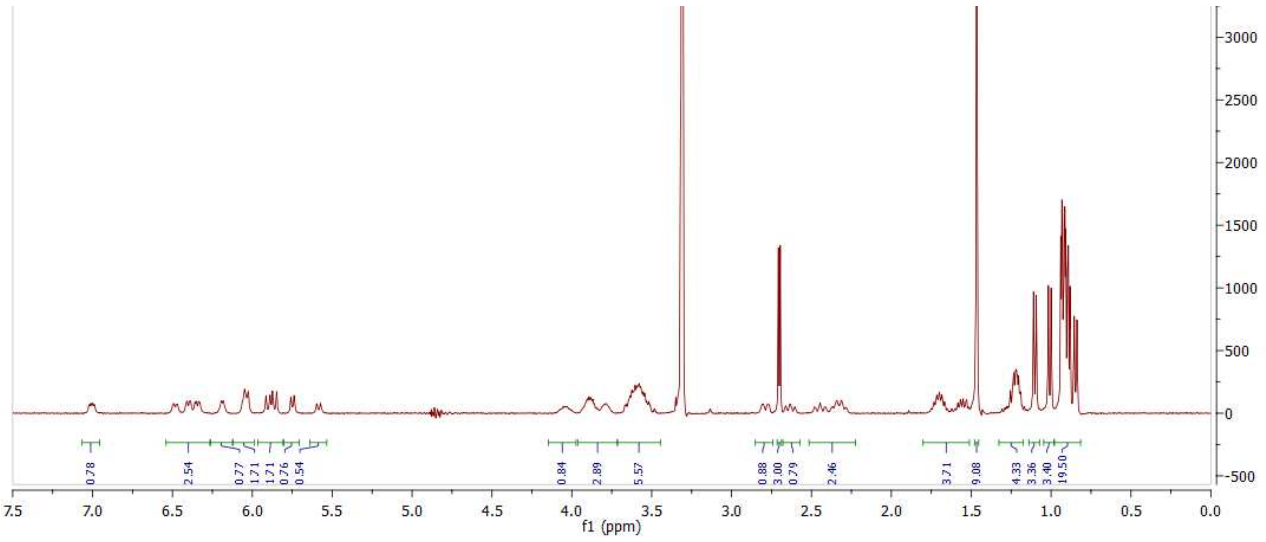

- **BocVal^{u}(^{inv}Ala)^{u}Leu^{u}Val^{u}Ala^{u}Leu^{u}NHMe (32):**

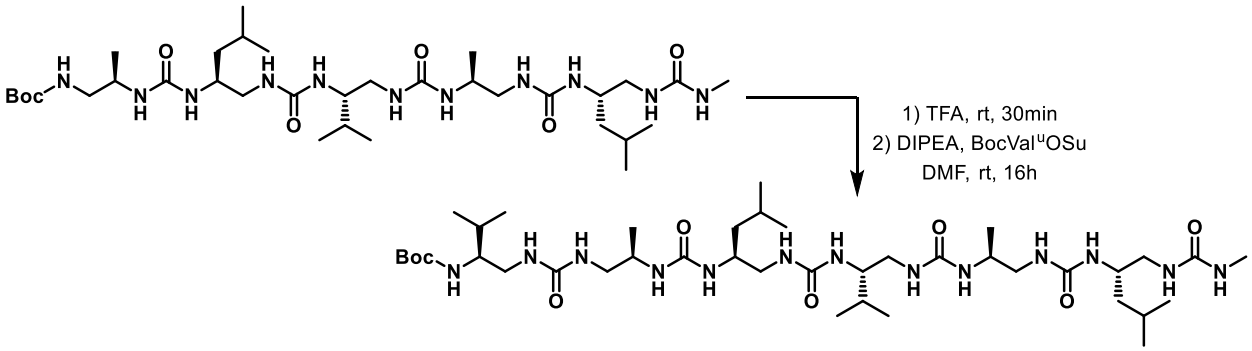

Boc(^{inv}Ala)^{u}Leu^{u}Val^{u}Ala^{u}Leu^{u}NHMe was dissolved in TFA and stirred at room temperature for 30 min. The acid was removed by three successive co-evaporations with Toluene. The residue was dried under high vacuum for 5h.
The resulting oil was dissolved in DMF (3mL/mmol) and stirred. DIPEA (3eq) was added to the reaction mixture and the pH was checked to be above 9 after which BocValOSu (1.2eq) was added to the TFA salt mixture. The reaction was left to stir overnight.
Ethyl Acetate was added to the reaction mixture. The mixture was washed with $KHSO_4$ (3x1.5mL, 1M solution), $NaHCO_3$ (3x1.5mL, sat. solution) and brine (2x1mL, sat. solution). After the first washing with $NaHCO_3$ a precipitate was formed. After filtration, the precipitated was determined to be the expected tetramer.
The aqueous layer was re-extracted with EtOAc (2x10mL). The combined organic layers were dried and concentrated *in vacuo* to afford the crude product as a yellow oil.

The crude product was purified by flash chromatography using a CH_2Cl_2/MeOH 100:0 ➡ 90:10 gradient system as eluent.

η= 60%

^{1}H NMR (400 MHz, CD_3OH) δ 6.65 (t, *J* = 8.9 Hz, 2H), 6.54 – 6.34 (m, 3H), 6.27 – 6.09 (m, 3H), 6.05 (d, *J* = 9.2 Hz, 1H), 5.98 (d, *J* = 10.3 Hz, 1H), 5.90 (d, *J* = 10.1 Hz, 1H), 5.39 (d, *J* = 9.2 Hz, 1H), 4.04 (s, 1H), 3.95 – 3.77 (m, 4H), 3.74 – 3.45 (m, 7H), 2.70 (d, *J* = 4.7 Hz, 3H), 2.68 – 2.26 (m, 5H), 1.80 – 1.51 (m, 5H), 1.48 (s, 9H), 1.34 – 0.81 (m, 37H).

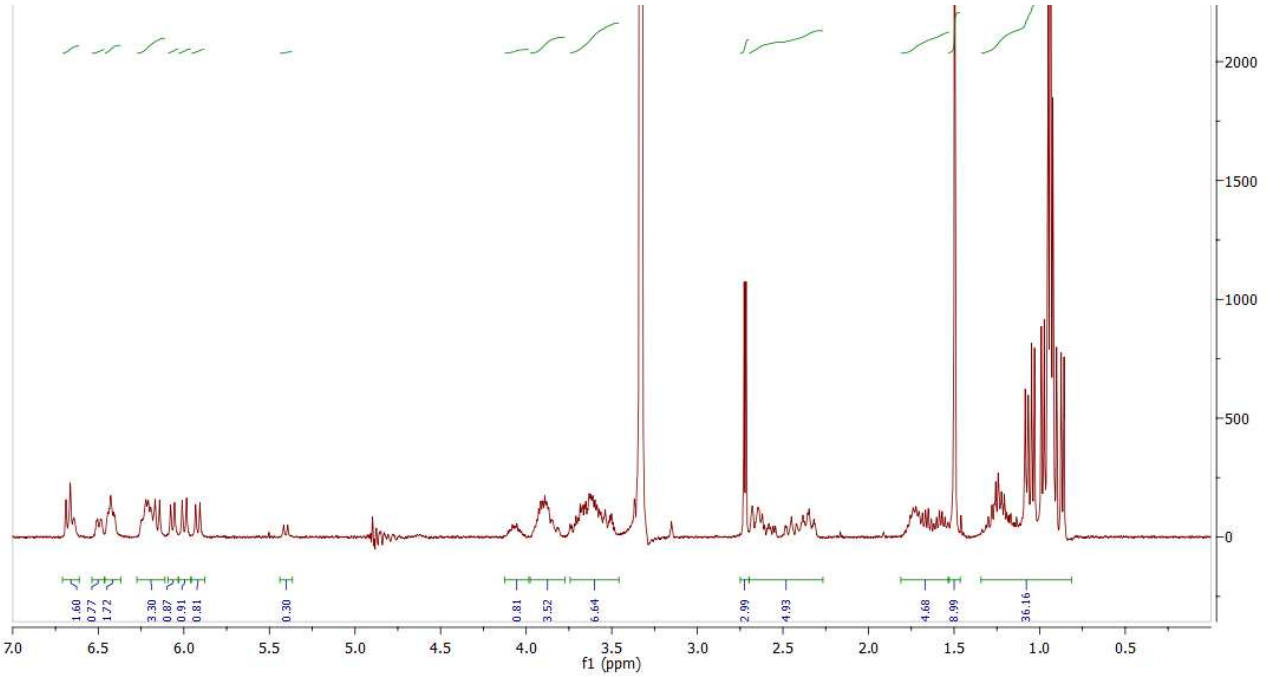

- **$(CF_3)_2$PhNHCO-Val^{u}(^{inv}Ala)^{u}Leu^{u}Val^{u}Ala^{u}Leu^{u}NHMe (C47):**

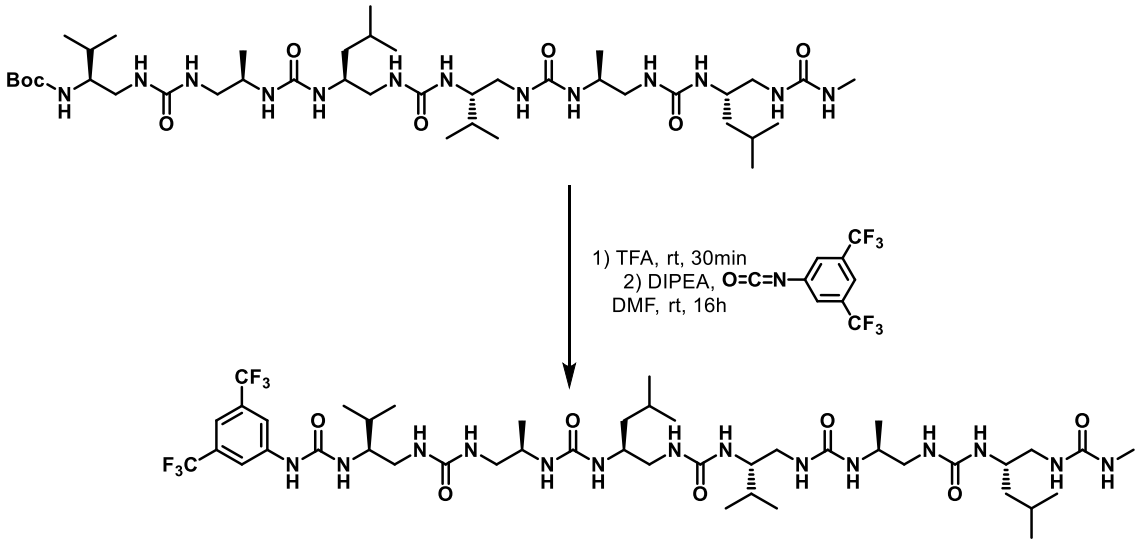

BocVal^{u}(^{inv}Ala)^{u}Leu^{u}Val^{u}Ala^{u}Leu^{u}NHMe was dissolved in TFA and stirred at room temperature for 30 min. The acid was removed by three successive co-evaporations with Toluene. The residue was dried under high vacuum for 5h.
The resulting oil was dissolved in DMF (3mL/mmol) and stirred. DIPEA (3eq) was added to the reaction mixture and the pH was checked to be above 9 after which3,5-Bis(trifluoromethyl)phenyl isocyanate (1.5eq) was added to the TFA salt mixture. The reaction was left to stir overnight.
Ethyl Acetate was added to the reaction mixture. The mixture was washed with $KHSO_4$ (3x1.5mL, 1M solution), $NaHCO_3$ (3x1.5mL, sat. solution) and brine (2x1mL, sat. solution). After the first washing with $NaHCO_3$ a precipitate was formed. After filtration, the precipitated was determined to be the expected tetramer.
The aqueous layer was re-extracted with EtOAc (2x10mL). The combined organic layers were dried and concentrated *in vacuo* to afford the crude product as a yellow oil.

The crude product was purified by flash chromatography using a CH_2Cl_2/MeOH 100:0 ➡ 90:10 gradient system as eluent.

η =64.4%

^{1}H NMR (400 MHz, CD_3OH) δ 8.03 (s, 2H), 7.51 (s, 1H), 6.63 (d, *J* = 7.8 Hz, 1H), 6.49 – 6.31 (m, 4H), 6.27 – 6.13 (m, 4H), 6.02 (dd, *J* = 22.1, 9.8 Hz, 2H), 5.74 (dd, *J* = 20.0, 9.6 Hz, 2H), 4.12 – 3.98 (m, 1H), 3.98 – 3.50 (m, 11H), 2.80 – 2.59 (m, 6H), 2.50 – 2.30 (m, *J* = 25.2, 12.6 Hz, 3H), 1.85 – 1.64 (m, 3H), 1.55 (tt, *J* = 11.6, 5.9 Hz, 1H), 1.34 – 1.13 (m, 5H), 1.12 – 0.81 (m, 32H).

^{13}C NMR (75 MHz, MeOD) δ 162.27, 162.01, 161.65, 161.39, 160.78, 158.18, 143.22, 133.85, 133.41, 132.98, 132.54, 130.05, 126.44, 122.84, 118.96, 115.67, 56.48, 56.27, 47.15, 46.87, 46.30, 46.08, 44.60, 44.35, 43.79, 42.85, 31.85, 26.85, 26.18, 25.81, 23.56, 23.50, 22.76, 22.41, 20.07, 20.05, 18.64, 18.35, 17.75.

HRMS: m/z calculated for $C_{44}H_{77}F_6N_{14}O_7^+$ $[M+H]^+$ 1027.5998, found 1027.6000.

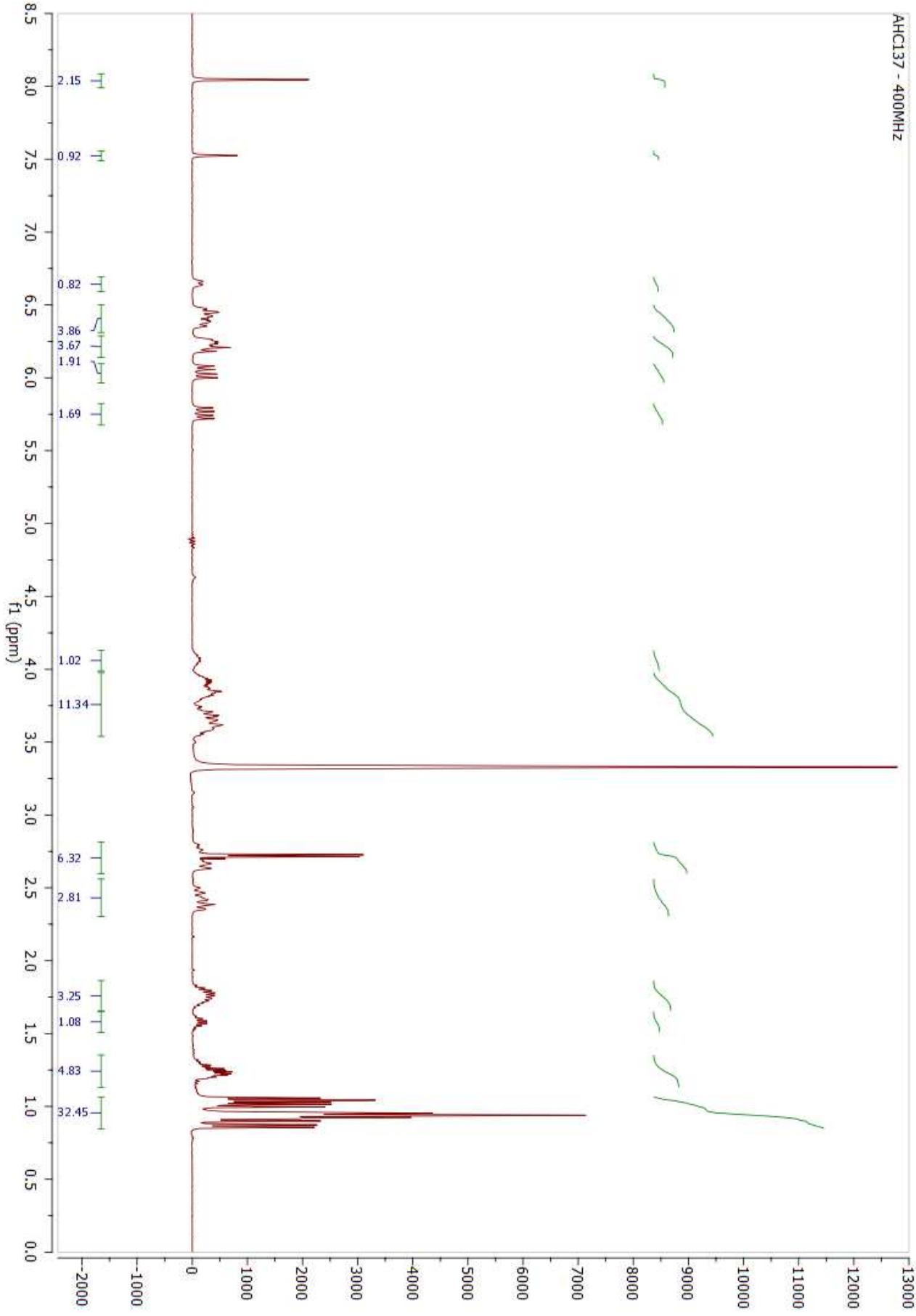
AHC137 - 400MHz
f1 (ppm)
2.15
0.92
0.82
3.86
3.67
1.91
1.69
1.02
11.34
6.32
2.81
3.25
1.08
4.83
32.45

- **Boc(^{inv}Val)^{u}Leu^{u}Val^{u}Ala^{u}Leu^{u}NHMe (30):**

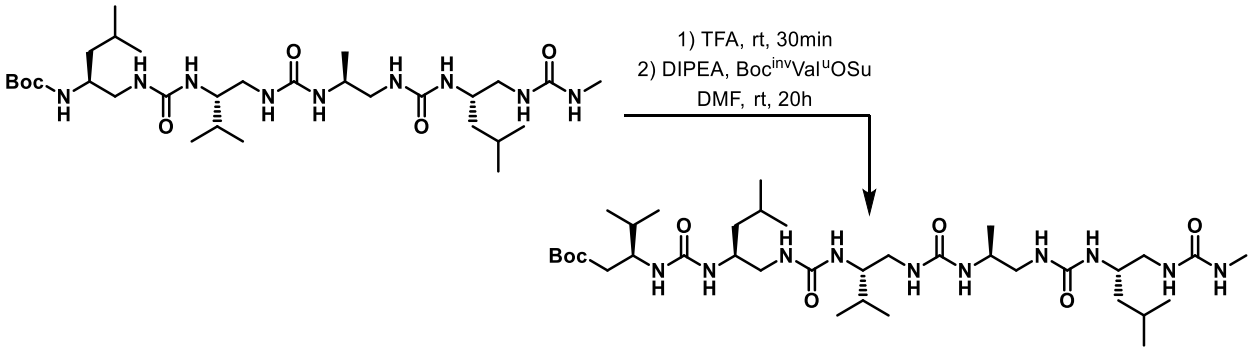

Boc-Leu^{u}-Val^{u}-Ala^{u}-Leu^{u}-NHMe was dissolved in TFA and stirred at room temperature for 30 min. The acid was removed by three successive co-evaporations with Toluene. The residue was dried under high vacuum for 5h.
The resulting oil was dissolved in DMF (1.5mL/mmol) and stirred. DIPEA (3eq) was added to the reaction mixture and the pH was checked to be above 9. Boc^{inv}AlaOSu (1.2eq) was dissolved in DMF (1.5mL/mmol) and added to the TFA salt mixture using a syringe pump set at 125µL/h. The reaction was left to stir for 20h (addition and reaction time combined) at room temperature.

Ethyl Acetate was added to the reaction mixture. The mixture was washed with $KHSO_4$ (3x1.5mL, 1M solution), $NaHCO_3$ (3x1.5mL, sat. solution) and brine (2x1mL, sat. solution). After the first washing with $NaHCO_3$ a precipitate was formed. After filtration, the precipitated was determined to be the expected tetramer.

The aqueous layer was re-extracted with EtOAc (2x10mL). The combined organic layers were dried and concentrated *in vacuo* to afford the crude product as a white solid.

The crude product was purified by flash chromatography using a CH_2Cl_2/MeOH 100:0 ➡ 90:10 gradient system as eluent.

η = 48%

^{1}H NMR (400 MHz, CD_3OH) δ 6.89 (s, 1H), 6.48 – 6.29 (m, 3H), 6.19 (d, *J* = 4.8 Hz, 1H), 6.05 (d, *J* = 9.1 Hz, 2H), 5.88 (dd, *J* = 20.3, 10.0 Hz, 2H), 5.76 (d, *J* = 8.4 Hz, 1H), 5.59 (d, *J* = 9.6 Hz, 1H), 4.12 – 3.81 (m, 3H), 3.73 – 3.35 (m, 7H), 2.70 (d, *J* = 4.7 Hz, 3H), 2.68 – 2.57 (m, 1H), 2.56 – 2.24 (m, 3H), 1.81 – 1.52 (m, 5H), 1.46 (s, 9H), 1.32 – 1.17 (m, 4H), 1.07 – 0.79 (m, 29H).

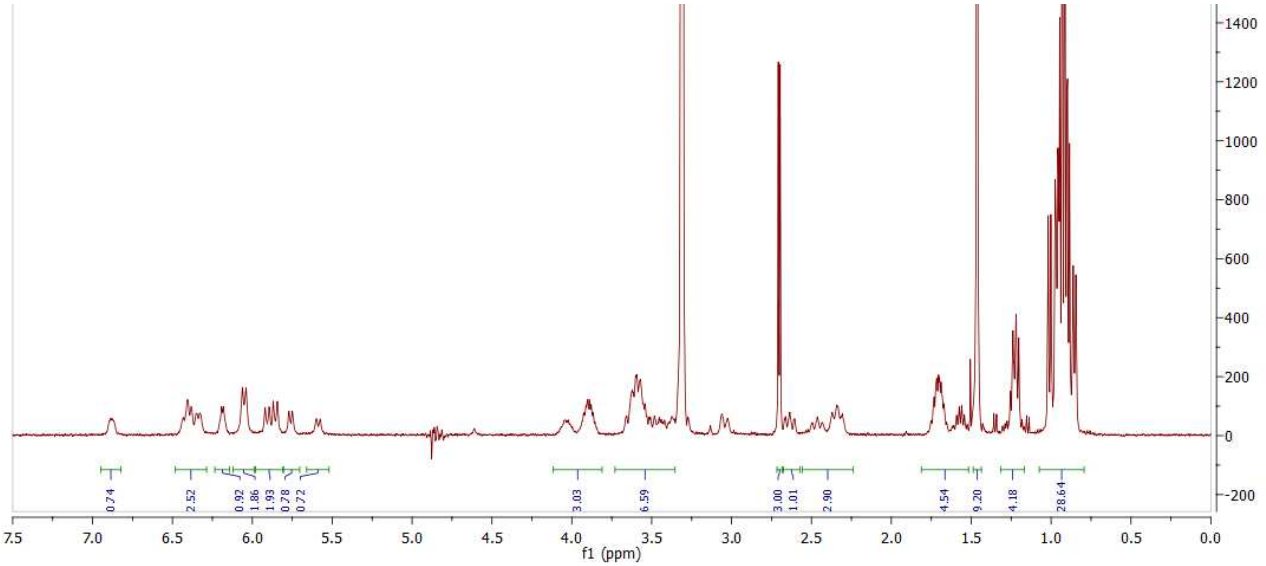

- **BocVal^{u}(^{inv}Val)^{u}Leu^{u}Val^{u}Ala^{u}Leu^{u}NHMe (33):**

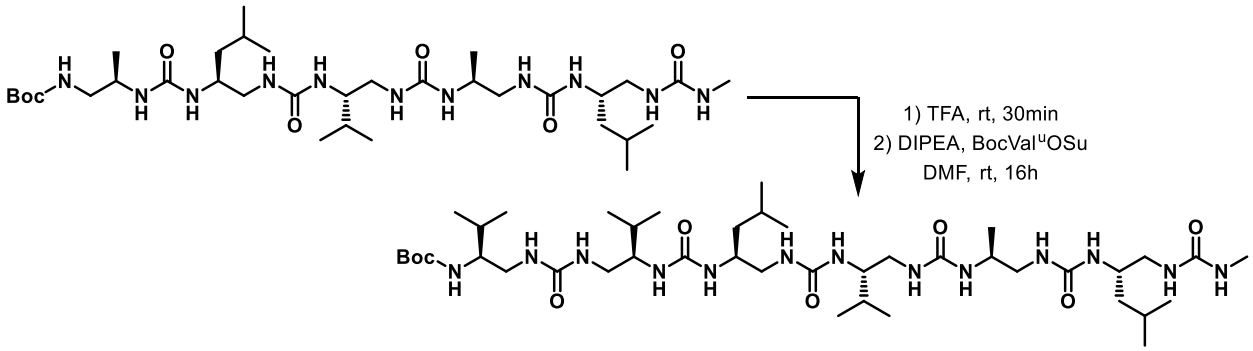

Boc(^{inv}Val)^{u}Leu^{u}Val^{u}Ala^{u}Leu^{u}NHMe was dissolved in TFA and stirred at room temperature for 30 min. The acid was removed by three successive co-evaporations with Toluene. The residue was dried under high vacuum for 5h.

The resulting oil was dissolved in DMF (3mL/mmol) and stirred. DIPEA (3eq) was added to the reaction mixture and the pH was checked to be above 9 after which BocValOSu (1.2eq) was added to the TFA salt mixture. The reaction was left to stir overnight.

Ethyl Acetate was added to the reaction mixture. The mixture was washed with $KHSO_4$ (3x1.5mL, 1M solution), $NaHCO_3$ (3x1.5mL, sat. solution) and brine (2x1mL, sat. solution). After the first washing with $NaHCO_3$ a precipitate was formed. After filtration, the precipitated was determined to be the expected tetramer.

The aqueous layer was re-extracted with EtOAc (2x10mL). The combined organic layers were dried and concentrated *in vacuo* to afford the crude product as an off-white solid.

The crude product was purified by flash chromatography using a CH_2Cl_2/MeOH 100:0 ➡ 90:10 gradient system as eluent.

η = 81.9%

^{1}H NMR (400 MHz, CD_3OH) δ 6.63 (dd, *J* = 27.9, 8.9 Hz, 2H), 6.42 (t, *J* = 8.8 Hz, 3H), 6.25 – 6.00 (m, 5H), 6.00 – 5.88 (m, 2H), 5.38 (d, *J* = 9.7 Hz, 1H), 4.14 – 3.96 (m, 1H), 3.89 (s, 2H), 3.78 – 3.42 (m, 8H), 2.70 (d, *J* = 4.7 Hz, 3H), 2.67 – 2.22 (m, 5H), 1.79 – 1.50 (m, 6H), 1.47 (s, 9H), 1.29 – 1.10 (m, 4H), 1.06 – 0.83 (m, 34H).

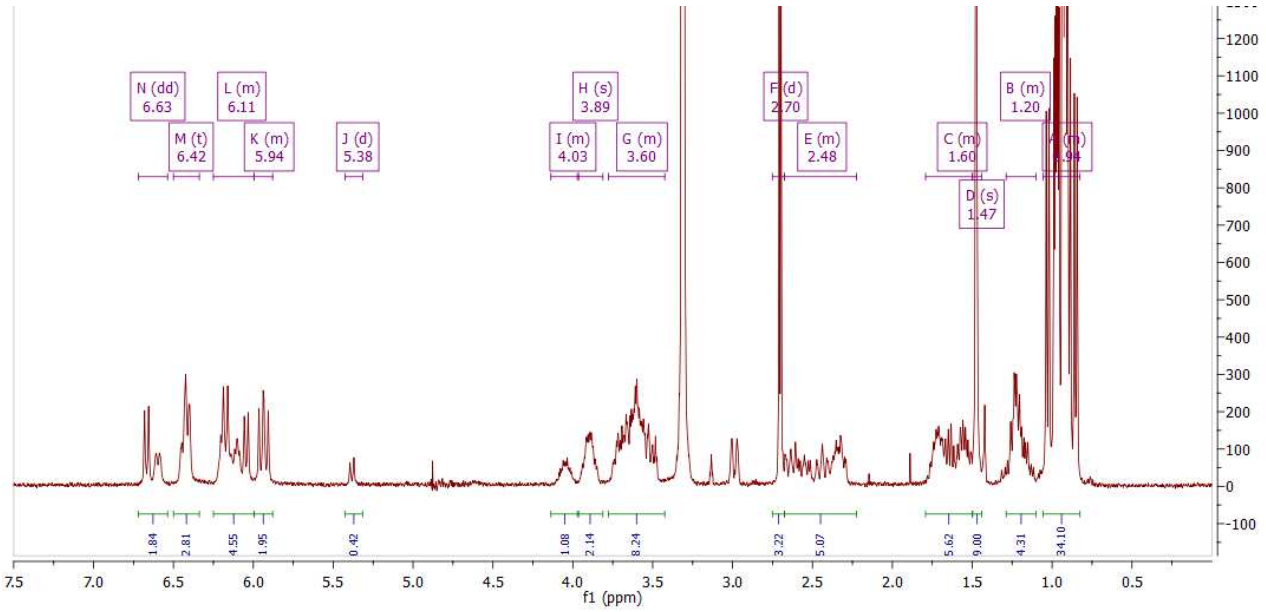

- **$(CF_3)_2$PhNHCO-Val^u(^{inv}Val)^{u}Leu^{u}Val^{u}Ala^{u}Leu^{u}NHMe (C46):**

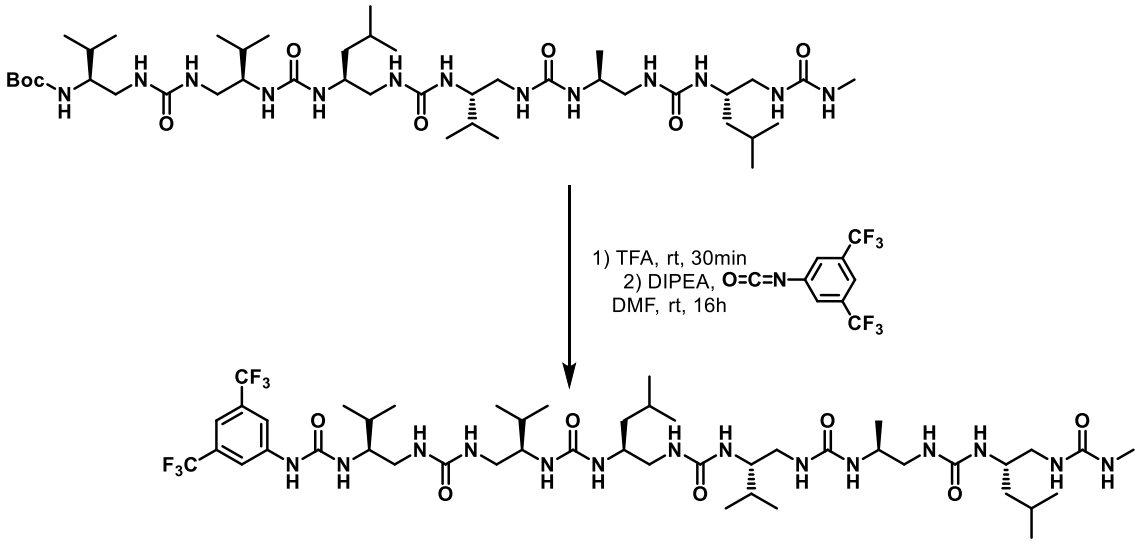

BocVal^u(^{inv}Val)^{u}Leu^{u}Val^{u}Ala^{u}Leu^{u}NHMe was dissolved in TFA and stirred at room temperature for 30 min. The acid was removed by three successive co-evaporations with Toluene. The residue was dried under high vacuum for 5h.

The resulting oil was dissolved in DMF (3mL/mmol) and stirred. DIPEA (3eq) was added to the reaction mixture and the pH was checked to be above 9 after which 3,5-Bis(trifluoromethyl)phenyl isocyanate (1.5eq) was added to the TFA salt mixture. The reaction was left to stir overnight.

Ethyl Acetate was added to the reaction mixture. The mixture was washed with $KHSO_4$ (3x1.5mL, 1M solution), $NaHCO_3$ (3x1.5mL, sat. solution) and brine (2x1mL, sat. solution). After the first washing with $NaHCO_3$ a precipitate was formed. After filtration, the precipitated was determined to be the expected tetramer.

The aqueous layer was re-extracted with EtOAc (2x10mL). The combined organic layers were dried and concentrated *in vacuo* to afford the crude product as a yellow oil.

The crude product was purified by flash chromatography using a CH_2Cl_2/MeOH 100:0 ➡ 90:10 gradient system as eluent.

η = 51.5%

^{1}H NMR (400 MHz, CD_3OH) δ 8.00 (s, 2H), 7.52 (s, 1H), 6.58 (d, *J* = 8.5 Hz, 1H), 6.49 – 6.33 (m, 3H), 6.32 – 6.00 (m, 5H), 5.91 (dd, *J* = 33.3, 10.1 Hz, 2H), 5.60 (d, *J* = 9.6 Hz, 1H), 4.16 – 3.50 (m, 11H), 2.91 (d, *J* = 14.0 Hz, 1H), 2.79 – 2.58 (m, 5H), 2.58 – 2.30 (m, 3H), 1.87 – 1.65 (m, 3H), 1.57 (td, *J* = 13.4, 6.8 Hz, 1H), 1.48 – 1.16 (m, 6H), 1.10 – 0.83 (m, 32H), 0.77 (d, *J* = 6.7 Hz, 3H).

^{13}C NMR (75 MHz, MeOD) δ 162.16, 162.01, 161.62, 161.41, 161.33, 158.20, 143.15, 133.86, 133.42, 132.98, 132.54, 130.03, 126.43, 122.83, 119.08, 115.77, 57.40, 57.40, 56.52, 56.52, 56.26, 56.26, 47.12, 46.26, 46.14, 44.55, 44.19, 43.76, 42.99, 41.13, 31.87, 31.77, 30.43, 26.86, 26.14, 25.81, 23.56, 23.52, 22.75, 22.42, 20.09, 20.05, 19.99, 19.82, 18.69, 18.65, 18.41.

HRMS: m/z calculated for $C_{46}H_{81}F_6N_{14}O_7^+$ $[M+H]^+$ 1055.6311, found 1055.6287.

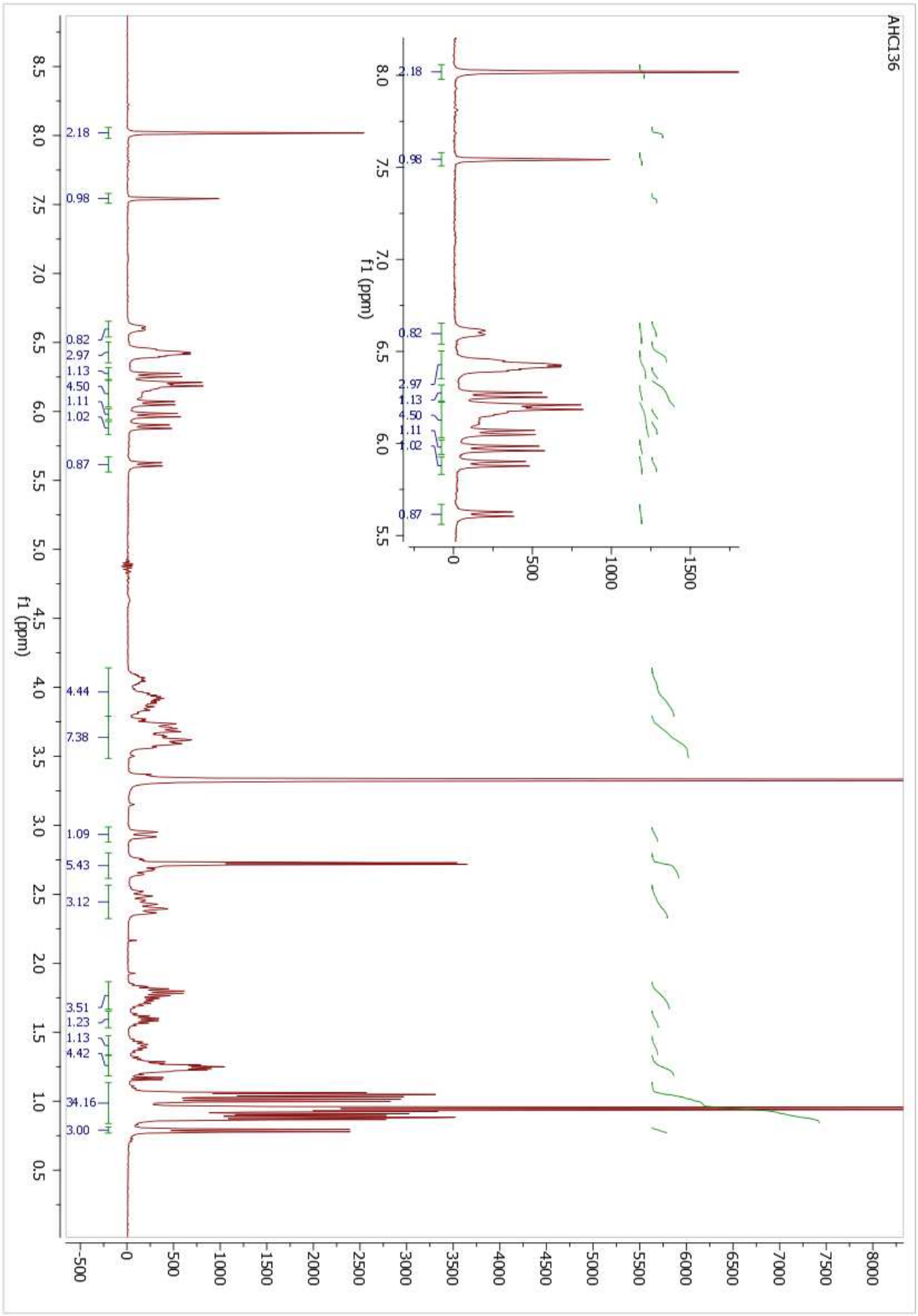
AHCl36
f1 (ppm)
2.18
0.98
0.82
2.97
1.13
4.50
1.11
1.02
0.87
4.44
7.38
1.09
5.43
3.12
3.51
1.23
1.13
4.42
34.16
3.00

- **BocVal^{u}NHCH(Me)CH_2-N_3 (35):**

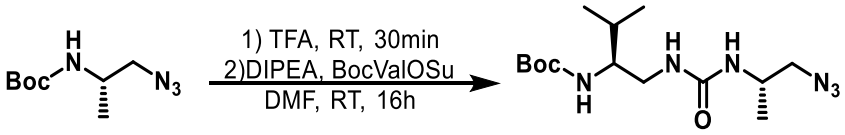

Boc NHCH(Me)CH_2-N_3 **(34)** was dissolved in TFA and stirred at room temperature for 30 min. The acid was removed by three successive co-evaporations with Toluene. The residue was dried under high vacuum for 4h.

The resulting oil was dissolved in acetonitrile (3mL/mmol) and stirred. DIPEA (3eq) was added to the reaction mixture and the pH was checked to be above 9 after which BocValOSu (1.2eq) was added to the TFA salt mixture. The reaction was left to stir overnight.

The acetonitrile was evaporated under reduced pressure and the residue was dissolved in Ethyl Acetate. The mixture was washed with $KHSO_4$ (3x1.5mL, 1M solution), $NaHCO_3$ (3x1.5mL, sat. solution) and brine (2x1.5mL, sat. solution). After the first washing with $NaHCO_3$, a precipitate was formed and filtered off. The combined organic layers were dried and concentrated *in vacuo* to afford the crude product as a yellow oil

The crude product was triturated in cold Et_2O to afford the pure compound as an off-white solid

η =100%

^{1}H NMR (300 MHz, MeOD) δ 6.34 (d, *J* = 9.5 Hz, 1H), 6.14 (d, *J* = 7.7 Hz, 1H), 5.87 (s, 1H), 4.02 – 3.82 (m, 1H), 3.57 – 3.36 (m, 2H), 3.32 – 3.00 (m, 2H), 1.74 (tt, *J* = 13.9, 7.0 Hz, 1H), 1.46 (s, 9H), 1.16 (d, *J* = 6.8 Hz, 3H), 0.97 – 0.89 (m, 6H).

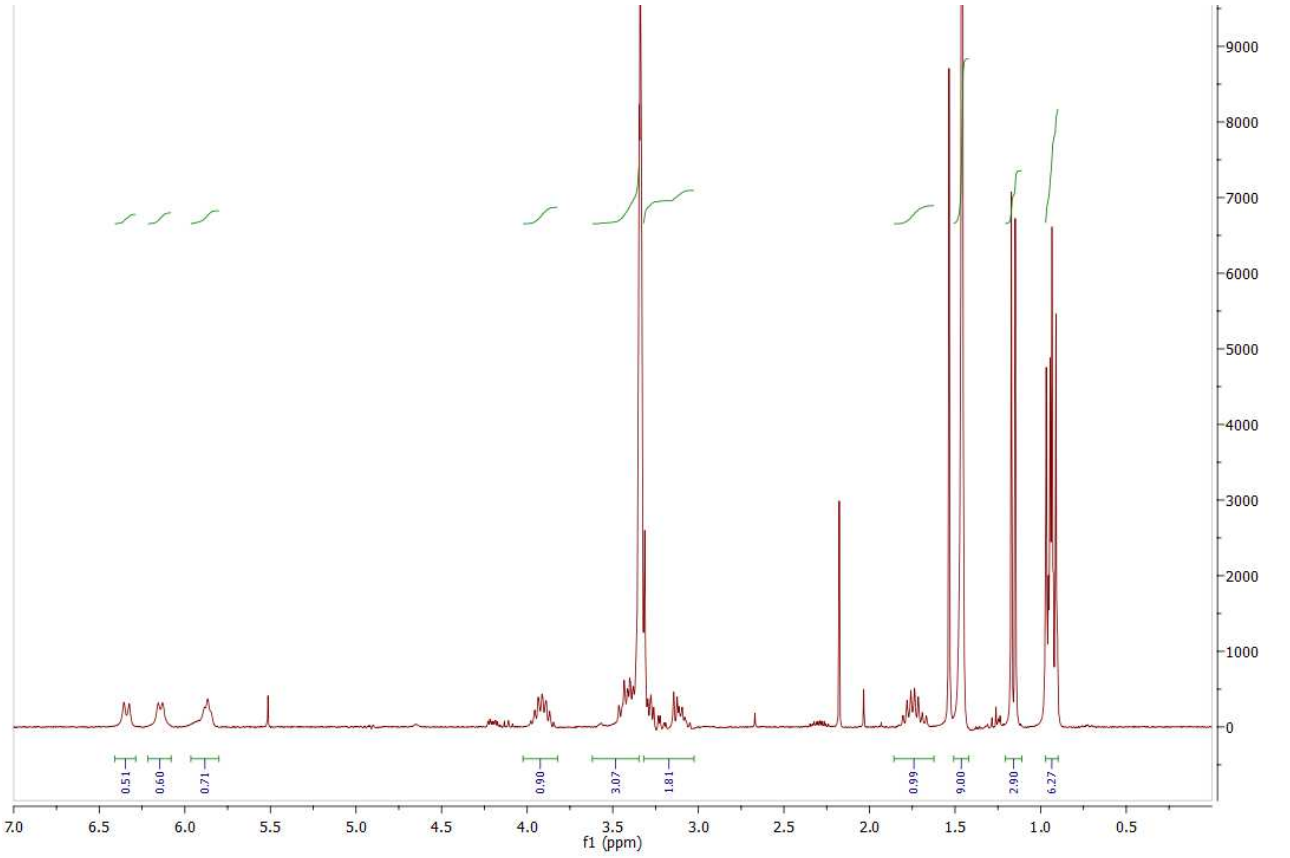

- **BocVal(Imidazolidinetrione)NHCH(Me)CH_2-N_3 (36):**

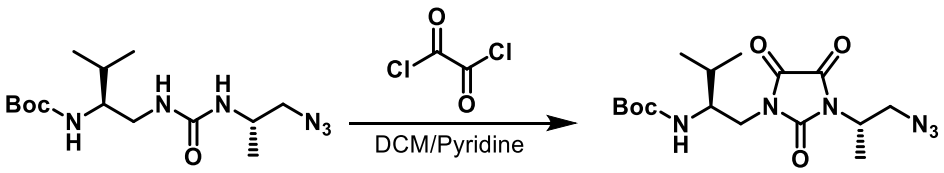

BocVal^{u}NHCH(Me)CH_2-N_3 **(35)** was dissolved in a mixture of CH_2Cl_2/Pyridine (50:50). Oxalyl chloride (1eq.) was added leading to smoke and precipitate formation. The reaction was left to stir at room temperature for 1h30 after which one more equivalent Oxalyl Chloride was added leading to more precipitation and smoke formation. The reaction was stirred for an additional 1h30.

The CH_2Cl_2 was evaporated and EtOAc was added. The organic layer was washed with HCl (0.5N, 2x10mL), dried over $MgSO_4$ and concentrated *in vacuo*.

The product was purified by column chromatography using a Petroleum ether/EtOAc gradient (100/0 ➡ 90/10)

η = 48%

^{1}H NMR (300 MHz, $CDCl_3$) δ 4.45 (m, 1H), 3.90 (m, 2H), 3.74 – 3.55 (m, 3H), 1.94 – 1.74 (m, 1H), 1.59 (s, 9H), 1.54 (d, J = 7.0 Hz, 3H), 1.04 (dd, J = 8.1, 7.0 Hz, 6H).

^{13}C NMR (75 MHz, CD_3OH) δ 157.41, 157.02, 153.70, 78.75, 54.77, 52.35, 41.71, 30.09, 27.31, 18.62, 17.55, 14.38.

HRMS: m/z calculated for $C_{16}H_{26}N_6O_5Na^+$ $[M+Na]^+$ 405.1857, found 405.1965

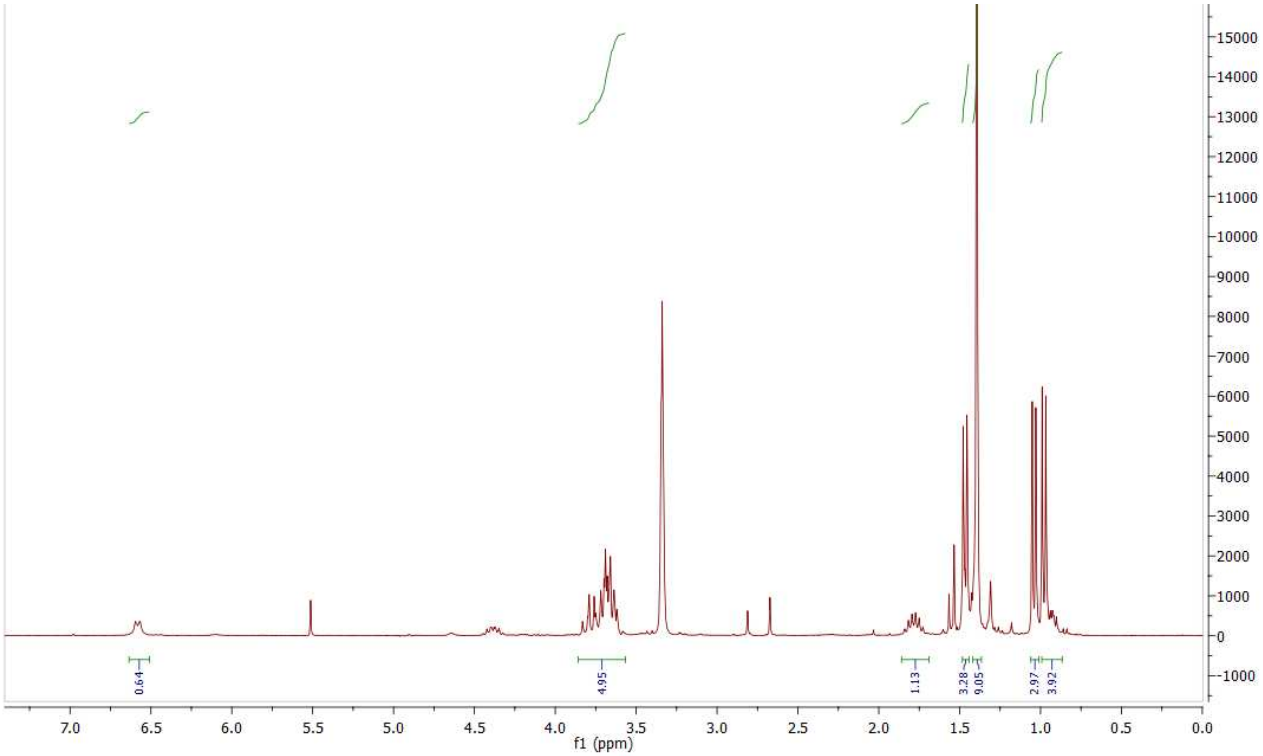

- **Catalytic test reaction:**

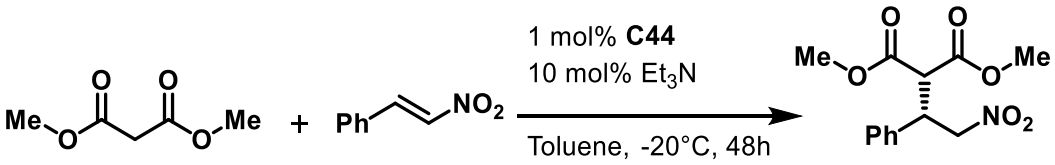

A glass tube was loaded with catalyst **C44** (0.5mg, 0.5µmol), toluene (0.5mL) and *trans*-β-nitrostyrene (74.6mg, 0.5mmol). The mixture was cooled to -20°C before addition of dimethylmalonate (0.11mL, 1mmol) and triethylamine (21µL, 0.15mmol). The reaction was stirred at -20°C for 48h.

The mixture was quenched with 1N HCl (2mL) and extracted with dichloromethane (3x2mL). The combined organic layers were washed with brine (2mL), dried over $MgSO_4$ and concentrated *in vacuo* to afford the crude product as a yellow oil.

The crude material was purified by column chromatography using a hexane/ethyl acetate (90:10) system as eluent.

The physical appearance of the product was observed to be dependent on the enantiomeric purity with the higher enantiomerically pure product resulting in a crystalline white solid whereas the racemic mixture was obtained as a colorless oil.

^{1}H NMR (300 MHz, $CDCl_3$) δ 7.36 – 7.20 (m, 5H), 4.99 – 4.80 (m, 1H), 4.25 (td, *J* = 8.7, 5.6 Hz, 1H), 3.77 (s, 1H), 3.57 (s, 1H).

The enantiomeric excess was determined by HPLC (Chiralpak® AD-H; flow: 1mL/min; hexane/*i*PrOH 75:25; λ=210nm): major enantiomer t_R= 12.7min; minor enantiomer t_R=8.4min; *ee*=97%

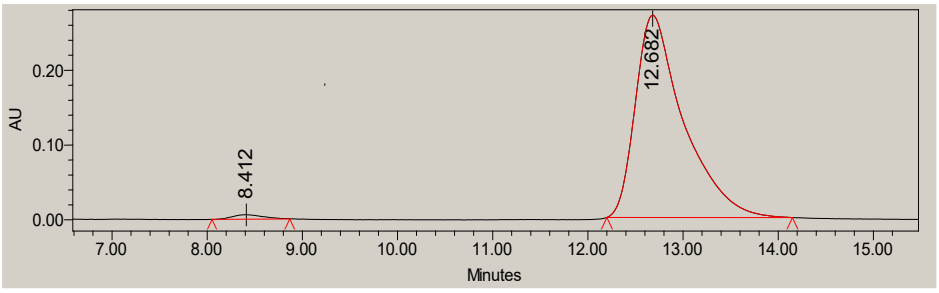

	Retention time	% Area
2	12.682	98.67
1	8.412	1.33

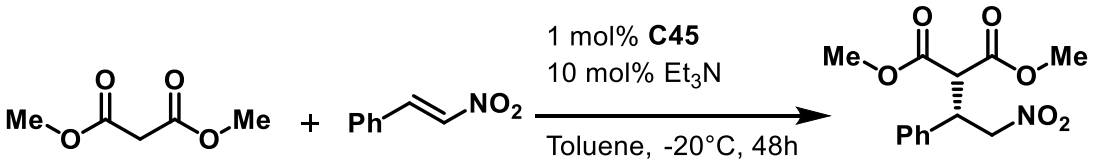

A glass tube was loaded with catalyst **C45** (0.5mg, 0.5µmol), toluene (0.5mL) and *trans*-β-nitrostyrene (74.6mg, 0.5mmol). The mixture was cooled to -20°C before addition of dimethylmalonate (0.11mL, 1mmol) and triethylamine (21µL, 0.15mmol). The reaction was stirred at -20°C for 48h.

The mixture was quenched with 1N HCl (2mL) and extracted with dichloromethane (3x2mL). The combined organic layers were washed with brine (2mL), dried over $MgSO_4$ and concentrated *in vacuo* to afford the crude product as a yellow oil.

The crude material was purified by column chromatography using a hexane/ethyl acetate (90:10) system as eluent.

The enantiomeric excess was determined by HPLC (Chiralpak® AD-H; flow: 1mL/min; hexane/*i*PrOH 75:25; λ=210nm): major enantiomer t_R= 12.4min; minor enantiomer t_R=8.3min; *ee*=78%

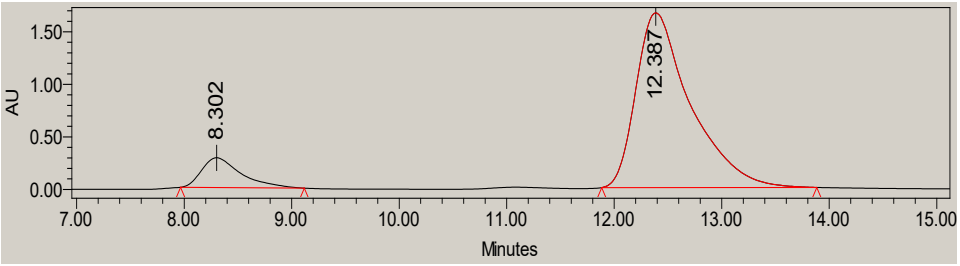

	Retention time	% Area
2	12.387	89.04
1	8.302	10.96

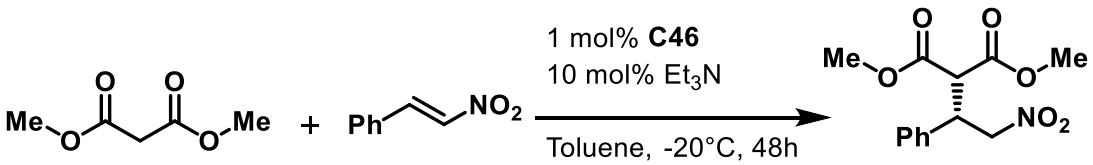

A glass tube was loaded with catalyst **C46** (0.5mg, 0.5µmol), toluene (0.5mL) and *trans*-β-nitrostyrene (74.6mg, 0.5mmol). The mixture was cooled to -20°C before addition of dimethylmalonate (0.11mL, 1mmol) and triethylamine (21µL, 0.15mmol). The reaction was stirred at -20°C for 48h.

The mixture was quenched with 1N HCl (2mL) and extracted with dichloromethane (3x2mL). The combined organic layers were washed with brine (2mL), dried over $MgSO_4$ and concentrated *in vacuo* to afford the crude product as a yellow oil.

The crude material was purified by column chromatography using a hexane/ethyl acetate (90:10) system as eluent.

The enantiomeric excess was determined by HPLC (Chiralpak® AD-H; flow: 1mL/min; hexane/*i*PrOH 75:25; λ=210nm): major enantiomer t_R= 12.5min; minor enantiomer t_R=8.3min; *ee*=84%

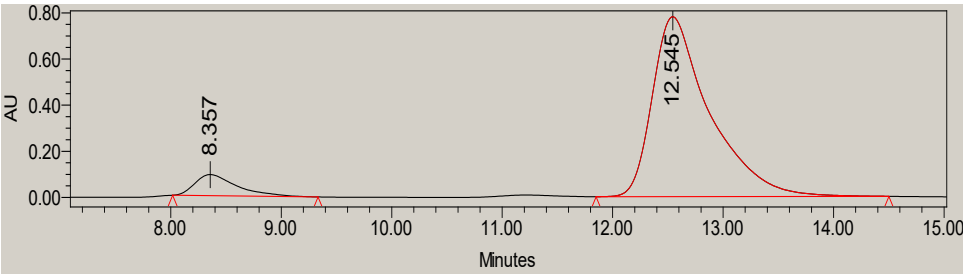

	Retention time	% Area
2	12.545	92.10
1	8.357	7.90

Extension of reactivity:

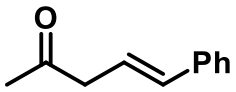

(E)-5-phenylpent-4-en-2-one (40):

Benzaldehyde (530.6mg, 5mmol), powdered Indium (1.148g, 10mmol, 2eq) and $InCl_3$ (553mg, 2.5mmol, 0.5eq) were charged in a round bottom flask and dissolved in a 1:1 mixture of THF and H_2O (30mL, 6mL/mmol). Methyl vinyl ketone (1.051g,15mmol, 3eq) was added and the mixture was stirred at room temperature for 8h, after which 15mL HCl 1N were added and the mixture was stirred for an additional 30 minutes. The reaction mixture was extracted with ethyl acetate (4x20mL) and the combined organic layers were washed with brine (30mL), dried over $MgSO_4$ and concentrated *in vacuo* to afford the crude product as a yellow oil.

The crude material was purified by flash chromatography using a 100/0 to 96/4 gradient of hexane/ethyl acetate, yielding the pure product as a yellow liquid.

η=38.4%

^{1}H NMR (300 MHz, $CDCl_3$) δ 7.40 – 7.20 (m, 5H), 6.48 (d, J = 15.9 Hz, 1H), 6.31 (dt, J = 15.9, 7.0 Hz, 1H), 3.34 (d, J = 6.9 Hz, 2H), 2.21 (s, 3H).

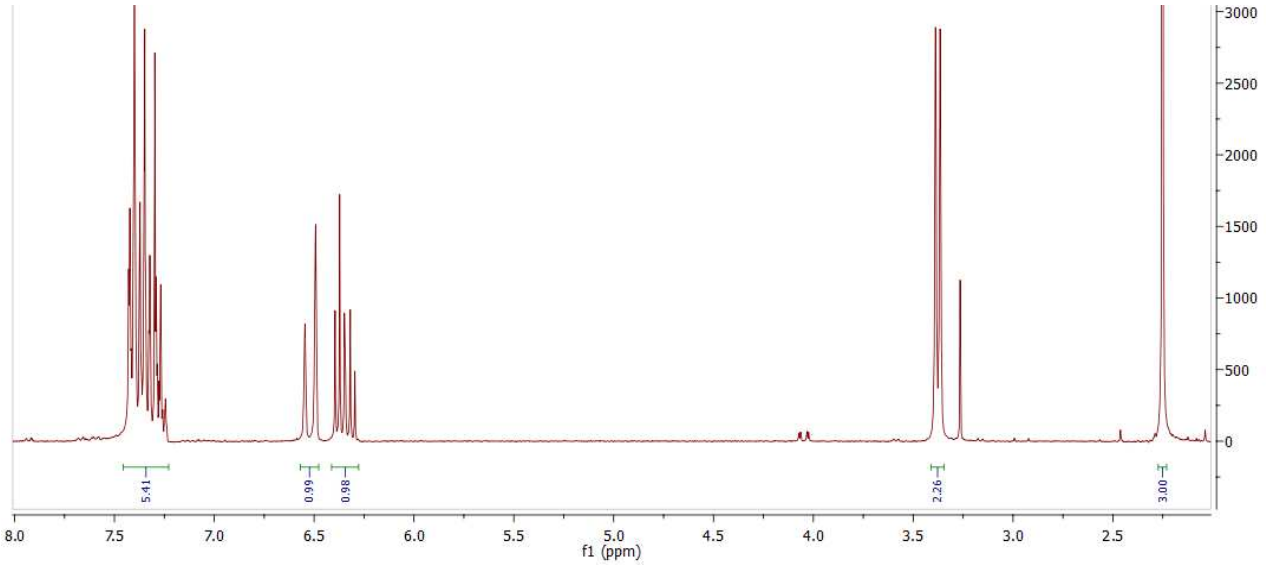

Catalytic reaction:

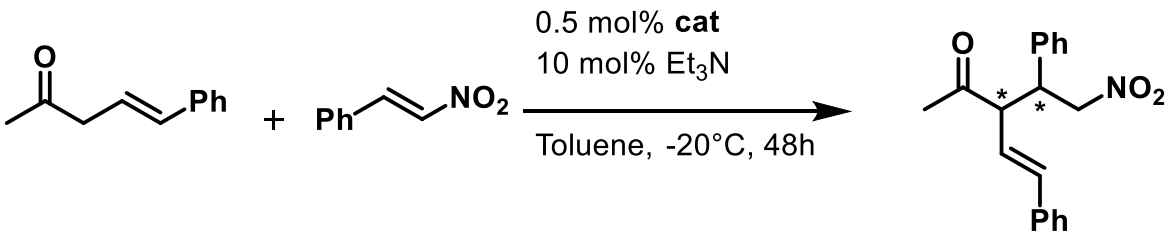

The previously synthesised enone **(40)** (64.1mg, 0.4mmol, 2eq), nitrostyrene (29.83mg, 0.2mmol) and the catalyst (1.04mg, 1µmol, 0.5mol%) were charged in a 5mL glass tube. Added 0.2mL of a solution of Et_3N in Toluene (0.1mol/L, 20µmol, 0.1eq) and stirred the resulting mixture at -20°C.
The reaction was monitored by ^{1}H NMR from aliquots taken from the reaction mixture (See chapter 2, *Extension of reactivity*)

Syntheses concerning chapter 3

Synthesis of α- and β- chlorinated sulfides as electrophiles

- **Ethyl Benzyl sulfide (42):**

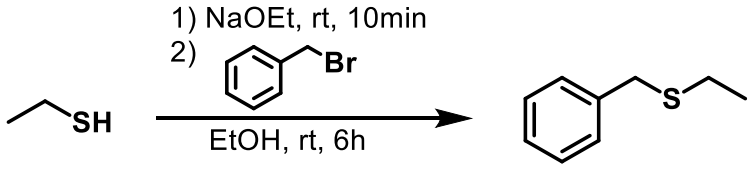

Ethanethiol was dissolved in EtOH (2mL/mmol). Sodium ethoxide (2eq) was added to the thiol solution leading to a strong yellow coloration immediately. The mixture thus obtained was stirred at room temperature for 10 minutes before benzyl bromide (1eq) was added drop wise. The reaction was stirred at room temperature for 6h (TLC in 100% n-Hexane). Once the reaction is complete, water and DCM (20mL each) were added to the mixture and the two layers were separated. The aqueous layer was extracted with DCM (2x10mL). The combined organic layers were washed with NaOH (2N, 2x10mL) and brine (15mL), dried over $MgSO_4$ and concentrated under reduced pressure to afford the crude product as a yellow oil.

The product was purified by column chromatography using 100% n-Hexane as the eluent.

Aspect: colorless oil **η=76.5%**

^{1}H NMR: (300 MHz, $CDCl_3$) δ 7.35-7.26, (m, 5H), 3.75 (s, 2H), 2.45 (q, *J* = 7.4 Hz, 2H), 1.26 (t, *J* = 7.4 Hz, 3H).

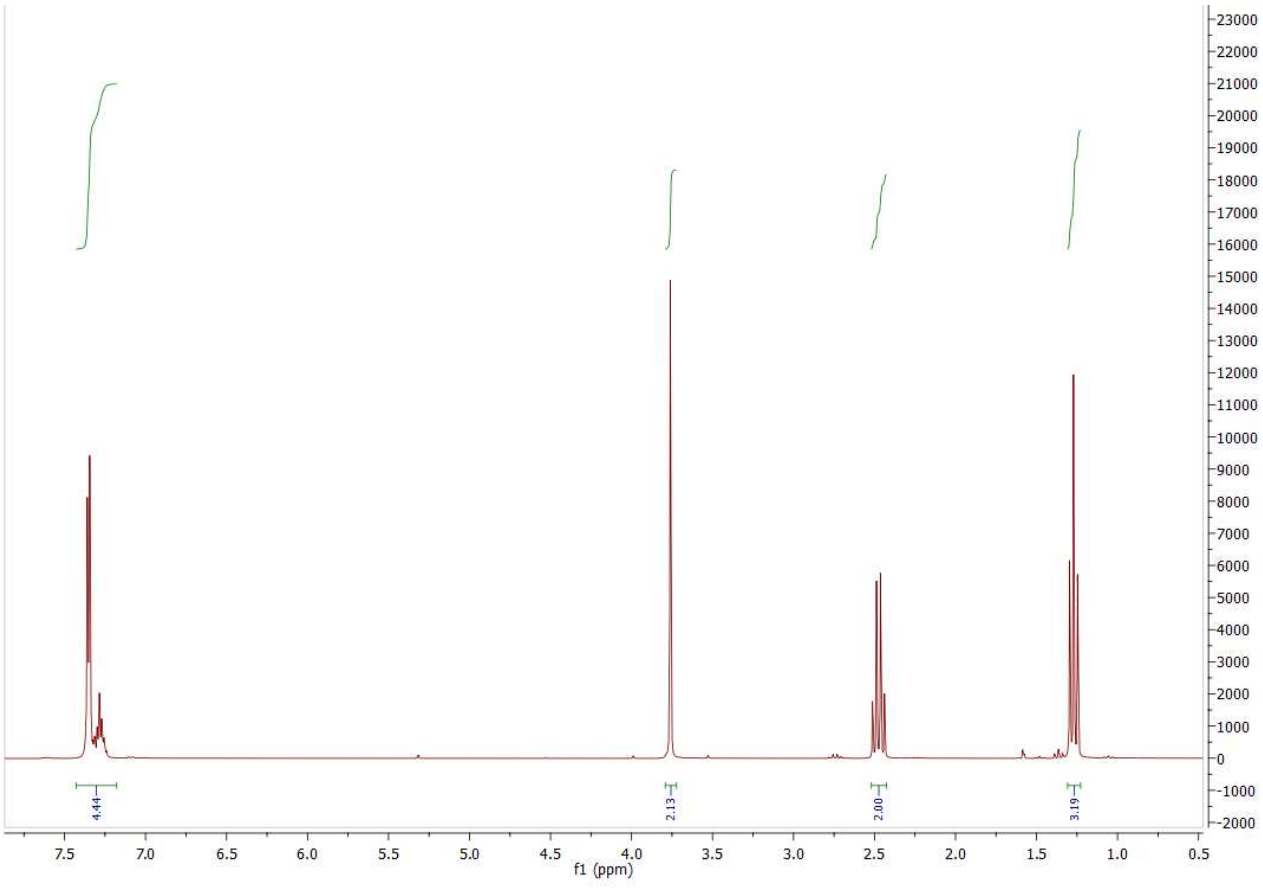

- **Ethyl 4-Nitrobenzyl sulfide[2] :**

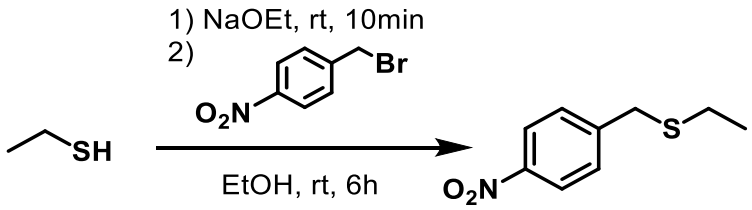

In an addition funnel, Ethanethiol was dissolved in EtOH (2mL/mmol). Sodium ethoxide (2eq) was added to the thiol solution leading to a strong yellow coloration immediately. The mixture thus obtained was left to react for 10 minutes while stirred manually. 4-nitrobenzyl bromide (1.2eq) dissolved in EtOH and stirred at room temperature for 5min before adding the sodium thiolate solution dropwise. The reaction was stirred at room temperature for 4h (TLC in 95:5 n-Hexane/EtOAc). Once the reaction is complete, the solvent was removed by evaporation. Water was added to the residue and extracted with DCM .The two layers were separated and the organic layer washed with water twice. Dried the combined organic layers over $MgSO_4$ and concentrated under reduced pressure to afford the crude product as a pale yellow oil.

Purification by column chromatography was attempted, however no single eluent mixture was capable to separate the compound from the impurity.

The crude product's NMR shows the desired compound has been formed but an impurity remains.

^{1}H NMR: (300 MHz, $CDCl_3$) δ 8.18 (d, *J*= 8.7Hz, 2H), 7.48 (d, *J*= 8.6Hz, 2H), 3.78 (s, 3H), 2.44 (q, *J* = 7.4 Hz, 3H), 1.23 (t, *J* = 7.4 Hz, 3H).

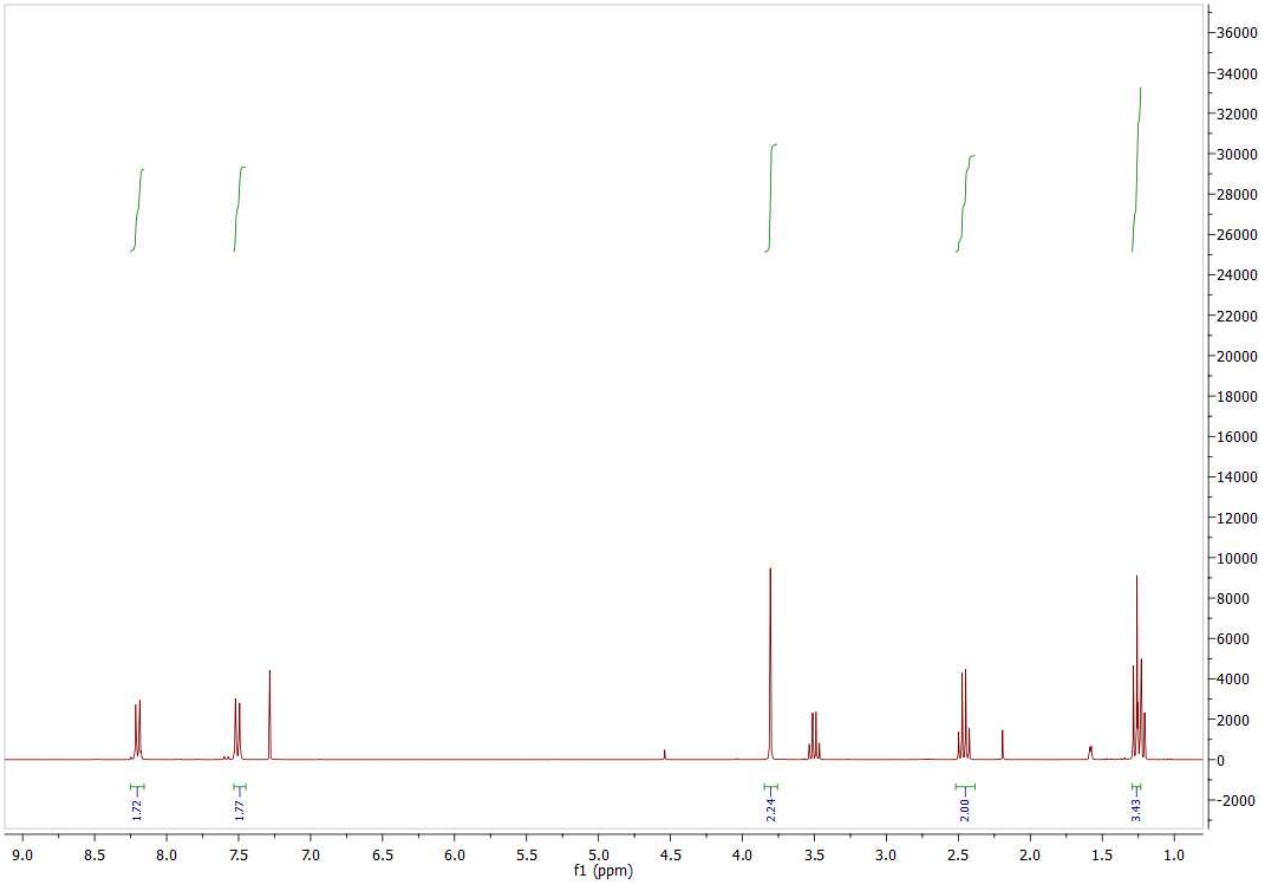

[2] H.L. Holland, F.M. Brown, B.G. Larsen ,*Tetrahedron: Asymmetry*, **1995**, *Vol. 6 (N.7)*, p. 1561-1567

- **Ethyl 3,5-Difluorobenzyl sulfide :**

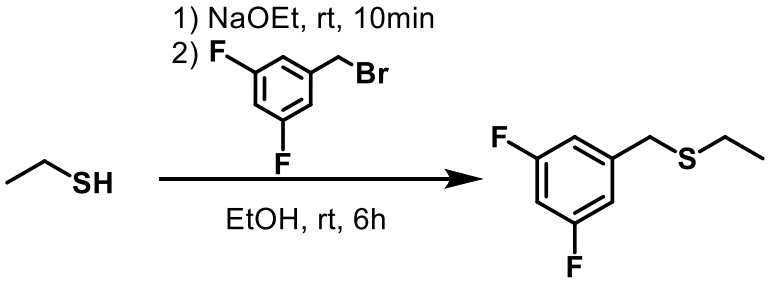

Ethanethiol was dissolved in EtOH (2mL/mmol). Sodium ethoxide (2eq) was added to the thiol solution leading to a strong yellow coloration immediately. The mixture thus obtained was stirred at room temperature for 10 minutes before 3,5-Difluorobenzyl bromide (1eq) was added dropwise. The reaction was stirred at room temperature for 6h (TLC in 100% n-Hexane). Once the reaction is complete, water and DCM (20mL each) were added to the mixture and the two layers were separated. The aqueous layer was extracted with DCM (2x10mL). The combined organic layers were washed with NaOH (2N, 2x10mL) and brine (15mL), dried over $MgSO_4$ and concentrated under reduced pressure to afford the crude product as a yellow oil.

The product was purified by column chromatography using 100% n-Hexane as the eluent.

Aspect: colorless oil **η=63%**

^{1}H NMR: (300 MHz, $CDCl_3$) δ 6.86 (dd, *J* = 8.1, 2.2 Hz, 2H), 6.74 – 6.62 (m, 1H), 3.67 (s, 2H), 2.44 (q, *J* = 7.4 Hz, 2H), 1.23 (t, *J* = 7.4 Hz, 3H).

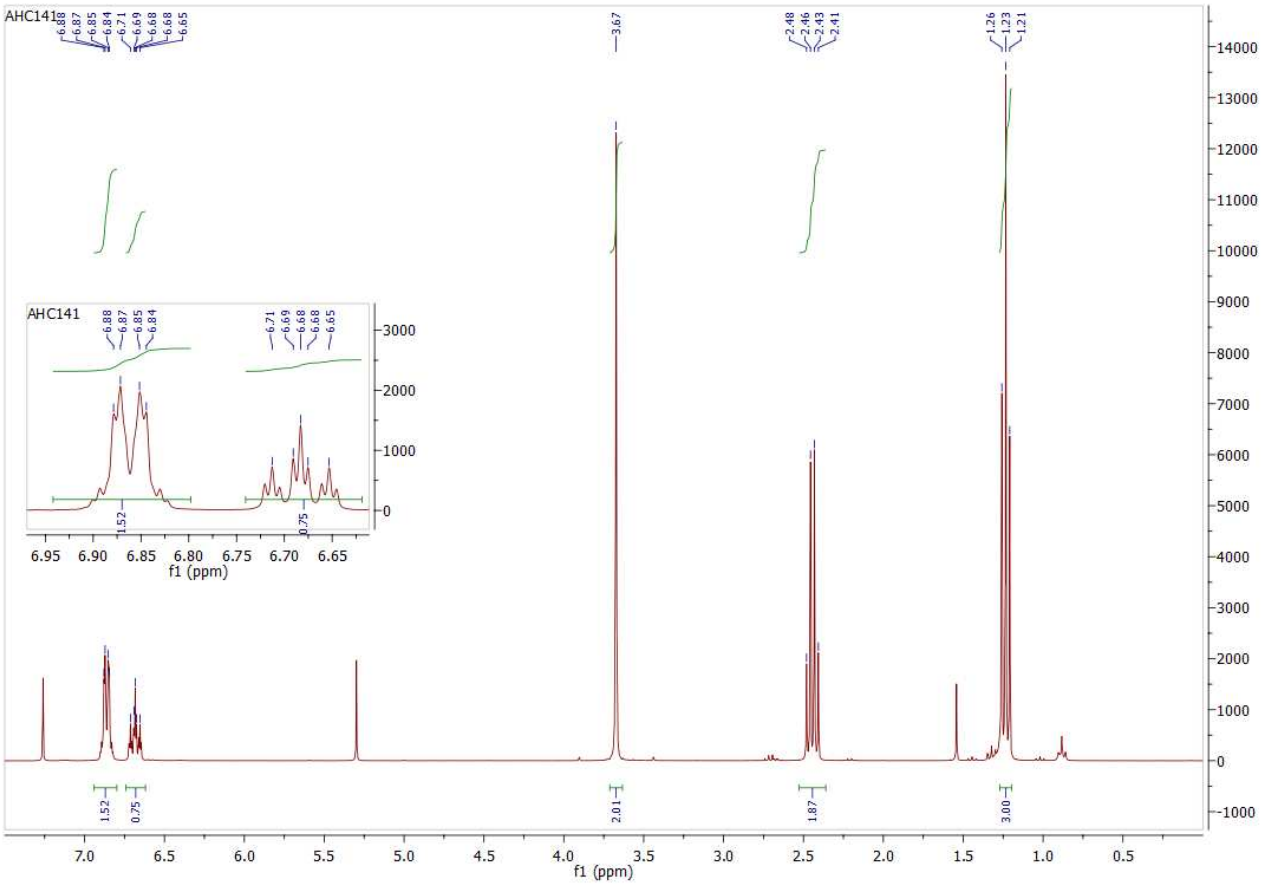

- **α-Chloro Ethyl Benzyl sulfide[3] (43):**

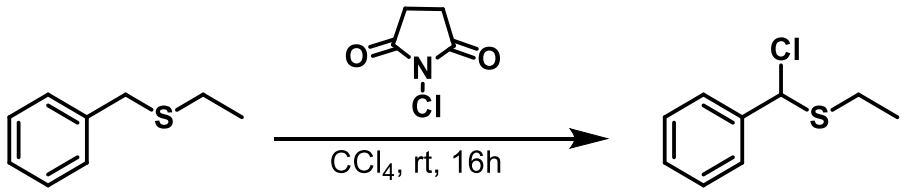

The previously obtained ethylbenzyl sulfide was dissolved in carbon tetrachloride (2mL/mmol) and cooled to 4°C. N-Chlorosuccinimide (1eq) was dissolved in carbon tetrachloride (2mL/mmol) and added dropwise to the sulfide solution. The reaction was stirred at 4°C overnight (TLC conditions: 95/5 Hex/EtOAc). The reaction mixture was filtered to remove the insoluble. The solvent was removed under reduced pressure to afford the crude product as a yellow oil.

Purification by column chromatography was attempted by using a 95/5 n-Hexane/EtOAc mixture as eluent but was unsuccessful, leading to degradation of the material.

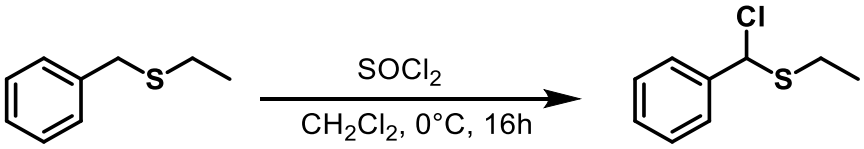

The previously obtained ethylbenzyl sulfide was dissolved in dichloromethane (2mL/mmol) and cooled to 0°C. Thionyl chloride (1eq) was dissolved in carbon tetrachloride (2mL/mmol) and added dropwise to the sulfide solution. The reaction was stirred at 0°C overnight (TLC conditions: 95/5 Hex/EtOAc). TLC indicates no reaction has taken place.

[3] D.L. Tuleen, T. Stephens, *J. Org. Chem.*, **1969**, *Vol. 34 (No.1)*, p 31-35

- **Ethyl Phenyl sulfide[4] (45):**

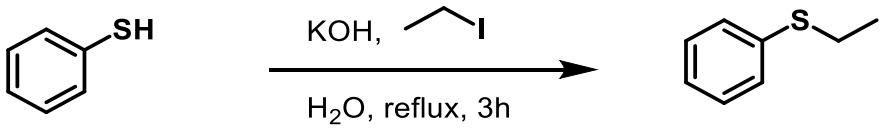

A round bottom flask was charged with thiophenol (20mmol) and a solution of KOH (30mmol, 1.5eq) in water (1.3mL/mmol) was slowly added. After stirring at room temperature for 10 minutes, ethyl iodide (22mmol, 1.1eq) was added to the reaction mixture and stirred at room temperature for 1h and refluxed for 3h.

Added Ethyl Acetate to the reaction mixture, separated the two layers, washed the organic layer with water (3x15mL) and brine (2x10mL). The combined organic layers were dried over $MgSO_4$ and concentrated *in vacuo* to afford the crude product as a pale yellow liquid. The crude NMR indicated the presence of the desired product as well as some leftover alkane halide.

The product was purified by column chromatography using hexane as the eluent.

η=96%

^{1}H NMR (300 MHz, $CDCl_3$) δ 7.42 – 7.25 (m, 4H), 7.25 – 7.14 (m, 1H), 2.97 (q, *J* = 7.4 Hz, 2H), 1.34 (t, *J* = 7.4 Hz, 3H)

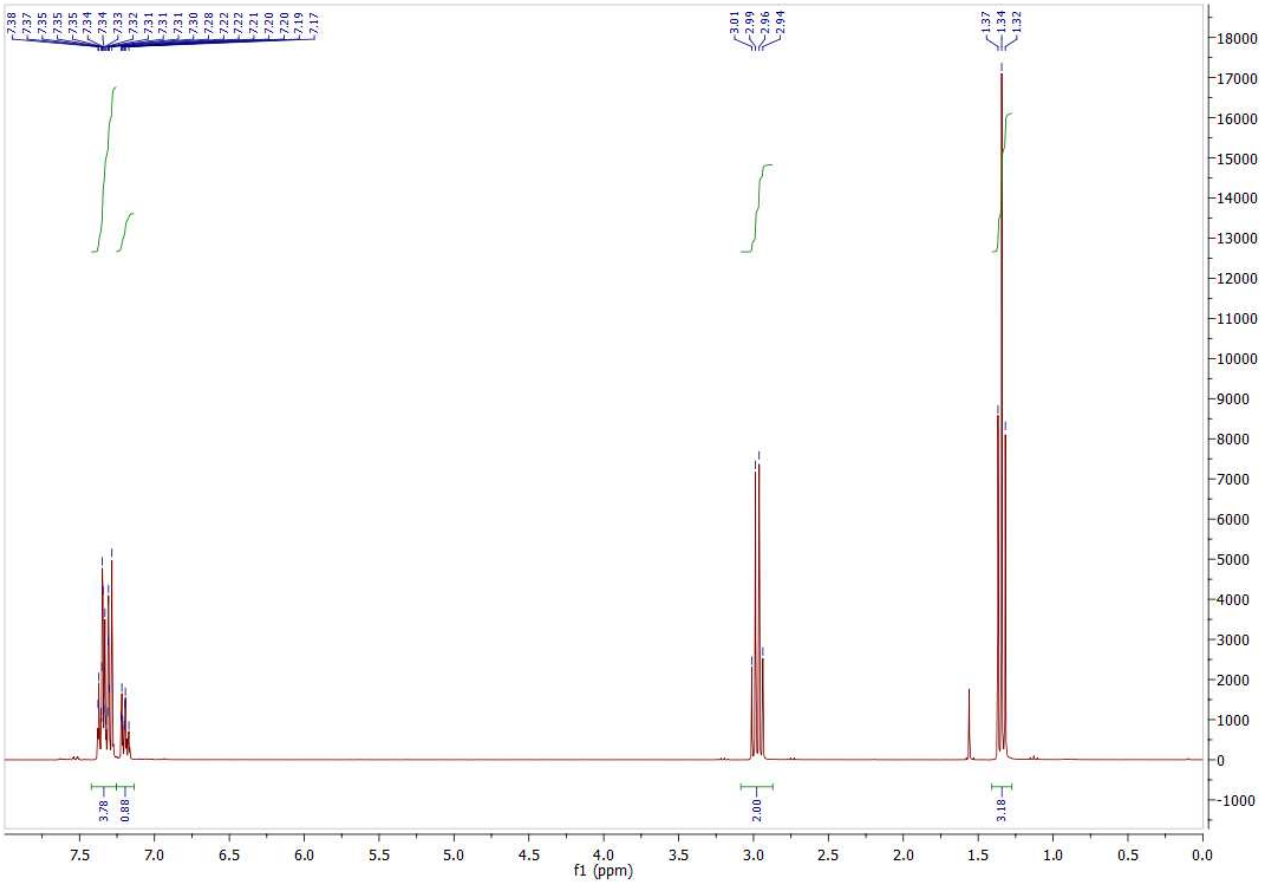

[4] D. Antoniak, M. Barbasiewicz, *Org. Lett.*, **2019**, *21 (23)*, 9320-9325

- **α-Chloro Methyl Phenyl sulfide :**

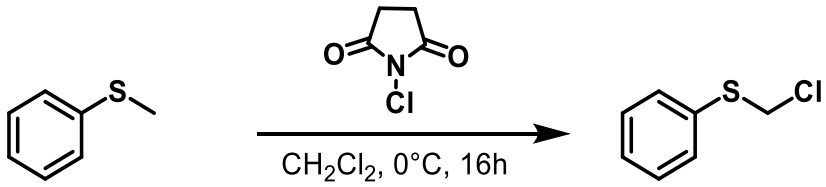

Thioanisole (7.668mmol) was dissolved in CH_2Cl_2 (2mL/mmol) and cooled in an ice bath. Finely powdered NCS (7.668mmol, 1eq) was added carefully and the reaction was left to stir overnight at 0°C. (During the night, the reaction shifts color to fluorescent yellow).
The insoluble were filtered off and the solvent was evaporated to afford the crude product as a yellow liquid. The crude NMR indicates that the desired product has formed however some impurities are still present.
The desired compound could not be isolated by column chromatography (possible degradation of the product on silica)

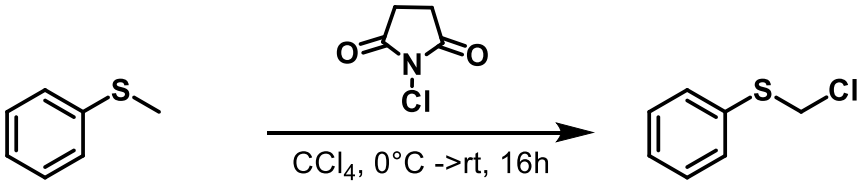

Thioanisole (42.271mmol) was dissolved in CCl_4 (0.5mL/mmol) and cooled in an ice bath. Finely powdered NCS (42.271mmol, 1eq) was added carefully and the reaction was left to stir overnight while letting the temperature rise back to ambient. (During the night, the reaction shifts color to yellow).
The insolubles were filtered off and the solvent was evaporated to obtain the pure product as a yellow liquid.

η=91.8%

^{1}H NMR (300 MHz, $CDCl_3$) δ 7.60 – 7.47 (m, 2H), 7.42 – 7.31 (m, 3H), 4.98 (s, 2H).

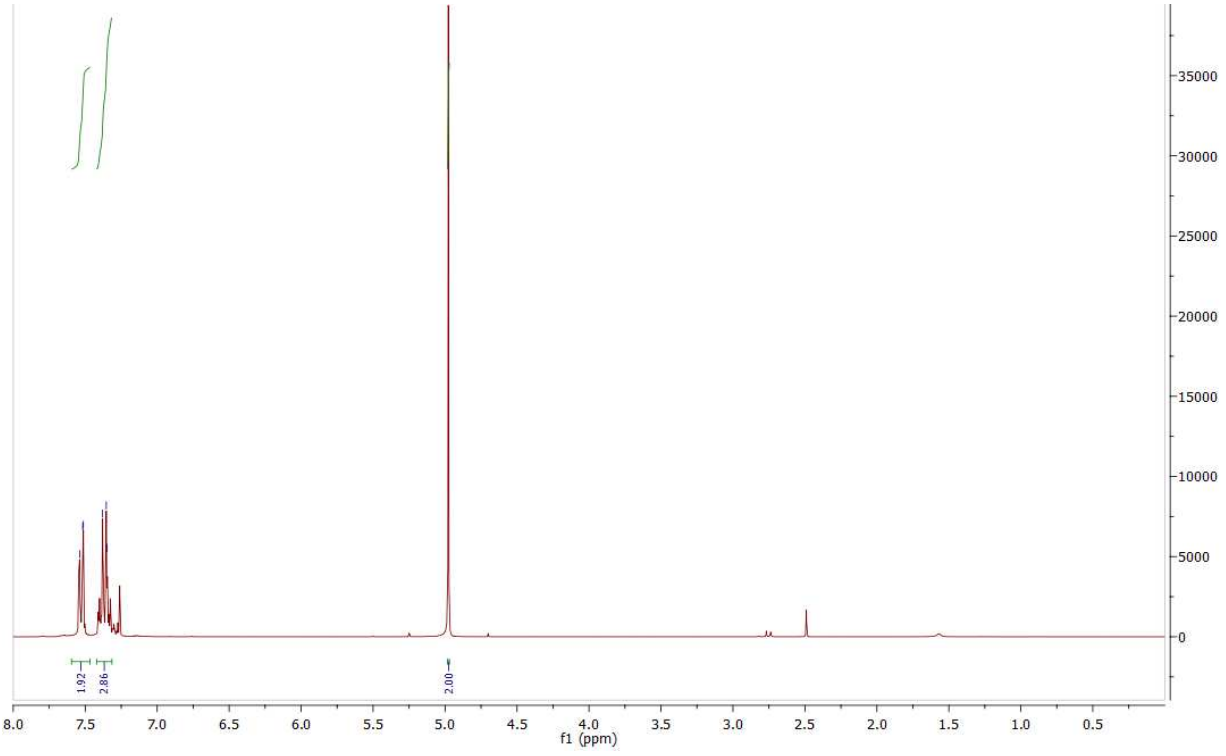

- **α-Chloro Ethyl Phenyl sulfide (46):**

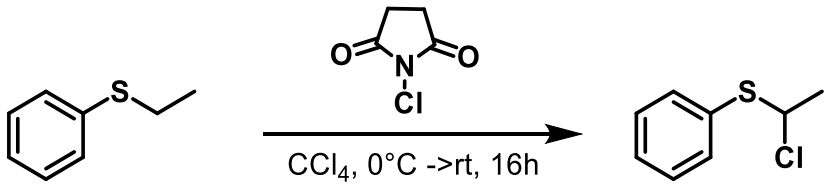

The previously obtained sulfide (19.2mmol) was dissolved in CCl_4 (1mL/mmol) and cooled in an ice bath. Finely powdered NCS (19.2mmol, 1eq) was added carefully and the reaction was left to stir overnight while letting the temperature rise back to ambient. (During the night, the reaction shifts color to yellow).

The insoluble were filtered off and the solvent was evaporated to obtain the product as a yellow liquid.

η=80%

^{1}H NMR (300 MHz, $CDCl_3$) δ 7.59 – 7.52 (m, 1H), 7.43 – 7.33 (m, 2H), 5.42 (q, *J* = 6.7 Hz, 1H), 1.89 (d, *J* = 6.7 Hz, 3H).

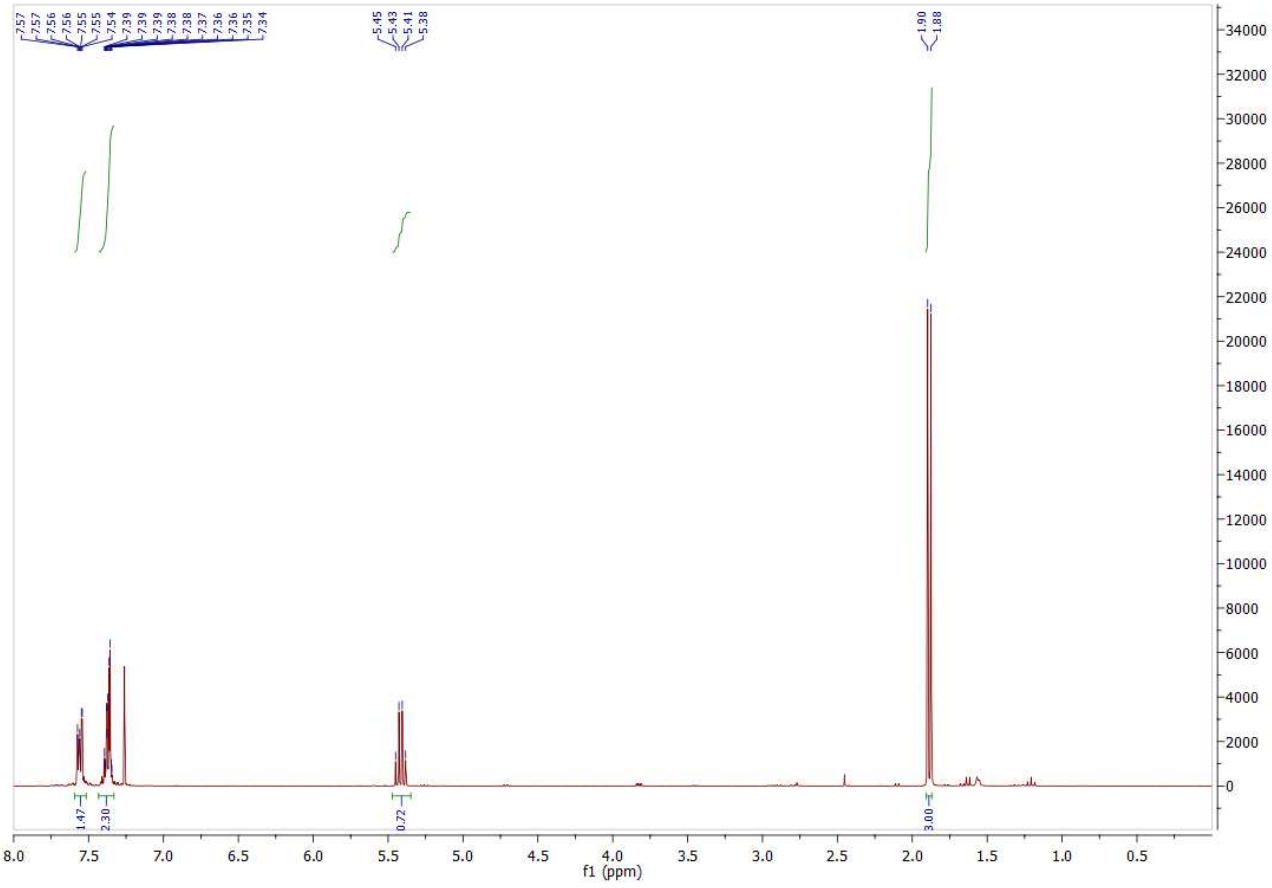

- **2-chloro-1,2-diphenylethyl(methyl)sulfide[5] (61):**

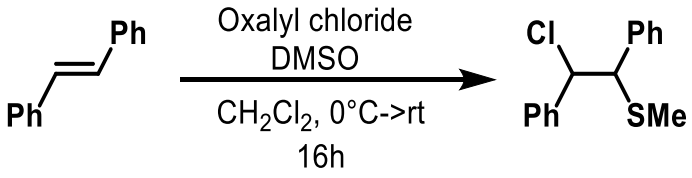

In a two-necked round bottom flask equipped with a condenser and a dropping funnel, dissolved DMSO (1.7mL, 24mmol, 2.4eq) in DCM (10mL). The resulting mixture was cooled to 0°C before a solution of oxalyl chloride (1mL, 12mmol, 1.2eq) in DCM (10mL) was added dropwise. After 10min at 0°C, *trans*-stilbene (1.802g, 10mmol) was added and the reaction mixture was allowed to warm to room temperature. The reaction was left to stir overnight at room temperature.

Triethylamine (7mL, 50mmol, 5eq) was added and the reaction was stirred for an additional 10min before it was successively washed with aqueous NH_4Cl (30mL) and brine (2x30mL). The combined organic layers were dried over $MgSO_4$ and concentrated under reduced pressure to afford the crude product as a yellow solid.

NMR analysis of the crude material shows 10% conversion of stilbene to the desired product.

- **1-Chloro-2-(methylthio)cyclopentane[5] (63):**

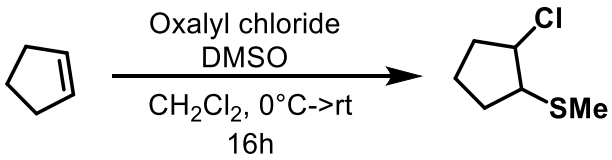

In a two-necked round bottom flask equipped with a condenser and a dropping funnel, dissolved DMSO (1.7mL, 24mmol, 2.4eq) in DCM (10mL). The resulting mixture was cooled to 0°C before a solution of oxalyl chloride (1mL, 12mmol, 1.2eq) in DCM (10mL) was added dropwise. After 10min at 0°C, cyclopentene (681.1mg, 10mmol) was added and the reaction mixture was allowed to warm to room temperature. The reaction was left to stir overnight at room temperature.

Triethylamine (7mL, 50mmol, 5eq) was added and the reaction was stirred for an additional 10min before it was successively washed with aqueous NH_4Cl (30mL) and brine (2x30mL). The combined organic layers were dried over $MgSO_4$ and concentrated under reduced pressure to afford the crude product as a yellow solid.

NMR analysis of the crude material shows 8% conversion of cyclopentene to the desired product.

[5] L. Lan, Y. Gao, T. Zhang, Y. Liu, B. Sun, H. Tian, *Synth. Commun.*, **2019**, *Vol 49 (4)*, 539-549

- **2-chloro-1,2-diphenylethyl(ethyl)sulfide (alternative pathway)[6]:**

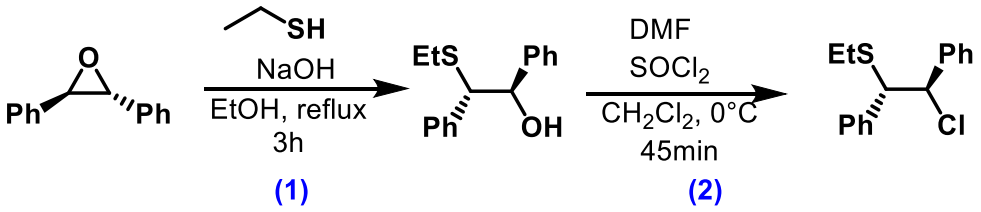

***rac*-(*S*,R**) 2-hydroxy-1,2-diphenylethyl(ethyl)sulfide (65)**

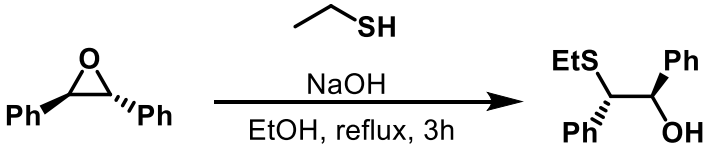

Trans-Stilbene oxide (10.191mmol) was dissolved in EtOH (10mL/mmol). Sodium hydroxide (10.191mmol, 1eq) and Ethanethiol (10.191mmol, 1eq) were added and the reaction was refluxed for 3h.
The solvent was removed under reduced pressure. Et_2O (50mL) and H_2O (40ml) were added to the residue before the layers were separated. The aqueous layer was washed with Et_2O (3x10mL) and the combined organic layers were dried over $MgSO_4$ and concentrated under reduced pressure to afford the crude product as a brown oil with some precipitate.

The crude material was purified by column chromatography using a Hexane/Et_2O 90:10 ➡ 80:20

The purified product was obtained as a colourless solid.

r=68.7%

^{1}H NMR (300 MHz, $CDCl_3$) δ 7.35 – 7.27 (m, 8H), 4.97 (dd, *J* = 7.0, 3.1 Hz, 1H), 4.09 (d, *J* = 7.0 Hz, 1H), 2.23 (q, *J* = 7.4 Hz, 2H), 1.09 (t, *J* = 7.4 Hz, 3H)

[6] G. Pupo, F. Ibba, D. M. H. Ascough, A. C. Vicini, P. Ricci, K. E. Christensen, L. Pfeifer, J. R. Morphy, J. M. Brown, R. S. Paton, V. Gouverneur, *Science*, **2018**, *360*, 638-642

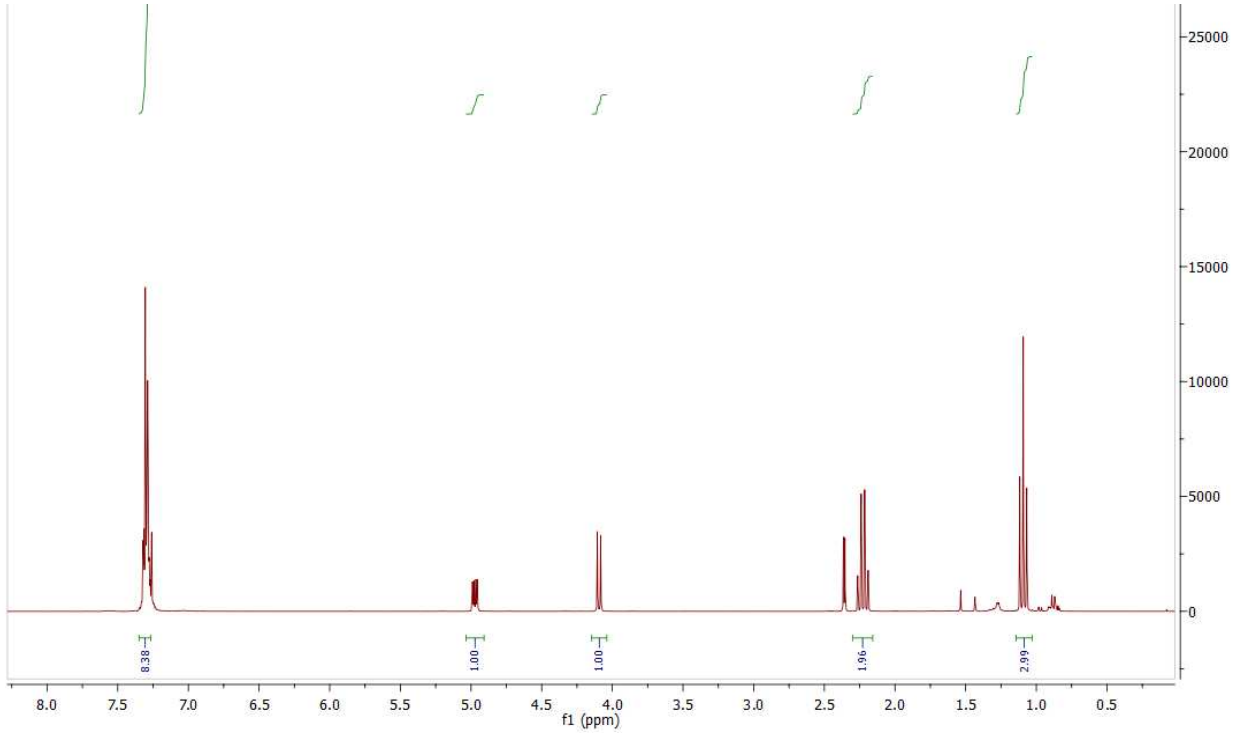

***rac*-(*S*,R**) 2chloro-1,2-diphenylethyl(ethyl)sulfide (66)**

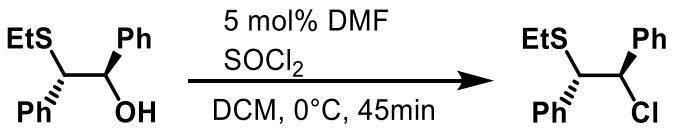

Dissolved the previously synthesised alcohol (7.003mmol) in dry dichloromethane (5mL/mmol). Degassed the flask and flushed it with argon and cooled the mixture to 0°C. Added DMF (0.35mmol, 0.05eq) and thionyl chloride (10.505mmol, 1.5eq) under inert atmosphere. The reaction was stirred at 0°C for 45min.

The volatiles were removed under reduced pressure to afford the product as a pale green solid.

r=92%

^{1}H NMR (300 MHz, $CDCl_3$) δ 7.47 (ddd, *J* = 7.1, 3.8, 2.5 Hz, 2H), 7.44 – 7.31 (m, 8H), 5.18 (d, *J* = 9.8 Hz, 1H), 4.36 (d, *J* = 9.8 Hz, 1H), 2.07 (q, *J* = 7.4 Hz, 2H), 1.03 (t, *J* = 7.4 Hz, 3H)

^{13}C NMR (75 MHz, $CDCl_3$) δ 139.79, 139.62, 128.89, 128.80, 128.62, 128.56, 128.55, 128.06, 127.85, 126.63, 66.59, 56.85, 26.36, 14.29.

HRMS: m/z calculated for $C_{16}H_{17}S$ $[M\text{-}Cl]^+$ 241.1051, found 241.1092

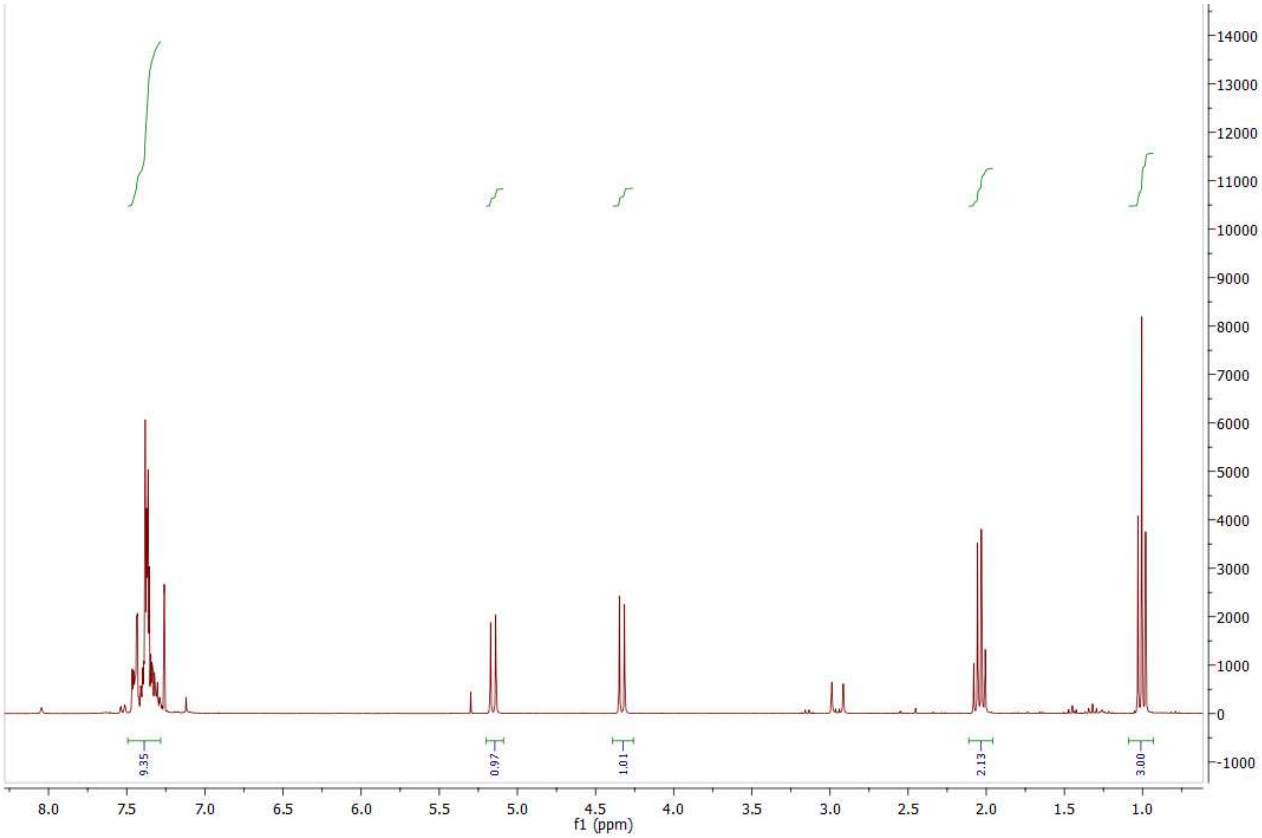
14000
13000
12000
11000
10000
9000
8000
7000
6000
5000
4000
3000
2000
1000
0
-1000
9.35
0.97
1.01
2.13
3.00
8.0
7.5
7.0
6.5
6.0
5.5
5.0
4.5
4.0
3.5
3.0
2.5
2.0
1.5
1.0
f1 (ppm)

- **(*S*,S**) 2-chloro-1,2-diphenylethyl(methyl)sulfide :**

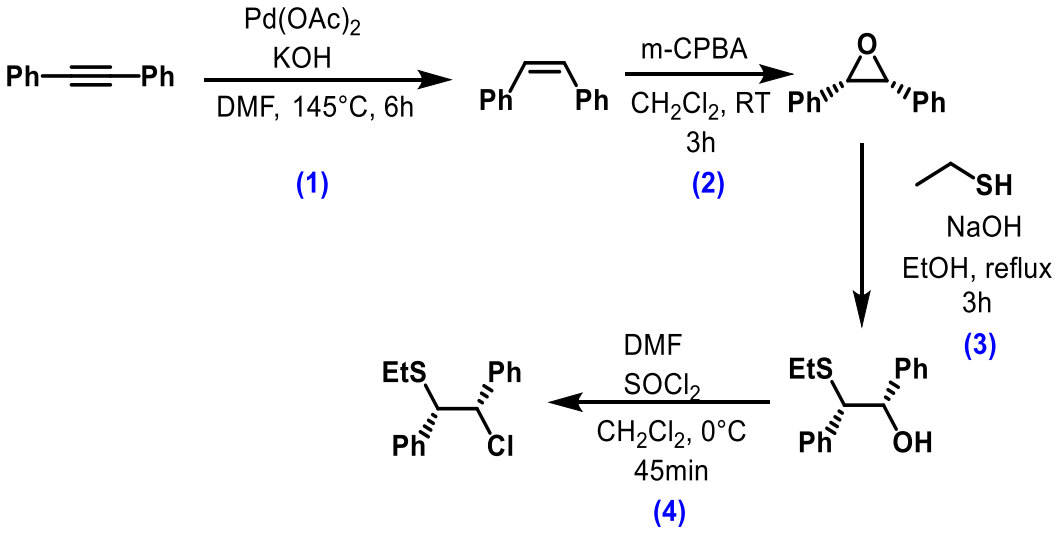

Cis-stilbene (90)[7]:

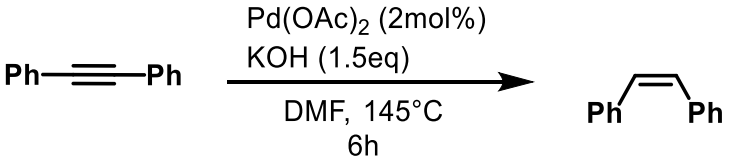

A thick-walled sealable tube was charged with diphenylacetylene (11.221mmol), KOH (16.831mmol, 1.5eq) and $Pd(OAc)_2$ (0.224mmol, 0.02eq). DMF (2mL/mmol) was added and the medium was flushed with Argon. The tube was sealed and the mixture was stirred at 145°C for 6h.

The mixture was cooled to room temperature and EtOAc was added. The reaction mixture was filtered over a celite pad. The filtrate was washed with water (3X30ml) and brine (30mL). The combined organic layers were dried over $MgSO_4$ and concentrated under reduced pressure. The crude product was obtained as an orange oil and was used without further purification as no separation conditions could be found. ^1H NMR data indicates a 97:3 ratio of Cis/Trans Stilbene isomers.

η= 67.5%

[7] J. Li, R. Hua, T. Liu, *J. Org. Chem.*, **2010**, *75(9)*, 2966-2970

Cis-stilbene oxide (91)[8]:

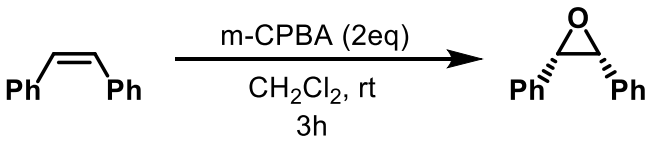

The previously synthesized cis-stilbene (5.610mmol) was dissolved in DCM (5mL/mmol) and m-CPBA (11.220mmol, 2eq) was added to the mixture. The reaction was stirred for 3h at room temperature. After 3h, the mixture was transferred to a separtin funnel and washed with a saturated Na_2CO_3 solution (25mL). The aqueous layer was extracted with DCM (2x20mL) and the combined organic layers were dried over $MgSO_4$ and concentrated *in vacuo* to afford the crude product as an orange oil.

Syn isomer: **^{1}H NMR (300 MHz, $CDCl_3$)** 7.20 – 7.10 (s, 9H), 4.37 (s, 2H)

Anti isomer: **^{1}H NMR (300 MHz, $CDCl_3$)** δ 7.45 – 7.29 (m, 10H), 3.87 (S, 2H)

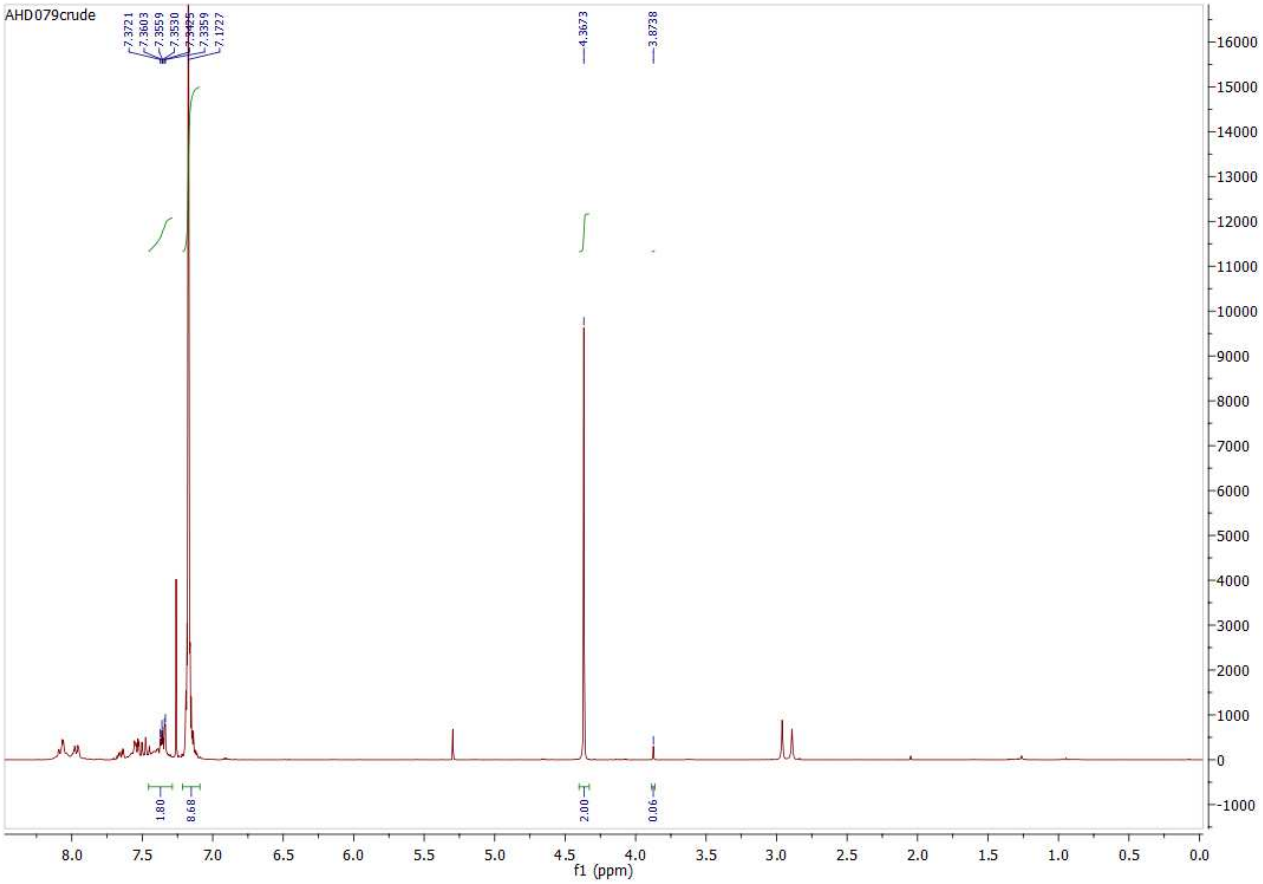

[8] T. Mori, Y. Takeuchi, M. Hojo, *Tet. Lett.* , **2020***, 61(8)*, 151518

(*S*,S) 2-hydroxy-1,2-diphenylethyl(ethyl)sulfide (92):**

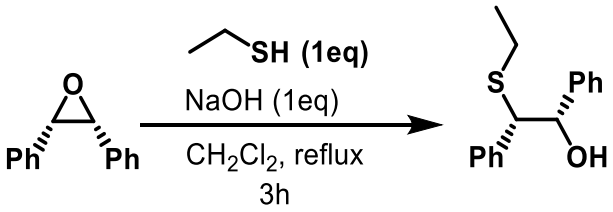

Dissolved cis-stilbene oxide (18.544mmol) in EtOH (1mL/mmol). Added NaOH (18.544mmol, 1eq) and ethanethiol (18.544mmol, 1eq) and stirred at reflux for 3h.

The mixture was cooled to room temperature and the solvent was evaporated. Water (50mL) and Et_2O (50mL) were added and the layers were separated. The aqueous layer was extracted with Et_2O (2x30mL) and the combined organic layers were dried over $MgSO_4$ and concentrated under reduced pressure to afford the crude product as an orange oil.

The crude product was purified by column chromatography using Hexane/Et_2O (90:10) as eluent.

(S,S*)/(S*,R*)* ratio: 10:1

η= 64.3%

(S,S*)* isomer: **^{1}H NMR (300 MHz, $CDCl_3$)** δ 7.23 – 7.06 (m, 9H), 4.84 (dd, *J* = 8.6, 2.5 Hz, 1H), 4.01 (d, *J* = 8.6 Hz, 1H), 2.45 (qd, *J* = 7.4, 1.2 Hz, 2H), 1.19 (t, *J* = 7.4 Hz, 3H).

(S,R*)* isomer: **^{1}H NMR (300 MHz, $CDCl_3$)** δ 7.37 – 7.24 (m, 1H), 4.97 (dd, *J* = 7.0, 3.1 Hz, 1H), 4.09 (d, *J* = 7.0 Hz, 1H), 2.23 (q, *J* = 7.4 Hz, 1H), 1.09 (t, *J* = 7.4 Hz, 1H)

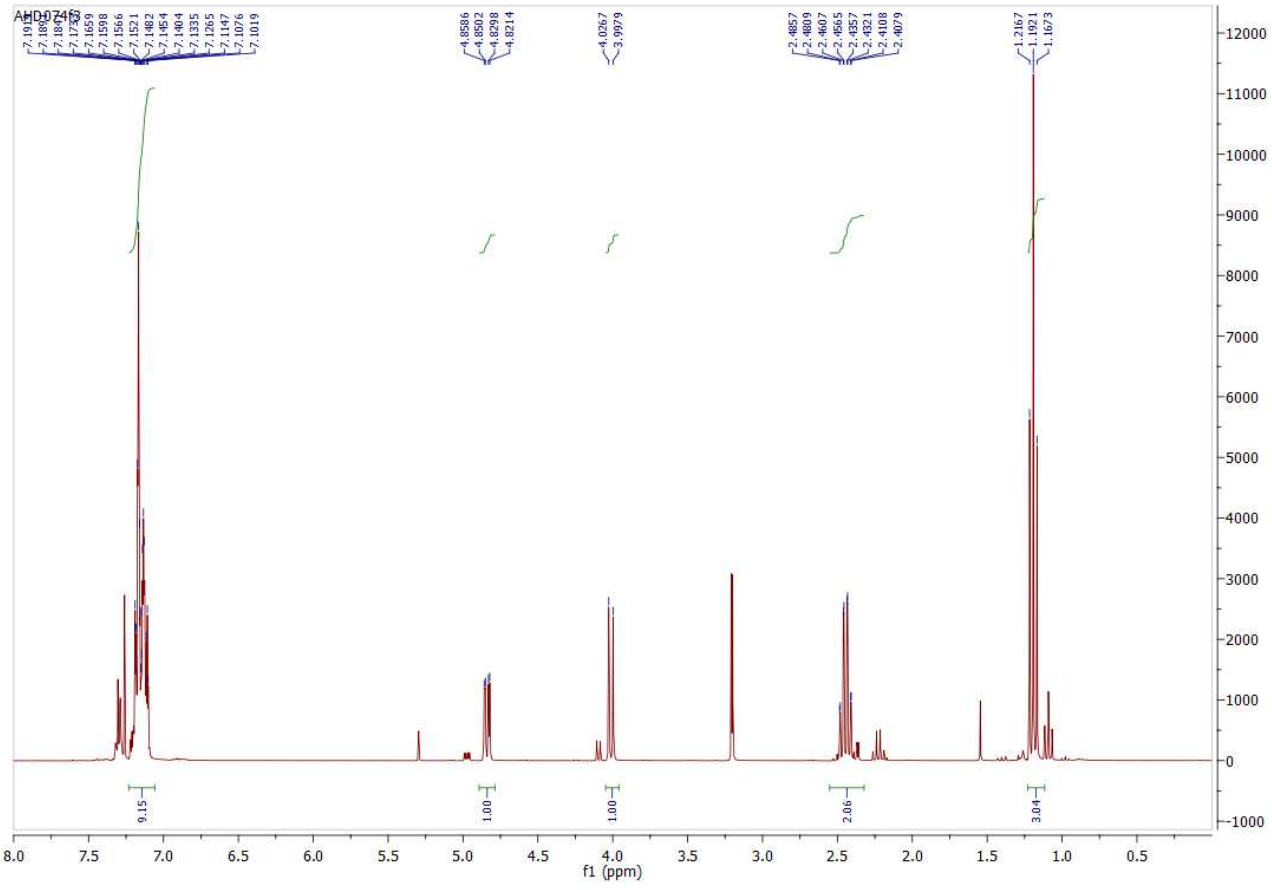

(*S*,S) 2chloro-1,2-diphenylethyl(ethyl)sulfide:**

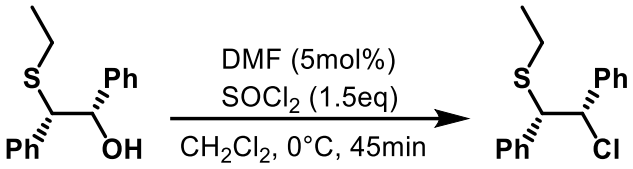

The previously synthesized alcohol (11.927mmol) was dissolved in DCM (2mL/mmol) and cooled to 0°C. Dry DMF (0.596mmol, 0.05eq) and $SOCl_2$ (17.891mmol, 1.5eq) were successively added and the reaction was stirred for 45min at 0°C.

The volatiles were removed under vacuum and the crude product was obtained as an orange oil, becoming a yellow solid after being cooled.

η=71%

Syn isomer: **^{1}H NMR (300 MHz, $CDCl_3$)** δ 7.23 – 7.08 (m, 9H), 5.19 (d, *J* = 8.3 Hz, 1H), 4.41 (d, *J* = 8.3 Hz, 1H), 2.45 – 2.24 (m, 2H), 1.16 (t, *J* = 7.4 Hz, 3H).

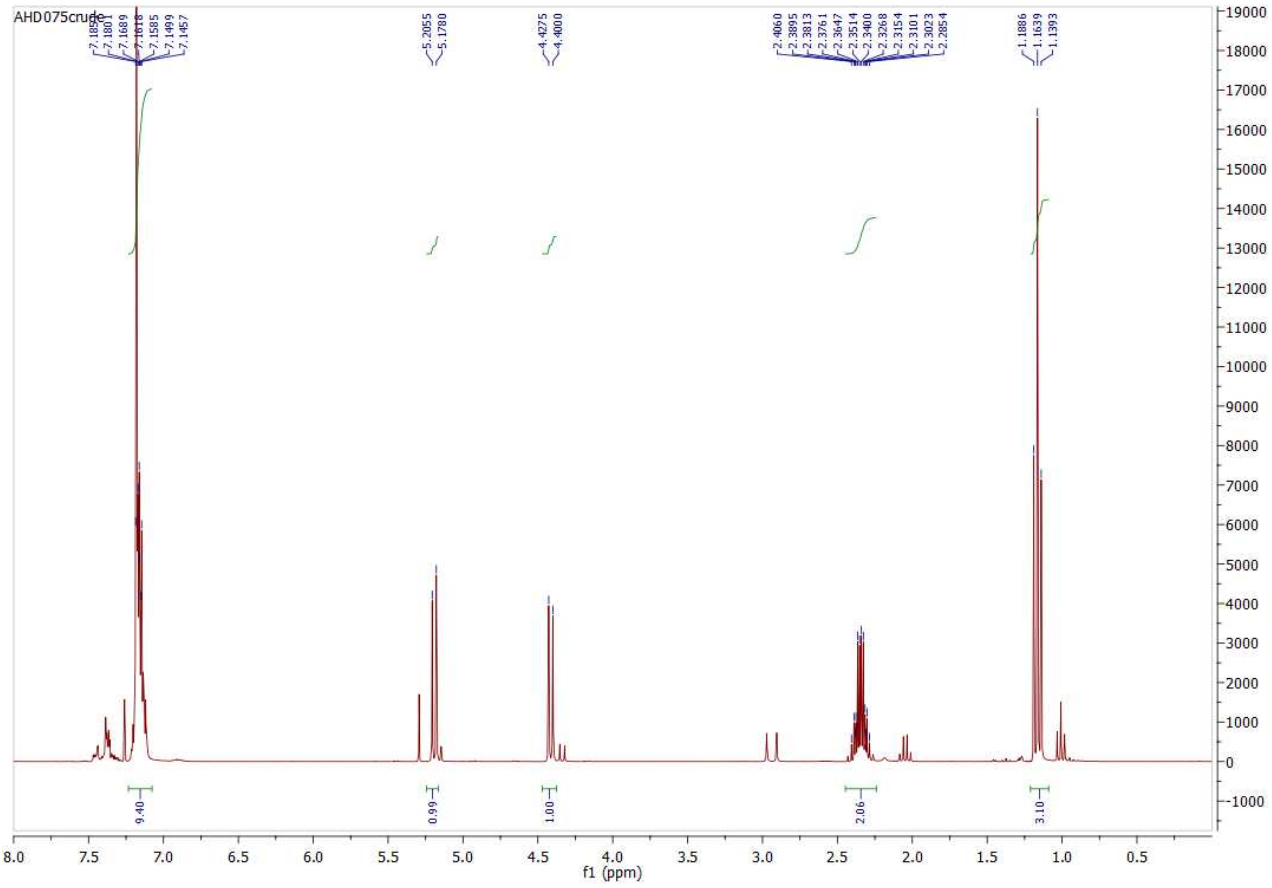

(*S*,S) 2chloro-1,2-diphenylethyl(ethylphenyl)sulfide (93):**

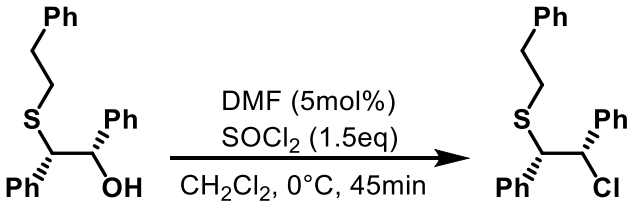

The previously synthesized alcohol (3.477mmol) was dissolved in DCM (2mL/mmol) and cooled to 0°C. Dry DMF (0.174mmol, 0.05eq) and $SOCl_2$ (5.215mmol, 1.5eq) were successively added and the reaction was stirred for 45min at 0°C.

The volatiles were removed under vacuum and the crude product was obtained as an orange oil, becoming a yellow solid after being cooled.

η=100%

^{1}H NMR (300 MHz, $CDCl_3$) δ 7.32 – 6.97 (m, 14H), 5.15 (d, *J* = 8.4 Hz, 1H), 4.36 (d, *J* = 8.4 Hz, 1H), 2.87 – 2.68 (m, 2H), 2.62 – 2.50 (m, 2H).

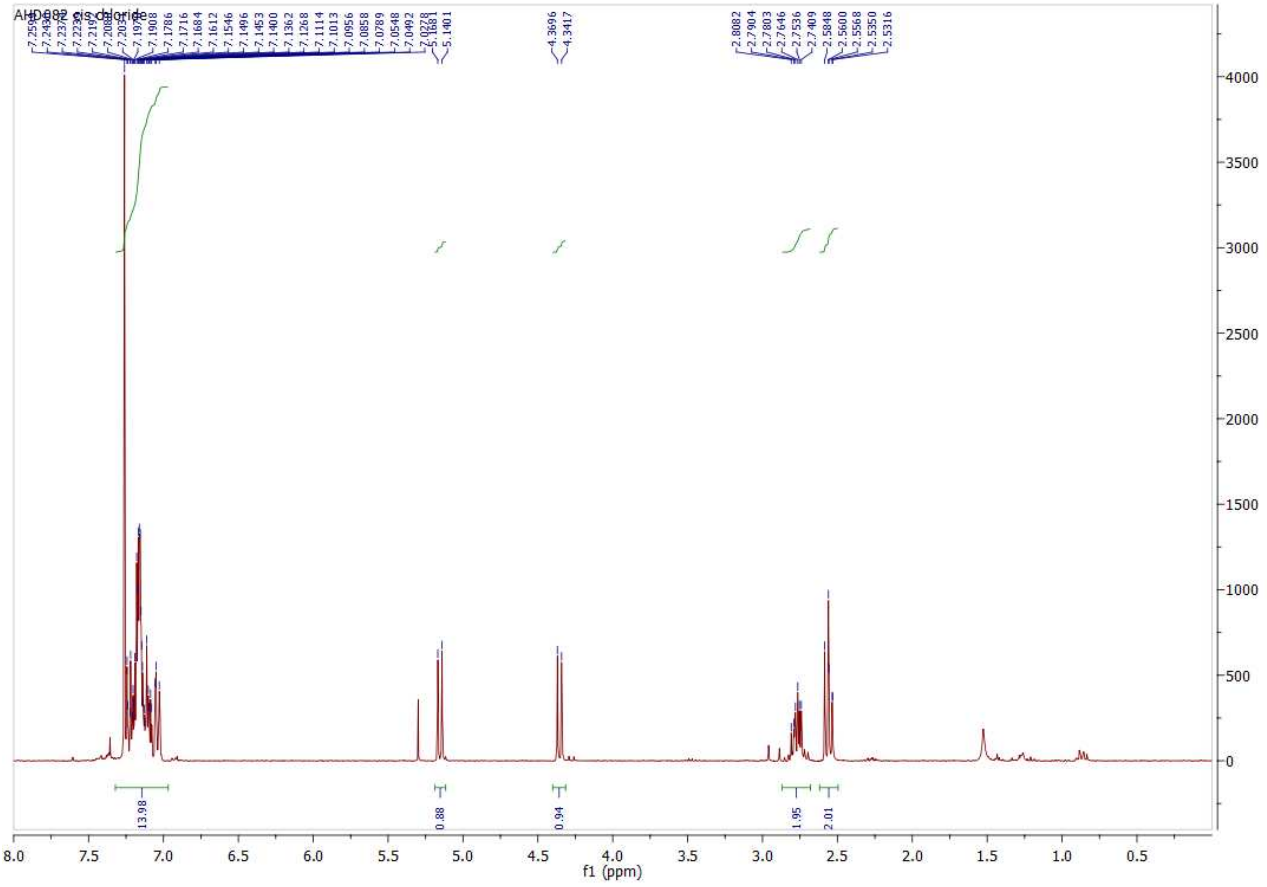

(*S*,R) 2chloro-1,2-diphenylethyl(ethylphenyl)sulfide (71):**

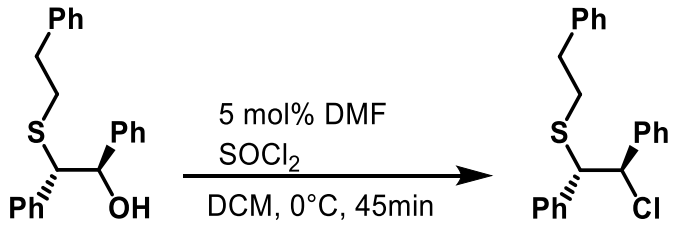

The previously synthesized alcohol (3.477mmol) was dissolved in DCM (2mL/mmol) and cooled to 0°C. Dry DMF (0.174mmol, 0.05eq) and $SOCl_2$ (5.215mmol, 1.5eq) were successively added and the reaction was stirred for 45min at 0°C.

The volatiles were removed under vacuum and the crude product was obtained as an orange oil, becoming a yellow solid after being cooled.

η=100%

^{1}H NMR (300 MHz, $CDCl_3$) δ 7.47 – 7.28 (m, 10H), 7.25 – 7.13 (m, 3H), 6.93 (dd, *J* = 7.8, 1.6 Hz, 2H), 5.13 (d, *J* = 9.8 Hz, 1H), 4.28 (d, *J* = 9.8 Hz, 1H), 2.69 – 2.49 (m, 2H), 2.33 – 2.17 (m, 2H).

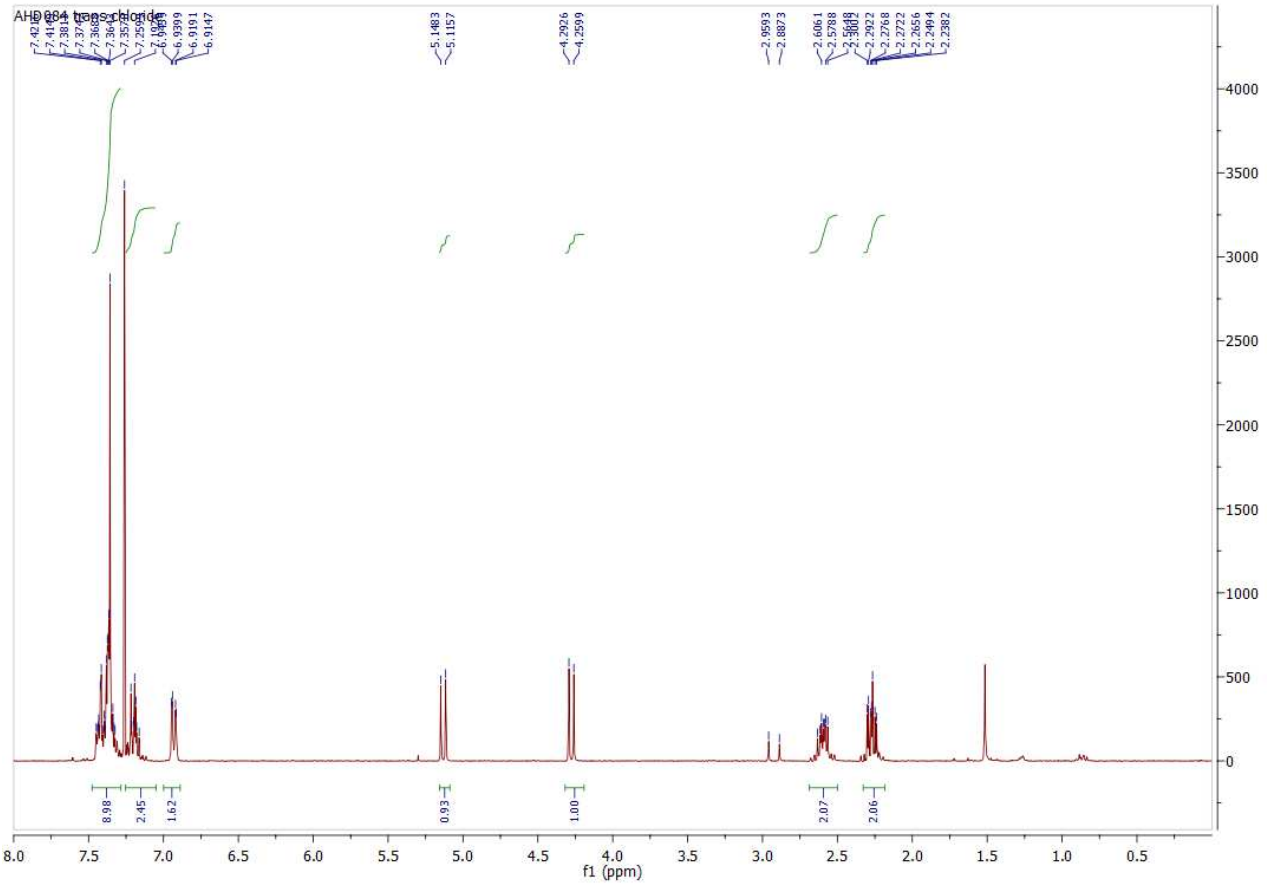

(R*,R*)2-(benzylthio)cyclohexan-1-ol (68):

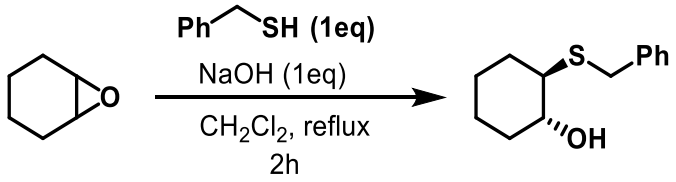

Cyclohexene oxide (5.095 mmol) was dissolved in EtOH (2mL/mmol). Sodium hydroxide (5.095mmol, 1eq) and benzyl thiol (5.095mmol, 1eq) were subsequently added to and the reaction mixture was stirred at reflux for 2 hours (TLC in Hexane/Et_2O, 90:10). The solvent was evaporated and a 1:2 mixture of water and Et_2O was added to the residue. The layers were separated, the aqueous layer was extracted with Et_2O (3x15mL) and the combined organic layers were dried over $MgSO_4$ and concentrated *in vacuo* to afford the crude product as a pale yellow oil.

The crude product was purified by column chromatography using a Hexane/Et_2O (85:15) system as eluent.

η=72%

^{1}H NMR (300 MHz, $CDCl_3$) δ 7.38 – 7.21 (m, 4H), 3.79 (dd, *J*= 12.9, 2.8 Hz, 2H), 3.43 – 3.21 (m, 1H), 2.69 (s, 1H), 2.55 – 2.29 (m, 1H), 2.14 – 1.92 (m, 2H), 1.84 – 1.61 (m, 2H), 1.56 – 1.08 (m, 5H).

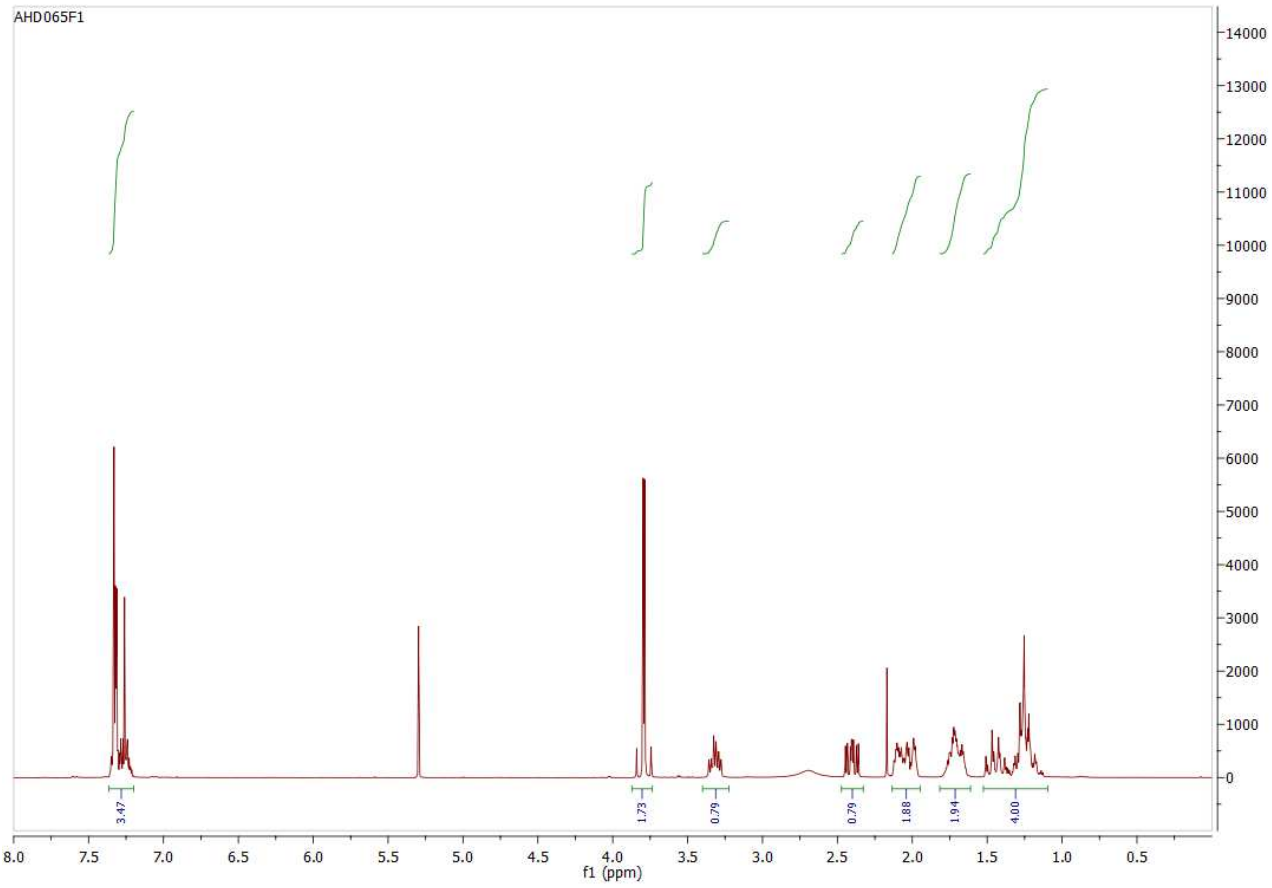

(R*,R*)benzyl(2-chlorocyclohexyl)sulfide (69):

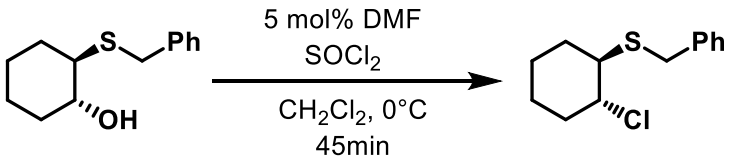

The previously synthesized alcohol (3.477mmol) was dissolved in DCM (2mL/mmol) and cooled to 0°C. Dry DMF (0.174mmol, 0.05eq) and $SOCl_2$ (5.215mmol, 1.5eq) were successively added and the reaction was stirred for 45min at 0°C.

The volatiles were removed under vacuum and the crude product was obtained as an orange oil, becoming a yellow solid after being cooled.

η=100%

^{1}H NMR (300 MHz, $CDCl_3$) δ 7.42 – 7.18 (m, 4H), 4.04 (td, *J* = 7.0, 3.7 Hz, 1H), 3.85 (dd, *J*=13.3, 1.68Hz, 2H), 2.81 (td, *J* = 7.1, 4.2 Hz, 1H), 2.38 – 2.04 (m, 2H), 1.84 – 1.27 (m, 7H).

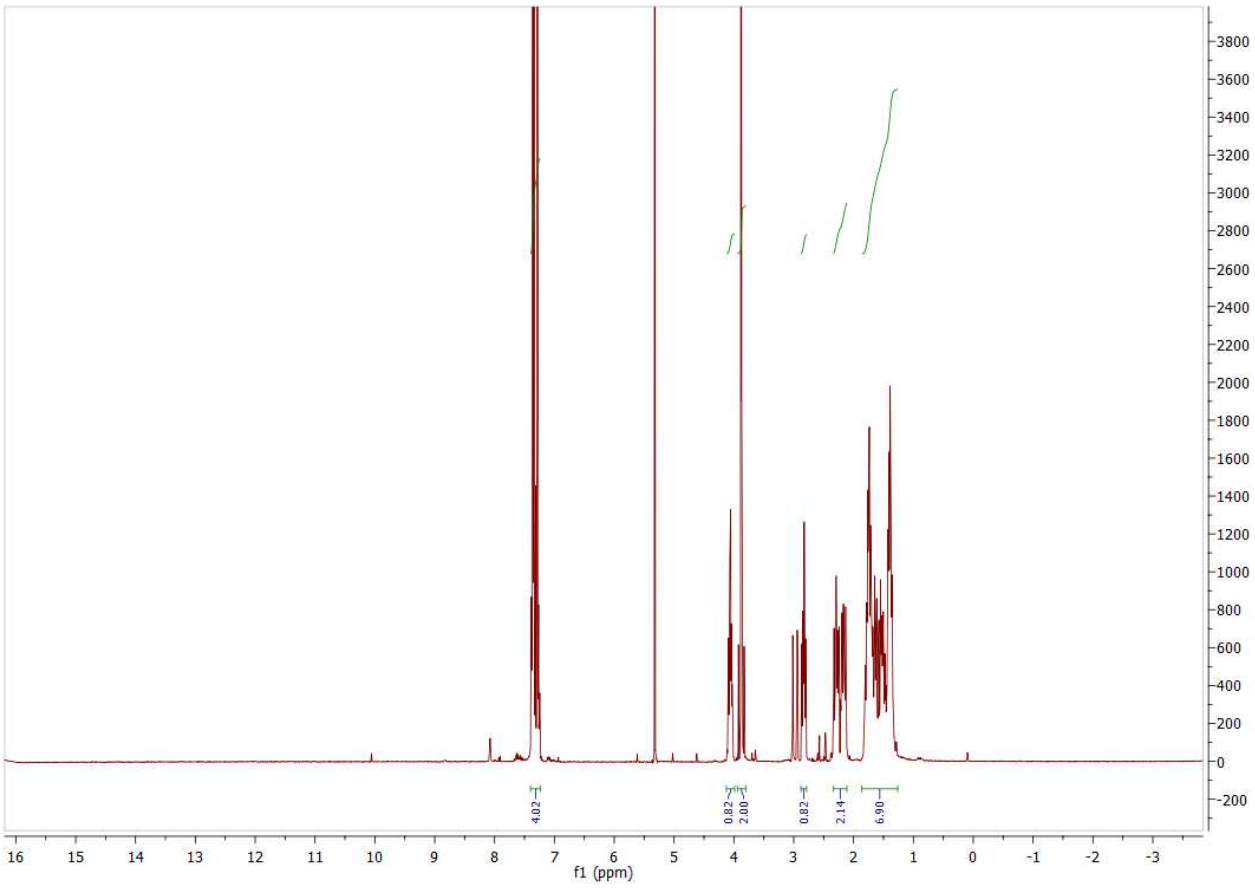

***rac*-(*S*,R**)-1,2-diphenyl-2-(pyridin-2-ylthio)ethan-1-ol**

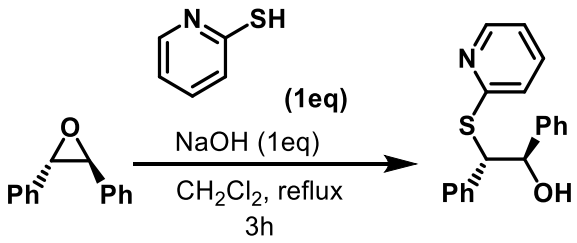

Trans-Stilbene oxide (10.191mmol) was dissolved in EtOH (10mL/mmol). Sodium hydroxide (10.191mmol, 1eq) and Ethanethiol (10.191mmol, 1eq) were added and the reaction was refluxed for 3h.
The solvent was removed under reduced pressure. Et_2O (50mL) and H_2O (40ml) were added to the residue before the layers were separated. The aqueous layer was washed with Et_2O (3x10mL) and the combined organic layers were dried over $MgSO_4$ and concentrated under reduced pressure to afford the crude product as a vivid orange oil.

The crude material was purified by column chromatography using a Hexane/Et_2O 90:10 ➔ 80:20

The purified product was obtained as a yellow oil.

η=36.9%

^{1}H NMR (300 MHz, $CDCl_3$) δ 8.48 (ddd, *J* = 5.0, 1.8, 0.9 Hz, 1H), 7.50 (ddd, *J* = 8.0, 7.4, 1.9 Hz, 1H), 7.30 – 7.10 (m, 9H), 7.10 – 7.01 (m, 3H), 5.34 (d, *J* = 4.0 Hz, 1H), 5.29 (d, *J* = 4.0 Hz, 1H).

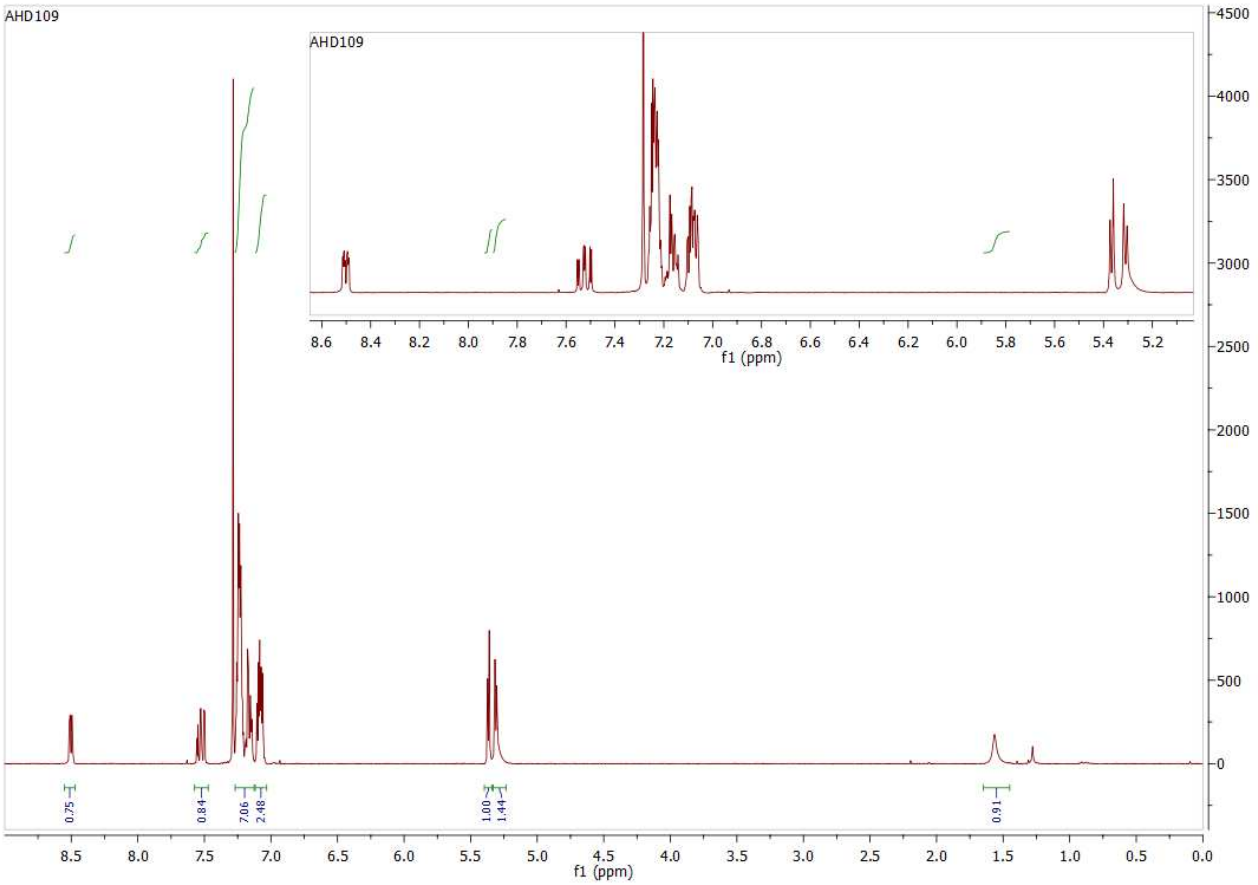

***rac*-(*S*,R**) 2-((-2-chloro-1,2-diphenylethyl)thio)pyridine**

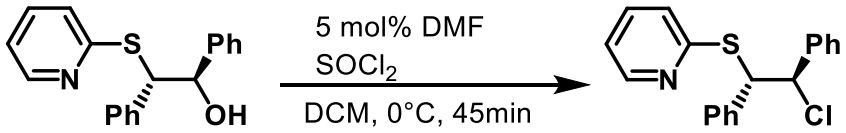

The previously synthesized alcohol (3.477mmol) was dissolved in DCM (2mL/mmol) and cooled to 0°C. Dry DMF (0.174mmol, 0.05eq) and $SOCl_2$ (5.215mmol, 1.5eq) were successively added and the reaction was stirred for 45min at 0°C.

The volatiles were removed under vacuum and the crude product was obtained as an orange foam, becoming a yellow solid after being cooled.

η=61.3%

^{1}H NMR (300 MHz, $CDCl_3$) δ 8.53 (dd, *J* = 5.7, 1.4 Hz, 1H), 7.83 (td, *J* = 7.9, 1.6 Hz, 1H), 7.60 – 7.30 (m, 9H), 7.26 – 7.11 (m, 3H), 6.49 (d, *J* = 9.4 Hz, 1H), 5.43 (d, *J* = 9.4 Hz, 1H).

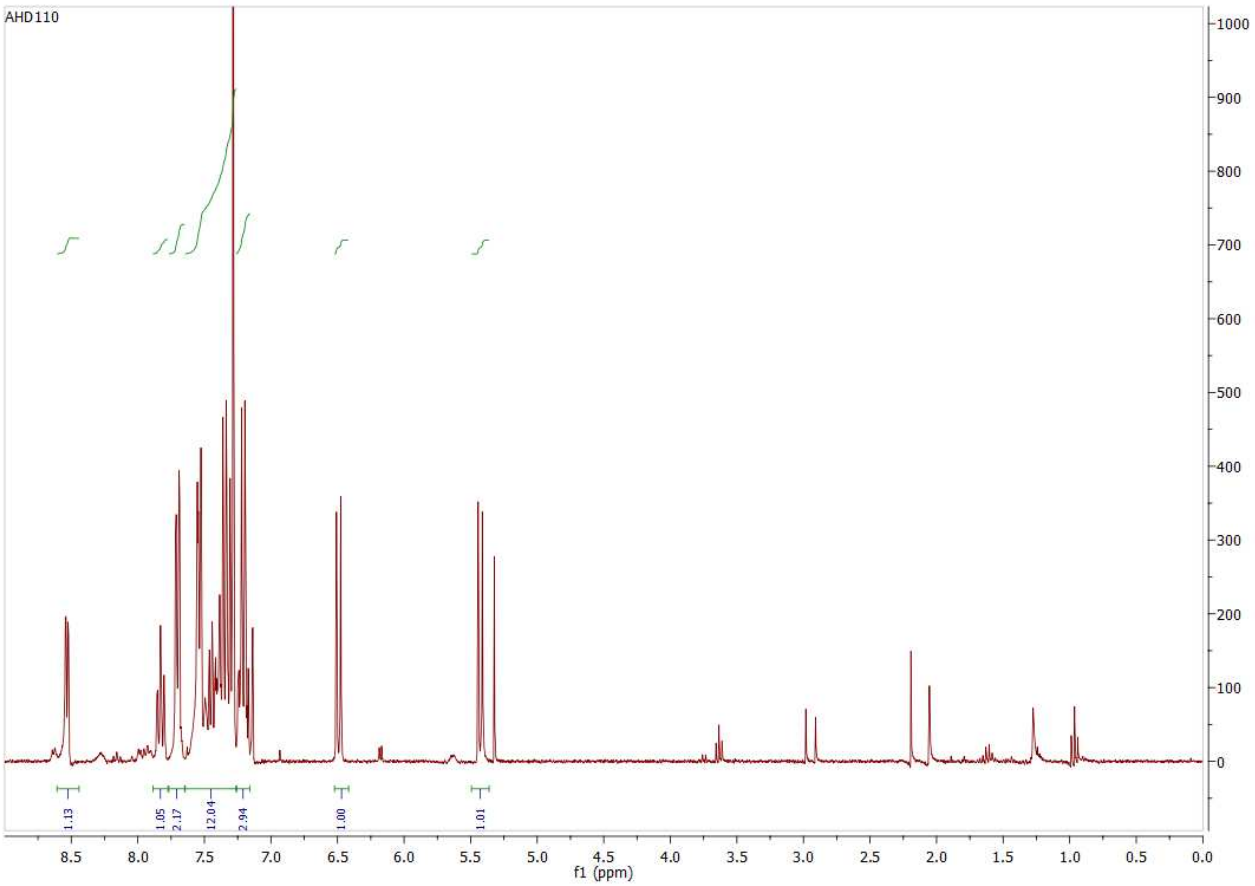

Catalytic test reaction:

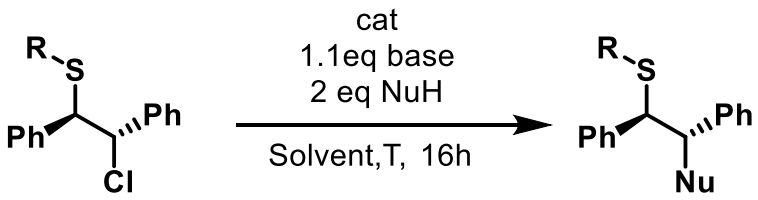

Reference conditions: The sulfenyl chloride (0.5mmol) was charged in a 5mL glass tube. Toluene (1mL/mmol) and the nucleophile (2 eq) were subsequently added. The reaction vessel was cooled to -10°C before the base was added and the reaction mixture was left to stir overnight.

The conversion was monitored by taking an aliquot from the mixture and NMR analysis.

The reaction mixture was washed with 1N HCl (2mL/mmol). The combined organic layers were dried over $MgSO_4$ and concentrated *in vacuo* to afford the crude product which was purified by column chromatography.

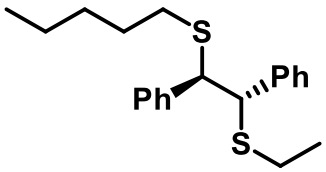

Ethyl((1S*,2R*)-2-(pentylthio)-1,2-diphenylethyl)sulfane

Purified by column chromatography using a Hexane/Et_2O (99:1) eluent system to afford a pale yellow oil.

^{1}H NMR (300 MHz, $CDCl_3$) δ 7.43 – 7.26 (m, 10H), 4.27 – 4.15 (m, 2H), 2.20 – 1.96 (m, 4H), 1.44 – 1.24 (m, 4H), 1.21 – 1.09 (m, 3H), 1.02 (t, *J* = 7.4 Hz, 3H), 0.81 (t, *J* = 6.7 Hz, 2H).

^{13}C NMR (75 MHz, $CDCl_3$) δ 140.55, 140.49, 129.87, 128.92, 128.67, 128.66, 128.60, 128.23, 127.53, 55.68, 55.44, 31.82, 30.91, 28.70, 25.79, 22.13, 14.17, 13.89.

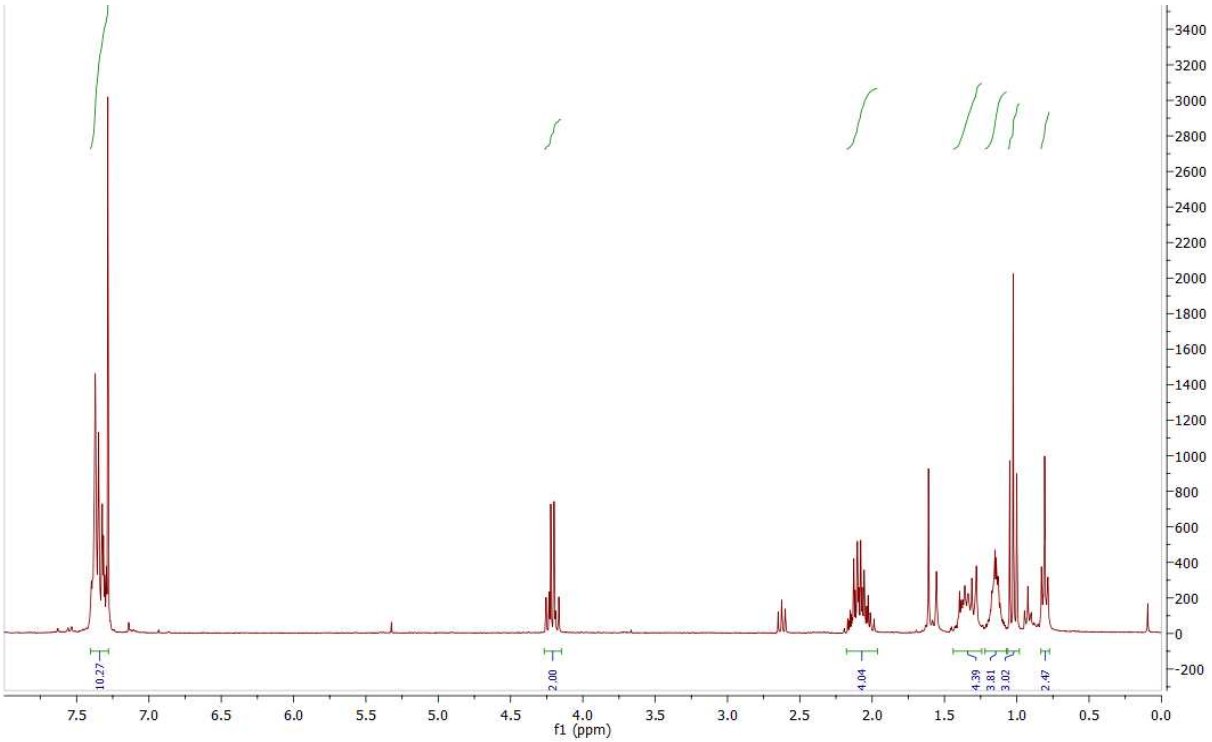

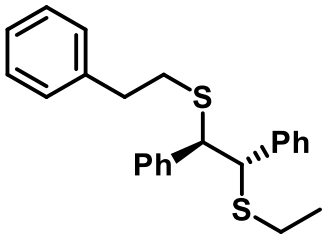

Ethyl((1S*,2R*)-2-(phenethylthio)-1,2-diphenylethyl)sulfane

Purified by column chromatography using a Hexane/Et_2O (99:1) eluent system to afford a pale yellow oil.

^{1}H NMR (300 MHz, $CDCl_3$) δ 7.45 – 7.27 (m, 11H), 7.26 – 7.13 (m, 2H), 6.95 (d, *J* = 6.3 Hz, 2H), 4.26 – 4.16 (m, 2H), 2.72 – 2.50 (m, 2H), 2.40 – 2.27 (m, 2H), 2.16 – 2.00 (m, 2H), 1.02 (t, *J* = 7.4 Hz, 3H).

^{13}C NMR (75 MHz, $CDCl_3$) δ 128.90, 128.81, 128.60, 128.46, 127.85, 127.75, 126.33, 55.88, 55.49, 36.10, 33.26, 29.86, 25.91.

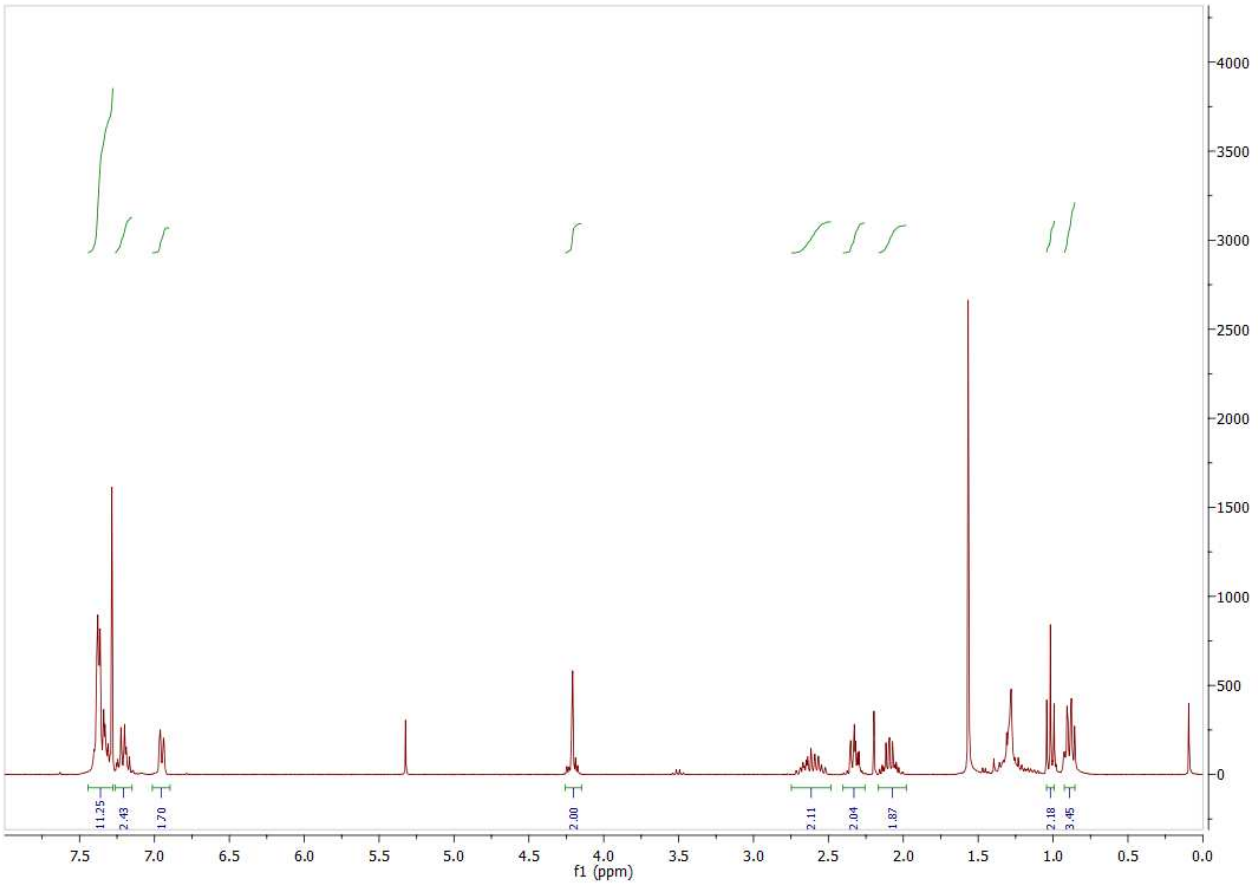

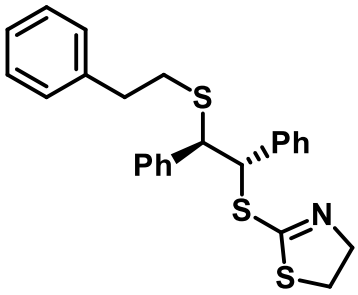

2-(((1S*,2R*)-2-(phenethylthio)-1,2-diphenylethyl)thio)-4,5-dihydrothiazole

Purified by column chromatography using a Hexane/Et_2O (90:10) eluent system to afford a white solid.

^{1}H NMR (300 MHz, $CDCl_3$) δ 7.36 – 7.13 (m, 13H), 7.04 – 6.96 (m, 2H), 5.30 (d, *J* = 8.4 Hz, 1H), 4.38 (d, *J* = 8.4 Hz, 1H), 4.13 – 4.03 (m, 2H), 3.25 (t, *J* = 8.0 Hz, 2H), 2.78 – 2.58 (m, 2H), 2.48 – 2.40 (m, 2H).

^{13}C NMR (75 MHz, $CDCl_3$) δ 140.71, 129.54, 128.99, 128.80, 128.68, 128.61, 128.55, 128.42, 128.34, 127.22, 126.51, 118.69, 52.09, 50.75, 36.13, 32.75, 29.85, 27.66.

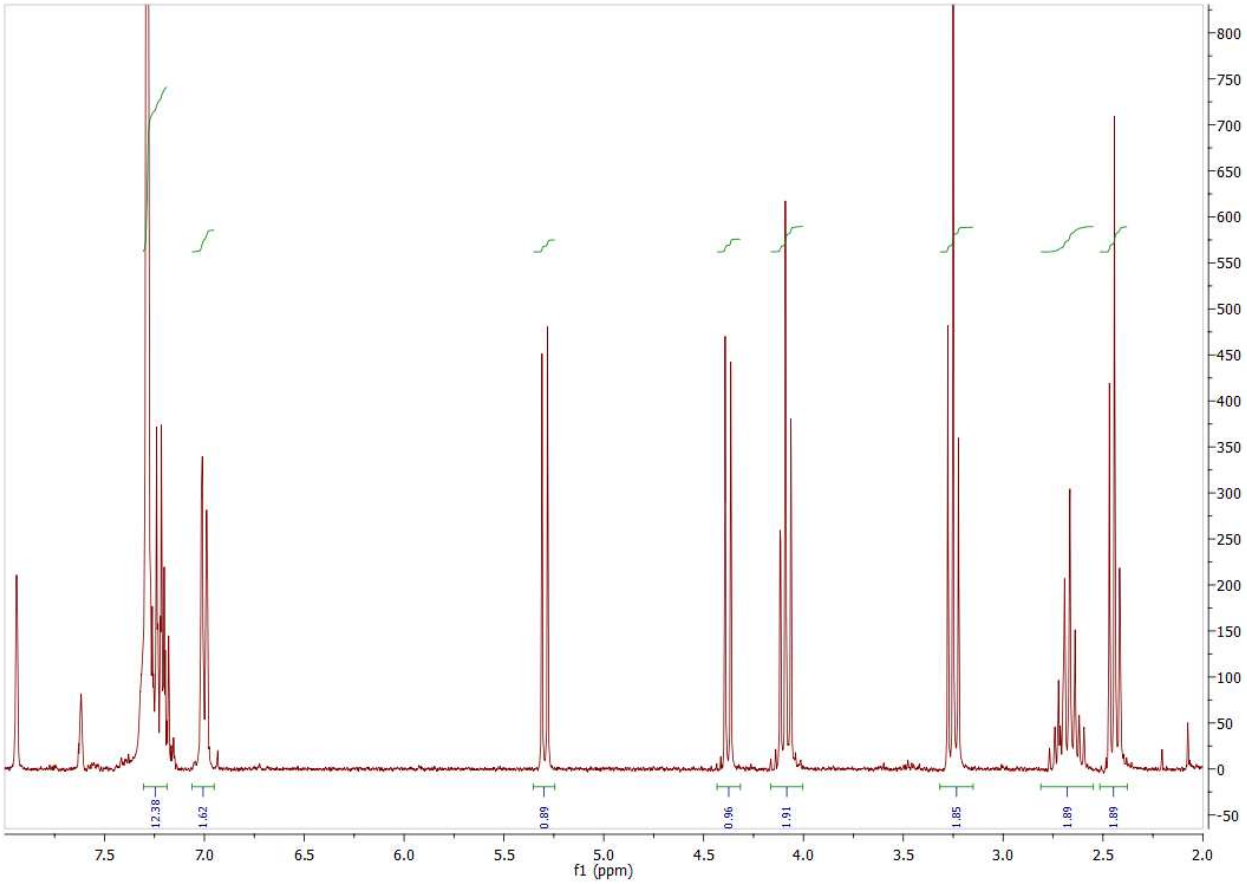

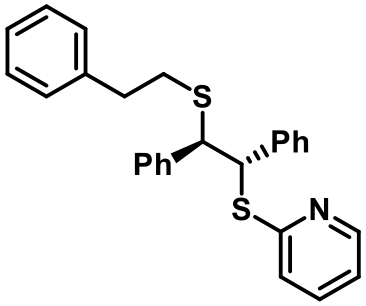

2-(((1S*,2R*)-2-(phenethylthio)-1,2-diphenylethyl)thio)pyridine

Purified by column chromatography using a Hexane/Et_2O (90:10) eluent system to afford a white solid.

^{1}H NMR (300 MHz, $CDCl_3$) δ 8.42 – 8.38 (m, 1H), 7.42 – 7.13 (m, 15H), 7.02 – 6.88 (m, 3H), 5.56 (d, *J* = 8.6 Hz, 1H), 4.46 (d, *J* = 8.6 Hz, 1H), 2.77 – 2.57 (m, 2H), 2.49 – 2.40 (m, 2H).

^{13}C NMR (75 MHz, $CDCl_3$) δ 149.31, 135.92, 129.69, 129.04, 129.02, 128.86, 128.73, 128.64, 128.55, 128.41, 128.26, 128.10, 128.02, 127.55, 127.52, 126.28, 123.24, 119.80, 56.05, 54.25, 36.07, 33.55.

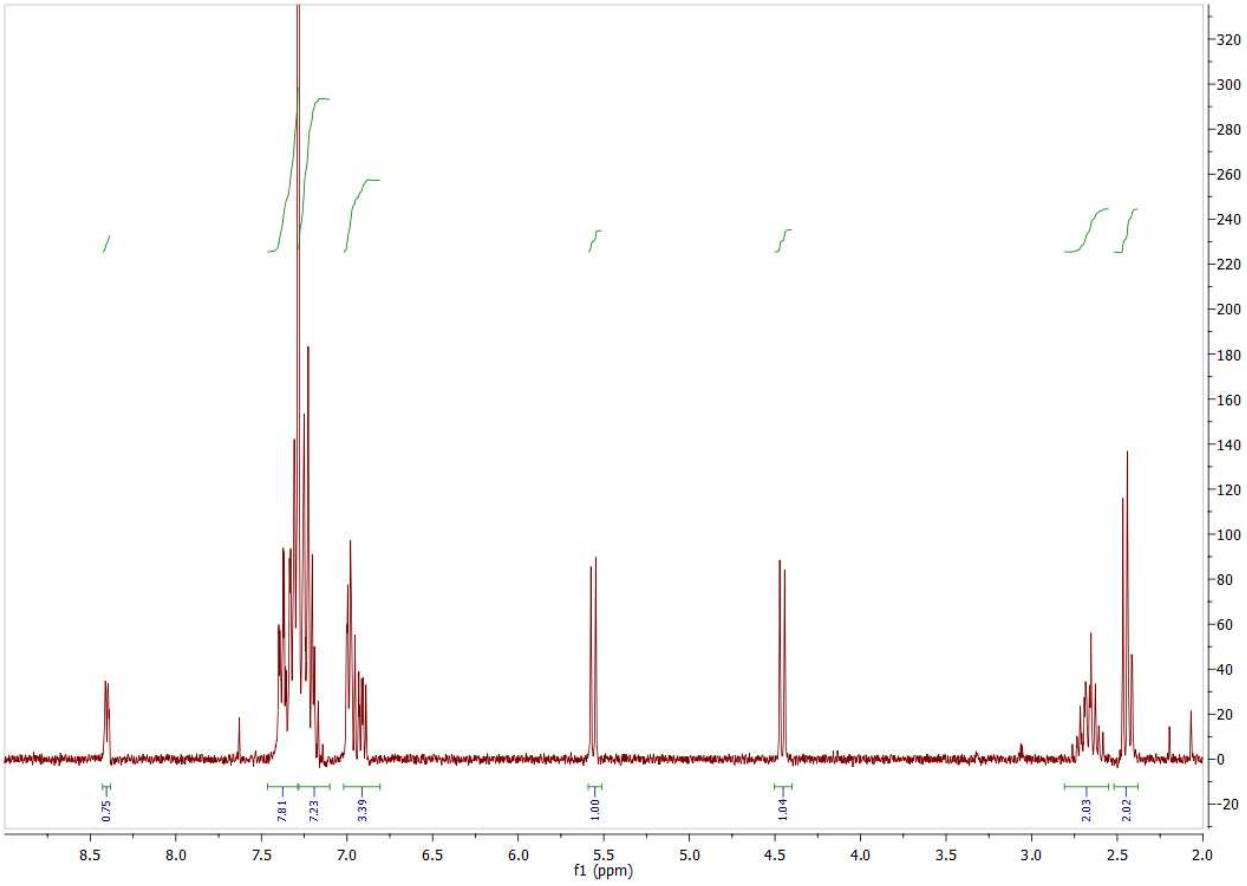

Titre : Catalyse asymétrique biomimétique avec des foldamères hélicoidaux bioinspirés

Résumé :

L'organocatalyse est une méthodologie qui connait un développement rapide, permettant de réaliser des transformations chimiques complexes dans le contexte général de la chimie durable (procédés sans métaux, recyclage des catalyseurs…). Les applications potentielles incluent l'élaboration rapide d'éléments de base avancés et utiles pour le développement pharmaceutique. Malgré de grandes réalisations, les organocatalyseurs souffrent généralement de certaines limitations comme une faible accélération de la réaction, d'un taux de rotation catalytique faible et de la nécessité de quantités importantes de catalyseur pour obtenir une bonne conversion et sélectivité. Afin de répondre à ces limitations, des catalyseurs incorporant de plus en plus de fonctions d'interaction afin d'exercer un contrôle plus important sur l'état de transition de réactions ont été des axes de recherche populaires. Un second axe consistant à utiliser des catalyseurs pré-structurés, analogues simplifiés des enzymes à également commencé à être étudié. Les foldamères d'oligourées développées par notre laboratoire ont précédemment démontré la capacité de catalyse dans le cadre de la réaction d'additions de composés 1,3-dicarbonylés aux nitroalcènes avec de très faibles charges catalytiques et d'excellentes stéréosélectivités. Les travaux présentés font suite à ces résultats et ont pour but d'étudier le mécanisme d'interaction du catalyseur, puis d'explorer de nouvelles réactions catalysées par nos foldamères.

Mots clés : Organocatalyse, Foldamères, Biomimétique, Hélices

Title : Biomimetic asymmetric catalysis with bioinspired helical foldamers

Abstract :

Organocatalysis is a rapidly expanding methodology enabling challenging chemical transformations to be performed in the broad context of sustainable chemistry (metal-free procedures, catalyst recycling…). Potential applications include the rapid elaboration of advanced and useful building blocks for pharmaceutical development. Despite major achievements, organocatalysts generally suffer from low rate acceleration and turnover and the need for relatively high amounts to achieve good conversion and selectivity. In order to address these limitations, catalyst structures incorporating increasing numbers of interacting functions to better control the transitions state of reactions have been a popular axis of research. A second, more recent approach has been the use of pre-organised catalysts, which can be viewed as simplified enzyme analogues. In this context, the oligourea foldamers developed by our group have previously been shown to catalyse the addition of 1,3-dicarbonyl compounds to nitroalkenes with low catalyst loading and excellent stereoselectivities. The works presented hereby come in continuation of these previous results with the main objectives being the study of the mechanism of interaction between the catalyst and substrates, and the exploration of new potential reactions catalysed by our foldamers.

Keywords : Organocatalysis, Foldamers, Biomimetic, Helices

Unité de recherche

Guichard Peptidomimetic group, UMR 5245 CBMN, 2 Rue Robert Escarpit, 33607 PESSAC